The Development and Application of a Distribution Class LMP Index

Final Project Report

Power Systems Engineering Research Center

Empowering Minds to Engineer
the Future Electric Energy System

The Development and Application of a Distribution Class LMP Index

Final Project Report

Project Team

Gerald T. Heydt, Project Leader
Arizona State University

Kory Hedman
Arizona State University

Shmuel Oren
Univ. of California, Berkeley

PSERC Publication 13-38

July 2013

For information about this project, contact

Gerald T. Heydt
Arizona State University
Department of Electrical Engineering
P.O. Box 875706
Tempe, AZ 85287-5706
Phone: 480 965-8307
Fax: 480 965-0745
Email: heydt@asu.edu

Power Systems Engineering Research Center

The Power Systems Engineering Research Center (PSERC) is a multi-university Center conducting research on challenges facing the electric power industry and educating the next generation of power engineers. More information about PSERC can be found at the Center's website: http://www.pserc.org.

For additional information, contact:

Power Systems Engineering Research Center
Arizona State University
527 Engineering Research Center
Tempe, Arizona 85287-5706
Phone: 480-965-1643
Fax: 480-965-0745

Notice Concerning Copyright Material

Acknowledgements

This is the final report for the Power Systems Engineering Research Center (PSERC) research project titled "The Development and Application of a Distribution Class Locational Margin Price Index" (project M-25). We express our appreciation for the support provided by PSERC's industry members and by the National Science Foundation under the Industry / University Cooperative Research Center program.

The authors thank industry collaborators including Baj Agrawal, Simon Chiang, Luther Dow, Alan Dulgeroff, Xiaoming Feng, Richard Kafka, W. Doug McLaughlin, Jim Price, Robert Saint, Shimo Wang, Xing Wang, and Steven Whisenant. Special acknowledgement is given to Mr. Whisenant for his careful reading of the text.

Project researcher Dr. Qiuwey Wu was supported by a fellowship from the Danish Agency for Science, Technology and Innovation (DASTI) during his research stay in the Department of Industrial Engineering and Operational Research (IEOR) at the University of California Berkeley from February to May 2012.

Executive Summary

The essence of the PSERC project "The Development and Application of a Distribution Class Locational Marginal Price Index" is to examine the details of the proposed use of a pricing signal in power distribution systems much like the locational marginal price is used in transmission systems. The project work is reported in three volumes as described below. The first volume focuses on how a modified form of a locational marginal price can be calculated and used in distribution systems. The second volume focuses in on a specific application, namely electric vehicle charging. The third volume provides mathematical rigor in the calculation of the distribution locational marginal price.

The main motivation for this work is a central tenet of 'the Smart Grid," namely the use of measurements and signals in electric power systems to maximize the efficacy of the system. In this way, the maximal and most cost efficient use of the system assets are attained.

Volume I: Applications and Calculation of a Distribution Class Locational Marginal Price

In Volume I, the topical coverage is the calculation and use of a pricing signal in distribution systems for energy and power management, and for the identification of components of the system that are stressed.

This volume presents an overview of the calculation and application of locational marginal prices in electric power systems particularly pertaining to the distribution system. The focus is on methods of performing the calculation of this near real time pricing signal. The terminology proposed is a *distribution locational marginal price* or DLMP. Alternative formulations and the calculation of locational prices in distribution engineering is conjectured and discussed. Much in the same way that locational marginal prices are decomposed into an energy cost, a congestion cost, and an active power loss cost, the DLMP is assumed to decompose into the same three terms. The use of quadratic programming for the calculation of the DLMP is proposed and illustrated. A small four bus test bed exemplifies the concept and then the concept is expanded to the IEEE 34 bus 'standard' distribution system. Alternatives for the calculation are predicated on alternative commercial software that is readily available in the power engineering community. The results are presented, and approximations for the inclusion of losses are reviewed. Active power losses in the system are modeled and incorporated by two different methods. These calculation methods are applied to the IEEE 34 bus system. The results from each method are compared to results found using the PowerWorld simulator.

The application of energy management using the DLMP to control loads is briefly analyzed. This analysis entails the use of the DLMP to cause certain controllable loads to decrease when the DLMP is high, and vice-versa. Tests are done to illustrate the impact of energy management using DLMPs for residential, commercial, and industrial controllable loads. Results showing the dynamics of the loads are shown. The main conclusion is

that the calculation of the DLMP can be done rapidly, and transmitted to energy management devices at the distribution system loads. It is further concluded that the calculation of the DLMP can be done with readily available, commercial software.

The use and characteristics of Matlab function FMINCON are presented in an appendix. Some remarks and examples for potential users of this software are given.

Volume II: Distribution Locational Marginal Pricing for Optimal Electric Vehicle Charging Management

This volume of the final report presents an integrated distribution locational marginal pricing method designed to alleviate congestion induced by electric vehicle (EV) loads in future power systems. In the proposed approach, the distribution system operator (DSO) determines distribution locational marginal prices (LMPs) by solving the social welfare optimization of the electric distribution system which considers EV aggregators as price takers in the local DSO market and accounts for price elasticity of conventional household load. Supply busses connecting the distribution system to the transmission grid are treated as generators with marginal costs set to the locational marginal prices for each bus. These LMPs are determined by the transmission system operator and treated in our model as exogenous inputs.

Nonlinear optimization has been used to solve the social welfare optimization problem in order to obtain the DLMPs which propagate the LMPS throughout the transmission network so as to alleviate distribution level congestion while meeting the conventional household load and the EV charging load. The efficacy of the proposed approach was demonstrated by mean of a case study using the Bus4 distribution system of the Roy Billinton Test System (RBTS) and superimposing on it EV charging load based on Danish driving data. The case study results show that the integrated DLMP methodology can successfully alleviate the congestion caused by EV loads. It is also shown mathematically that the socially optimal charging schedule can be implemented through a decentralized mechanism where loads respond autonomously to the posted DLMPs by maximizing their individual net surplus. .

Volume III: A Distribution-Class Locational Marginal Price Index for Enhanced Distribution Systems

The third volume compares the distribution-class locational marginal price (DLMP) mechanism to existing pricing mechanisms and it presents an integrated transmission and distribution model that incorporates the DLMP.

The smart grid initiative is the impetus behind changes that are expected to culminate into an enhanced distribution system with the communication and control infrastructure to support advanced distribution system applications and resources such as distributed generation, energy storage systems, and price responsive loads. The DLMP is proposed, in

this report, as an enabler of the advanced applications of the enhanced distribution system. The DLMP is proposed to be a control signal that can incentivize price sensitive distribution system resources to behave optimally in a manner that benefits economic efficiency and system reliability and that can optimally couple the transmission and the distribution systems.

This volume presents an integrated framework that couples the transmission and distribution systems models together. The DLMP is calculated from a two-stage optimization problem, which includes a transmission system and a distribution system OPF. An iterative framework that ensures accurate representation of the price sensitive resources in a distribution system for the transmission system problem, and vice versa, is developed and its convergence is discussed.

As part of the DLMP framework, a direct current optimal power flow (DCOPF) formulation that endogenously captures the effect of real power losses is discussed, i.e., a lossy DCOPF formulation is proposed. The formulation uses piecewise linear functions to linearly approximate real power losses. This report provides, with a theoretical proof, the breakdown of the loss approximation technique when non-positive DLMPs/LMPs occurs and discusses a mixed integer linear programming formulation to correct the breakdown.

The DLMP is numerically illustrated in traditional and enhanced distribution systems and its superiority to contemporary pricing mechanisms is demonstrated through the actions of price responsive loads. A combined transmission and distribution systems test model is created based on the IEEE 30-bus test system and the Roy Billinton Test System (RBTS). Results show that, as flexible resources increase, the impact of the inaccuracy of contemporary pricing schemes becomes significant. At high elasticity, aggregate load consumption deviated from the optimal consumption by up to about 45 percent when using a flat rate or a time-of-use rate. The individual load consumption incentivized by a real-time price deviated by up to 25 percent at high elasticity. The superiority of the DLMP is more pronounced when important distribution network conditions are not reflected by contemporary prices. The individual load consumption incentivized by the real-time price deviated by up to 90 percent from the optimal consumption in a congested, meshed distribution network. While the DLMP internalizes congestion management, the consumption incentivized by the real-time-price caused overloads.

This volume provides two primary conclusions: a) The DLMP is shown to be superior to existing pricing mechanisms in the distribution system. b) The primary benefit of the DLMP mechanism is the impact it can have on both the distribution system and the transmission system. Prior work has primarily focused on calculating DLMPs as opposed to extracting the flexibility of distribution system resources to benefit transmission system operations. Thus, this report proposes a framework that optimally integrates the transmission and distribution system operations together via an iterative framework that utilizes the DLMP as a control signal to align distribution system resource operations with transmission system objectives.

Project Publications

Akinbode, O., and K. W. Hedman, "Effect of fictitious losses on LMPs in the DCOPF with piecewise linear approximation of losses," *IEEE PES General Meeting 2013*, pp. 1-5, July 2013. Selected to participate in the Best Papers Forum.

Ruoyang, Li, and Quwei, Wu and Shmuel S. Oren, "Distribution Locational Marginal Pricing for Optimal Electric Vehicle Charging Management", Working paper, Submitted to IEEE Transactions on Power Systems (3rd round of review) 2013

Sathyanarayana, B. R., and G. T. Heydt, "Sensitivity-based pricing and optimal storage utilization in distribution systems," *IEEE Transactions on Power Systems*, accepted for publication 2013.

Singhal, N., and K. W. Hedman, "An integrated transmission and distribution systems model with distribution-based LMP (DLMP) pricing," *NAPS Conference*, pp. 1-6, September 2013.

Steffan, N., and G. T. Heydt, "Quadratic programming and related techniques for the calculation of locational marginal prices in power distribution systems," *Proc. North American Power Symposium,* Champaign IL, September 2012.

Student Theses

Akinbode, Oluwaseyi Wemimo *A Distribution-class Locational Marginal Price (DLMP) Index for Enhanced Distribution Systems*. Master's Thesis, Arizona State University, Tempe, AZ, May 2013. (Advisor: K. Hedman)

Steffan, Nicholas M. *Applications and calculation of a distribution class locational marginal price*. Master's Thesis, Arizona State University, Tempe, AZ, May 2013. (Advisor: G. Heydt)

Intentionally Blank Page

Volume I

Applications and Calculation of a Distribution Class Locational Marginal Price

Nicholas M. Steffan
G. T. Heydt
Arizona State University

Information about Volume I, contact

Gerald T. Heydt
Arizona State University
Department of Electrical Engineering
P.O. BOX 875706
Tempe, AZ 85287-5706
Phone: 480 965-8307
Fax: 480 965-0745
Email: heydt@asu.edu

Power Systems Engineering Research Center

The Power Systems Engineering Research Center (PSERC) is a multi-university Center conducting research on challenges facing the electric power industry and educating the next generation of power engineers. More information about PSERC can be found at the Center's website: http://www.pserc.org.

For additional information, contact:

Power Systems Engineering Research Center
Arizona State University
527 Engineering Research Center
Tempe, Arizona 85287-5706
Phone: 480-965-1643
Fax: 480-965-0745

Notice Concerning Copyright Material

Table of Contents

List of Figures

List of Tables

Nomenclature

A	Coefficients of the state vector in inequality constraints
A_{eq}	Coefficients of the state vector in equality constraints
b	Right hand sides of inequality constraints of the form $Ax \leq b$
B_{eq}	Right hand sides of equality constraints of the form $A_{eq}\,x = b_{eq}$
c	Coefficients of the linear terms in a cost function
C	Cost
CAISO	California ISO
d	Right hand sides of equality constraints of the form $Ex = d$
DAM	Day ahead market
DLMP	Distribution Locational Marginal Price
E	Coefficients of the state vector in equality constraints
EMS	Energy management system
ERCOT	Electric Reliability Council of Texas
F	Function to minimized
FERC	Federal Energy Regulatory Commission
FREEDM	The Future Renewables Electric Energy Delivery and Management
FUN	Call function for FMICON in MATLAB
IEEE	Institute of Electrical and Electronics Engineers
IFM	Integrated Forward Market
IPP	Independent power producer
ISO	Independent system operator
ISO-NE	ISO New England
KKT	Karush-Kuhn-Tucker
L	Lagrangian function to be minimized
LB	Lower bound
LMP	Locational Marginal Price
LP	Linear programming

μ	Lagrangian multiplier
MRTU	Market Redesign and Technology Upgrade
NYISO	New York Independent System Operator
NYPP	New York Power Pool
P	Power
PJM	Pennsylvania-Jersey-Maryland Interconnection
PLL	Phase locked loops
PWM	Pulse width modulated
Q	Coefficients of the quadratic terms in a cost function
QP	Quadratic programming
r	Resistance
SMD	Standard market design
SQP	Sequential quadratic programming
UB	Upper bound
x	A state vector that gives the system operating point
Y	Admittance
Z	Impedance

Chapter 1: Locational marginal prices and their application and calculation in distribution systems

1.1 Motivation for this project

Locational marginal pricing has been used in transmission systems for over a decade [1]. It has served as an adept measurement of variations in prices and bottlenecks within the transmission system. There is no measurement such as this currently in distribution systems, although proponents of the Smart Grid have proposed additional measurements in distribution systems. As government and industry influences push towards a "smarter" grid, the application of a distribution based locational marginal price (DLMP) could be very useful. The DLMP would be very similar to that of the transmission system in that it would as accurately as possible display the cost for one additional unit of energy to be supplied to a particular bus. Where the transmission system is commonly defined as the cost for one additional megawatt to be supplied, it might make more sense to define the DLMP as the cost of one additional kilowatt.

The DLMP could then serve many purposes. Most obviously it could show price variations throughout the distribution grid, but others as well. The application of a DLMP could identify which components cause high prices within the system. With this information, it could be determined where improvements in the system would be most beneficial. Improvements such as additional lines, distributed generation or even distribution level storage could be implemented to lower costs of the system. Additionally the DLMP could serve as a pricing structure for consumer level energy management. Consumers could obtain information from the DLMP and react to the prices, choosing whether to continue consuming or to reduce load. This control would not only save consumers money, but it could also help reduce the peak load in times of high prices.

1.2 Project researchers

The project researchers are listed in Table 1.1.

1.3 Period of performance

The project period of performance was from August 15, 2011 to August 14, 2013.

1.4 Objectives of the study

Recently, a variation of the LMP concept has been proposed for distribution systems, e.g., [2]. In distribution engineering, a pricing signal could be used for local control

[3,4]. As an example, when pricing signals are high, local energy storage (e.g., in electric vehicles [5]) could be controlled to 'discharge' to alleviate the high energy cost condition. Conversely, when the pricing signal is low, energy storage elements could be controlled to 'store' energy. Such a mechanism has the advantage of leveling distribution system demand and concurrently increasing load factor.

Table 1.1 Project researchers and advisors

University researchers		Industry advisors	
G. Heydt	Principal investigator, ASU	Baj Agrawal	APS
S. Oren	Researcher, UCB	Simon Chiang	PG&E
K. Hedman	Researcher, ASU	Luther Dow*	Quanta Technology
N. Steffan	Graduate research assistant, ASU	Alan Dulgeroff	Sempra Utilities
		Xiaoming Feng	ABB
		Richard Kafka*	Pepco Holdings
		W. Doug McLaughlin	Southern Co.
		Jim Price	CAISO
		Robert Saint	NRECA
		Shimo Wang*	Southern California Edison
		Xing Wang	Areva T&D
		Steven Whisenant	Duke Energy

*Retired from the project in 2013 ASU = Arizona State University
UCB = University of California - Berkeley

As stated previously, the DLMP would be defined as the cost to produce on additional kilowatt to a particular bus. This research aims to show the application of the DLMP in multiple sized systems. A very small system will be used as well as a slightly larger system from IEEE. For these two systems, different optimizing methods will be used to calculate the DLMP to illustrate:

- The inclusion of active losses
- To evaluate accuracy of the solution
- To include or exclude such phenomena as reactive power limits, PV versus PQ buses, and voltage controlled buses
- To show illustrations of the calculation method.

1.5 Literature review

Locational marginal prices

The present structure of LMPs was originally developed by Hogan of Harvard University in the early and mid 1990s [6]. Over a decade ago numerous markets around the world adapted location marginal pricing for their grids. The issues related to locational marginal prices, their calculation and use include:

> "adequacy of models and tools being used for economic dispatch, unit commitment and the calculation of the LMP; addressing infeasibilities; interpreting LMP components; physical and marginal loss pricing; recovering 'as bid' costs for the generators etc." [7]

Reference [1] outlines the history of how LMPs have been applied to contemporary power marketing:

- 1992: The Energy Policy Act is passed. FERC initiates the transition to competitive bulk energy markets
- April 1997: PJM becomes the first association of interconnected electric systems, or power pool, to officially operate as a regional transmission organization and independent system operator (RTO/ISO)
- July 1997: New England (ISO-NE) is declared an ISO.
- July 1999: ISO-NE implements wholesale energy markets.
- December 1999: New York Independent System Operator (NYISO) formally takes over control and operation of bulk transmission and generation dispatch in New York from New York Power Pool (NYPP).
- 2003: ISO-NE adopts an LMP scheme as part of its transition to a so-called SMD.
- April 2009: California ISO (CAISO) goes live with a fully nodal LMP market. The Market Redesign and Technology Upgrade (MRTU) project establishes an LMP real-time market and a day-ahead market (DAM). This combination, known as the Integrated Forward Market (IFM), is designed to co-optimize energy, reserves, and capacity, balancing supply and demand.
- December 2010: ERCOT goes live with a fully nodal LMP market and DAM.

Contemporary applications of LMPs

Locational marginal prices conventionally are the cost to deliver one additional megawatt hour to a given bus within a power system. The calculation includes optimal dispatch, line and generation constraints, and potentially additional equality and inequality constraints. Locational Marginal Prices are a pricing method used to establish the price for energy purchases and sales at specific location and under a specific operating regime. Contemporary practice is that LMPs are calculated through a linear programming (LP) process. The LP minimizes the total energy cost for the entire area subject to constraints that repre-

sent the physical limitations of the power system. For example, at the New England ISO, the linear programming process yields three portions of the LMP corresponding to the energy component, the loss component and congestion component [8] as seen in (1.1). The energy component does not depend on the physical location in the system, while the loss and congestion components are uniquely calculated at each specific system bus,

$$LMP = LMP_{energy} + LMP_{congestion} + LMP_{loss}. \quad (1.1)$$

Equation (1.1) is an approximation: the actual LMP is the cost to deliver the next unit of energy to a specific bus, and only to the degree that this incremental cost can be decomposed and resolved into three distinct components indicated in (1.1) is this expression valid. Gross discusses (1.1) as an approximation in [32]. Specifically, in [32], the decomposition shown in (1.1) is discussed in terms of its accuracy and validity. For purposes of the present work, the decomposition shown is used. A common calculation method to obtain the LMPs is linear programming because (1.1) can be written in approximate terms by linearizing the power flow equations. However, the loss term in (1.1) is often omitted. In transmission systems, the active power losses are in the range of 2 to 5%. The unique characteristics of each individual bus are what cause price differentiation between each bus.

In transmission systems, LMPs have value in revenue pricing and identification of bottlenecks in the system. Since their implementation they have become one of the most popular methods for congestion management in many markets worldwide. As a result of their current structure, LMPs not only reveal current energy prices, but help price other ancillary services as well. [7].

1.6 Energy management systems

Numerous companies offer home energy management systems. Companies like General Electric, Schneider Electric, Hitachi and others provide a system that a home owner can use to control their home [9]. In the case of the Schneider electric product it "allows homeowners to reduce or shift energy use during peak times and helps electricity providers improve grid efficiency and network reliability" [10]. When referring to load control the device can be used for remote monitoring and management of HVAC compressors, water heaters, pool pumps and other power circuits.

These types of systems however are manually driven where a more automatically driven system is based on the DLMP is proposed later in this report. With the high probability of increased distributed generation and storage there is a need to have a more automatic energy management system. Other 'automatic' systems have been proposed. In [11] a system based on control through cloud computing is proposed. In this system the load is controlled based on peak power times and mitigates power based on connected appliances. In addition to [11], more proposals for energy management are listed in Table 1.2 as well as

different projects by the Electric Power Research Institute (EPRI) in Table 1.3. The material in Table 1.3 is abstracted from [31].

Table 1.2 Energy management proposals

Load(s) Controlled	Basic Strategy	Reference
Home appliances based on a given schedule; has distributed generation and storage capabilities	Assigns dynamic priority to a household appliance according to the type of appliance and its current status. In accordance with the assigned priority, the use of household appliances is scheduled considering renewable energy capability	[11]
Controls household load based on appliances and cost	Consists of price prediction, a load scheduler and energy consumption monitor. The electricity pricing models provide the price prediction capability. The load scheduler is used to control the residential load with an aim at reducing the total energy cost and the smart meter and smart switchers are utilized to collect and monitor the energy consumption in the house	[28]
Individual homes major appliances and lighting	A smart home control system that can assign tasks to suitable components. It can automatically gather physical sensing information and efficiently control various consumer home devices.	[29]

Table 1.3 EPRI projects on energy management

Title	Abstract
Energy Management Systems for Commercial Buildings:	Approximately 25,000 commercial buildings in the United States have energy management systems. Planners estimate that by 1990 another 80,000 systems will be in use. This primer on commercial building energy management systems describes their functions, components, and design options
Assessment of Commercial Building Automation and Energy Management Systems for Demand Response Applications:	An overview of commercial building automation and energy management systems with a focus on their capabilities (current and future), especially in support of demand response (DR). The report includes background on commercial building automation and energy management systems; a discussion of demand response applications in commercial buildings, including building loads and control strategies; and a review of suppliers' building automation and energy management systems
Commercial Building Energy Management Systems Handbook: Opportunities for Reducing Costs and Improving Comfort:	This document is written for the commercial building owner, manager, or developer without a technical background but wanting to understand and evaluate recommendations for energy savings or comfort made by energy consultants and/or building engineers. It provides an overview of commercial building heating, ventilating, air-conditioning (HVAC), and lighting systems, and of the energy management systems (EMSs) that control comfort and provide energy savings.
Integration of Utility Energy Management Technologies into Building Automation Systems:	The challenges with managing peak demand are expected to worsen as de-carbonization, plant retirement, renewable integration, and electric vehicle rollouts unfold. One solution to this problem is in better management of the demand side. This study is focused on commercial buildings, which account for approximately 27% of all electricity used in the United States and have a large impact on demand since much of the consumption falls during business hours, which tend to correspond with peak demand windows
Standard Interfaces for Smart Building Integration:	Electricity systems in the United States are changing to accommodate increasing levels of distributed energy resources and demand responsive loads. Commercial buildings are positioned to play a central role in this change. With advances in energy generation and storage technologies, process management, and controls, commercial buildings are increasingly able to provide a range of grid supportive functions

1.7 Organization of this report

The remainder of this report will be organized into five additional chapters. Chapter two will discuss the process of using quadratic programming to minimize a cost. In addition it will discuss how the 'FMINCON' function in Matlab can potentially be used to approximate the losses. Chapter three will take the theory in chapter two and apply it to calculating the DLMP using quadratic programming. Both a small example and larger example will be analyzed. Chapter four is a continuation of chapter three but with the application of losses. Comparison of the three methods proposed in this report will be made against PowerWorld simulator. Chapter five discusses the role of the DLMP and it uses for energy management. In this chapter, the DLMP is used in various ways to control the load of the system. Chapter six ends the report with a conclusion, recommendations and future work.

An appendix contains comments on Matlab function FMINCON. Execution time and convergence is discussed and illustrated.

Chapter 2: The theory and application of quadratic programming in power distribution engineering

2.1 Definition of the quadratic programming problem

Quadratic programming (QP) is the optimization of a quadratic function. Mathematically, consider the extremization of the scalar function *c(x)*,

$$f(x) = \frac{1}{2}x^T Qx + c^T x \tag{2.1}$$

where the objective function has a vector valued argument *x*, a vector of *n* rows, *Q* is a constant *n* by *n* matrix, and *c* is a constant *n*-vector. In the case where $Q = 0$, the problem is solved by linear programming (LP). The constraints of (2.1) are

$$Ax \leq b \tag{2.2}$$

$$Ex = d \tag{2.3}$$

where *A* is an *m* by *n* matrix and *E* is a *k* by *n* matrix.

Quadratic programming is commonly solved by the Karush-Kuhn-Tucker (KKT) method. This method entails the creation of the Lagrangian function,

$$L(x, \mu) = cx + \frac{1}{2}x^T Qx + \mu(Ax - b) \tag{2.4}$$

where μ is a *m*-dimensional row vector. The conditions for a local minimum are as follows [10],

$$\frac{\partial L}{\partial x_j} \geq, \quad j = 1, \dots, n \qquad\qquad c + x^T Q + \mu A \geq 0$$

$$\frac{\partial L}{\partial \mu_j} \leq, \quad i = 1, \dots, m \qquad\qquad Ax - b \leq 0$$

$$x_j \frac{\partial L}{\partial x_j} = 0, \quad j = 1, \dots, n \qquad\qquad x^T (c + x^T Q + \mu A) = 0$$

$$\mu_i g_i(x) = 0, \quad i = 1, \dots, m \qquad\qquad \mu(Ax - b) = 0$$

$$x_j \geq 0, \quad j = 1, \dots, n \qquad\qquad x \geq 0$$

$$\mu_j \geq 0, \quad i = 1, \dots, n \qquad\qquad \mu \geq 0.$$

Reference [13] also discusses this formulation. In essence, the KKT method causes the last term in (2.4) to be zero. This happens by virtue of either the term μ as zero, or the coefficient of μ as zero (this occurs row by row when the elements in (2.4) are vectors). To solve, rearrange the inequality constraints with nonnegative slack variables *y, v* inserted, and the KKT conditions can now be written as follows,

$$xQ + \mu^T A^T - y = c^T \tag{2.5}$$

$$Ax + v = b \tag{2.6}$$

$$x \geq 0, \quad \mu \geq 0, \quad y \geq 0, \quad v \geq 0 \tag{2.7}$$

$$y^T x = 0, \quad \mu v = 0. \tag{2.8}$$

Eqs. (2.5-2.8) are linear and LP is applied to obtain a solution [12]. This is the method used in Matlab.

Appendix A contains a more detailed discussion of the Matlab implementation of QP, namely quadprog. Also in the appendix, a discussion appears for a MATLAB solver for the minimization of a nonlinear *f(X)* of general configuration (not simply quadratic) using the KKT method. This optimization in-line function is FMINCON.

2.2 Formulation of DLMP using quadratic programming

The application of quadratic programming is a process of taking real world functions and constraints and applying them to the process above. The function that will be minimized is associated with costs of the system. Those costs are the result of fuel (generation) and system related costs (congestion and losses). The equality and inequality constraints are derived from the characteristics of the system. Line data such as resistances, impedances and thermal limit, as well as load data and generation capacity all can contribute to these constraints. So to follow the formulas above, *Q* and *c* in equation (2.5) are derived from costs and *A, b, E* and *d* are due primarily line and load data.

2.3 Inclusion of losses

The inclusion of line losses in the above formulation is problematic because quadratic programming, at least in the classic formulation shown in section 2.1, does not permit nonlinear constraints. Losses are generally not negligible in distribution systems (estimates vary as to the percentage of losses, but generally 3 to 7% active power losses are reasonable estimates). Additionally, there are losses in the distribution transformers at the points of common coupling.

There are many approaches to the inclusion of losses with one being linearization. However, in this paper another approach is offered: relaxation of the loss term by inclusion in the objective function. If the function *f(x)* is augmented with an additive term that captures the cost of the losses, the minimization of *f(x)* (i.e., calculation of $f^* = f(x^*)$) will give an approximate solution to the constrained optimal dispatch. Subsequently, the loads specified can be increased by a small amount to calculate the change in f^*. Then the LMP at the bus at which the load was increased is calculated as the change in f^*.

To effectuate the approach outlined above, modify the *f(x)* formulation as used in the lossless case,

$$f(x) = C(x) + \frac{f(x^*)}{P_{load_1}+\cdots+P_{load_i}}[P_{loss_1} + \cdots + P_{loss_i}] \tag{2.9}$$

where *C(x)* is the total cost of generation without considering losses. In (2.9), the coefficient of the second term is the approximate generation cost expressed in $/MWh, the sum term at the end of (2.9) represents the total system-wide active power losses. Therefore the entire second term in (2.9) is the approximate cost of active power losses. Assuming $f^* = f(x^*)$ to be the optimum (i.e., minimum operating cost) solution, and the total cost calculated including losses, then

$$f(x) = \frac{C(x)}{1 - \frac{P_{loss_1} + \cdots}{P_{load_1} + \cdots}} \tag{2.10}$$

It is interesting to note that in (2.9), the term *f(x*)* is taken to be a constant, and differentiation of (2.9) then treats *f(x*)* as a constant. Of course, if *f(x)* on the right hand side of (2.9) were taken as a variable, the derivative of *f(x)* with respect to *x* would nonetheless be zero because *f(x)* is being extremized (minimized in this case).

As the LMP is defined as the cost to deliver one more megawatt for one hour for a given location, then the DLMP can be formulated as,

$$DLMP = \frac{f(x(t+1)) - f(x(t))}{P_{load}(t+1) - P_{load}(t)} \tag{2.11}$$

where $f(x(t+1))$ is the new total cost due to load change $P_{load}(t+1)$, $f(x(t))$ is the total cost determined previously, i.e., at load $P_{load}(t)$. This is the approach taken to include line losses. It is noted, however, that the model for the losses is approximate.

Note that the proposed formulation as given in (2.11) disallows the use of classically formulated QP because of the nonlinear term in *f(x)*. This term occurs due to the inclusion of losses in the model. Modern commercially available software is used to solve the lossy case shown here. For example, Matlab uses function FMINCON which can be

used in this application. FMINCON uses Sequential Quadratic Programming (SQP) [13] which is a variant of the Kuhn-Tucker approach. The basis of SQP is to model the minimization problem at x_k by a quadratic sub-problem and to use the solution to find a new point x_{k+1}. The explanation of FMINCON and SQP in general appears in [14,15].

The Kuhn-Tucker approach uses the exclusion conditions: in (2.4), the $\mu(AX-b)$ term must be such that either the μ_i term is zero or the $(AX-b)_i$ term is zero. There is one such exclusion condition for each inequality constraint, and therefore one assumes that the number of cases to be checked is proportional to 2^d where d is the number of inequality constraints and d is the dimension of μ. The actual Matlab code uses various procedures to reduce the dimensionality of the problem, but nonetheless, the execution speed is *not an advantage* of FMINCON. Also, in large scale problems, excessive memory requirements have been reported [16]. In distribution system applications, neither the execution time nor the memory requirements were found to be problematic, but these are marked for potential problems in some large scale applications. Note that in typical distribution engineering applications, the number of line limits to be applied as constraints is not large, and many could be dropped from consideration because of the robustness of the systems (i.e., the line limits are not reached in any credible steady state system operating condition).

Chapter 3: Calculation of DLMPs

3.1 Locational marginal prices for power distribution systems

The process to calculate the distribution based LMP will be explained in this chapter. Using the concepts explained in Chapter 2 an example using a small four bus system will be used to display the DLMP concept. The concept will then be expanded and applied to the IEEE 34 bus test bed. Both the lossless and lossy cases are illustrated. Figure 3.1 shows the general approach taken in these examples.

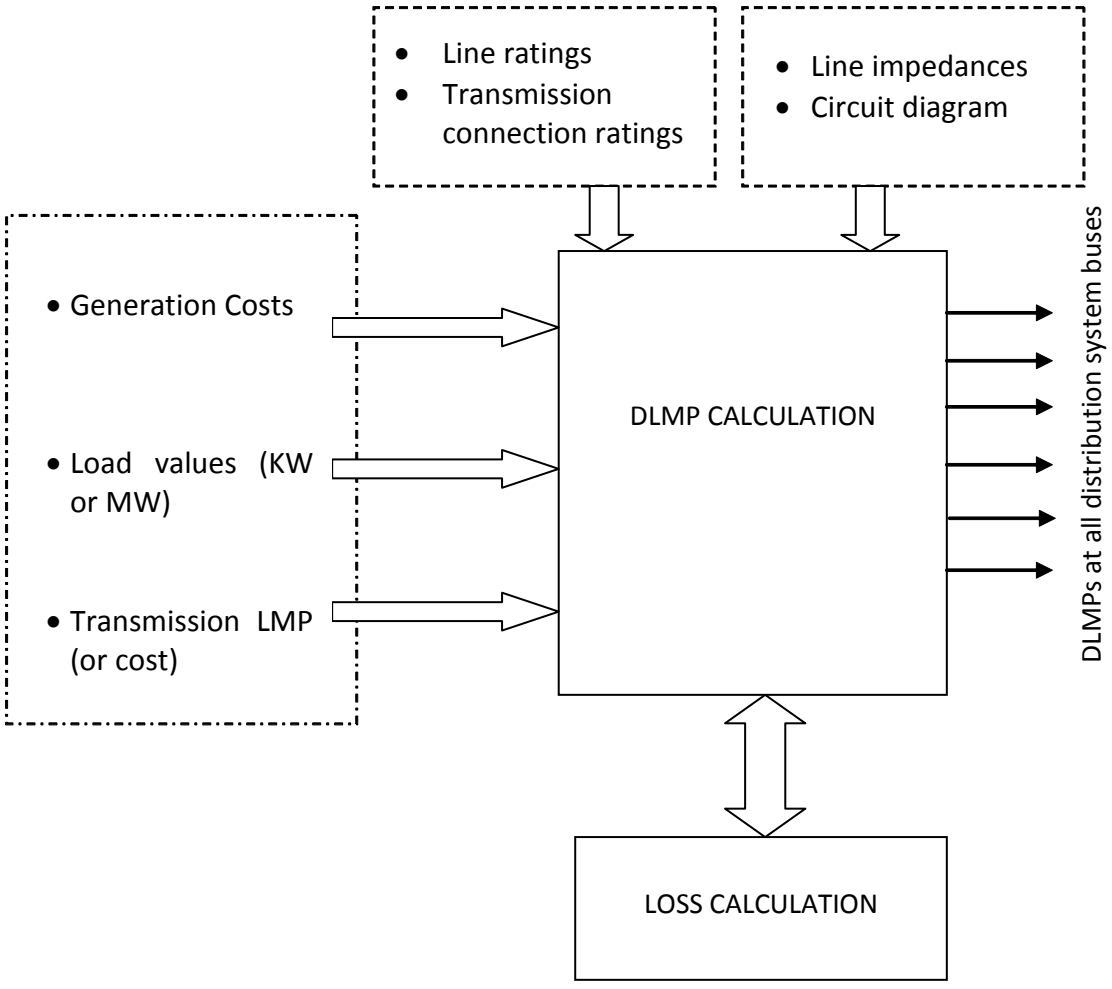

Figure 3.1 General approach to the calculation of a distribution LMP

3.2 Illustrative small example

For purposes of illustrating the algorithms in Chapter 2, a small example is offered. Figure 3.2 shows a four-bus networked system with line data shown in Table 3.1. In the system, there are two sources P_1 and P_2 with corresponding cost functions (P_i in MW, C_i in \$/h),

$$C_1 = 2P_1 + 0.1P_1^2 \tag{3.1}$$

$$C_2 = 1.5P_2 + 0.12P_2^2 \tag{3.2}$$

Two cases are considered: the lossless case, and the lossy case.

3.2.1 Lossless case

The lossless case is considered first by assuming that the line impedances shown in Table 3.1 are all reactive (i.e., $R = 0$). The loads P_3 and P_4 both are less than or equal to 30 MW. It is desired to obtain the constrained economic dispatch for this system. Using a base power of 10 MW, let the bus loads be represented as $P_i > 0$. Then the problem is,

$$Min \quad \frac{1}{2}X^T \begin{bmatrix} 20 & 0 & \cdots & 0 \\ 0 & 24 & & \\ \vdots & & \ddots & \vdots \\ 0 & & \cdots & 0 \end{bmatrix} X + [20 \quad 15 \quad ...]X$$

$$X = [P_1 \quad P_2 \quad P_3 \quad P_4 \quad P_{l1} \quad P_{l2} \quad P_{l3} \quad P_{l4} \quad \delta_2 \quad \delta_3 \quad \delta_4\ ]^{\mathrm{T}}.$$

The conservation of active power at each bus is,

$$\begin{bmatrix} -1 & 0 & 0 & 0 & 1 & 1 & 0 & 0 \\ 0 & -1 & 0 & 0 & -1 & 0 & 1 & 1 \\ 0 & 0 & 1 & 0 & 0 & -1 & -1 & 0 \\ 0 & 0 & 0 & 1 & 0 & 0 & 0 & -1 \end{bmatrix} \begin{bmatrix} P_1 \\ P_2 \\ P_3 \\ P_4 \\ P_{l1} \\ P_{l2} \\ P_{l3} \\ P_{l4} \end{bmatrix} = 0$$

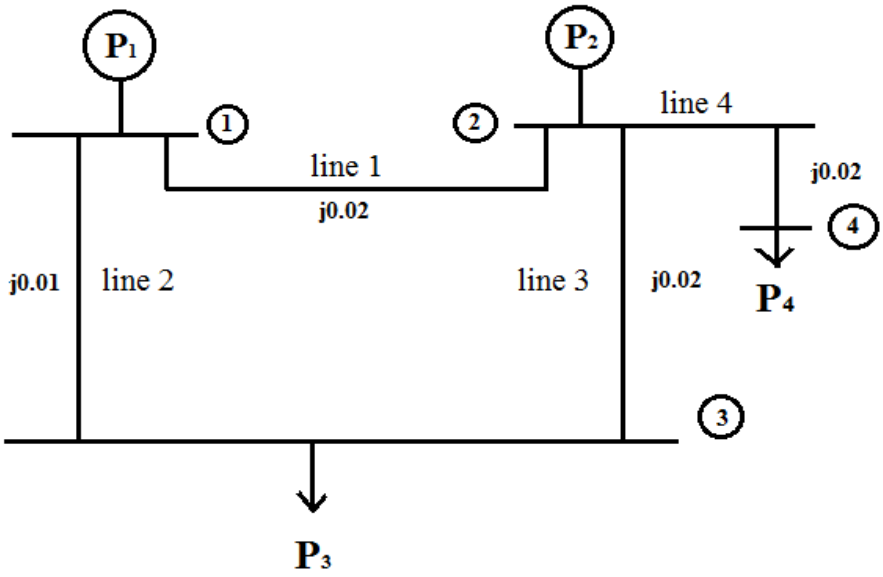

Figure 3.2 An illustrative example of quadratic programming to calculate the DLMP

Table 3.1 Line ratings for example system shown in Figure 3.2

Line	Line impedance (p.u., 10 MVA base)	Rating (MW)
1-2	0.0025+ $j0.02$	15
1-3	0.0013 + $j0.01$	15
2-3	0.0030 + $j0.02$	25
2-4	0.0040 + j0.02	30

The line active power flows are,

$$P_{l1} = \frac{\delta_1 - \delta_2}{x_{12}} \qquad P_{l2} = \frac{\delta_1 - \delta_3}{x_{13}} \qquad P_{l3} = \frac{\delta_2 - \delta_3}{x_{23}}$$

$$P_{l4} = \frac{\delta_2 - \delta_4}{x_{24}} \qquad \delta_1 = 0.$$

The line constraints are (in per unit),

$$|P_{l1}| \le 1.5 \quad |P_{l2}| \le 1.5 \quad |P_{l3}| \le 2.5 \quad |P_{l4}| \le 3.0$$

Using the QUADPROG function in Matlab, the optimum operating cost results are obtained and shown in Figs. 3.3 and 3.4. Using (2.11), the DLMP for bus 3 is calculated and shown in Figure 3.4.

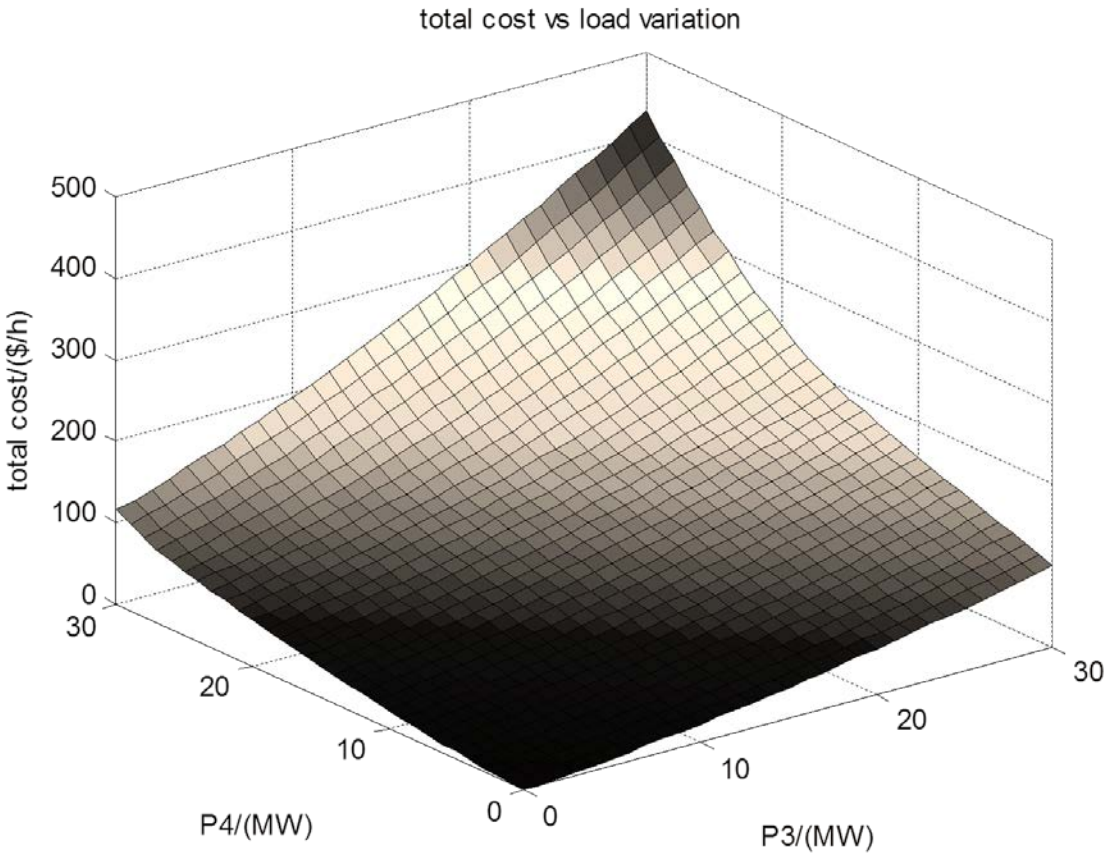

Figure 3.3 Results obtained for a constrained economic dispatch, P3 and P4 are loads – lossless case

The results in Figure 3.3 show a contoured map of the DLMP at buses three and four. As the load of each bus varies from zero to 30 MW, the DLMP at each bus is affected. The total load is set up in a way so that it is always equal to 30 MW. For instance is the load at bus three is five, bus four will be 25.

3.2.2 The lossy case

The same example shown in Figure 3.2 is reconsidered with losses included (i.e., $R \geq 0$ as shown in Table 3.1). The formulation is as in (2.10). For this case,

$$f(x) = \frac{20P_1 + 10P_1^2 + 15P_2 + 12P_2^2}{1 - \frac{P_{loss1} + P_{loss2} + P_{loss3} + P_{loss4}}{P_3 + P_4}}$$

where

$$P_{loss(i)} = {P_{li}}^2 R_{li}$$

$$X = [P_1 \quad P_2 \quad P_3 \quad P_4 \quad P_{l1} \quad P_{l2} \quad P_{l3} \quad P_{l4} \quad \delta_2 \quad \delta_3 \quad \delta_4\ ]^T$$

The formulation shown here is used in Matlab function FMINCON, and the resulting DLMP is shown in Figure 3.4. Abscissas and ordinates are superimposed so that quantitative comparisons can be made with lossy results. Bus P4 has been set to four different values and bus P3 is gradually increased.

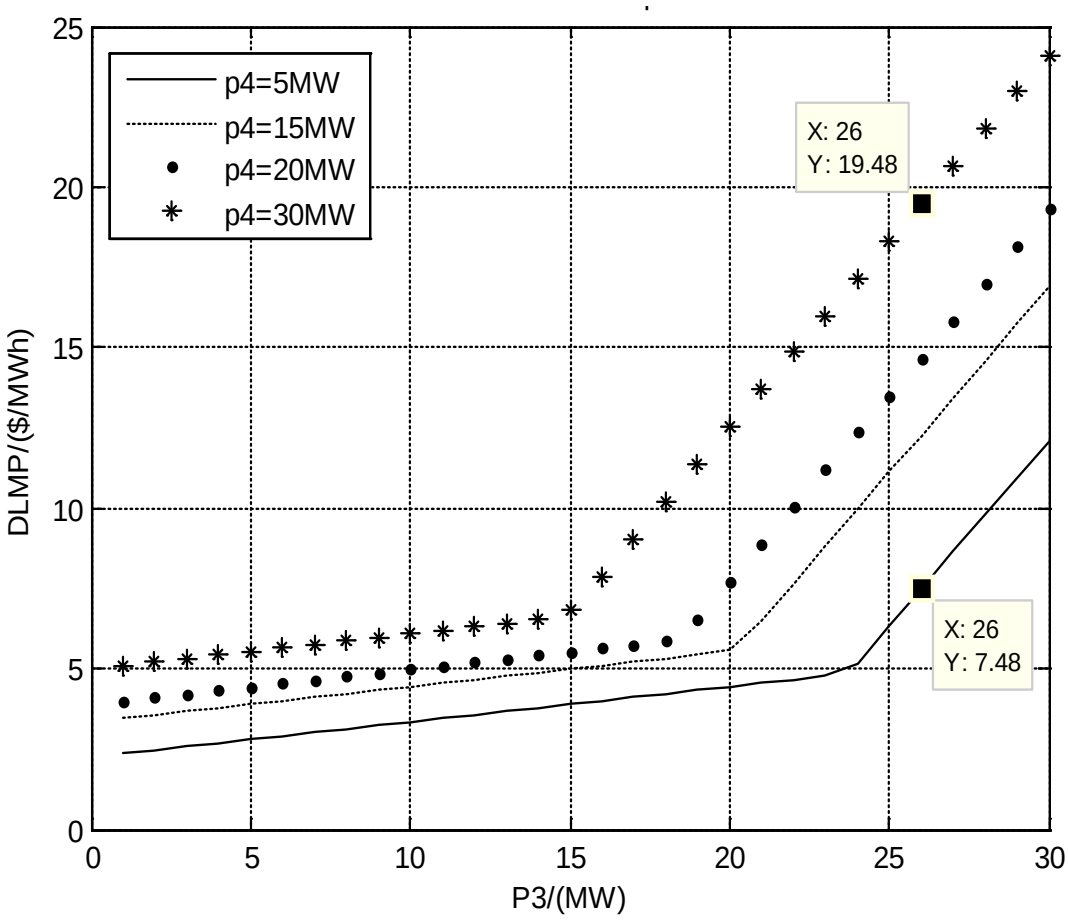

Figure 3.4 Result obtained for a constrained economic dispatch, P3 and P4 are loads – lossless case

The constraints are the same as those for the previous lossless example. Using the FMINCON function in Matlab, the optimum (minimum) total cost is obtained and shown in Figure 3.5 and the DLMP for bus 3 with loss are obtained and shown in Figure 3.6. Note that abscissa and ordinates are shown in the figure so that a comparison with Figure 3.6 can be made.

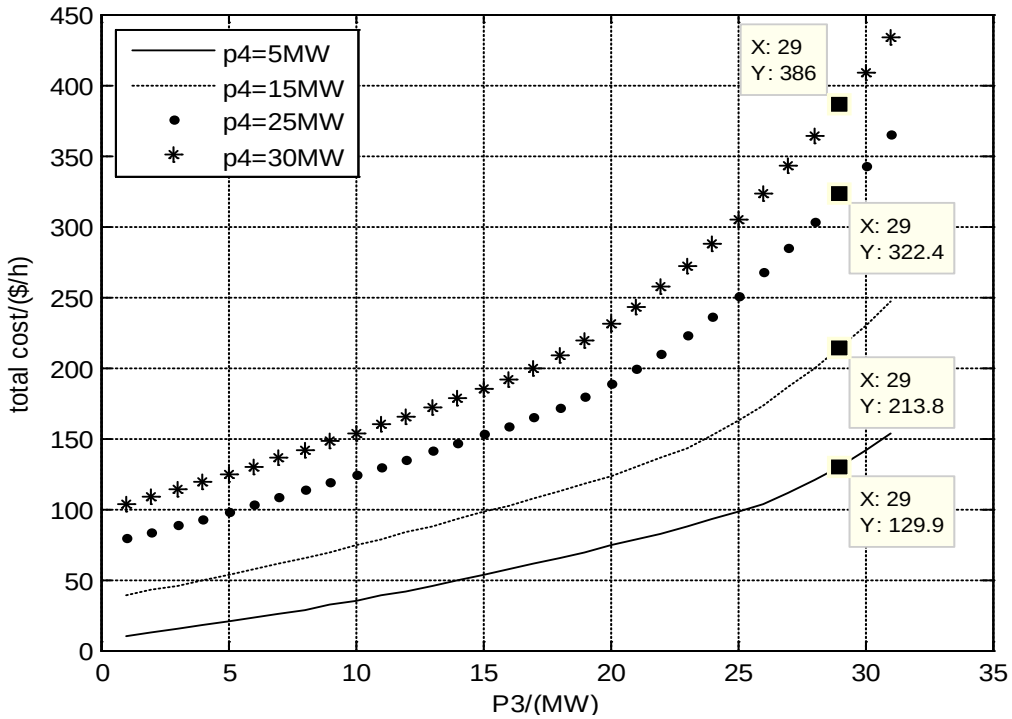

Figure 3.5 Result obtained for a system with constraint considering losses, P3 and P4 are loads

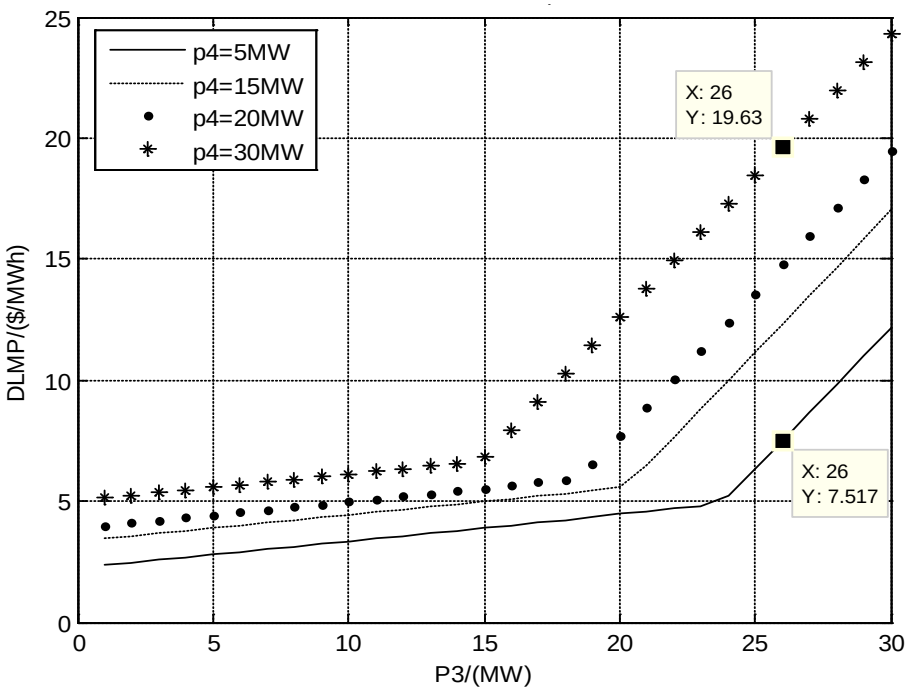

Figure 3.6 Result obtained for a system with constraint considering losses, P3 and P4 are loads

The results in Figure 3.6 show a slightly higher DLMP in the lossless case as compared to the results of the no loss case in Figure 3.4. The resistances of the system are low creating low losses. A system with higher resistance values should see higher losses.

3.3 Illustration using the IEEE 34 bus test bed

A test bed used is selected from an IEEE repository of test systems [17]. The intent is to demonstrate the DLMP calculation on a larger system for which some published results are available. This is a 34 bus distribution test bed and for purposes of this work the system has been modified as follows:

- Distributed generation was inserted at buses 800, 836 and 854, renamed 1, 2 and 3 respectively
- All single phase buses have been eliminated
- The symmetrical component transformation was used: $Z_{line} = T^{1} Z_{abs} T = Z_{sc}$ for given data which give the three phase bus impedance matrix Z
- Unbalanced lines were ignored and only the positive sequence was considered
- Distributed loads (i.e. 802 to 806) were placed as spot loads at the bus which is 'upstream' in the feeder.
- Changes to the system have been reflected in Figure 3.7, and the system data are in Appendix A.

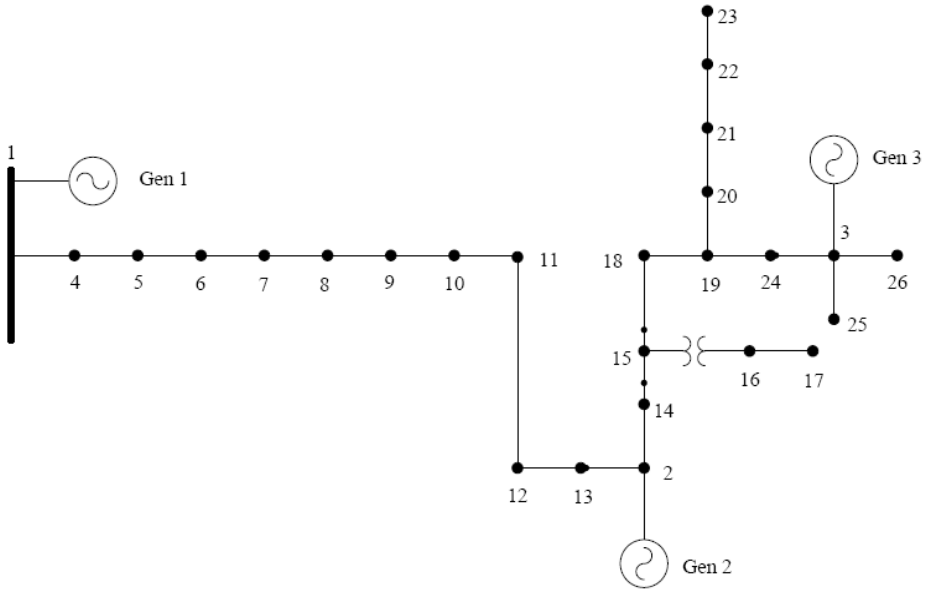

Figure 3.7 System diagram with single phase lines removed and generation inserted

The following cost data were used at buses 1, 2, and 3,

$$C_{P1} = 3.75 * 10^{-2} P_1 + 9.38 * 10^{-5} P_1^2$$
$$C_{P2} = 4.50 * 10^{-2} P_2 + 9.30 * 10^{-5} P_2^2$$
$$C_{P3} = 4.00 * 10^{-2} P_3 + 9.90 * 10^{-5} P_3^2$$

The analysis procedure is as follows:

- Convert line data and load data to per unit using a 500 kVA base, 24.9 kV
- Form the admittance matrix Y_{bus}
- Use QUADPROG in MATLAB solve for the LMP for the lossless case
- Use FMINCON to simulate case with losses (see Appendix A).

The DLMP in the no loss case was found to be identical at all buses in the system. This 'lossless' DLMP was 0.0728 $/kWh (the same value is found at every system bus). The lossy case is solved and gives results shown in Table 3.2. Figure 3.8 shows contours of similarly valued DLMP regions superimposed on the system diagram.

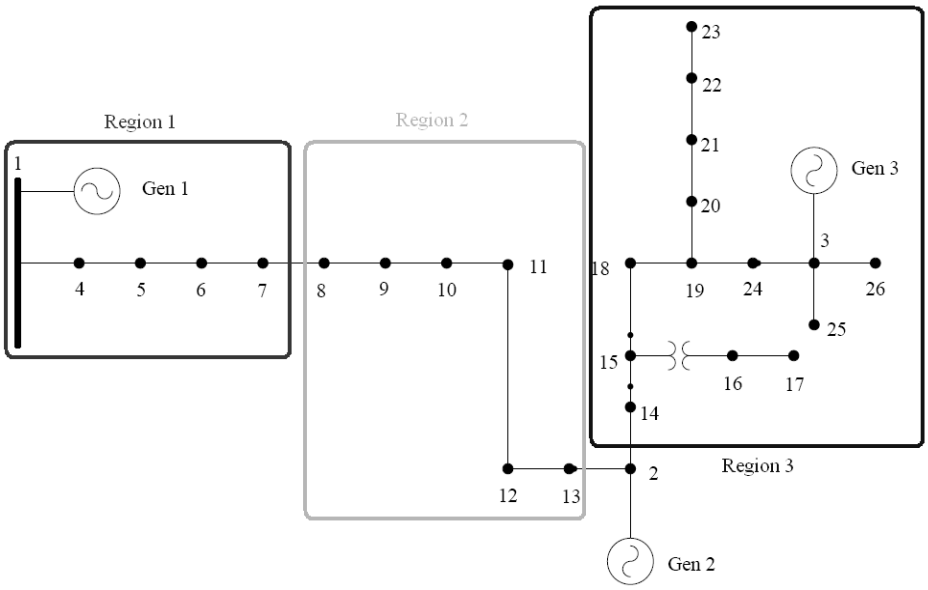

Figure 3.8 System diagram with similar DLMP regions. Region 1: 0.0726-0.0730$/kW; Region 2: 0.0732-0.0735$/kW; Region 3: 0.0742-0.0749$/kW

3.4 Discussion: application of DLMPs

As the power system transitions into the future, the implementation of smart meters and distributed generation will create an application for DLMPs [18-21]. The DLMP could help support cost effective growth of new technologies and could be used as a road map for

new renewable distributed generation. That is, in regions with high DLMP, greater investments could be made in distribution system assets. Another application of the DLMP might be in pricing energy and power differently at different buses. In [22], Heydt conjectures that a DLMP signal might be used in a future power distribution system control: the idea is to use a DLMP to control energy storage at the distribution level. This concept is being promoted as part of the Future Renewable Electric Energy Distribution Management (FREEDM) center (a National Science Foundation supported Engineering Research Center).

Table 3.2 Results for a distribution LMP calculated for the IEEE 34 bus system, lossy case

Bus	DLMP $/pu.h	DLMP $/kWh	Bus	DLMP $/pu.h	DLMP $/kWh
1*	36.2829	0.0726	14	37.1001	0.0742
2*	36.7765	0.0736	15	37.1002	0.0742
3*	37.1253	0.0743	16	37.4300	0.0749
4	36.2922	0.0726	17	37.4300	0.0749
5	36.2979	0.0726	18	37.1206	0.0742
6	36.4028	0.0728	19	37.1431	0.0743
7	36.5249	0.0730	20	37.1446	0.0743
8	36.6218	0.0732	21	37.1517	0.0743
9	36.6218	0.0732	22	37.1548	0.0743
10	36.6233	0.0732	23	37.1551	0.0743
11	36.6370	0.0733	24	37.1371	0.0743
12	36.6771	0.0734	25	37.1253	0.0743
13	36.7742	0.0735	26	37.1256	0.0743

* indicates generation bus

Figure 3.9 shows a ‘Generation II’ control scheme for distribution systems. Various inputs are brought to a point of calculation of the DLMP, and the DLMPs are distributed to smart loads and other distributed controls. Intelligent fault management (IFM) may be integrated into the system. The building blocks of the concept illustrated are electronic controls, phase locked loops (PLLs) and pulse width modulated (PWM) controllers. The FREEDM center relates to the electronic control of power distribution systems.

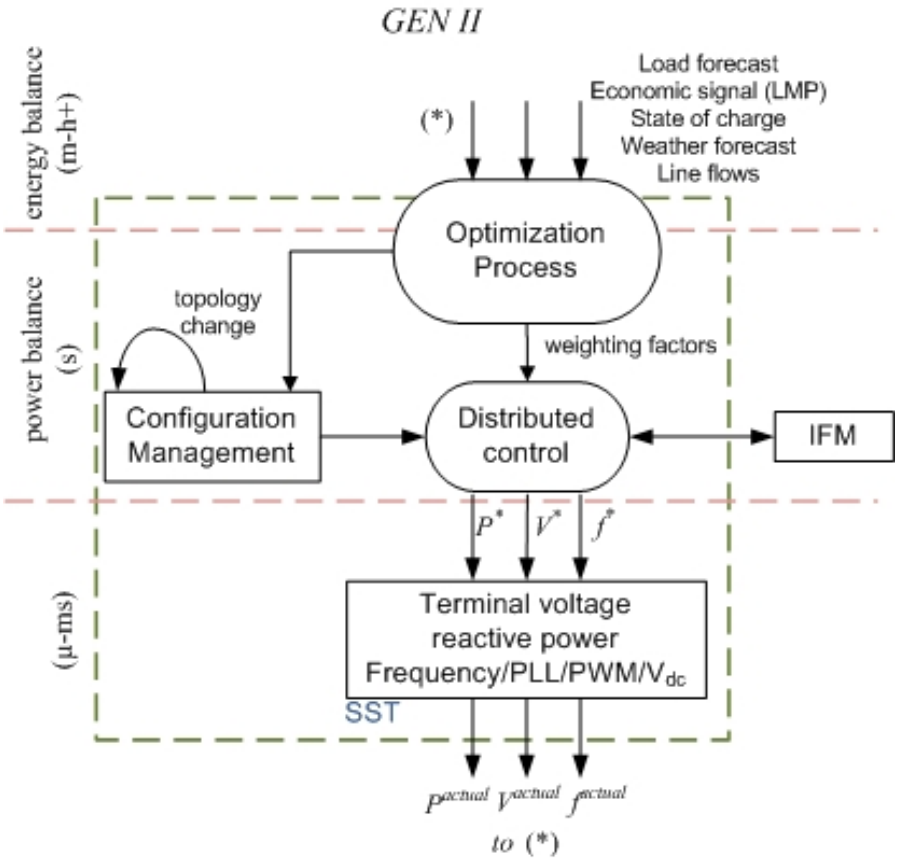

Figure 3.9 A conceptual picture of a 'Generation II" electronically controlled distribution system

3.5 Conclusions

The use of quadratic programming and the FMINCON application in common software has been demonstrated to find the DLMP within a small distributed grid. When comparing the results of the no losses case to the results found in the lossy case the effects of losses on the system can be viewed. The largest DLMP of the system is found to be about 6.45% higher than the value found in the lossless case and 9.15% higher than the lowest value of the lossy case. According to [23] the average losses within the transmission and distribution systems are about 7%. More of the losses are found in the distribution system compared to the transmission system thus the increases found in the DLMP throughout the system are in line with what would be expected in real distribution system.

Chapter 4: DLMP calculation for the lossy case using loss factors

4.1 Motivation for the use of loss factors

In Chapter 3, a technique for the calculation of DLMPs for the lossy case was presented. That method was based on the Karush Kuhn Tucker method as implemented in FMINCON, a Matlab mainline program. Because of the significant run times of FMINCON, additional ways of calculating the DLMP have been explored. One technique is to use a concept from the method of B-coefficients [24] in which optimal dispatch is done for the lossy case using loss penalty factors. The central idea is to apply a pre-calculated penalty factor to generator incremental operating costs to model losses. That is, the higher the losses produced by a generator, the higher the penalty factor, and therefore the higher the penalized incremental operating cost. In the case of DLMP calculation, instead of calculating a penalty factor that is applied to the generation incremental cost, the penalty is applied to pre-calculated DLMPs at system buses, and the penalty is intended to capture the level of system losses due to loading at the specified bus. Figure 4.1 shows the general proposed concept.

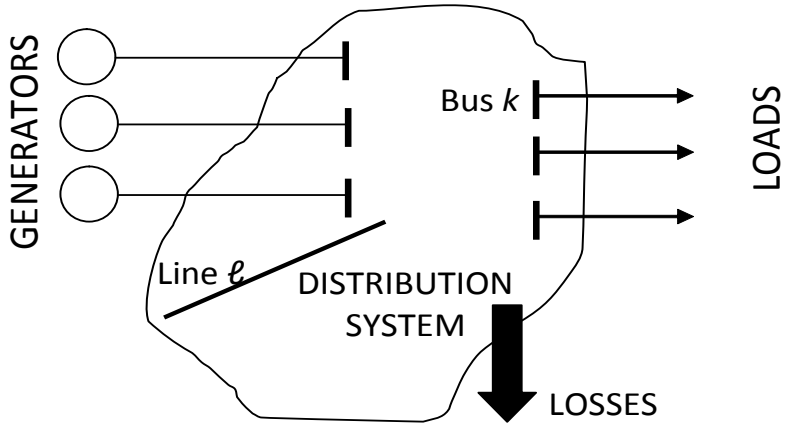

Figure 4.1 Concept of losses in a distribution system

4.2 Calculation of loss penalty factors

A way to calculate an appropriate loss factor for each bus is presented as follows:

- Run the lossless OPF using 'quadprog' as seen in Chapter 2 and calculate all the bus voltage phase angles (δ) in the distribution system.
- Calculate the total active power loss P_{loss} in the system by calculating the $I_\ell^2 R_\ell$ losses for every line.
- Calculate Y_{bus} and convert to Z_{bus} with all the generators grounded. Examine $(Z_{bus})_{kk}$ for load bus k. This is $r_{kk}+jX_{kk}$. Assume that at each load bus the contribution to the losses P_{loss} is proportional to approximately $r_{kk}(P_{kk})^2$.

- The fractional loss at each load bus *k* is,

$$P_{loss\ due\ to\ load\ k} = P_{Lk} = \frac{r_{kk}(P_k)^2}{\sum_\ell P_\ell^2 r_{\ell\ell}} P_{loss}$$

where *k* is the specific load bus for which the DLMP is sought, and ℓ refers to the system lines.

- Add P_{Lk} to the original precalculated DLMP (i.e., the precalculated DLMP using quadprog),

$$DLMP_k^{'} = DLMP_k \left(1 + \frac{P_{Lk}}{P_k}\right).$$

4.3 Application of the loss factor method to the 34 bus test bed

An example using the methods of Section 4.2 has been applied to the IEEE 34 bus system. The system diagram for the 34 bus system is reproduced in Figure 4.2. The original QP DLMP was calculated then each calculated loss factor was appropriately applied to each non-generation bus. Table 4.1 shows the common (data given) load profile. Table 4.2 taken directly from [17] shows the load at bus 17 equally distributed between buses 16 and 17. The results are shown in Table 4.1.

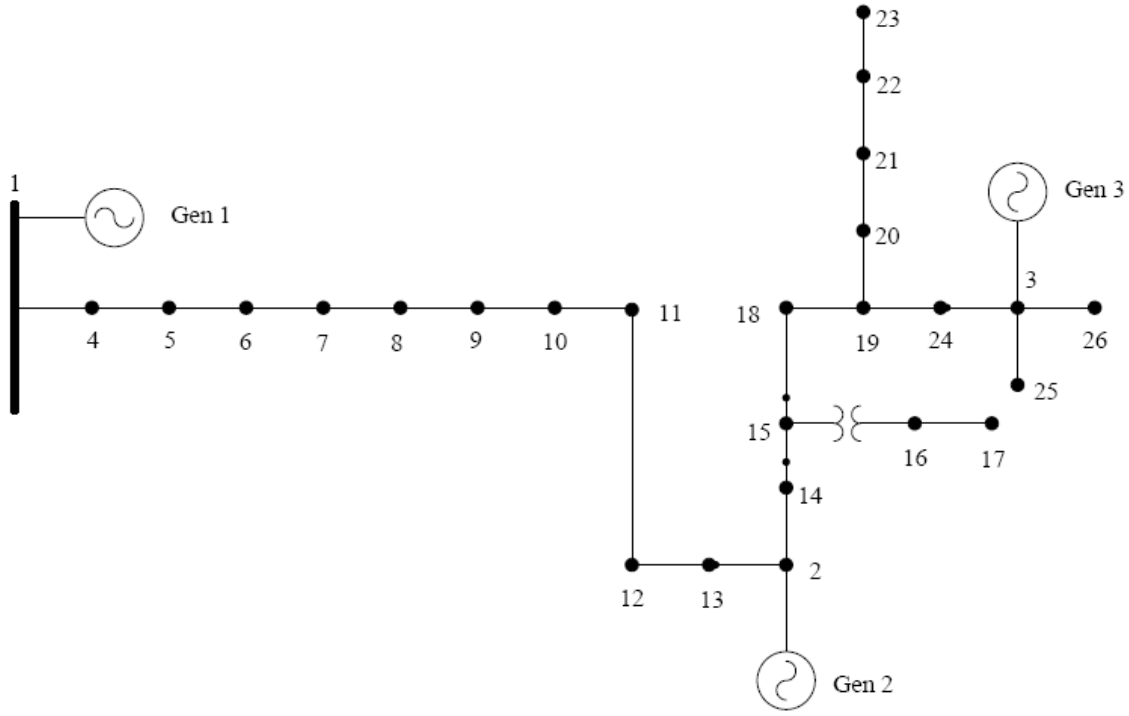

Figure 4.2 Test bed: 34 bus system

A few noticeable characteristics are displayed in the results. Most notably is that load immediately adjacent to the non-generation side of the system transformer experiences the highest increases in the DLMP. Bus 16 reflects that in Table 4.1 and in Table 4.2. The next largest contributor to a higher DLMP is load size. Buses with a large load see a much greater percent change in comparison to smaller loads. The final factor that influences the DLMP is distance from generation. While not as impactful as load size, it clearly contributes to the DLMP change.

Table 4.1 Table with loss factors applied to DLMP

Bus Number	Load (pu)	QP LMP	Loss Factor DLMP	% Change	Multiplier
4	0.1	0.0883	0.0883	0.00%	1.0000
5	0	0.0883	0.0883	0.00%	1.0000
6	0	0.0883	0.0883	0.00%	1.0000
7	0	0.0883	0.0883	0.00%	1.0000
8	0	0.0883	0.0883	0.00%	1.0000
9	0	0.0883	0.0883	0.00%	1.0000
10	0.007	0.0883	0.0883	0.00%	1.0000
11	0.01	0.0883	0.0883	0.00%	1.0000
12	0.008	0.0883	0.0883	0.00%	1.0000
13	0.03	0.0883	0.0883	0.00%	1.0000
14	0	0.0883	0.0883	0.00%	1.0000
15	0.015	0.0883	0.0883	0.00%	1.0000
16	0	0.0883	0.089	0.79%	1.0079
17	0.5	0.0883	0.0883	0.00%	1.0000
18	0.05	0.0883	0.0895	1.36%	1.0136
19	0.15	0.0883	0.0883	0.00%	1.0000
20	0.006	0.0883	0.0883	0.00%	1.0000
21	0.3	0.0883	0.0885	0.23%	1.0023
22	0.0233	0.0883	0.0884	0.11%	1.0011
23	0.06	0.0883	0.0883	0.00%	1.0000
24	0.14	0.0883	0.0883	0.00%	1.0000
25	0.08	0.0883	0.0883	0.00%	1.0000
26	0.018	0.0883	0.0886	0.34%	1.0034

Table 4.2 Table with calculated loss factors applied to DLMP and load at bus 17 distributed to buses 16 and 17

Bus Number	Load (pu)	QP LMP	Loss Factor DLMP	% Change	Multiplier
4	0.1	0.0896	0.0896	0.00%	1.0000
5	0	0.0896	0.0896	0.00%	1.0000
6	0	0.0896	0.0896	0.00%	1.0000
7	0	0.0896	0.0896	0.00%	1.0000
8	0	0.0896	0.0896	0.00%	1.0000
9	0	0.0896	0.0896	0.00%	1.0000
10	0.007	0.0896	0.0896	0.00%	1.0000
11	0.01	0.0896	0.0896	0.00%	1.0000
12	0.008	0.0896	0.0896	0.00%	1.0000
13	0.03	0.0896	0.0896	0.00%	1.0000
14	0	0.0896	0.0896	0.00%	1.0000
15	0.015	0.0896	0.0896	0.00%	1.0000
16	0.25	0.0896	0.0902	0.67%	1.0067
17	0.25	0.0896	0.0896	0.00%	1.0000
18	0.05	0.0896	0.0908	1.34%	1.0134
19	0.15	0.0896	0.0896	0.00%	1.0000
20	0.006	0.0896	0.0896	0.00%	1.0000
21	0.3	0.0896	0.0898	0.22%	1.0022
22	0.0233	0.0896	0.0897	0.11%	1.0011
23	0.1	0.0896	0.0896	0.00%	1.0000
24	0.14	0.0896	0.0896	0.00%	1.0000
25	0.08	0.0896	0.0896	0.00%	1.0000
26	0.018	0.0896	0.0897	0.11%	1.0011

4.4 Proportioning active power losses in the penalty factor loss approximation

In the optimization of generation sources as described above, a method has been proposed based on penalty factors (see Sections 4.2 and 4.3). The loss penalty factors account for the impact of losses on cost; but, as stated above, there is no inclusion in the model for the need for generation to produce power to balance and accommodate active power losses.

At this point, the concept is to attribute losses to each system generator based on the "distance" from each generator. For this purpose, consider a general distribution system as shown in Figure 4.3. In this figure, three generation sources are depicted. Regions I, II, and III are established based on the electrical distance (i.e., point to point impedance) from a load bus to a generator. Thus the load at bus L in Figure 4.3 is evaluated to determine whether the point to point impedance L – N, L to T, or L to U is smallest. Then L is taken to be in the region associated with the smallest impedance. In Figure 4.3, this is shown as bus L in region I. This procedure is repeated for all the load buses. The result is exemplified by Figure 4.3.

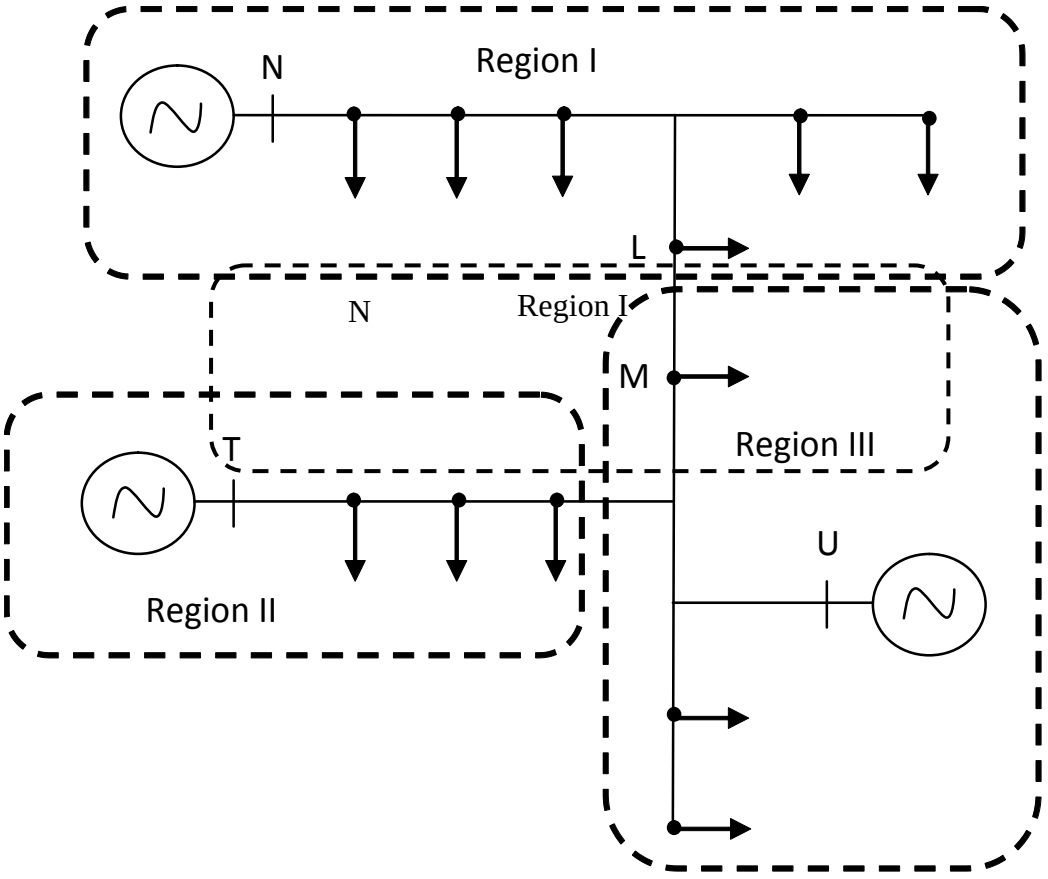

Figure 4.3 General distribution system

The foregoing procedure is applied to the IEEE 34 bus system shown in Figure 4.2. The result is shown in Figure 4.4. Generator #1 lies in region I which contains buses 4-8;

generator #2 lies in region II which contains buses 9-17; and generator #3 lies in region #3 which contains buses 18-26.

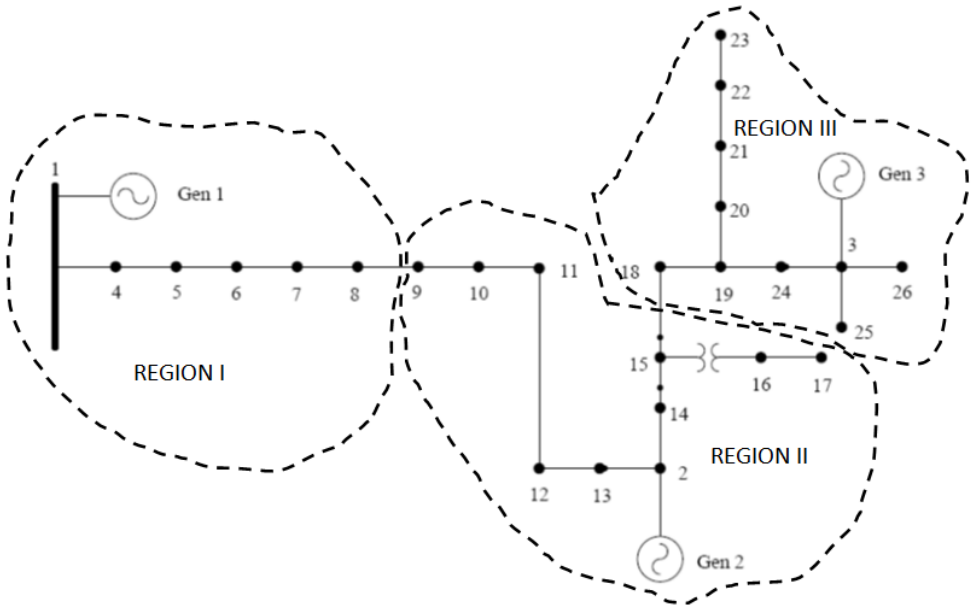

Figure 4.4 The IEEE 34 bus test bed with regions I, II, and III superimposed, used to identify attribute losses to generation.

In order to apportion losses among the several generators, the total load inside each identified region is divided the total load of the entire system. The resulting percentage is used to proportion the losses to each region. The proportioned loss is added to the generation in that region. The basic concept is written for the generalized case as,

$$P_{attributed\ to\ generator\ k} = \frac{Total\ load\ in\ region\ k}{Total\ system\ load} * [Total\ system\ active\ power\ losses].$$

The loss apportioning method is applied to the 34 bus test bed and results are shown in Table 4.3.

Table 4.3 Example of proportioning losses for the IEEE 34 bus test bed

Region	No loss generation level (kW)	Buses	Load (kW)	% of total load	Load added to generation* (kW)	New generator setting (kW)
1	0.543	4-8	0.1	6.68%	0.001108662	0.54411
2	0.4671	9-17	0.57	38.07%	0.006319375	0.47342
3	0.4893	18-26	0.8273	55.25%	0.009171963	0.49847

* The total loss found by this method is 0.0166 kW.

The loss apportioning method shown here has the following disadvantages and weaknesses:

- Reactive power is not modeled
- The load flow equations are not modeled.

The advantages of the approach are:

- The method is simple and completely repeatable
- The calculation is fast – even for large distribution systems.

Of course, the salient question relates to the accuracy of the apportioning method. This is discussed using the 34 bus test bed as an example below.

4.5 Optimal dispatch using PowerWorld

In PowerWorld, optimal power flow studies (OPFs) are solved using a linear programming (LP) approximation. In the standard mode, 'Simulator' solves the power flow equations using a Newton-Raphson power flow study algorithm. With the optimal power flow enhancement (an 'add on'), 'Simulator OPF' in PowerWorld can also solve many of the system control equations using an Optimal Power Flow algorithm. Specifically, Simulator OPF uses a linear programming OPF implementation. In the Simulator OPF, the LP OPF determines the optimal solution by iterating between a solved case that was obtained using a standard power flow algorithm, and then solving a linear programming problem to change the system controls. The latter is done to remove any limit violations [25]. The results of the base case using PowerWorld can be seen in Figure 4.3 and the load data in Table 4.4. The PowerWorld solution clearly displays the generation in MW at P1, P2 and P3 as well as the marginal cost in $/MWh. The loads are very small so they are depicted as zeros on a MW scale in Figure 4.3.

4.6 Comparison of results of the several methods

The results from each method used to calculate the DLMP and the operating costs are shown in Tables 4.5-4.8 and graphically in Figures 4.6-4.8. Table 4.5 shows the linear and quadratic costs of each trial. Each trial has a different set of cost functions. Trial A uses an original set of cost functions used throughout the project. Trial B uses a set of cost functions that are very similar and trial C uses a set with constant linear terms but varying quadratic terms. The first calculation method, namely 'QuadProg no loss', shows the results from a purely quadratic programming calculation only. There are no losses calculated in the system. The second method, labeled as 'FMINCON', uses the loss approximation method via the FMINCON function in Matlab. This method has been detailed in Sections 2.3 and 3.2.2, and in Appendix A. The third method, 'QP with loss approximation', uses the loss

approximation method detailed in Sections 4.1 and 4.4. The final column shows the results calculated using PowerWorld.

Table 4.4 System load data (modified IEEE 34 bus test bed)

Bus Number	Load (pu)	Bus Number	Load (pu)
4	0.1	16	0.25
5	0	17	0.25
6	0	18	0.05
7	0	19	0.15
8	0	20	0.006
9	0	21	0.3
10	0.007	22	0.0233
11	0.01	23	0.06
12	0.008	24	0.14
13	0.03	25	0.08
14	0	26	0.018
15	0.015		

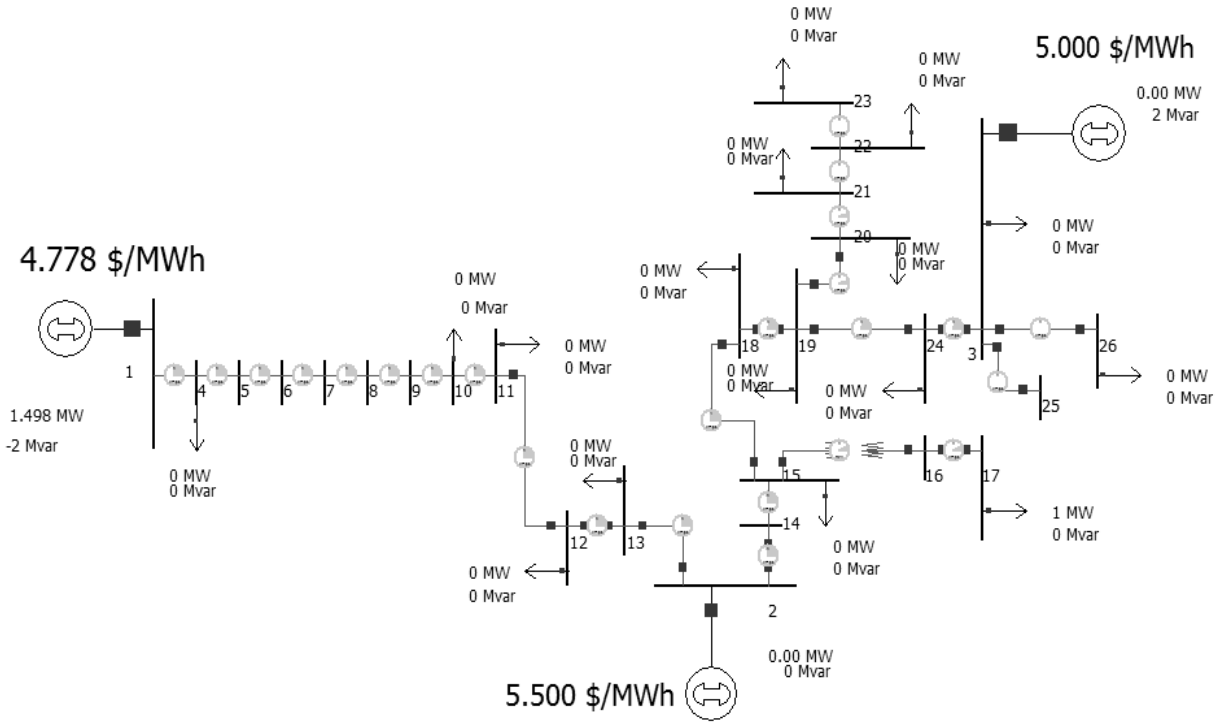

Figure 4.5 PowerWorld results (34 bus test bed)

The marginal costs indicated at buses 1, 2, and 3 are the marginal costs at the operating point indicated in Table 4.4.

Table 4.5 The coefficients of a quadratic cost function for three different test trials

Cost coefficients of each trial ($/h)					
Trial A		Trial B		Trial C	
Linear*	Quadratic*	Linear*	Quadratic*	Linear*	Quadratic*
3.75	9.38	3.75	9.40	3.75	9.38
4.50	9.30	3.76	9.30	3.75	9.30
4.00	9.90	3.74	9.50	3.75	9.90

*Linear terms are multiplied by ($*10^{-3}$) and quadratic terms are multiplied by ($*10^{-6}$)

Table 4.6 Trial A – Original test case

Calculation Methods				
Solution	QuadProg no loss	FMINCON	QP with loss approximation‡	PowerWorld
P1 (kW)	0.543	0.5283	0.54411	1.498
P2 (kW)	0.4671	0.4689	0.47342	0
P3 (kW)	0.4893	0.5022	0.49847	0
Linear cost term**	0.06095	0.06100	0.06165	0.05618
Quadratic cost term**	0.00014	0.00014	0.00014	0.00014
Total calculated cost***	0.0611	0.0611	0.06179	0.0563

*The total cost is the linear cost term plus the quadratic cost term
** In arbitrary cut consistent units, may be interpreted as $/h
‡Losses served by generation as described in Section 4.4

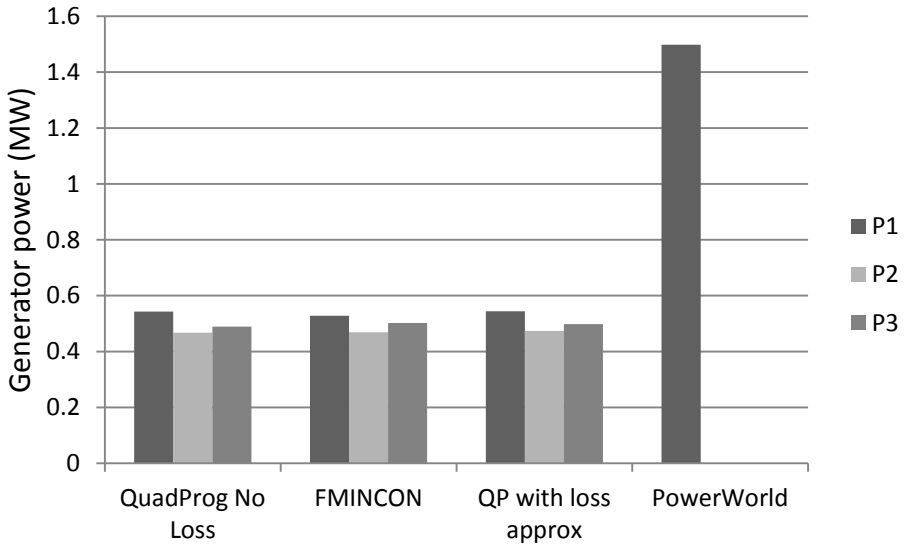

Figure 4.6 Graphical representation of trial A

Table 4.7 Trial B using similar cost functions

Calculation Methods				
Solution	QuadProg no loss	FMINCON	QP with loss approximation‡	PowerWorld
P1 (kW)	0.4997	0.5283	0.50081	1.498
P2 (kW)	0.504	0.4689	0.51032	0
P3 (kW)	0.4955	0.5022	0.50467	0
Linear cost term**	0.05622	0.05622	0.05684	0.05618
Quadratic cost term**	0.00014	0.00014	0.00014	0.00014
Total calculated cost***	0.0564	0.0564	0.05699	0.0563

*The total cost is the linear cost term plus the quadratic cost term
** In arbitrary cut consistent units, may be interpreted as $/h
‡Losses served by generation as described in Section 4.4

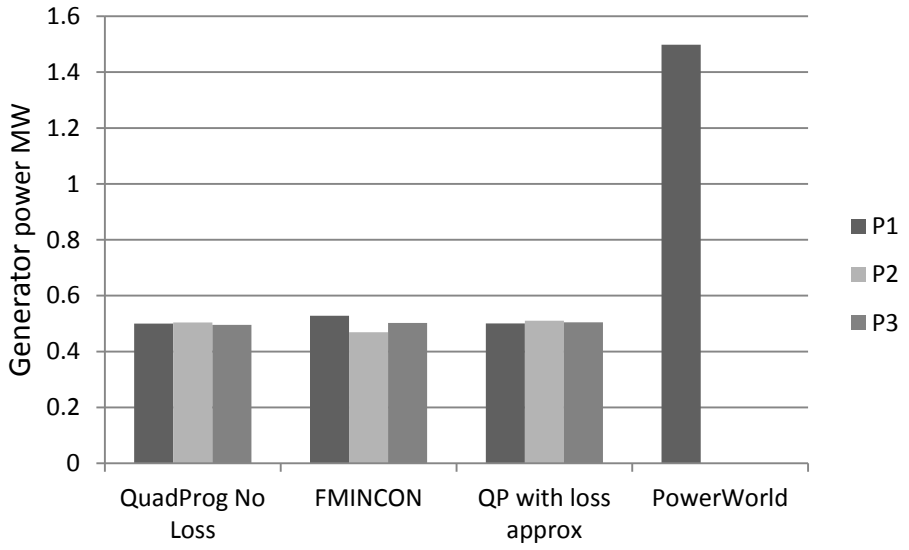

Figure 4.7 Graphical representation of trial B

Table 4.8 Trial C – test using constant linear term

Calculation Methods				
Value	QuadProg no loss	FMINCON	QP with loss approximation‡	PowerWorld
P1 (kW)	0.5072	0.4939	0.50831	0.489
P2 (kW)	0.5116	0.5128	0.51792	0.509
P3 (kW)	0.4806	0.4926	0.48977	0.48
Linear cost term**	0.05623	0.05622	0.05685	0.05543
Quadratic cost term**	0.00014	0.00014	0.00014	0.00014
Total calculated cost***	0.0564	0.0564	0.05699	0.0556

*The total cost is the linear cost term plus the quadratic cost term
** In arbitrary cut consistent units, may be interpreted as $/h
‡Losses served by generation as described in Section 4.4

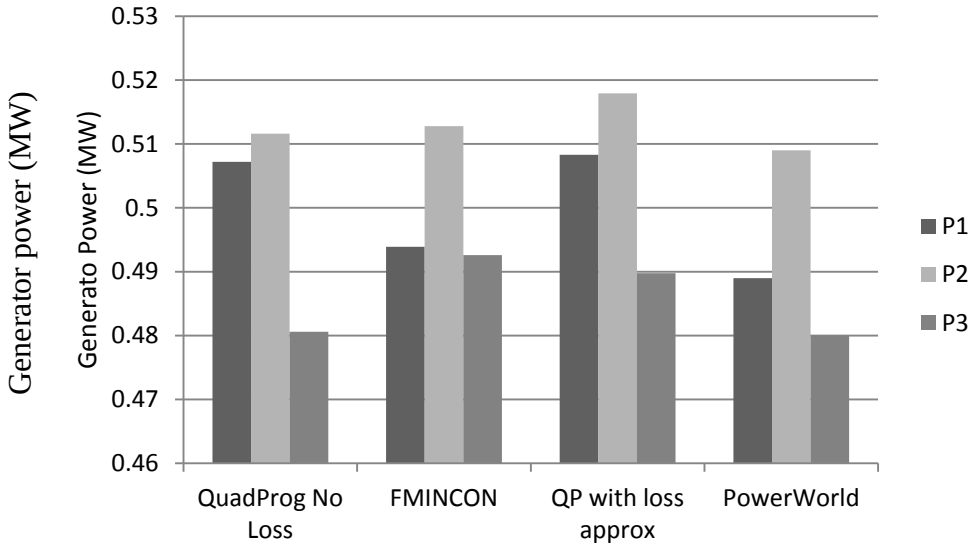

Figure 4.8 Graphical representation of trial C

The results from each trial show that the linear component of the cost function plays a large role in determining the dispatch. Table 4.9 shows a comparison of the assumed characteristics of each solution method. The variance in each method is likely due to the solution method each one takes. Not surprisingly the 'FMINCON' and the 'QP with loss approximation' are higher than the no loss QP method. Since these are just extensions to include losses of the QP method the results are reasonable. One potential reason for the difference between the three new proposed methods and PowerWorld is that PowerWorld solves the system by changing the quadratic costs into a piece-wise linear programming problem. This is less exact and could be the cause for the slightly lower total costs. There are also likely differences in how MATLAB and PowerWorld solve iteratively. Tables 4.10 and 4.11 show the percent difference in the results compared to PowerWorld regarding total load and total cost. Some other possible reasons for the variance in total load and total cost are:

- PW was created for large scale systems; does better with transmission system, megawatts not kilowatts
- In PW, DLMP (seen as bus marginal cost) is constant throughout system, while the other methods solve for the DLMP individually
- The three new proposed methods don't take into account reactive power.

Table 4.9 A comparison of assumed characteristics of solution methods for the calculation of DLMPs

Method used	Models losses	Iterative	PQ and PV buses modeled	Linearize cost function	Load flow equations modeled	Quadratic cost function mod-eled
QuadProg no loss	N	Y	N	N	N	Y
FMINCON	Y	Y	N	N	N	Y
QuadProg with losses	Y	Y	N	N	N	Y
PowerWorld	Y	Y	Y	Y*	Y	N*

*Piecewise linear representation of the cost function is used
N = NO Y = YES

Table 4.10 Percent difference from PowerWorld results regarding total load

Trial	QuadProg no loss	FMINCON	QP with loss approximation‡
A	0.09%	0.09%	1.20%
B	0.08%	0.09%	1.19%
C	1.45%	1.44%	2.57%

Table 4.11 Percent difference from PowerWorld results regarding total cost

Trial	QuadProg no loss	FMINCON	QP with loss approximation‡
A	8.53%	8.53%	9.75%
B	0.18%	0.09%	1.19%
C	1.44%	1.44%	2.50%

In each trial, the total load difference was less than 2.57% as obtained found from PowerWorld. The proposed new systems were not as close to the results of PowerWorld when it came to total cost. When each cost had a similar or exactly the same linear cost as in trials B and C, the total cost was not much different varying as much as only 2.5%. However, in trial A where the linear cost of the system was much more diverse, the total cost of the system was approximately 9% higher than the PowerWorld cost.

Chapter 5: Energy management

5.1 Introduction

The previous chapter displayed the application and calculation of a distribution based locational marginal price. In this chapter, further applications involving energy management within the IEEE 34 bus test bed will be demonstrated. In most applications, energy management will primarily be based on the DLMP, that is, it will adjust based on original DLMP values. Different examples below will show how different factors affect the energy management.

Before going through the examples on how an energy management system (EMS) coinciding with a DLMP can be used, the possible applications for a realistic EMS should be discussed.

5.2 Example 1: the role of DLMP set points

Depending on the system parameters (e.g., costs, load values, line ratings) the DLMP will vary from load to load. The energy management system created looks at the initial values of the DLMP and applies energy management system 'multipliers'. In the real world this would be either load reduction or an increasing of the load with some sort of storage. Assuming there is some desired range of DLMP value, convergence to this value can vary depending location of the DLMP set points set up within the system. Figure 5.1 depicts a visualization of the ranges for a DLMP. Each range would have an associated multiplier. The EMS would view the previous DLMP data and apply the appropriate multiplier. The range where the multiplier is one or no change is the desired range of DLMP for the system to be in.

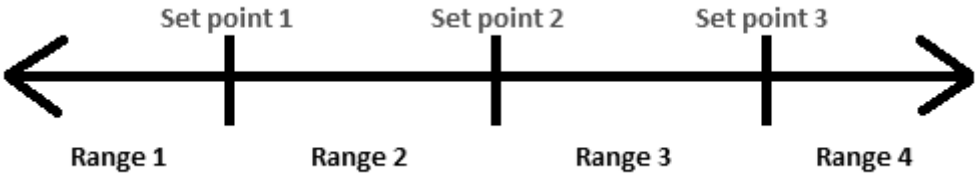

Figure 5.1. Visualization of different DLMP multiplier ranges.

Adjusting the location of the set points can have varying effects on the speed of the convergence of the DLMP. In Figure 5.2 the system converges to the desired range after 4 units of time. Figure 5.3 is the result of reducing the size of the desired range of DLMP. In this scenario it takes the system much longer than 10 units of time and does not even show signs of convergence at all. It is clear the placement on the DLMP set points can have a significant impact on the speed and completion towards convergence of a desired DLMP.

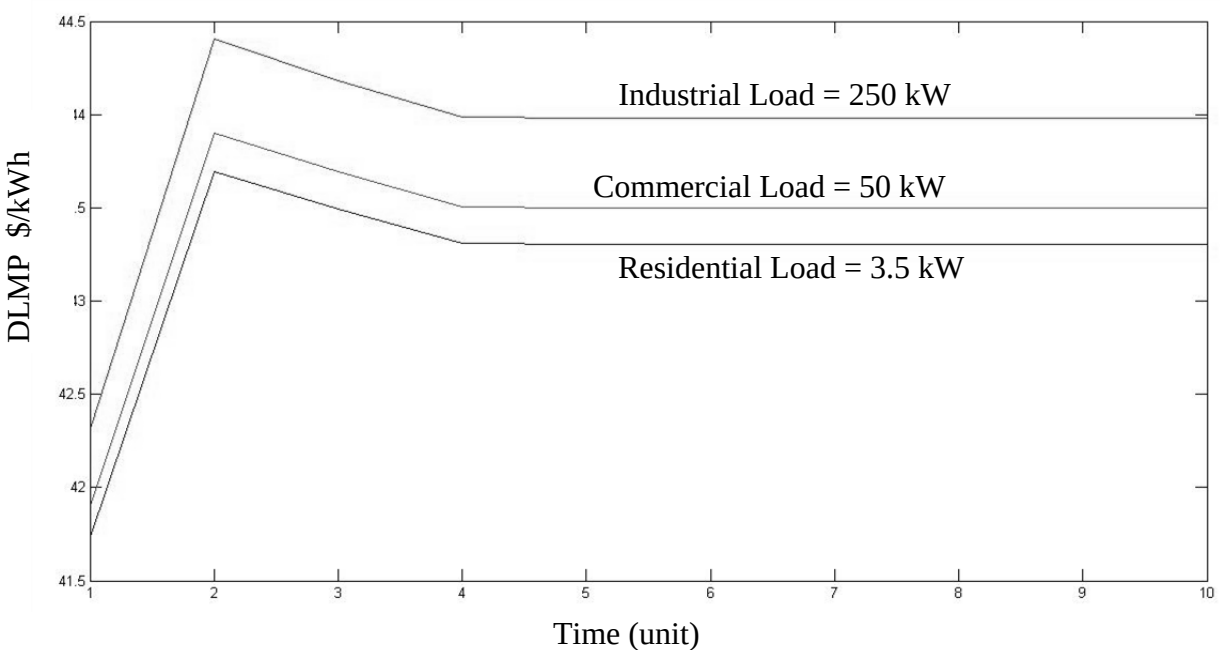

Figure 5.2 Faster DLMP convergence with a wider desired range

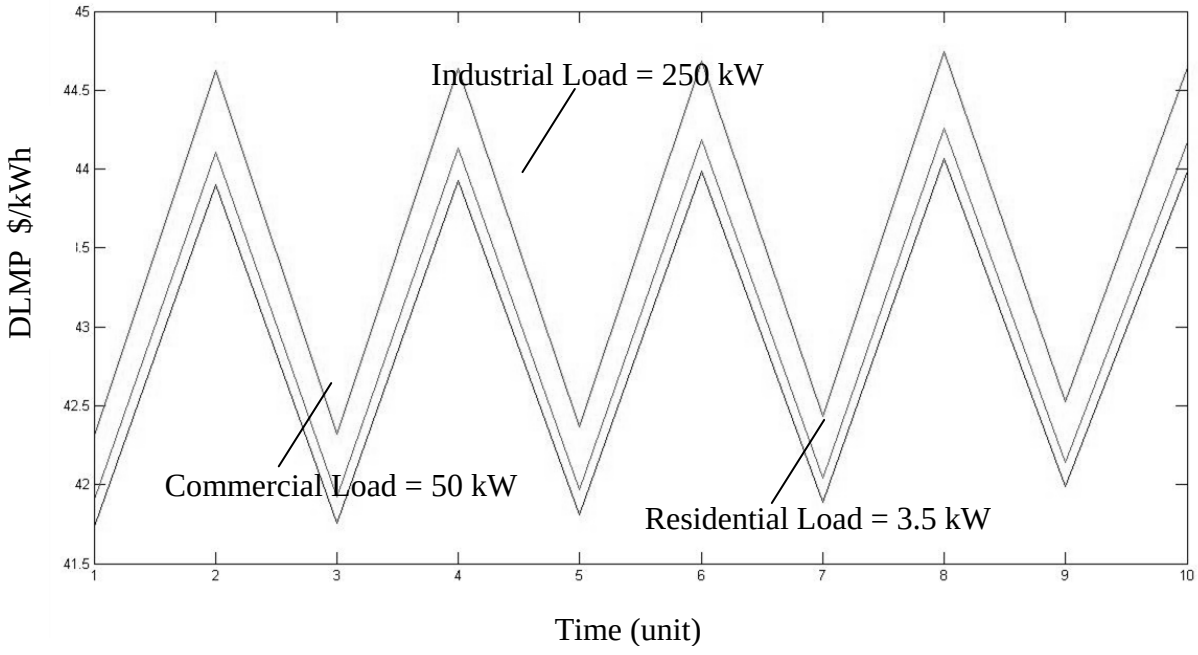

Figure 5.3 No DLMP convergence with a reduced desired range

5.3 Example 2: the role of energy management systems 'multipliers'

As said previously the 'multipliers' of the system would act as either load increase such as implementing storage or a load shedding. The severity of the load increase can drastically change the DLMP. Two different runs were performed. The first, "run A" had a large variance in load manipulation. As much as 50% of the load could be shed based on what range the DLMP fell in. The second trial, "run B", had far less variance. A maximum of 10% could be reduced at one time. The multipliers of each range are located in Table 5.1 and the results are in Figures 5.3 and 5.4.

Table 5.1 Range multipliers for each run*

Name	Range 1 multiplier	Range 2 multiplier	Range 3 multiplier	Range 4 multiplier
Run A	0.5	0.75	1	1.25
Run B	0.9	0.95	1	1.05

*The range multipliers are the factors that are applied to each load

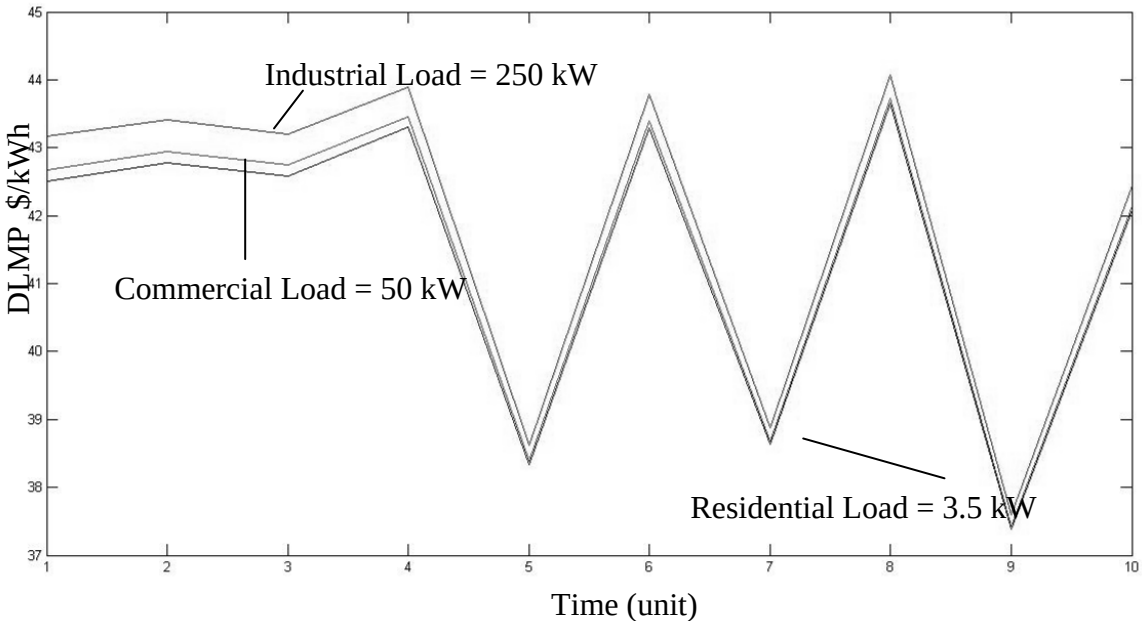

Figure 5.4 DLMPs with large variance in 'multipliers' namely the multipliers used in Trial A

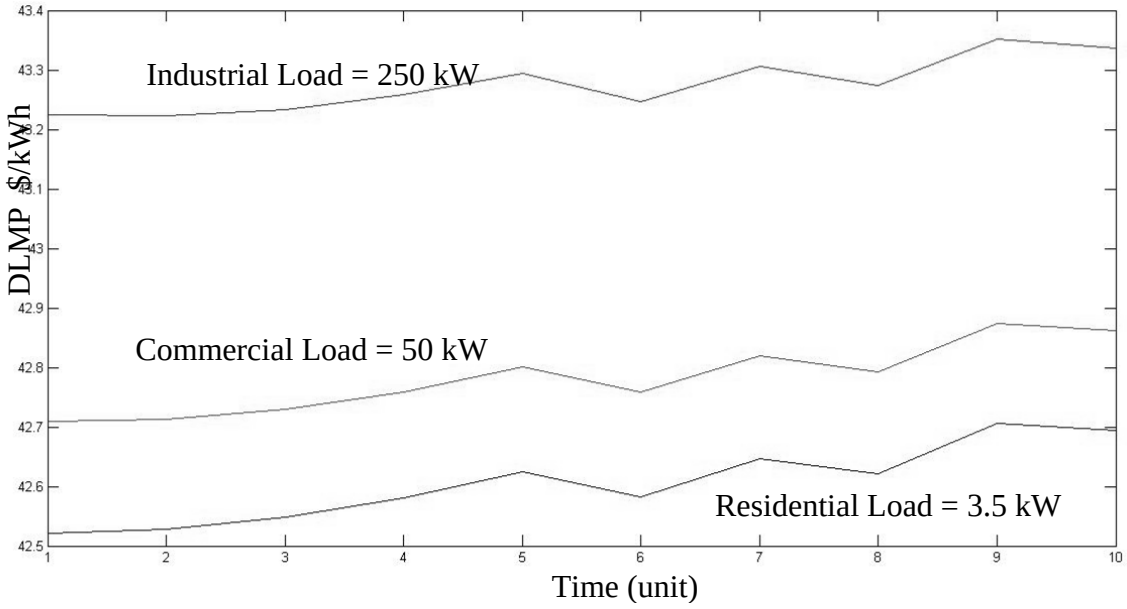

Figure 5.5 DLMPs with small variance in 'multipliers', namely the multipliers used are for Trial B

The figures show how much this can affect the DLMP. In the case of having large multipliers the industrial load DLMP varied from 44 to 38. However, in the run with smaller multipliers, the industrial load varied from less than 43.4 and greater than 43.2.

5.4 Example 4: load control using DLMP with a single load

In Sections 5.2 and 5.3 each bus of the system was increased or decreased based on its own DLMP. Conversely, this section looks into how individual DLMPs change based a single load having an energy management system based on the DLMP. Buses 2, 8 and 26 of Figure 4.2 are controlled in the system in three different trials and their load values and load type are seen in Table 5.2. The results of each run are shown in Figures 5.6 and 5.7.

Table 5.2 Controlled load data

Bus Number	Load Value	Load Type
2	50 kW	Commercial
8	3.5 kW	Residential
26	250 kW	Industrial

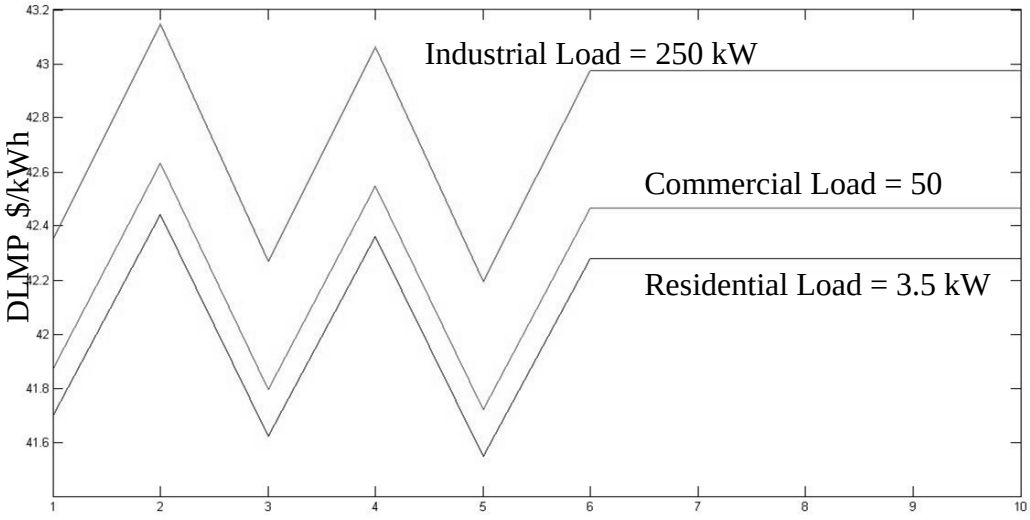

Figure 5.6 Single industrial load (bus 26) altering load based on DLMP

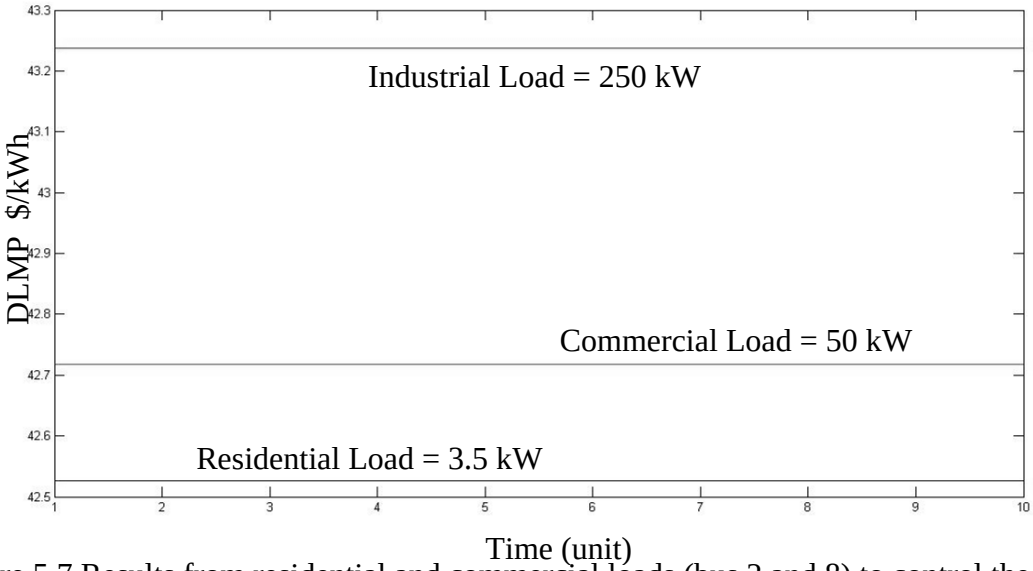

Figure 5.7 Results from residential and commercial loads (bus 2 and 8) to control the load, using load data in Table 5.2

When the industrial load is changed the system sees a variant DLMP. This is likely due to the larger percentage of total load this bus has compared to the others. However when in the case of the industrial and residential loads, the change is insignificant to the DLMP as it remains constant. This of course is also dependent on the settings of the 'set point' as discussed in Section 5.2.

5.5 Conclusions

A few approaches to the use of the DLMP as a pricing based method for energy management have been discussed in this chapter. The underlying concept is that a single home, neighborhood or entire distribution network could use DLMP signals to control loads. The user could identify which loads are controllable and what strategy might be employed to control load based on price. This could be done either from the utility perspective or the homeowner depending on the deployment of certain technologies. Many contemporary smart meters are able to give present load values immediately, which is the primary real time data needed to calculate the DLMP. It is likely that only a few selective loads have the ability to be controlled. Any load with this type of control would require technologies such as Wi-Fi integrated appliances to control the load. As an example, ZigBee technology has been used for energy management [28, 29]. Deployment of energy management using DLMP to save money would likely be customer driven rather than utility driven.

An additional application relates to the use of the DLMP as a signal that can be used to identify heavily used assets in the distribution system. The potential utility company application would be that the DLMP is used to identify which distribution assets need to be enhanced.

The effects of DLMP set points in the controller and the ‘multiplier’ (in the form of load shedding and storage) have also been discussed in this section. The set points in the controller determine the time response of the load. The ‘multipliers’ discussed in this chapter also have a significant impact on the time response of the energy management system.

Chapter 6: Conclusions, recommendations, and future work

6.1 Conclusions

The main and secondary conclusions of this research are outlined in Tables 6.1 and 6.2. The tables include conclusions and application areas. The selected application areas are 'Calculation Methods', 'DLMP applications', 'DLMP results' and 'Energy Management'.

Table 6.1 Main conclusions of this research

Description	*Application Area*
The application of present techniques for the calculation of transmission LMPs in distribution systems can be transported to distribution engineering.	DLMP applications
Quadratic programming is effective in finding the minimal operating cost (quadratic expressions for fuel costs assumed).	Calculation methods
FMINCON can be used for the indicated optimization and results compare favorably with PowerWorld.	DLMP results
Modeling active power losses using loss factors gives results that are close to PowerWorld results.	DLMP results
The use of DLMPs as a fundamental control signal for energy management could be effective.	Energy management
Distributed generation will have significant effects on the DLMP.	DLMP applications

Table 6.2 Secondary conclusions of this research

Description	*Application Area*
Calculation time to obtain the DLMP is faster using the described method with loss factors – as compared to the use of FMINCON.	Calculation methods
Costs increase in moving from source to load in a radial distribution system.	DLMP applications
The use of FMINCON and the use of the method of loss factors for the calculation of DLMPs give results that do not agree well with PowerWorld (e.g., approximately 9% discrepancies). The discrepancy appears to exacerbate when the generation operating cost functions differ widely.	DLMP results
The DLMP is an indicator for assets (e.g., lines and transformers) needing improvement in the distribution system	DLMP applications

6.2 Recommendations and future considerations

Table 6.3 contains topical areas for future work. Issues and recommendations are presented in the table. Not considered in this report is the role of a DLMP type 'signal' with regard to compensating a customer or an independent power producer (IPP) for generating power. Also not considered is the cost of compensation to an IPP for moving power in a portion of the distribution system under that IPP's control. These are important practical questions that should be considered in future work.

Table 6.3 Issues and recommendations for future work

Recommendations and Future Explorations	
Issue	Recommendation
DLMP should be applied to networked distribution systems	Explore test systems with a mesh configuration; note differences in cost and still include distributed generation. Could be usefully applied to new construction neighborhoods with smart meters that have implemented distributed generation and possibly storage.
Determining the best location for distributed generation	Develop software to identify optimal location of distributed generation; compare total cost and individual DLMP at each bus to determine optimal locations for the generation.
Consider time varying LMPs in the transmission system	Consider having system adapt to changing transmission LMP as well as time varying distributed generation.
Public acceptability of paying for electricity based on home location	Conduct market research to determine homeowner opinion of subject. Consider developing incentive programs if DLMP is found to be helpful in lowering utility total cost.
Methods have only been applied to 34 bus system	Apply to larger distribution network. Look at percent change in total cost and total load compared to PowerWorld as before. Note change in percentage differences based on each scenario.
Consider energy storage.	Model energy storage.
Utilization of more complex generation cost 'curves' (e.g., tabular costs)	Use of alternative optimization methods.

References

[1] Mandhir Sahni, Richard Jones, Yunzhi Cheng, "Beyond the crystal ball: locational marginal price forecasting and predictive operations in U.S. power markets," *IEEE Power & Energy Magazine,* July/August 2012, pp. 35-42.

[2] Bharadwaj R. Sathyanarayana, G. T. Heydt, "A roadmap for distribution energy management via multiobjective optimization," *Proc. IEEE Power and Energy Society General Meeting*, Minneapolis MN, July 25 – 29, 2010, Paper #2010GM0655.

[3] R. F. Arritt, R. C. Dugan, "Distribution system analysis and the future smart grid," IEEE Transactions on Industry Applications, v. 47, No. 6, December 2011, pp. 2343 – 2350.

[4] A. H. Noureddine, A. T. Alouani, A. Chandrasekaran, "An optimal control strategy for power distribution system operation," Proc. 22nd North American Power Symposium, October 1990, pp. 327 – 335.

[5] D. P. Tuttle, R. Baldick, "The evolution of plug-in electric vehicle – grid interactions," IEEE Transactions on Smart Grid, v. 3, No. 1, pp. 500 – 505.

[6] Western Area Power Administration Rocky Mountain Region, "Locational marginal pricing overview," available at:
www.wapa.gov/rm/LMP%20Overview%20v%2010-30-02.ppt

[7] E. Litvinov, "Design and operation of the locational marginal prices-based electricity markets," *IET Gener. Transm. Distrib.,* 2010, Vol. 4, Iss. 2, pp. 315–323.

[8] New England Independent System Operator, "Locational marginal pricing (LMP) frequently asked questions," accessed at:
http://www.iso-ne.com/support/faq/lmp/index.html

[9] B. Asare-Bediako, W. L. Kling, P. F. Ribeiro, "Home energy management systems: Evolution, trends and frameworks," *47th International Universities Power Engineering Conference (UPEC),* , pp. 1-5, 4-7, Sept. 2012.

[10] Schneider Electric, "Wiser home energy management system", available at:
http://products.schneider-electric.us/products-services/products/energy-management-systems/residential-energy-management-system/wiser-home-energy-management-system1/wiser-home-energy-management-system/

[11] Jinsung Byun; Insung Hong; Sehyun Park; , "Intelligent cloud home energy management system using household appliance priority based scheduling based on prediction of

renewable energy capability," *IEEE Transactions on Consumer Electronics,* vol. 58, no. 4, pp. 1194-1201, November 2012.

[12] P. A. Jensen, J. F. Bard, "Nonlinear programming methods S2 quadratic programming," Operations Research Models and Methods, University of Texas at Austin.

[13] J. N. Nocedal, S. J. Wright, Numerical Optimization, Springer, Series in Operations Research, 1999.

[14] Mathworks, "Constrained nonlinear optimization problems," available at:
www.mathworks.com/help/toolbox/optim/ug/brnoxzl.html

[15] Ilan Kroo, Joaquim Martins, "Optimization and MDO: Taxonomy and Examples" Ch. 4, SQP Methods, Research Consortium for Multidisciplinary System Design, Stanford – MIT Design Consortium, available at:
http://acdl.mit.edu/mdo/mdo_06/

[16] Miao Fan, "Probabilistic power flow studies to examine the influence of photovoltaic generation on transmission system reliability," Ph.D. Comprehensive Report, Arizona State University, Department of Electrical, Computer, and Energy Engineering, Tempe AZ, April, 2012.

[17] IEEE Power and Energy Society, "IEEE 34 node test feeder," 2004, [Online]. Available:
http://ewh.ieee.org/soc/pes/dsacom/testfeeders/index.html

[18] S. S. S. R. Depuru; Lingfeng Wang; Devabhaktuni, V.; Gudi, N.; "Smart meters for power grid — challenges, issues, advantages and status," IEEE PES *Power Systems Conference and Exposition (PSCE),* pp. 1-7, 20-23 March 2011.

[19] Hui Hou, Jianzhong Zhou, Yongchuan Zhang, Xiongkai He, "A brief analysis on differences of risk assessment between smart grid and traditional power grid," *Fourth International Symposium on Knowledge Acquisition and Modeling (KAM),* pp. 188-191, 8-9 Oct. 2011.

[20] P. P. Varaiya, F. F. Wu, J. W. Bialek, "Smart operation of smart grid: risk-limiting dispatch," *Proceedings of the IEEE,* vol. 99, no. 1, pp. 40-57, Jan. 2011.

[21] P. Samadi, H. Mohsenian-Rad, R. Schober, V. W. S. Wong, "Advanced demand side management for the future smart grid using mechanism design," *IEEE Transactions on Smart Grid* , vol. 3, no. 3, pp. 1170-1180, Sept. 2012.

[22] G. Heydt, "The next generation of power distribution systems," *IEEE Transactions on Smart Grid*, v. 1, No. 3, December, 2010, pp. 225 – 235.

[23] U.S. Energy Information Administration, “Frequently asked questions” [Online]. Available:
http://www.eia.gov/tools/faqs/faq.cfm?id=105&t=3

[24] O. Elgerd, “Electric energy systems theory: an introduction”, McGraw Hill Book Publishers, New York, 1983.

[25] PowerWorld system help command. Search query ‘Optimal Power Flow’

[26] Mathworks system help. Matlab search query ‘FMINCON’

[27] N. Steffan, G. T. Heydt, "Quadratic programming and related techniques for the calculation of locational marginal prices in distribution systems," *Proc. North American Power Symposium,* pp. 1-6, 9-11 Sept. 2012.

[28] Danping Ren; Hui Li; Yuefeng Ji, "Home energy management system for the residential load control based on the price prediction," *IEEE Online Conference on Green Communications (GreenCom),* pp. 1-6, 26-29 Sept. 2011

[29] Dae-Man Han; Jae-Hyun Lim, "Smart home energy management system using IEEE 802.15.4 and zigbee," *IEEE Transactions on Consumer Electronics*, vol. 56, no. 3, pp. 1403-1410, Aug. 2010

[30] R. H. Byrd, J. C. Gilbert, J. Nocedal, "A trust region method based on interior point techniques for nonlinear programming," *Mathematical Programming*, Vol. 89, No. 1, pp. 149–185, 2000.

[31] Electric Power Research Institute online database.

[32] T. Orfanogianni, G. Gross, “A general formulation for LMP evaluation,” *IEEE Transactions on Power Systems*, v. 22, No. 3, pp. 1163 – 1173, 2007.

Appendix A: The utilization and performance of Matlab function FMINCON

A.1 Function FMINCON: a brief description

The Matlab function FMINCON is an optimization routine based on the 'interior point' method [30]. As stated in the Matlab 'help' command, the function "FMINCON attempts to find a constrained minimum of a scalar function of several variables starting at an initial estimate. This is generally referred to as constrained nonlinear optimization or nonlinear programming."

A.2 Function FMINCON and its implementation in Matlab

Matlab function FMINCON is an automated optimization tool. Function FMINCON finds a constrained minimum of a nonlinear multivariable function of several variables. It attempts to minimize the function subject to linear and non-linear equality and inequality constraints. FMINCON uses Sequential Quadratic Programming (SQP) which is a variant of the Kuhn-Tucker approach. The basis of SQP is to model the minimization problem at x_k by a quadratic sub-problem and to use the solution to find a new point x_{k+1} -- this is a search. FMINCON has options for four different algorithms to solve the equation. They are '*sqp*', '*active-set*', '*interior-point*' and '*trust region reflective*'. Figure A.1 shows the pseudocode for a quadratic programming problem.

The call for FMINCON is set up in the following:

X = FMINCON(FUN,X0,A,B,Aeq,Beq,LB,UB)

FMINCON starts at an initial point *X0* and finds a minimum *X* to the function FUN. The function is subject to the linear inequalities $A*X \leq B$ and linear equalities $Aeq*X = Beq$. The function FUN accepts input *X* and returns a scalar function value *F* evaluated at X. Initial value *X0* may be a scalar, vector, or matrix. LB and UB are a set of lower and upper bounds on the variables, *X*, so that a solution is found in the range $LB \leq X \leq UB$ [26].

$$\min_x f(x) \text{ such that } \begin{cases} c(x) \leq 0 \\ ceq(x) = 0 \\ A \cdot x \leq b \\ Aeq \cdot x = beq \\ lb \leq x \leq ub, \end{cases}$$

PSEUDOCODE

Figure A.1 A quadratic programming pseudocode taken from Matlab [27]

A.3 Execution time of FMINCON

The run time of FMINCON has been found to be long and variant based on the optimization set and starting point x0 used by the program. Investigation into different parameters of the 'optimset' and starting point (x0) of FMINCON was done to find the performance of the software. The approach taken is purely experimental. Consider two different test beds,

$$f_1 = (x_1 - 1)^2 + (x_2 - 12 + \cdots + (x_{50} - 50)^2 \tag{A.1}$$

$$f_2 = \sum_{i=1}^{50} (x_i - i)^2. \tag{A.2}$$

In order to investigate the performance of FMINCON, parameters x0 and 'optimset' are varied. Considering (A.1) first, varying the starting point x0, three possible variations are studied and listed below. The equations (A.3) – (A.5) define the X) value for three tests. For convenience, the tests shall be denominated as run A.3, A.4, and A.5 respectively. The three cases studied are:

$$X0 = \begin{pmatrix} 0 \\ 0 \\ 0 \\ \vdots \\ 0 \end{pmatrix} \tag{A.3}$$

$$X0 = \begin{pmatrix} 1 \\ 2 \\ 3 \\ \vdots \\ 50 \end{pmatrix} - 0.1 * \begin{pmatrix} 1 \\ 1 \\ 1 \\ \vdots \\ 1 \end{pmatrix} \tag{A.4}$$

$$X0 = \begin{pmatrix} 1 \\ 2 \\ 3 \\ \vdots \\ 50 \end{pmatrix} \tag{A.5}$$

The timing difference when solving (A.1) was explored using the three different X0 values that are shown in (A.3) – (A.5). No modification to the 'optimset' of FMINCON was done. Each initial value x0 (A.3-A.5) was run twice using the 'sqp' algorithm type and twice using the 'active-set' type. The total run time was recorded in Table A.1. Each initial value was run again 25 times in each algorithm type and the average time was recorded in Table A.2.

The results depicted in Tables A.1 and A.2 show that there is a benefit to initiating the search near the solution. The run times are about four times longer in A.3 as compared to starting *exactly* on the answer as in run A.5. The difference between the average run times of starting at the solution as compared to very close to the solution ranges from about

30-75% longer per run when starting at an X0 value displaced by 0.1 in each row of the vector X0 as indicated in (A.4).

A.4 Solution accuracy for FMINCON

Using the run (A.2), the different 'Algorithms' of the optimset of FMINCON were varied to investigate the error and value obtained (*F**). The results are displayed in Table A.3

Table A.1 Run times with different X0 values for examples (A.3) – (A.5)

X0 value*	Algorithm Type	Time (s)	fval
A.3	sqp	21.5737	$1.6271*10^{-12}$
A.3	sqp	19.5066	$1.6271*10^{-12}$
A.3	active-set	22.0704	$5.4432*10^{-10}$
A.3	active-set	20.9760	$5.4432*10^{-10}$
A.4	sqp	6.6423	$2.3819*10^{-12}$
A.4	sqp	6.6989	$2.3819*10^{-12}$
A.4	active-set	5.9303	$2.3827*10^{-12}$
A.4	active-set	6.1320	$2.3827*10^{-12}$
A.5	sqp	4.2784	0
A.5	sqp	3.6210	0
A.5	active-set	6.7066	0
A.5	active-set	5.0039	0

*The contents of this column show the 'run number' for tests performed

Table A.2 Average time after 25 runs for examples (A.3)-(A.5)

X0 value*	Algorithm Type	Time (s)
A.3	sqp	21.2264
A.3	active-set	21.9850
A.4	sqp	8.1359
A.4	active-set	6.7765
A.5	sqp	4.6500
A.5	active-set	5.211

*The contents of this column show the 'run number' for tests performed, the actual X0 values are shown in equations (A.3) – (A.5)

Table A.3 Solution error in FMINCON for run (A.2)

Algorithm Type	F*	Error in x*	ΔT (s)
Active-set	~2.4	~1.5	0.07-0.042
Interior-point	Bad away from x*	Does not solve	0.026-0.075
sqp	~2.4	~1.5	0.034-0.072
Trust-region-reflective	~2.4 ‡	~1.5	0.04-0.05

‡ This method produces an automated warning that advises the user that the method can not be used.

A.5 OPTIMSET parameters for MATLAB

The parameters of OPTIMSET are used in MATLAB for various optimization parameters. They are:

- Display - Level of display [off | iter | notify | final]
- MaxFunEvals - Maximum number of function evaluations allowed [positive integer]
- MaxIter - Maximum number of iterations allowed [positive scalar]

- TolFun - Termination tolerance on the function value [positive scalar]
- TolX - Termination tolerance on X [positive scalar]
- FunValCheck - Check for invalid values, such as NaN or complex, from user-supplied functions [{off} | on]
- OutputFcn - Name(s) of output function [{[]} | function]
- All output functions are called by the solver after each iteration.
- PlotFcns - Name(s) of plot function [{[]} | function]
- Function(s) used to plot various quantities in every iteration [26].

Volume II

Distribution Locational Marginal Pricing for Optimal Electric Vehicle Charging Management

Shmuel S. Oren
Ruoyang Li
University of California at Berkeley

Qiuway Wu
Danish Technical University, Copenhagen

For information about Volume II, contact

Shmuel S. Oren
Department of Industrial Engineering and Operations Research
University of California at Berkeley
Etcheverry Hall 4119
Berkeley, CA 94720-1777
Phone: (510) 642-1836 or 5484
Fax: (510) 642-1403
Email: oren@ieor.berkeley.edu
URL: http://www.ieor.berkeley.edu/~oren/

Power Systems Engineering Research Center

The Power Systems Engineering Research Center (PSERC) is a multi-university Center conducting research on challenges facing the electric power industry and educating the next generation of power engineers. More information about PSERC can be found at the Center's website: http://www.pserc.org.

For additional information, contact:

Power Systems Engineering Research Center
Arizona State University
527 Engineering Research Center
Tempe, Arizona 85287-5706
Phone: 480-965-1643
Fax: 480-965-0745

Notice Concerning Copyright Material

Table of Contents

List of Figures

List of Tables

Intentionally Blank Page

1. INTRODUCTION

1.1 Nomenclature

$D_{l,i}$ Power transfer distribution factor (PTDF) coefficient of line l with respect to a unit injected at node i

$E_{i,t}$ EV charging energy limit at time period t at node i

K_l MVA capacity of line l

N Set of all nodes

N_c Subset of demand nodes

N_n Subset of non-demand nodes

$P_{DLMP,i,t}$ Distribution locational marginal price at time period t at node i of the distribution grid

$P_{i,t}(\tau_i, t)$ Benefits from using demand τ_i at time period t at node i

$P_{LMP,t}$ System locational marginal price (LMP) at time period t for the node feeding the distribution grid

$S_{i,0}$ Initial aggregate battery state of charge (SOC) at node i

$S_{i,t}^-$ Minimum aggregate battery SOC at time period t at node i

$S_{i,t}^+$ Maximum aggregate battery SOC at time period t at node i

T Planning periods for optimization

$c_{i,t}$ Conventional household demand at time period t at node i

g The subset of generation node(s)

p_t Dual variables for total power flow balance constraints

$q_{g,t}$ Generation supplied to the distribution grid at time period t

$r_{g,t}$ Net active power import/export at time period t at generation node g (positive for import)

$r_{i,t}$ Net active power import/ export at time period t at node i (positive for import)

$x_{i,t}$ EV charging energy at time period t at node i

$\kappa_{i,t}^-$ Dual variables for aggregate EV minimum SOC constraints

$\kappa_{i,t}^+$ Dual variables for aggregate EV maximum SOC constraints

$\lambda_{l,t}^-$ Dual variables for negative line flow constraints

$\lambda_{l,t}^+$ Dual variables for positive line flow constraints

$\mu_{i,t}^-$ Dual variables for EV minimum charging energy constraints

$\mu_{i,t}^+$ Dual variables for EV maximum charging energy constraints

$\xi_{i,t}$ Dual variables for conventional household demand constraints

$\rho_{i,t}$ Dual variables for demand node power balance constraints

$\tau_{i,t}$ Demand variables at time period t at node i

$\omega_{g,t}$ Dual variables for generation node power balance constraints

$\omega_{i,t}$ Dual variables for non-demand node net active power import/output constraints

1.2 Overview of the Problem

Environmental concerns and the quest for energy supply independence have resulted in increasing penetration of renewable energy sources (RES) and a move toward electrification of transportation. Consequently, electric vehicles (EVs) are expected to play a significant role in the future power systems and distribution networks. Increased use of EVs will reduce the green house gas (GHG) emission from the transport sector by replacing conventional internal combustion engine (ICE) vehicles while also serving as distributed energy storage that can mitigate uncertainties arising from intermittent RES.

Numerous studies have addressed vehicle-to-grid (V2G) technology to investigate the technical and commercial feasibility of providing ancillary service to the grid from EVs. The capacity from EVs and the economic return to participate in peak power, spinning reserve and regulation markets have been explored in [1]-[3]. It was concluded that EV fleet operators can receive significant economic returns and the ancillary services from EVs can supply operating reserves or storage to support large scale renewable energy integration. The effectiveness of using EVs to provide peak load shaving and extra flexibility has been illustrated in [4] and [5] while aggregator based optimal EV charging algorithms for unidirectional V2G are used. It is shown in [6] that EV storage systems can support the operation of power system with high wind power penetration by supplying power back to the grid if there are proper incentives to do so.

However, the deployment of a large number of EVs will challenge power system operations especially for distribution networks if there is no proper coordination of the EV charging. Grid congestion results from demand patterns that induce flows exceeding design limits. Congestion from EVs can be observed at the medium voltage (MV) level, as demonstrated by a number of studies [7]-[10]. It was also noted that the problems are likely to originate on the distribution network, and as such, analysis of these networks should be conducted as the primary stage of EV induced congestion [10]-[12].

Grid congestion depends on a number of factors including local grid rating and topology, penetration and distribution of EVs, and charging management procedures. Coordinated charging appears to be an effective means of allowing increased penetration of EVs without violating grid constraints. There is some diversity regarding the optimal manner in which to coordinate charging and the proposed objectives for such coordination include minimization of losses [8], maximization of EV penetration [10], and minimization of customer charging costs [13]-[14]. The study conducted in [13] shows that the computational power required to handle grid constraints at the distribution level in the linear programming optimization of EV charging management is quite significant.

There are many approaches to implement congestion management in transmission systems, depending on the electricity market structure. The congestion management methods can be categorized into three groups: Optimal Power Flow (OPF) based method, price area congestion control method and transaction-based methods [15]. The OPF based congestion management method is based on a centralized optimization and is considered to be the most accurate and effective congestion management method. Price-based

congestion management controls congestion by generation re-dispatch in response to congestion prices within an OPF framework [16].

In the existing work on load management techniques and other methods for alleviating congestions from EVs, there is no integrated method which has a closed loop solution accounting for conventional demand elasticity and EV demand shifting characteristics. In order to address this problem, the distribution locational marginal pricing (DLMP) method is proposed for electric distribution networks in order to alleviate congestion induced by EVs. In the proposed method, the distribution system operator (DSO) determines the distribution locational marginal prices (DLMPs) by solving the social welfare optimization for the electric distribution network which considers EV aggregators as price takers in the local DSO market and demand elasticity for residential energy consumption. It is assumed that all the EV aggregators are economically rational, i.e. their objective is to maximize their individual surplus.

1.3 Report Organization

The report is arranged as follows. The mathematical formulation of the integrated DLMP method and the determination of DLMPs are presented in Section 2. In Section 3, the EV aggregator based optimal charging management is described. The alleviation of congestion induced by EVs within electric distribution networks is explained in Section 4. Case studies were conducted using the BUS 4 distribution networks of the Roy Billinton Test System (RBTS) [17] and the Danish driving data, and the case study results are presented in Section 5 with detailed discussion followed by the conclusion section.

2. DETERMINATION OF DISTRIBUTION LOCATIONAL MARGINAL PRICES USING INTEGRATED OPTIMIZATION

The system LMPs are determined by minimizing the cost of generations with the physical constraints of the transmission system respected, which exposes producers and consumers to the marginal cost of electricity delivery at different locations. The LMPs can be decomposed into three components: marginal cost of generation, marginal cost of losses and marginal cost of congestion [18].

The LMPs can be computed by either AC optimal power flow (ACOPF) or DC optimal power flow (DCOPF). The DCOPF is widely used and is considered to be sufficient for LMP calculation due to its computational efficiency and approximation accuracy [19]. The DCOPF has also been employed by several software tools for chronological LMP simulation and forecasting, such as ABB GridViewTM, Siemens Promod, GE MAPSTM and PowerWorld [20].

The DCOPF was adopted in the derivation of DLMPs as a practical approach to address the computational complexity resulting from the large number of nodes within the electric distribution network. In the proposed DLMP algorithm, the DSO determines the DLMPs for the next day by solving a constrained social welfare maximization problem.

The mathematical formulation in [21]-[23] has been modified to make it more general to allow economic allocation for both conventional household demand and EV charging energy. The mathematical formulation of the DSO optimization problem is presented in (1) to (9),

Objective Function

$$\max \sum_{i\in N_c}\sum_{t\in T}\int_0^{c_{i,t}} P_{i,t}(\tau_i,t)d\tau_{i,t} - \sum_{t\in T} P_{LMP,t}\,q_{g,t} \tag{1}$$

subject to

$$\sum_{i\in N} r_{i,t} = 0 \quad \forall t\in T \qquad (p_t) \tag{2}$$

$$-K_l \le \sum_{i\in N} D_{l,i} r_{i,t} \le K_l \quad \forall l\in L, \forall t\in T \qquad (\lambda_{l,t}^-, \lambda_{l,t}^+) \tag{3}$$

$$r_{i,t} = 0 \quad \forall i\in N_n, \forall t\in T \qquad (\omega_{i,t}) \tag{4}$$

$$r_{g,t} + q_{g,t} = 0 \quad \forall t\in T \qquad (\omega_{g,t}) \tag{5}$$

$$r_{i,t} = c_{i,t} + x_{i,t} \quad \forall i\in N_c, \forall t\in T \qquad (\rho_{i,t}) \tag{6}$$

$$c_{i,t} \ge 0 \quad \forall i\in N_c, \forall t\in T \qquad (\xi_{i,t}) \tag{7}$$

$$0 \le x_{i,t} \le E_{i,t} \quad \forall i\in N_c, \forall t\in T \qquad (\mu_{i,t}^-, \mu_{i,t}^+) \tag{8}$$

$$S_{i,t}^- \le S_{i,0} + \sum_{t'\le t-1} x_{i,t'} - \sum_{t'\le t} d_{i,t'} \le S_{i,t}^+ \quad \forall i\in N_c, \forall t\in T\setminus\{1\} \qquad (\kappa_{i,t}^-, \kappa_{i,t}^+) \tag{9}$$

The DSOs objective is to maximize the social surplus in (1) subject to the lossless energy-balance constraints in (2), the transmission constraints in (3), the non-demand

node constraints in (4), generation node balance constraints in (5), the demand node balance constraints in (6), the conventional household demand non-negativity constraints in (7), the charging energy limit constraints in (8) and the driving requirement constraints in (9).

For the demand node balance constraints in (6), the assumption is that EVs only charge energy at the location they belong to, which requires that the energy import $r_{i,t}$ is the sum of the conventional household demand $c_{i,t}$ and EV demand $x_{i,t}$ at time period t at node i. The elastic conventional household demand $c_{i,t}$ is constrained to be non-negative in (7). The EV demand $x_{i,t}$ is constrained between 0 and charging energy limit $E_{i,t}$ at time period t at node i in (8). $E_{i,t}$ varies over time to reflect the availability of EVs across hours. The SOC of EV batteries at time period t at node i is the sum of its initial SOC and total charging energy $x_{i,t}$ up to time period $t-1$ minus the total driving energy requirement $d_{i,t}$ up to time period t. The SOC is constrained between minimum SOC $S_{i,t}^{-}$ and maximum SOC $S_{i,t}^{+}$ in (9). The variables in parentheses next to each constraint denote the Lagrange multipliers corresponding to that constraint.

The objective function consists of two components, social value of meeting the conventional demand, given by the area under the demand functions, and the cost of satisfying both the EV demand and the conventional demand as shown in (1). The benefit of the EV demand is not included in the objective function since that component is constant, as long as the EV demand is met within the day, and is not affected by the charging schedule. Instead, a constraint requiring that the EV demand be met by the schedule is included. To be more specific, the object function in (1) can be further decomposed into three terms as shown in (10),

$$\begin{aligned}&\sum_{i\in N_c}\sum_{t\in T}\int_0^{c_{i,t}} P_{i,t}(\tau_i,t)d\tau_{i,t} - \sum_{t\in T} P_{LMP,t}\,q_{g,t} = \sum_{i\in N_c}\sum_{t\in T}\int_0^{c_{i,t}} P_{i,t}(\tau_i,t)d\tau_{i,t} - \sum_{t\in T} P_{LMP,t}\sum_{i\in N_c}(c_{i,t}+x_{i,t})\\ &= \sum_{i\in N_c}\sum_{t\in T}\int_0^{c_{i,t}} P_{i,t}(\tau_i,t)d\tau_{i,t} - \sum_{t\in T} P_{LMP,t}\sum_{i\in N_c} c_{i,t} - \sum_{t\in T} P_{LMP,t}\sum_{i\in N_c} x_{i,t}\end{aligned} \tag{10}$$

where $\sum_{i\in N_c}\sum_{t\in T}\int_0^{c_{i,t}} P_{i,t}(\tau_i,t)d\tau_{i,t} - \sum_{t\in T} P_{LMP,t}\sum_{i\in N_c} c_{i,t}$ is the social welfare corresponding to the conventional demand and $\sum_{t\in T} P_{LMP,t}\sum_{i\in N_c} x_{i,t}$ is the EV charging cost.

The KKT optimality conditions for the social welfare optimization problem are summarized in (11) to (28),

$$P_{i,t}(c_{i,t}) - \rho_{i,t} + \xi_{i,t} = 0 \quad \forall i \in N_c, \forall t \in T \tag{11}$$

$$-p_t - \sum_{l\in L}(\lambda_{l,t}^{+} - \lambda_{l,t}^{-})D_{l,i} + \rho_{i,t} = 0 \quad \forall i \in N_c, \forall t \in T \tag{12}$$

$$-p_t - \sum_{l\in L}(\lambda_{l,t}^{+} - \lambda_{l,t}^{-})D_{l,i} + \omega_{i,t} = 0 \quad \forall i \in N_n, \forall t \in T \tag{13}$$

$$-p_t - \sum_{l\in L}(\lambda_{l,t}^{+} - \lambda_{l,t}^{-})D_{l,g} + \omega_{g,t} = 0 \quad \forall t \in T \tag{14}$$

$$-P_{LMP,t} + \omega_{g,t} = 0 \quad \forall t \in T \tag{15}$$

$$-\rho_{i,t}-(\mu_{i,t}^{+}-\mu_{i,t}^{-})-\sum_{t'\geq t+1}(\kappa_{i,t'}^{+}-\kappa_{i,t'}^{-})=0 \quad \forall i\in N_c,\forall t\in T\setminus\{|T|\} \tag{16}$$

$$-\rho_{i,t}-(\mu_{i,t}^{+}-\mu_{i,t}^{-})=0 \quad \forall i\in N_c,\forall t=|T| \tag{17}$$

$$\sum_{i\in N} r_{i,t}=0 \quad \forall t\in T \tag{18}$$

$$r_{i,t}=0 \quad \forall i\in N_n,\forall t\in T \tag{19}$$

$$r_{g,t}+q_{g,t}=0 \quad \forall t\in T \tag{20}$$

$$r_{i,t}=c_{i,t}+x_{i,t} \quad \forall i\in N_c,\forall t\in T \tag{21}$$

$$\lambda_{l,t}^{-}\geq 0\perp\sum_{i\in N}D_{l,i}r_{i,t}+K_l\geq 0 \quad \forall l\in L,\forall t\in T \tag{22}$$

$$\lambda_{l,t}^{+}\geq 0\perp K_l-\sum_{i\in N}D_{l,i}r_{i,t}\geq 0 \quad \forall l\in L,\forall t\in T \tag{23}$$

$$\xi_{i,t}\geq 0\perp c_{i,t}\geq 0 \quad \forall i\in N_c,\forall t\in T \tag{24}$$

$$\mu_{i,t}^{-}\geq 0\perp x_{i,t}\geq 0 \quad \forall i\in N_c,\forall t\in T \tag{25}$$

$$\mu_{i,t}^{+}\geq 0\perp E_{i,t}-x_{i,t}\geq 0 \quad \forall i\in N_c,\forall t\in T \tag{26}$$

$$\kappa_{i,t}^{-}\geq 0\perp S_{i,0}+\sum_{t'\leq t-1}x_{i,t'}-\sum_{t'\leq t}d_{i,t'}-S_{i,t}^{-}\geq 0 \quad \forall i\in N_c,\forall t\in T\setminus\{1\} \tag{27}$$

$$\kappa_{i,t}^{+}\geq 0\perp S_{i,t}^{+}-S_{i,0}-\sum_{t'\leq t-1}x_{i,t'}+\sum_{t'\leq t}d_{i,t'}\geq 0 \quad \forall i\in N_c,\forall t\in T\setminus\{1\} \tag{28}$$

The KKT conditions yield the optimality for the primal problem and provide an economic interpretation of the Lagrange multipliers. The DLMPs are derived from the KKT conditions to provide price incentives for market participants to alleviate congestion and ensure efficient load allocation. By solving (12), (14) and (15), the marginal value of a unit of EV charging energy or conventional demand at time period t at node i, $\rho_{i,t}$, takes the form in (29),

$$\rho_{i,t}=P_{LMP,t}-\sum_{l\in L}(\lambda_{l,t}^{+}-\lambda_{l,t}^{-})D_{l,g}+\sum_{l\in L}(\lambda_{l,t}^{+}-\lambda_{l,t}^{-})D_{l,i}\ . \tag{29}$$

In the RBTS, the power transfer distribution factor (PTDF) coefficient associated with the generation node $D_{l,g}$ is set to be 0 to enable unlimited import from the grid to the distribution network, which simplifies (29) and yields (30),

$$\rho_{i,t}=P_{LMP,t}+\sum_{l\in L}(\lambda_{l,t}^{+}-\lambda_{l,t}^{-})D_{l,i}\ . \tag{30}$$

The DLMPs can be derived by combining (11) and (30),

$$P_{DLMP,i,t}=P_{i,t}(c_{i,t})=\rho_{i,t}-\xi_{i,t} \tag{31}$$

$$=P_{LMP,t}+\sum_{l\in L}(\lambda_{l,t}^{+}-\lambda_{l,t}^{-})D_{l,i}-\xi_{i,t} \tag{32}$$

The non-negativity constraints (7) can be excluded by implicitly assuming an interior solution with respect to these constraints, forcing the dual variable associated with the constraint $\xi_{i,t}=0$. This can be explained as: every conventional household consumes at least a small positive amount of energy. Under this assumption, the DLMPs become,

$$P_{DLMP,i,t} = P_{LMP,t} + \varphi_{i,t} \tag{33}$$

where $\varphi_{i,t} = \sum_{l \in L} (\lambda_{l,t}^{+} - \lambda_{l,t}^{-}) D_{l,i}$. The DLMPs can be interpreted as the sum of the reference price $P_{LMP,t}$ and the locational congestion markup $\varphi_{i,t}$, which is analogous to the marginal cost of congestion in the LMPs.

Noticing that the LMPs only optimize the dispatch of instantaneous demand, the DLMPs are designed to co-optimize the dispatch of both the instantaneous demand and the aggregated EV charging schedule over the planning interval. By rearranging (16) and (17), $\rho_{i,t}$ can be written as (34),

$$\rho_{i,t} = \begin{cases} -\mu_{i,t}^{+} + \mu_{i,t}^{-} - \sum_{t' \geq t+1} \kappa_{i,t'}^{+} + \sum_{t' \geq t+1} \kappa_{i,t'}^{-} & \forall i \in N_c, \forall t \in T \setminus \{|T|\} \\ -\mu_{i,t}^{+} + \mu_{i,t}^{-} & \forall i \in N_c, \forall t = |T| \end{cases} \tag{34}$$

where $-\mu_{i,t}^{+} + \mu_{i,t}^{-} - \sum_{t' \geq t+1} \kappa_{i,t'}^{+} + \sum_{t' \geq t+1} \kappa_{i,t'}^{-}$ is the marginal value of energy at non-terminal period $t \in T \setminus \{|T|\}$ at node i, and $-\mu_{i,t}^{+} + \mu_{i,t}^{-}$ is marginal value of energy at terminal period $t = |T|$ at node i. Combining (11) and (34) gives the DLMPs at time period t at node i as a linear combination of the dual variables associated with constraints of EVs,

$$P_{DLMP,i,t} = P_{i,t}(c_{i,t}) = \rho_{i,t} - \xi_{i,t} \tag{35}$$

$$= \begin{cases} -\mu_{i,t}^{+} + \mu_{i,t}^{-} - \sum_{t' \geq t+1} \kappa_{i,t'}^{+} + \sum_{t' \geq t+1} \kappa_{i,t'}^{-} - \xi_{i,t} & \forall i \in N_c, \forall t \in T \setminus \{|T|\} \\ -\mu_{i,t}^{+} + \mu_{i,t}^{-} - \xi_{i,t} & \forall i \in N_c, \forall t = |T| \end{cases} \tag{36}$$

$$= \begin{cases} -\mu_{i,t}^{+} + \mu_{i,t}^{-} - \sum_{t' \geq t+1} \kappa_{i,t'}^{+} + \sum_{t' \geq t+1} \kappa_{i,t'}^{-} & \forall i \in N_c, \forall t \in T \setminus \{|T|\} \\ -\mu_{i,t}^{+} + \mu_{i,t}^{-} & \forall i \in N_c, \forall t = |T| \end{cases} \tag{37}$$

where $\xi_{i,t} = 0$ assuming (7) does not bind.

The DLMPs defined by (33) and (37) can be interpreted as the equilibrium conditions for the electric distribution system market clearing. The market dynamics and the economic behavior of market participants under the DLMPs are discussed in the Section 3.

3. AGGREGATOR BASED OPTIMAL EV CHARGING MANAGEMENT

The EV charging management can take different forms: charging management controlled by individual EV users, aggregator based charging management and proper mixture of the two mechanisms. In this paper, the aggregator based EV charging management implementation is used.

In the aggregator based EV charging management concept, the EV aggregator is a profit-seeking entity, who takes care of the EV fleet on behalf of the EV users, ensures that the energy needs are satisfied, and provides customized service and charging solution. The objective of EV aggregators is to meet the energy needs of EV users with the minimum charging cost. It is also assumed that each EV aggregator only controls a small portion of the EVs so that EV aggregators do not have market power and act as price takers in the DSO market. The aggregator based EV optimal charging management can be described by the optimization problem in (38) to (40),

Objective Function

$$\min \sum_{t \in T} P_{DLMP,i,t} x_{i,t} \tag{38}$$

subject to

$$0 \le x_{i,t} \le E_{i,t} \qquad \forall t \in T \qquad (\mu_{i,t}^{-}, \mu_{i,t}^{+}) \tag{39}$$

$$S_{i,t}^{-} \le S_{i,0} + \sum_{t' \le t-1} x_{i,t'} - \sum_{t' \le t} d_{i,t'} \le S_{i,t}^{+} \quad \forall t \in T \setminus \{1\} \qquad (\kappa_{i,t}^{-}, \kappa_{i,t}^{+}) . \tag{40}$$

The constraints in (39) and (40) are to ensure that the EV charging energy and the EV battery SOC are within the specified limits. When the DLMPs, $P_{DLMP,i,t}$, are known to the EV aggregator, the optimization problem is a linear programming problem and the EV aggregator optimally decides $x_{i,t}$, the amount of energy to purchase in each hour, to minimize the charging cost subject to the charging power limit constraints and the driving requirement constraints. The optimality conditions of the EV charging are summarized in (41) to (52),

$$0 \le x_{i,t} \le E_{i,t} \qquad \forall t \in T \tag{41}$$

$$S_{i,t}^{-} \le S_{i,0} + \sum_{t' \le t-1} x_{i,t'} - \sum_{t' \le t} d_{i,t'} \le S_{i,t}^{+} \qquad \forall t \in T \setminus \{1\} \tag{42}$$

$$-P_{DLMP,i,t} - \mu_{i,t}^{+} + \mu_{i,t}^{-} - \sum_{t' \ge t+1} \kappa_{i,t'}^{+} + \sum_{t' \ge t+1} \kappa_{i,t'}^{-} = 0 \quad \forall t \in T \setminus \{|T|\} \tag{43}$$

$$-P_{DLMP,i,t} - \mu_{i,t}^{+} + \mu_{i,t}^{-} = 0 \quad \forall t = |T| \tag{44}$$

$$\mu_{i,t}^{-} \ge 0 \qquad \forall t \in T \tag{45}$$

$$\mu_{i,t}^{+} \ge 0 \qquad \forall t \in T \tag{46}$$

$$\kappa_{i,t}^{-} \ge 0 \qquad \forall t \in T \setminus \{1\} \tag{47}$$

$$\kappa_{i,t}^{+} \ge 0 \qquad \forall t \in T \setminus \{1\} \tag{48}$$

$$\mu_{i,t}^{-} x_{i,t} = 0 \qquad \forall t \in T \tag{49}$$

$$\mu_{i,t}^{+}(E_{i,t}-x_{i,t})=0 \qquad \forall t\in T \tag{50}$$

$$\kappa_{i,t}^{-}(S_{i,0}+\sum_{t'\le t-1}x_{i,t'}-\sum_{t'\le t}d_{i,t'}-S_{i,t}^{-})=0 \quad \forall t\in T\setminus\{1\} \tag{51}$$

$$\kappa_{i,t}^{+}(S_{i,t}^{+}-S_{i,0}-\sum_{t'\le t-1}x_{i,t'}+\sum_{t'\le t}d_{i,t'})=0 \quad \forall t\in T\setminus\{1\} \tag{52}$$

(41)-(42) are the primal feasibility conditions. (43)-(48) are the dual feasibility conditions. (49)-(52) are the complementarity conditions.

Theorem 1 The efficient allocation of EV charging of the DSO problem $x_{i,t}^{*}$ is optimal for each EV aggregator under the DLMPs, if the non-negativity constraint of conventional household demand (7) does not bind.

Proof: It has been shown that the optimal solution of the DSO problem $\{x_{i,t}^{*},\mu_{i,t}^{+*},\mu_{i,t}^{-*},\kappa_{i,t}^{+*},\kappa_{i,t}^{-*}\}$ also satisfies the optimality conditions of the EV aggregator's problem in (41)-(52).

The optimal solution of the DSO problem satisfies the KKT conditions (11)-(28). If (7) does not bind, the optimal solution of the DSO problem satisfies (37),

$$P_{DLMP,i,t}^{*}=\begin{cases}-\mu_{i,t}^{+*}+\mu_{i,t}^{-*}-\sum_{t'\ge t+1}\kappa_{i,t'}^{+*}+\sum_{t'\ge t+1}\kappa_{i,t'}^{-*} & \forall t\in T\setminus\{|T|\}\\ -\mu_{i,t}^{+*}+\mu_{i,t}^{-*} & \forall t=|T|\end{cases}.$$

This implies (43) and (44) hold under the optimal solution $\{x_{i,t}^{*},\mu_{i,t}^{+*},\mu_{i,t}^{-*},\kappa_{i,t}^{+*},\kappa_{i,t}^{-*}\}$. (41), (42) and (45)-(52) come directly from KKT conditions (25)-(28). Thus, the efficient allocation of EV charging from the DSO problem satisfies the optimality conditions of the EV aggregator's problem.

Corollary 1 The efficient allocation of the DSO problem $\{x_{i,t}^{*},c_{i,t}^{*}\}$ can be achieved in a decentralized system under the DLMPs, if the non-negativity constraint of conventional household demand (7) does not bind.

Proof: The conventional household demand $c_{i,t}^{*}$ is deterministic under the DLMPs. From Theorem 1, it is known that, under the DLMPs, the optimal solution of the EV aggregator's problem is the efficient allocation of EV charging of the DSO problem $x_{i,t}^{*}$. Therefore, the efficient allocation of the DSO problem can be achieved in the decentralized implementation.

4. ALLEVIATING CONGESTION FROM EVs WITHIN ELECTRIC DISTRIBUTION NETWORKS USING DLMP

The intention of the proposed DLMP concept is to alleviate congestion within electric distribution networks which might be caused by the EV charging demand. The congestion alleviation approach using DLMP is illustrated in Figure 1.

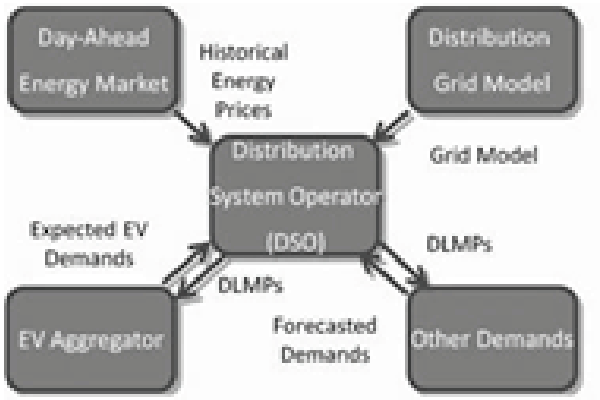

Figure 1: Congestion Alleviation from EVs using DLMPs

The DSO plays a major role in the DLMP based congestion management within electric distribution networks. The concept can be explained by the following steps.

- The DSO obtains the LMPs from the posted day-ahead energy prices.
- According to the EV data within the electric distribution network, the expected EV demand will be forecasted by the DSO with the assumption that all EV aggregators are minimizing their EV charging costs. Conventional demand will be forecasted by the DSO according to the posted energy prices.
- With the information on the forecasted demand, the DSO calculates the DLMPs at the electric distribution network level taking into account the electric distribution network topology.
- In the end, the DLMPs will be sent to all EV aggregators and retailers.

As it is proved in Theorem 1 and Corollary 1, after receiving the DLMPs from the DSO, EV aggregators and retailers will behave exactly as the DSO predicts. Consequently, the congestion on the electric distribution network will be properly managed, while it only requires EV aggregators and retailers to react rationally to the DLMPs by maximizing their individual net surplus. At this point, any additional information of distribution network grid or line congestion is redundant to the decision-making process of EV aggregators and retailers.

5. CASE STUDIES

In order to illustrate the efficacy of the proposed DLMP concept in alleviating congestion from EV demand, case studies have been conducted using the distribution network of the RBTS connected to Bus 4 with the Danish driving data.

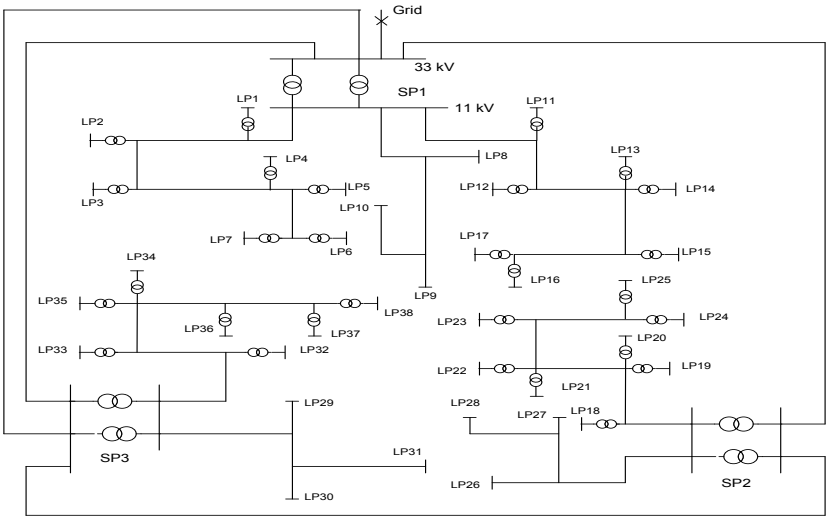

Figure 2: Single Line Diagram of Bus4 Distribution System of RBTS [17]

Figure 2 illustrates the single line diagram of the electric distribution system used in the case study. The electric distribution systems of the RBTS were designed following the general utility principles and practices regarding topology, ratings and load levels. They represent typical distribution networks. The BUS4 distribution system of the RTBS has a relatively complex topology and sufficient number of customers. Therefore, the BUS4 distribution system of the RTBS was chosen to carry out case studies. This MV distribution network is comprised of three supply points (SPs) connected to the main grid by 33 kV/11 kV transformers, 38 load points (LPs) and 66 feeders. The customer data are listed in Table 1.

Table 1: Customer Data

Number of Load Points	Load Points	Customer Type	Load Level Per Load Point (MW)		Number of Customers
			Average	Peak	
15	1-4, 11-13, 18-21, 32-35	Residential	0.545	0.8869	200
7	5, 14, 15, 22, 23, 36, 37	Residential	0.5	0.8137	200
7	8, 10, 26-30	Small User	1.0	1.63	1
2	9, 31	Small user	1.5	2.445	1
7	6, 7, 16, 17, 24, 25, 38	Commercial	0.415	0.6714	10
Total			24.58	40.00	4779

The customer data consist of customer type, peak and average loads and number of customers. There are 4779 customers in total in the electric distribution network. The inverse demand function at each bus is assumed to be linear with a price elasticity of −0.1. This level of demand price elasticity is consistent with empirical studies in [24].There are 7 feeders in the electric distribution network. Each of the lines is one of the three types listed in Table 2.

Table 2: Connection Line Types

Connection Line Type	Line Length (km)	Line Number
1	0.6	2 6 10 14 17 21 25 28 30 34 38 41 43 46 49 51 55 58 61 64 67
2	0.75	1 4 7 9 12 16 19 22 24 27 29 32 35 37 40 42 45 48 50 53 56 60 63 65
3	0.8	3 5 8 11 13 15 18 20 23 26 31 33 36 39 44 47 52 54 57 59 62 66

5.1 EV data

A non-homogenous EV fleet is used for the EV charging management studies. The EV battery size varies according to individual EV driving requirements. It is assumed that the maximum charging power is 1.1 kW (based on a 10 A, 110 V connection). A typical value of 0.15 kWh/km is used to calculate the energy consumption while driving [25]. The minimum and maximum EV battery SOC is set as 20% and 85%, respectively. The initial EV SOC varies by individual EV, and is set such that individual charging and driving requirements can be met. This is in accordance with the non-homogenous nature of EVs. A summary of the EV data is listed in Table 3.

Table 3: EV Data Summary

EV Parameter	EV Parameter Value
EV Battery Size	25 kWh
Charging Power	5.28 kW
Energy Consumption of Driving	150 Wh/km
Minimum SOC	20%
Maximum SOC	85%

5.2 Driving data

The Driving data used in the case studies are from the Danish National Travel Survey [25]. The Danish driving data were chosen for the case studies because the driving behavior in Denmark could be representative of the EV users' driving pattern. In Denmark, the average driving distance is about 40 km per day. Customers who need to drive a longer distance, might not choose to use EVs.

The Danish driving data are highly detailed and provide significant insight into the driving habits of Danish residents. The relevant data used in this study are driving stop and start time, distance during driving periods, and day type. The EV availability for charging is defined as the periods during which the EV is parked. The driving profile from the same day type as the LMPs is used to create a more consistent test case. The EV availability on a working day is illustrated in Figure 3. Each horizontal section represents a single EV, with the white colour representing availability to charge, and the black colour representing time periods when the EV is driving, and therefore is unavailable to charge.

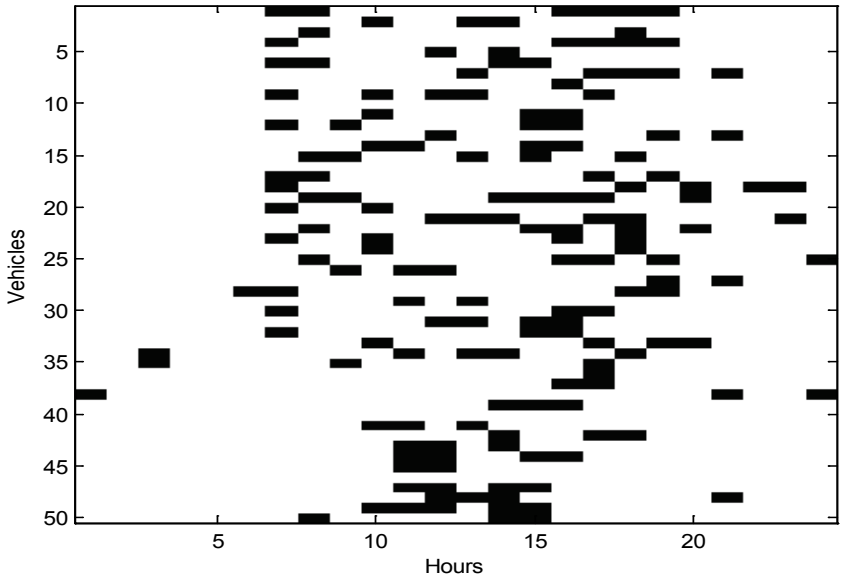

Figure 3: EV Availability on a Working Day

5.3 Case study results

Three case studies listed in Table IV have been carried out. The EV penetration is defined as the ratio of maximum EV charging demand divided by the conventional household demand. The maximum EV charging demand is the sum of the EV charging demand when all EVs charge simultaneously.

Table 4: Case Study Scenarios

Case Study No	Day Type	EV Penetration
1	Tuesday	100%
2	Saturday	100%
3	Thursday	500%

5.3.1 Case Study 1

The results of Case Study 1 are shown in Fiure. 4–Figure 6. Figure 4 and Figure 5 illustrate the effect of congestion alleviation on Line 1 when the DLMPs are introduced. Comparing with Figure 4, the EV loads are spread out under the DLMPs in Figure 5 and distributed among several hours with low LMPs, instead of charging all the EV loads in a single hour. In Figure 6, the line with circles is the system LMP curve and the solid lines are the DLMPs at different nodes. The DLMPs are slightly higher than the system LMPs on the buses downstream to the congested line in order to shift away the EV loads to avoid severe congestion.

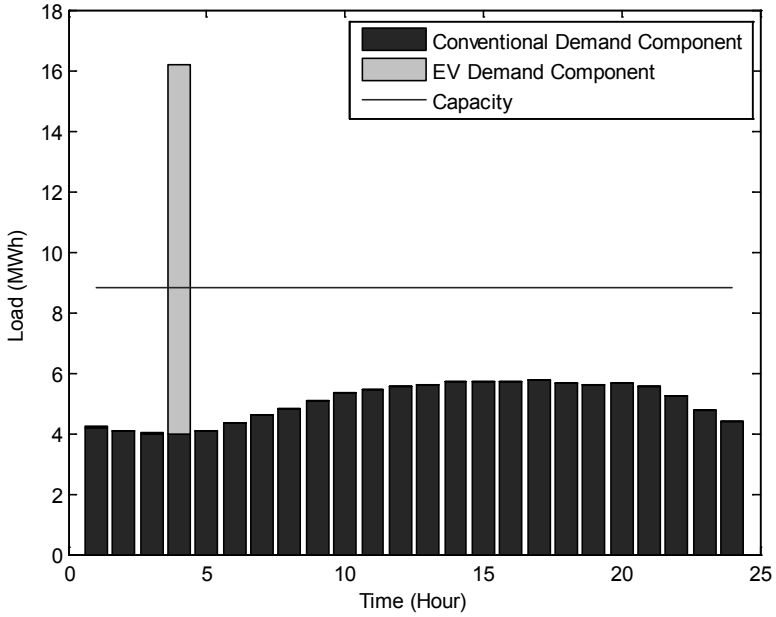

Figure 4: Line 1 Loading without DLMPs of Case 1

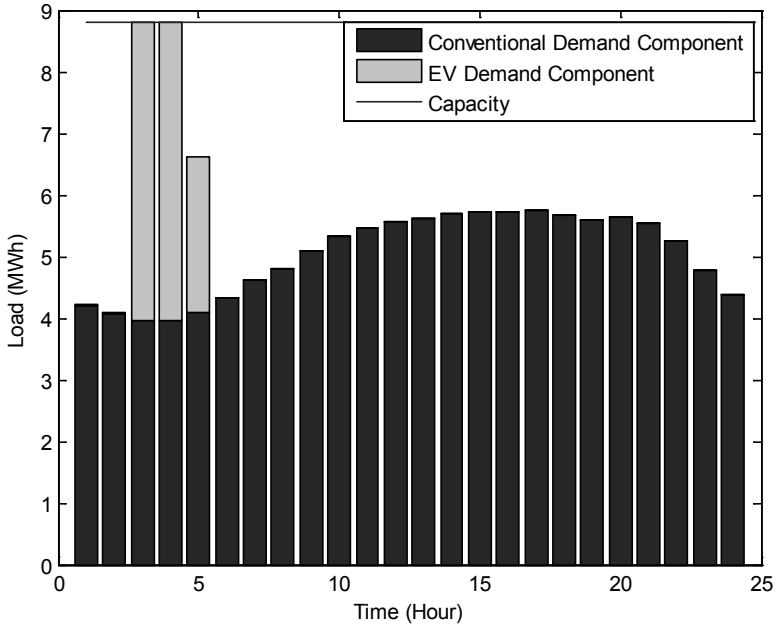

Figure 5: Line 1 Loading with DLMPs of Case 1

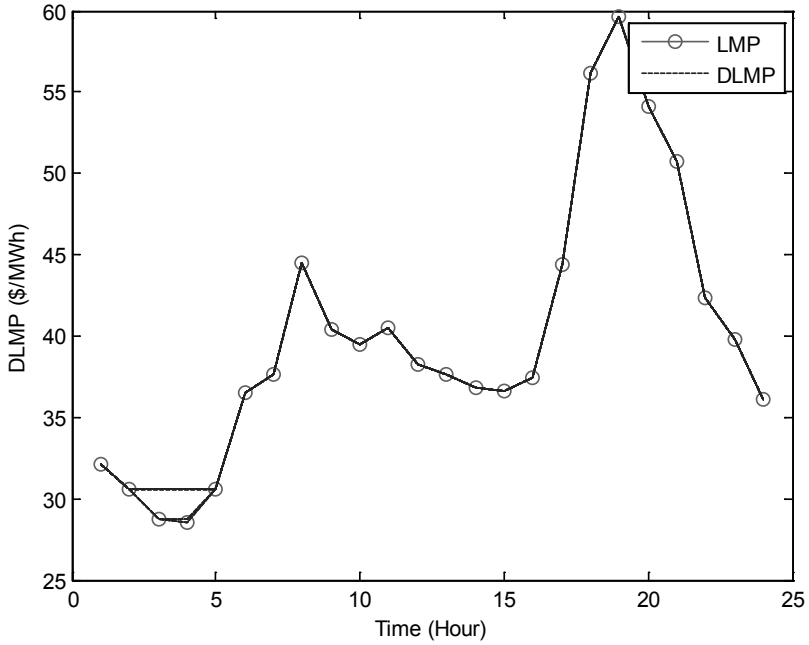

Figure 6: System LMPs and DLMPs of Case 1

5.3.2 Case Study 2

The results of Case Study 2 are shown in Figure 7-Figure 9. In Case Study 2, the system LMP profile is different from the one in Case Study 1. The low system LMPs occur both in the morning and in the afternoon. Without the DLMPs, congestion occurs in both of

the two periods on Line 1. With the proposed DLMP, it is shown in Figure 8 that the congestion can be successfully alleviated. The EV loads have been shifted to the adjacent low LMP hours.

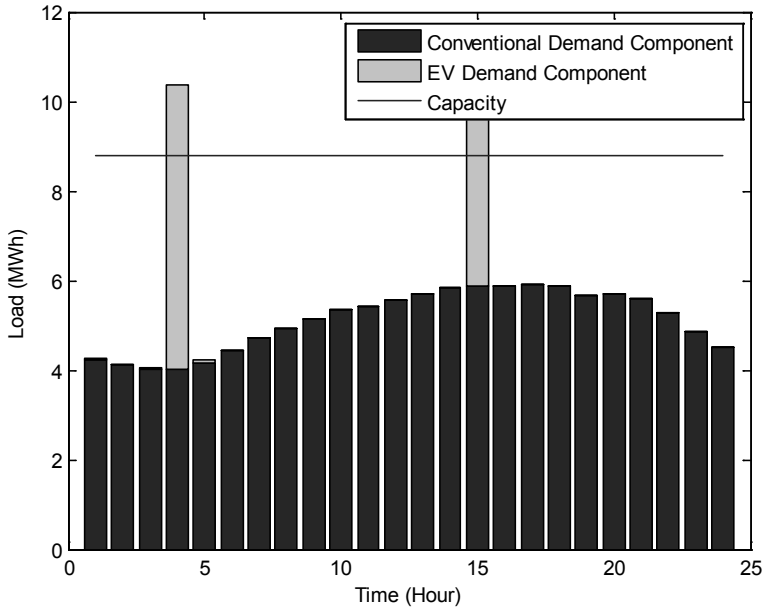

Figure 7: Line 1 Loading without DLMP of Case 2

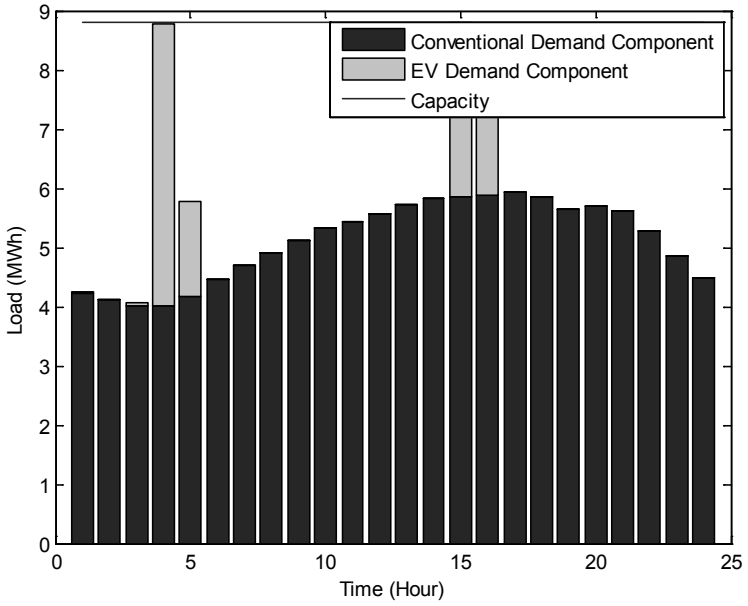

Figure 8: Line 1 Loading with DLMP of Case 2

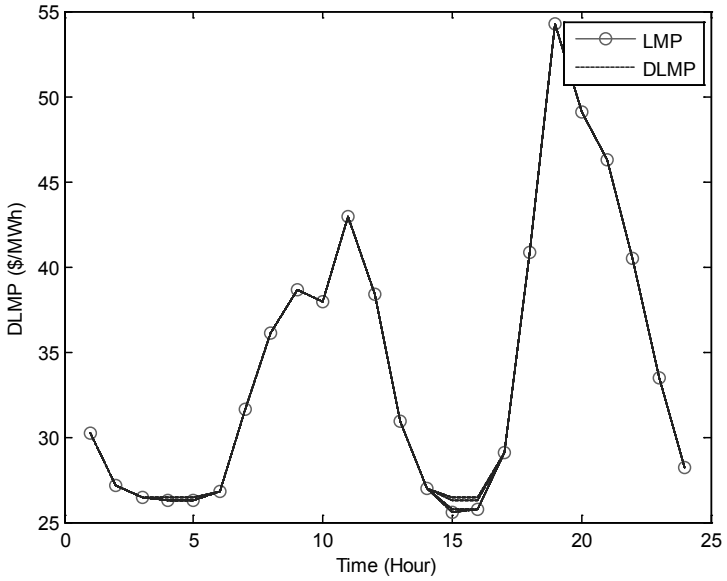

Figure 9: System LMPs and DLMPs of Case 2

5.3.3 Case Study 3

In Case Study 1 and Case Study 2, it is shown that DLMPs can alleviate the congestion induced by EVs under 100% EV penetration. In order to further illustrate the effectiveness of the proposed DLMP algorithm, studies with one projected future EV penetration levels have been conducted shown in Figure 10 and Figure 11 with 500% EV penetration.

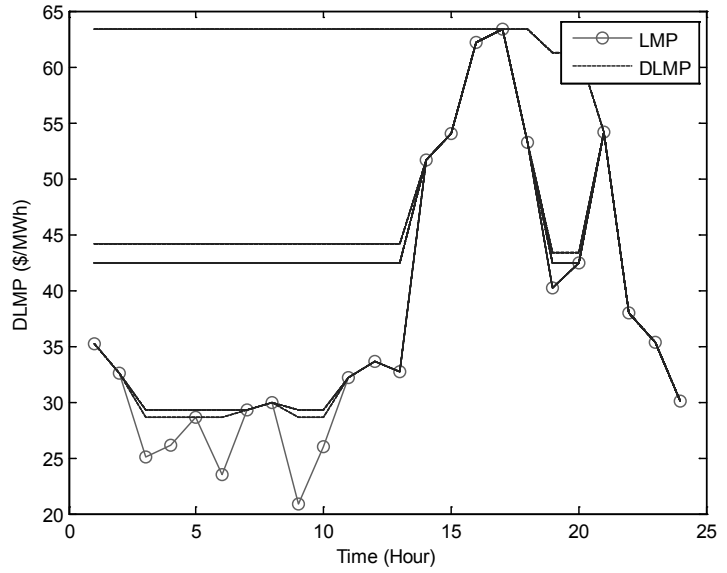

Figure 10: DLMP with 500% EV Penetration

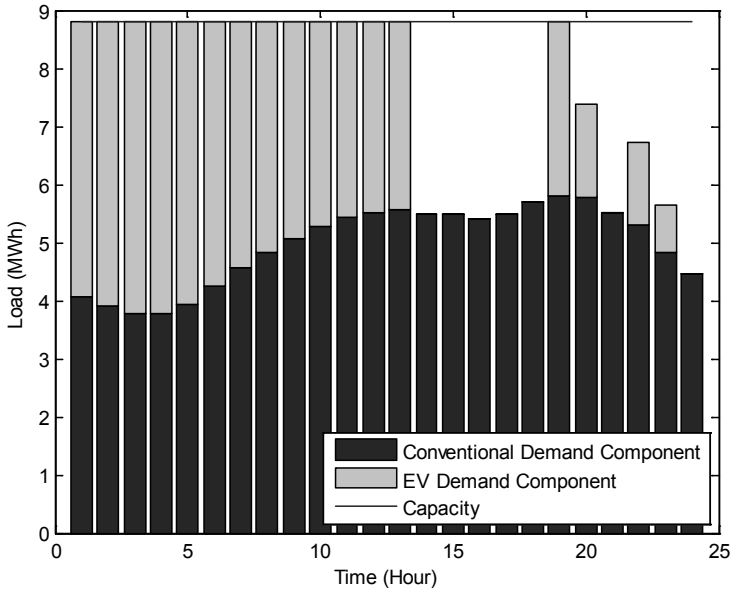

Figure 11: Line 1 Loading with 500% EV Penetration

With 500% EV penetration, the DLMPs are much higher than the system LMPs and the curve of DLMPs is flat in order to distribute the EV charging demand across time periods. Line capacity constraints are not violated shown in Figure 11. From the Case Study 3 results presented, it can be concluded that the DLMP algorithm is a promising approach even with very high EV penetration, which is very likely to come into existence in the future.

6. CONCLUSIONS

An integrated DLMP algorithm has been proposed in order to handle the congestion within electric distribution networks faced by the future energy industry. The proposed DLMP algorithm optimizes social welfare to determine the DLMPs. These DLMPs can be used as price signals for EV aggregators to menage congestion within the electric distribution networks. Case studies with the RBTS electric distribution network and the Danish driving data have shown the efficacy of the proposed DLMP concept under the assumption that EV aggregators are price takers in the DSO market and under the used demand price elasticity. In a very extreme scenario with 500% EV penetration, the congestion in the electric distribution network can be alleviated by introducing the DLMPs. Future work will mainly cover the extension of existing framework to the environment where DSO only have imperfect information on the LMPs and use the forecast LMPs in decision-making.

REFERENCES

[1] W. Kempton, and J. Tomic, "Vehicle-to-grid power fundamentals: calculating capacity and net revenue," *J. Power Sources*, vol. 144, no. 1, pp. 268–279, Jun. 2005.

[2] W. Kempton, and J. Tomic. *Vehicle-to-grid power implementation: from stabilizing the grid to supporting large-scale renewable energy*. J. Power Sources, vol. 144, no. 1, pp. 280-294, June 2005.

[3] J. Tomic, and W. Kempton. *Using fleets of electric-drive vehicles for grid support*. J. Power Sources, vol. 168, no. 2, pp. 459-468, June 2007.

[4] E. Sortomme, and M. A. El-Sharkawi. *Optimal Charging Strategies for unidirectional vehicle-to-grid*. IEEE Trans. Smart Grid, vol. 2. no. 1, pp. 131-138, March 2011.

[5] E. Sortomme, and M. A. El-Sharkawi. *Optimal Scheduling of Vehicle-to-Grid Energy and Ancillary Services*. IEEE Trans. Smart Grid, vol. 3. no. 1, pp. 351-359, March 2012.

[6] Y. Ma, T. Houghton, A. Cruden, and D. Infield. *Modeling the benefits of vehicle-to-grid technology to a power system*. IEEE Trans. Power Syst., vol. 27, no. 2, pp. 1012-1020, May 2012.

[7] G. T. Heydt. *The impact of electric vehicle deployment on load managment strategies*. IEEE Trans. Power App. Syst., vol. 1, no. 144, pp. 1253-1259, 1983.

[8] K. Clement-Nyns, E. Haesen, and J. Driesen. *The impact of charging plug-in hybrid electric vehicles on a residential distribution grid*. IEEE Trans. Power Syst., vol. 25, no. 1, pp. 371-380, February 2010.

[9] K.J. Dyke, N. Schofield, and M. Barnes. *The impact of transport electrification on electrical networks*. IEEE Trans. Ind. Electron., vol. 57, no. 12, pp. 3917-3926, December 2010.

[10] J. A. Pecas Lopes, F. J. Soares, and P. M. Rocha Almeida. *Integration of electric vehicles in the electric power system*. Proc. IEEE,vol. 99, no. 1, pp. 168-183, January 2011.

[11] M. Arindam, S. K. Kyung, J. Taylor and A. Giumento. *Grid impacts of plug-in electric vehicles on Hydro Quebec's distribution system*. *Proc.* 2010 IEEE PES Transmission and Distribution Conference and Exposition, pp. 1-7.

[12] J. Taylor, M. Maitra, D. Alexander and M. Duvall. *Evaluation of the impact of plug-in electric vehicle loading on distribution system operations*. Proc. 2009 IEEE Power & Energy Society General Meeting, pp. 1-6.

[13] O. Sundstrom, and C. Binding. *Flexible charging optimization for electric vehicles considering distribution grid constraints*. IEEE Trans. Smart Grid, vol. 3. no. 1, pp. 26-37, March 2012.

[14] N. Rotering, and M. Ilic. *Optimal charge control of plug-In hybrid electric vehicles in deregulated electricity markets*. IEEE Trans. Power Syst., vol. 26, no. 3, pp. 1021-1029, August 2010.

[15] R. D. Christie, B. F. Wollenberg and I. Wangensteen. *Transmission management in the deregulate environment*. Proc. IEEE, vol. 88, no. 2, pp. 170-195, February 2000.

[16] H. Glavitsch, and F. Alvarado. *Management of multiple congested congestions in unbounded operation of a power system*. IEEE Trans. Power Syst., vol. 13, no. 3, pp. 1013-1019, August 1998.

[17] R. N. Allan, R. Billinton, I. Sjarief, L. Goel and K. S. So. *A reliabiilty test system for educational purposes – basic distribution system data and results*. IEEE Trans. Power Syst., vol. 6, no. 2, pp. 813-820, May 1991.

[18] S. Stoft. *Power System Economics - Designing Markets for Electricity*, New York: IEEE Press & Wiley Interscience, 2002.

[19] F. Li, and R. Bo. *DCOPF-based LMP simulation: algorithm, comparison with ACOPF, and sensitivity*. IEEE Trans. Power Syst., vol. 22, no. 4, pp. 1475-1485, November 2007.

[20] J. Yang, F. Li and L. A. A. Freeman. *A market simulation program for the standard market design and generation/transmission planning*. Proc. 2003 IEEE Power Energy Society General Meeting, pp. 442-446.

[21] J. Yao, I. Adler, and S. Oren. *Modeling and computing two-settlement oligopolistic equilibrium in a congested electricity network*. Operations Research, vol. 56, no. 1, pp. 34-47, January-February 2008.

[22] T. Limpaitoon, Y. Chen, and S. Oren. *The impact of carbon cap and trade regulation on congested electricity market equilibrium*. Journal of Regulatory Economics, vol. 40, pp. 237-260, 2011.

[23] W. Hogan. *Contract networks for electric power transmission*. Journal of Regulatory Economics, vol. 4, no. 3, pp. 211-242, 1992.

[24] I. L. Azevedo, M. G. Morgan, and L. Lave. *Residential and regional electricity consumption in the U.S. and EU: how much will higher prices reduce CO2emissions*? The Electricity Journal, vol. 24, no. 1, pp. 21–29, 2011.

[25] Q. Wu, A. H. Nielsen, J. Østergaard, S.T. Cha, F. Marra, Y. Chen and C. Traeholt. *Driving pattern analysis for electric vehicle (EV) grid integration study*. in Proc. Of 2010 IEEE PES Conference on Innovative Smart Grid Technologies Europe, pp. 1-6.

Volume III

A Distribution-Class Locational Marginal Price (DLMP) Index for Enhanced Distribution Systems

Oluwaseyi W. Akinbode
Kory W. Hedman
Arizona State University

Information about this project

For information about Volume III contact:

Kory W. Hedman
Arizona State University
Department of Electrical Engineering
P.O. BOX 875706
Tempe, AZ 85287-5706
Phone: 480 965-1276
Fax: 480 965-0745
Email: kory.hedman@asu.edu

Power Systems Engineering Research Center

The Power Systems Engineering Research Center (PSERC) is a multi-university Center conducting research on challenges facing the electric power industry and educating the next generation of power engineers. More information about PSERC can be found at the Center's website: http://www.pserc.org.

For additional information, contact:

Power Systems Engineering Research Center
Arizona State University
527 Engineering Research Center
Tempe, Arizona 85287-5706
Phone: 480-965-1643
Fax: 480-965-0745

Notice Concerning Copyright Material

Table of Contents

List of Tables

List of Figures

Nomenclature

AMI	Advanced Metering Infrastructure
b_d	Price associated with load bid *d*
B_k	Susceptance of line *k*
c_g	Linear operating cost of generator *g*
CBL	Customer baseline
COS	Cost-of-service regulation
CPP	Critical peak price
DCOPF	Direct current optimal power flow
DER	Distributed energy resources
DG	Distributed generation
DLMP	Distribution-class Locational Marginal Price
DMS	Distribution management system
D_n	Real power demand of inelastic load at bus *n*
$D_{n,d}$	Cleared real power demand quantity of bid *d* of price responsive load at bus *n*
DR	Demand response
DSM	Demand side management
EISA	Energy independence and security act
ESS	Energy storage system
F_k^+	Dual variable of line *k*'s upper line flow limit constraint (flowgate marginal price)
F_k^-	Dual variable of line *k*'s lower line flow limit constraint (flowgate marginal price)
FR	Flat rate
G_k	Conductance of line *k*
G_n	Set of generators at bus *n*
IEEE	Institute of Electrical and Electronics Engineers
IPP	Independent power producer
ISO	Independent system operator
KKT	Karush Kuhn Tucker
$k(n,;)$	Set of lines with bus *n* as the receiving bus
$k(;,n)$	Set of lines with bus *n* as the sending bus
LMP	Locational marginal price
LP	Load point
MILP	Mixed-integer linear programming
OPF	Optimal power flow
P_g	Real power output of generator *g*
P_g^{max}	Maximum real power capacity of generator *g*
P_g^{min}	Minimum real power capacity of generator *g*
P_k	Power flow on line *k* in the DCOPF model
$P_k^{\max}$	Maximum power flow limit of line *k*
P_k^{min}	Minimum power flow limit of line *k*
P_k^{mn}	Alternating current power flow from bus *n* to bus *m* on line *k*
P_k^{nm}	Alternating current power flow from bus *m* to bus *n* on line *k*
P_n^L	Total losses on all lines connected to and delivering power to bus *n*

P_n^R	Real power injected at bus *n* and withdrawn at reference bus *R*
$P_n(w)$	Real power injection at bus *n* as a function of *w*
PRL	Price responsive load
$PTDF_{k,n}^R$	Power transfer distribution factor
Q_g	Reactive power output of generator *g*
Q_g^{max}	Maximum reactive power capacity of generator *g*
Q_g^{min}	Minimum reactive power capacity of generator *g*
Q_{L_n}	Reactive power load at bus *n*
$Q_n(w)$	Reactive power injected at bus *n* as a function of *w*
RBTS	A distribution system test bed, 'Roy Billinton Test System'
RES	Renewable energy standard
RPS	Renewable portfolio standard
RTO	Regional transmission organization
RTP	Real-time price
r/x	Ratio of conductor resistance to reactance
S_k	Apparent power flow on line *k*
S_k^{max}	Maximum apparent power flow capacity of line *k*
S_k^{min}	Minimum apparent power flow capacity of line *k*
T	Period index
TOU	Time-of-use rate
u_i^{k+}	Binary variable of positive orthant segment *i*
u_i^{k-}	Binary variable of negative orthant segment *i*
V_m	Voltage magnitude of designated sending end bus *m*
V_n	Voltage magnitude of designated receiving end bus *n*
V_n^{max}	Maximum voltage magnitude at bus *n*
V_n^{min}	Minimum voltage magnitude at bus *n*
W	Bus voltage magnitude and angle variables of the power flow equation
α_i	Slope of segment *i*
γ_n	Dual variable of piecewise linear loss equation constraint of bus *n*
δ_g^+	Dual variable of generator *g*'s power output upper limit constraint
δ_g^-	Dual variable of generator *g*'s power output lower limit constraint
ξ_k	Dual variable of line *k*'s line flow equation constraint (susceptance marginal price)
θ_i^{k+}	Length of positive orthant segment *i*
θ_i^{k-}	Length of negative orthant segment *i*
$\theta_i^{\max}$	Maximum length of segment *i*
θ_m	Voltage angle of designated sending end bus *m*
θ_n	Voltage angle of designated receiving end bus *n*
θ_{nm}	Voltage angle difference between bus *n* and bus *m*
θ_{nm}^{max}	Maximum voltage angle difference between bus *n* and bus *m*
θ_{nm}^{min}	Minimum voltage angle difference between bus *n* and bus *m*
λ_n	Dual variable of bus *n*'s node balance constraint, i.e., LMP at bus *n*
Λ^+	Set of lines connected to a bus with a positive LMP
Λ^-	Set of lines connected to a bus with a non-positive LMP

μ_k	Dual variable of line k's angle difference approximation constraint
ρ_i^{k+}	Dual variable of positive orthant segment i's upper limit constraint
ρ_i^{k-}	Dual variable of negative orthant segment i's upper limit constraint

Chapter 1. Introduction

1.1 Research Premise

As competition became increasingly valued in the U.S. electric energy industry in the late 1990's and the early 2000's, spot pricing of electricity, proposed in [1], gained in popularity. Today, spot pricing in the form of locational marginal prices (LMP) has been implemented for transmission systems operated under the U.S. competitive bulk energy markets. As evidenced by its prevalence, the LMP index has been beneficial to both market and system operations. In market operation, the LMP index is an economically efficient price signal that can be used to incentivize market participant to behave optimally and in a manner that benefits social welfare [2]-[6]. In system operation, the LMP index is a valuable market-based tool for transparently managing congestion in the transmission network [3], [7]-[10].

Despite its benefit to the transmission system, LMPs are not used in the distribution system. The most prevalent distribution system prices, e.g., flat rates (FR) and time-of-use rates (TOU), are also independent of transmission system LMPs. This stems partly from the differences in the design and the operational paradigm of both systems. Unlike the transmission system, which is a highly meshed network and is routinely congested, most distributions systems are operated radially [46] (even though they may be designed as networks [32]) and have feeders and equipment that are overbuilt and oversized to avoid congestion [42], [43]. Similarly, while generators provide the transmission system a substantial amount of price sensitive and controllable resources, the distribution system has very limited generation within it and loads are treated as highly or perfectly inelastic. Consequently, operation of the contemporary distribution system is not usually characterized by the active power flow management and control and short-term economic efficiency that are major parts of the operational paradigm in the transmission system. In certain municipals, the transmission system LMP at the distribution proxy is used to price energy for some large industrial and commercial facilities as real-time prices (RTP) [66], [67]. Such prices, however, do not take into consideration the particulars of the distribution network.

With the smart grid initiative, the distribution system is evolving. The future distribution grid may look more like the transmission system with resources, such as price responsive loads (PRL), energy storage systems (ESSs), and distributed generators (DG) [43], [47], [53]. The smart grid initiative is expected to enhance the future distribution grid with the control and communications infrastructure to support such functions and applications [45], [47], [53]. The level of generation in the enhanced distribution system may be significant enough that future distribution grids that have a meshed network topology [43], [46] may be congested.

1.2 Report Scope

This report proposes the application of the LMP concept to the enhanced distribution system as a control signal to incentivize expected price sensitive and controllable distribution resources to behave optimally in a way that benefits economic efficiency and system operations both at the distribution and at the transmission level. The aim of this report is to define the distribution-class LMP (DLMP), develop its calculation and application framework, and demonstrate its advantage over existing distribution pricing schemes. The work discusses the properties of the DLMP and its benefits to economic efficiency and systems operations both at the transmission

and the distribution systems level. The work also discusses the framework for calculating the DLMP, which includes a two-staged optimization problem. Calculating the DLMP via a two-staged problem helps overcome the computational intractability that could possibly result from solving a unit commitment or an optimal power flow (OPF) problem for a single model of the transmission and the distribution systems. An iterative framework, between the stages of the optimization problem, is implemented to ensure accurate modeling of the price sensitive distribution system resources (DSR) and the distribution network conditions in one of the stages while the other stage captures the transmission system and its resources. While attractive, convergence of the iterative approach to a solution or to the optimal solution is not guaranteed. This convergence issue is included in the iterative framework discussions. A sampling approach is used in place of the iterative approach is some of the studies in this report to overcome the convergence problem of the iterative framework.

The two stages of the optimization process use a direct current optimal power flow (DCOPF) formulation that endogenously captures real power losses. The formulation overcomes the arbitrariness that results from using the slack or distributed slack bus method for approximating losses in a DCOPF formulation by using piecewise linear loss functions to approximate the non-linear real power loss function. Under certain conditions, such as the occurrence of a non-positive DLMP or LMP, the loss approximation technique incorrectly creates non-physical artificial losses to improve the objective function. The lossy DCOPF formulation and its breakdown are explained in detail in this work.

As a way of setting up the illustration of the advantages of the DLMP, the work discusses cost-of-service (COS) regulation ratemaking and various rates structures that can be obtained in the contemporary distribution system. The contemporary rate structures are compared to the DLMP in terms of the DSR behavior incentivized and economic efficiency.

The DLMP is expected to benefit economic efficiency and reliability at both the distribution and the transmission system level by aligning the behavior of price sensitive DSRs with system operational objectives. The DLMP will incentivize optimal consumption from PRL, optimal generation from DGs and optimal operation of ESSs in the enhanced distribution grid. Optimally coupling the transmission and the distribution system, achieved by the iterative process, means the efficiency gains in the distribution system can also be translated into efficiency gains at the bulk energy system level. The optimal coupling could enable the utilization of DSR for ancillary services. Accurately representing price sensitive distribution load in the bulk energy market could also positively impact market efficiency: price sensitive demand is the greatest cure for the exercise of market power.

1.3 Organization of the Report

This report is organized into seven chapters. The goal in Chapter 2 is to provide readers with the knowledge of the concepts that are critical to understand the technical details in the later chapters and the background to understand the motivation of this report. Chapter 2 provides information on LMPs and the OPF formulations used for calculating LMPs. Chapter 2 also provides information on COS regulation ratemaking and contemporary rate structures in the distribution system, the smart grid initiative, and a literature review of contemporary works on nodal pricing in the distribution system.

The focus in Chapter 3 is on the DLMP. The chapter defines the DLMP and discusses its properties and calculation and application framework. The chapter also discusses economic efficiency and the properties of the DLMP that provide the price signal the capability to improve economic efficiency as compared to contemporary distribution pricing schemes. The chapter argues strongly against perceived drawbacks, such as unfairness of locational prices in the distribution system and price volatility of the DLMP, and discusses the ultimate environment under which the DLMP is most applicable.

The mathematical optimization problem for calculating the DLMP is developed in Chapter 4. The DLMP is calculated based on a DCOPF formulation that uses piecewise linear functions to approximate real power losses. The piecewise linear approximation technique and the lossy DCOPF formulation are discussed. The breakdown of the loss approximation technique, under the condition of the occurrence of non-positive DLMPs/LMPs, is discussed, proven theoretically using duality theory and the Karush Kuhn Tucker (K.K.T.) conditions, and illustrated numerically. A mixed integer linear programming (MILP) based formulation that can be used when the breakdown occurs is presented in the chapter.

The lossy DCOPF formulation developed in Chapter 4 is used to calculate and numerically illustrate the DLMP in Chapter 5. DLMPs are calculated for a traditional distribution system, an enhanced distribution system with PRLs and an enhanced distribution system with congestion. The results of the study on the enhanced distribution system with PRL are used to illustrate the superiority of the DLMP to average prices distorted by cross-subsidies. The results are also evaluated for social welfare and used to illustrate the importance of the iterative framework.

Chapter 6 presents a comparison of the DLMP to a RTP, a TOU and a FR. The price signals are compared based on PRL consumption in a meshed distribution system with and without congestion. The flexibility of the PRLs is varied to study the impact of the inaccuracy of the RTP, TOU and FR as demand becomes more flexible. A study is also conducted on a congested distribution system to demonstrate the superiority of the DLMP in terms of internalizing the distribution system network and generation conditions and efficiently aligning the behavior of controllable resources with system operational objectives.

Chapter 7 is a concluding chapter. It provides a summary of the work in this report and discusses future work. Tables of the data used in conducting the various simulations in the report are in Appendix A.

Chapter 2. Background

This chapter provides the background knowledge necessary to understand the technical details in the subsequent chapters. The information in this chapter also provides context for this report. The chapter describes the LMP concept in Section 2.1 and the optimal power flow problem used for calculating LMPs in Section 2.2. Cost-of-service ratemaking and contemporary rate structures in the distribution system are examined in Section 2.3 and Section 2.4. A discussion of the smart grid initiative is provided alongside a discussion and literature review of contemporary work on the subject of distribution system nodal prices in Section 2.5. Section 2.6 is a concluding paragraph.

2.1 Locational Marginal Pricing (LMP)

The concept of pricing electricity based on the location and time of injection and withdrawal was proposed in [1]. In this work, Schweppe *et al.* stated the main goals of proposing the concept as:

i. economic efficiency
ii. equity
iii. utility control, operation, and planning
iv. freedom of choice.

By economic efficiency, the authors envisaged using spot prices to incentivize a customer's electricity usage to match the marginal cost of its electric utility. By equity, a customer's price reflects what it costs a utility to serve the customer, i.e., no or reduced cross-subsidy between customers. By utility control, operation and planning, the authors envisioned spot prices to reflect system conditions and the action motivated to be aligned with system control, operation, and planning objectives. By freedom of choice, the authors envisaged providing customers the freedom to choose how they use electricity, cost, and reliability. Owing to these benefits, particularly economic efficiency, equity, and control, operation and planning, and the deregulation of the utility industry, spot pricing of electricity in the form of LMP signals have become part of the design of competitive bulk energy markets in the U.S. [11]-[15].

A LMP is the cost to optimally deliver an increment of energy to a specific location on a grid while respecting the system's security and generation constraints. Although it is often thought of as the cost to supply an additional MW of load, the incremental energy that an LMP prices is not necessarily a MWh and it could be a negative increment, i.e., a decrement. A LMP is an economic signal used for system and market operations. It is calculated for a specific state of a power system and it reflects network conditions and supply and demand characteristics [3]. A LMP at a node on the grid captures the short-run marginal cost to generate an increment of energy and the effect on system congestion and system losses of delivering the increment of energy to a specific node on the grid.

Capturing the effect of the incremental consumption at a node, on system congestion and losses, provides the LMP its nodal property. That is, LMPs in the same system can vary from one node to another as a result of the contribution to losses and to congestion of the incremental consumption at different nodes. Congestion can occur in a system as a result of binding network se-

curity constraints, such as branch thermal limits or transient stability limits. If congestion occurs in a system, the cheapest available generator(s) will be prevented from supplying the incremental energy to be delivered to a node. Instead, the incremental energy must come from a more expensive generator or a combination of generators. The LMP at a node, whose incremental consumption impacts congestion, will be different from the LMP of nodes whose incremental consumption can be supplied by the cheapest generator available. Hence, LMP separation as a result of a binding network constraint can be said to reflect the cost to re-dispatch a system while still satisfying all network constraints and reliability requirements. LMP separation as a result of losses reflects the cost to procure energy losses, as a result of the impedance of system components, incurred to deliver an increment of energy to a specific node. If a system has no congestion and losses are ignored, as is in a lossless DCOPF, then the LMPs in the system will be the same at every node.

The nodal property of the LMP is very important because it provides the LMP its capability to reflect network conditions and its capability to price the individual contribution of consumption at a node to system conditions. As a result of the nodal property, the LMP can be used to incentivize price sensitive resources at a node to behavior appropriately in a manner that benefits efficiency and system reliability. This is an important benefit of the LMP to short-term operations and it is why LMPs are sometimes referred to as a tool for managing system operations. As an illustration, congestion in a system can make the LMP at a node very high, to incentivize price sensitive loads at the node to reduce consumption and generators at the node to increase their output in order to respect the limit of a constrained branch. The nodal property also provides important, albeit limited, economic signal in terms of long term planning and investment. For example, the LMP separation in a system can be used to identify where upgrades are needed and it could be a signal for locating generation resources. A generator may make more money by locating at a node with perpetually high LMP and LMPs can signify the most effective node to locate a resource to relieve congestion. When scarcity occurs, high LMPs can also indicate the need for entry of new resources into a market.

2.2 Optimal Power-flow (OPF)

LMPs are obtained as the dual variables of the node balance constraints of an optimal power-flow (OPF) problem. An OPF problem is an economic dispatch problem that takes into consideration operational constraints such as branch thermal limits. The goal of an OPF problem is to optimally select some controllable or independent variables to optimize a benefit within the limits of reliable operation. For an electricity market framework, the controllable variables include generator outputs and the objective is usually to maximize social welfare. If demand is elastic, then load consumption is also a controllable variable. Social welfare, which will be discussed in Chapter 3, is a measure of the benefits to both consumers and producers for participating in a market [4]. In the OPF framework, social welfare, also known as market surplus, is often evaluated based on the bids and offers by loads and generators respectively.

Equation (2.1) represents the objective function of an OPF problem where loads submit monotonically non-increasing step-wise demand bids and generators submit monotonically non-decreasing step-wise offer curves. The first term of the equation is the total consumer bid value. It is the sum, for all load bids d, of the product of the price associated with a load bid (b_d) and the cleared demand of the load bid (D_d). The bid price for a load represents the maximum value the

load places on consumption at a certain level. The second term is the total generation cost. It is the sum, for all generators g, of the product of the marginal cost (c_g) of a generator and the real power output (P_g) of the generator. An OPF problem with (2.1) as its objective is sometimes referred to as bid cost maximization problem, which is said to maximize the social welfare (when entities bid honestly) or the market surplus (when there is strategic bidding),

$$Maximize: \sum_{d} b_d D_d - \sum_{g} c_g P_g. \tag{2.1}$$

The representation in (2.1) assumes that demand is price responsive. Often times, electricity demand is viewed as perfectly inelastic with a fixed consumption regardless of price. In such a scenario, the first part of (2.1) is fixed as b_d for a perfectly inelastic load is also assumed fixed at a very high value of lost load (VoLL). For perfectly inelastic loads, the first part of (2.1) can be ignored or removed from the objective function. What is left is the maximization of a negative function, which is the same as minimizing the function. The objective function can, thus, be re-written as in (2.2) where generation cost is minimized. An OPF with (2.2) is referred to as a generation cost minimization problem,

$$Minimize: \sum_{g} c_g P_g. \tag{2.2}$$

The limits of reliable operation are defined in an OPF formulation by the constraints of the optimization problem. In general, these limits can be broadly categorized into three groups: power or node balance constraints, network constraints and generator constraints. Power balance constraints are equality constraints used to enforce conservation of energy. A power balance constraint requires the net power in a system to be zero, i.e., generation is equal to the sum of load and losses. Power balance constraints are usually enforced at each node in a system; hence, the name node balance constraint is frequently used. A node balance constraint enforces conservation of energy through Kirchhoff's Current Law (KCL). It forces the net power at a node to be zero. Network constraints are used to impose limits on network parameters, such as bus voltage magnitudes and angles, and line flows. By imposing limits on network parameters, network constraints define the reliability bounds of network elements and the network as a whole for operational purposes. For example, line flow limits are proxies for the thermal capacity of network elements and voltage angle limits are usually proxies for transient stability. Similar to network constraints, generator constraints define the reliable operating limits of the generators in a system.

OPF problems can be classified into two types: the alternating current OPF (ACOPF) and the DCOPF. While the objective function for both are the same and both OPF formulations have constraints that fall into the three categories of constraints discussed in the preceding paragraph, they use different power flow equations in the constraints. As the names imply, the ACOPF uses the AC power flow equations in (2.3) and (2.4). The DCOPF uses a linearized approximation of (2.3): shown in (2.15),

$$P_k^{nm} = |V_m^2|G_k - |V_m||V_n|(G_k \cos(\theta_m - \theta_n) + B_k \sin(\theta_m - \theta_n)) \tag{2.3}$$

$$Q_k^{nm} = -|V_m^2|B_k - |V_m||V_n|(G_k \sin(\theta_m - \theta_n) - B_k \cos(\theta_m - \theta_n)). \tag{2.4}$$

A generalized ACOPF formulation is shown in (2.5)-(2.12) [9]. Equation (2.5) is the objective function. Equation (2.6) and (2.7) are the node balance constraints. Equation (2.6) is the real power node balance constraint and (2.7) is the reactive power node balance constraint. Equations (2.8), (2.9) and (2.10) are the network constraints. Equation (2.8) is the proxy for the thermal limits of network branches. Equation (2.9) is the limit on bus voltage magnitudes and (2.10) is a proxy for transient stability limit. Equation (2.11) and (2.12) are the generator real and reactive power output limits. Note that *w* in the formulation represents the bus voltage magnitude and angle variables of the power flow equations,

$$Minimize: \sum_{g} c_g P_g \tag{2.5}$$

$subject\ to$:

$$P_n(w) + D_n - \sum_{g \in G_n} P_g = 0 \qquad \forall n \tag{2.6}$$

$$Q_n(w) + Q_{L_n} - \sum_{g \in G_n} Q_g = 0 \qquad \forall n \tag{2.7}$$

$$S_k^{min} \le S_k \le S_k^{max} \qquad \forall k \tag{2.8}$$

$$V_n^{min} \le V_n \le V_n^{max} \qquad \forall n \tag{2.9}$$

$$\theta_{nm}^{min} \le \theta_{nm} \le \theta_{nm}^{max} \qquad \forall n \tag{2.10}$$

$$P_g^{min} \le P_g \le P_g^{max} \qquad \forall g \tag{2.11}$$

$$Q_g^{min} \le Q_g \le Q_g^{max}. \qquad \forall g \tag{2.12}$$

As stated earlier, the DCOPF is a linear approximation of the ACOPF problem. To obtain the DCOPF, the AC real power flow equation is linearized by recognizing the following about the transmission system:

i. branch reactances are much larger than their resistances; therefore, the conductance term in the AC real power flow equations, (G_k), is approximately zero: this approximation essentially renders the DCOPF lossless
ii. bus angle differences are small; therefore, $\cos\theta_{nm}$ is approximately 1 and $\sin\theta_{nm}$ is approximately θ_{nm}
iii. bus voltage magnitudes ($|V_n|$ and $|V_m|$) are approximately 1 p.u.
iv. reactive power is ignored in the DCOPF as a result of the first three assumptions: reactive power generation is scheduled by system operators as needed to maintain a stable operating system

The preceding assumptions are used to develop the DC approximation of the real power flow equation and the DCOPF. Note that reactive power load is also ignored in the DCOPF formulation. A DCOPF formulation is shown in (2.13)-(2.18). Equation (2.13) is the objective function. Equation (2.14) is the node balance constraint. The first and the second terms in (2.14) represent the power flowing into a bus and the power flowing out of a bus respectively. Equation (2.15) is the DC approximation of the line flow equation. P_k, in (2.15), is the DC approximation of the real

power flow from a bus *m* to a bus *n*. Equation (2.16) is the real power branch flow limit and (2.17) is the transient stability limit proxy. Equation (2.18) is the generator real power output limit,

$$Minimize: \sum_{g} c_g P_g \tag{2.13}$$

$subject\ to$:

$$\sum_{\forall k(n,;)} P_k - \sum_{\forall k(;,n)} P_k - D_n + \sum_{g \in G_n} P_g = 0 \qquad \forall n \tag{2.14}$$

$$B_k(\theta_n - \theta_m) - P_k = 0 \qquad \forall k \tag{2.15}$$

$$P_k^{min} \leq P_k \leq P_k^{max} \qquad \forall k \tag{2.16}$$

$$\theta_{nm}^{min} \leq (\theta_n - \theta_m) \leq \theta_{nm}^{max} \qquad \forall n \tag{2.17}$$

$$P_g^{min} \leq P_g \leq P_g^{max}. \qquad \forall g \tag{2.18}$$

The DCOPF formulation in (2.13)-(2.18) can be re-formulated as in (2.19)-(2.23). In (2.19)-(2.23), the DC approximation of the power flow equation is further approximated using power transfer distribution factors (PTDFs). A PTDF ($PTDF_{k,n}^R$) is the linear sensitivity of the power flow on a line *k* to the real power injected at a bus *n* and withdrawn at a reference bus *R*. Equation (2.21) is a power balance constraint,

$$Minimize: \sum_{g} c_g P_g \tag{2.19}$$

$subject\ to$:

$$P_n^R + D_n - \sum_{g \in G_n} P_g = 0 \qquad \forall n \tag{2.20}$$

$$\sum_{n} P_n^R = 0 \tag{2.21}$$

$$P_k^{min} \leq \sum_{n} PTDF_{k,n}^R \cdot P_n^R \leq P_k^{max} \qquad \forall k \tag{2.22}$$

$$P_g^{min} \leq P_g \leq P_g^{max}. \qquad \forall g \tag{2.23}$$

The ACOPF, as a result of the AC power flow equation, is non-linear and non-convex and is as a non-linear programming problem. The DCOPF, with a linear objective function, is linear and convex, thereby making it a linear programming problem. The differences as a result of the power flow equation account for the advantages of the DCOPF over the ACOPF in terms of computation time and convergence. Non-linear programming problems are difficult to solve. According to [5], the computation time of an ACOPF problem could be 60 times greater than the computational time of a comparable DCOPF problem and the ACOPF often fails to converge to a solution or the global optimal solution. The ACOPF, however, is a full representation on the characteristics of the power system while the DCOPF is an approximate representation.

LMPs are the dual variables of the node balance constraint of either an ACOPF or a DCOPF problem. As such, LMPs represent the change to the objective function as an incremen-

tal change is made to the right hand side of the node balance constraint. With a bid surplus maximization objective, the LMP reflects the change in the market surplus as a change is made to the right hand side of the node balance constraint and the change in generation cost for a cost minimization problem. LMPs obtained from an ACOPF formulation will capture marginal cost of energy, congestion, and losses. LMPs obtained from the standard DCOPF will not have a marginal loss component, since the standard DCOPF is a lossless model. Loss approximation for a DCOPF formulation is discussed in Chapter 4.

2.3 Cost-of-Service Regulation Ratemaking

Electric utility companies are operated in a regulated environment. Under the "regulatory compact", utility companies, in exchange for being appointed as a franchised monopolies, are obligated to serve all customers in their service area, are subject to regulatory oversight that determines, amongst other things, distribution system rates and rate structures, and are allowed a fair rate-of-return on prudent investments [57], [60]. Ratemaking under this construct is termed the cost-of-service (COS) or rate-of-return regulation. COS regulation is governed by the notion that rates must be fair, reasonable, and non-discriminatory and utilities must be allowed a fair return on their investment [58] (see the classic work of J.C. Bonbright [56] for other objectives). Two issues are determined in a rate case under the COS regulation construct: the revenue requirement of a utility company and the rates and rate-structures to recover the revenue requirement [57] .

Revenue Requirement

The revenue requirement of a utility represents the best estimate, in the regulator's judgment, of the revenue that must be collected to recover the costs incurred by a utility to serve its customers and to provide a reasonable return on the utility's capital investments. A utility's revenue requirement includes the "prudent and necessary" operating costs required to service customers and a reasonable return on its rate base. The operating costs of a utility are expenses on labor, maintenance, fuel, insurance, and other recurring costs directly related to providing service [60]. It also includes expenses, such as taxes, asset depreciation, and franchise fees, which are not directly related to providing service [59], [60]. A utility is only allowed to recover its operating expenses. It is not allowed to make a return on them. Instead, a utility receives a reasonable return on its rate base.

A rate base is the value of a utility's asset minus the depreciated value of such assets [59]. Establishment of the revenue requirements of a utility can be contentious especially in regards to the investments that can be included in the rate base. In general, capital assets, such as transmission and distribution lines, transformers, fleet vehicles and power plants, are included in a rate base. The assets must, however, be "used and useful". The "used and useful" concept requires an asset to be in use for providing services and for the asset to be a prudent and necessary investment such that disruption of service may occur without it [59], [60]. In some municipals, utilities are allowed to include the carrying cost of capital during construction in their rate base once a facility meets the "used and useful" criterion. This concept is termed allowance for use during construction (AFUDC). For projects requiring huge capital burden, a utility could be allowed to include in its rate base, the carrying cost of capital while construction is still in progress. The concept is termed construction work in progress (CWIP). AFUDC and CWIP are controversial and may not be allowed in certain jurisdictions [60]. A rate base could also include the carrying

capital a utility must borrow to meet its obligations before customers pay. A regulator determines the fair rate-of-return allowed on a rate base. The rate must take into cognizance a utility's capital structure, equity and debt, and the fact that the costs of both are different. The rate-of-return a utility is allowed must be such that it can continue to attract capital. According to [57], it is theoretically the rate that would be demanded for an investment of similar value and risk in a competitive market.

The product of allowed rate-of-return and the established rate base is added to a utility's operating expenses to obtain the utility's revenue requirement. It is established for a test year, which could be an actual year in the past (based on utility records) or a year in the future (based on an extensive budgeting process) [60]. In both cases, changes are made to reflect additional costs since the test year, if established based on a past year, or expected costs by the test year, if established based on a future year. The test year is used to determine if rates need to be increased or decreased. The rate case process under the COS regulation construct is lengthy and rates are established for long periods, e.g., a year to three years.

Rate Design

Once the revenue requirement of a utility has been established, rates are designed to recover the revenue. Rate design starts with the determination of customer classes. Customer classes vary from state to state and could include residential classes, general service classes, and agricultural classes. A rate class must be determined based on a rational set of commonalities between the rate class members. For example, the homogenous characteristic could include load characteristics, delivery voltage, and end use. The revenue requirement is allocated amongst the customer classes. Before allocation, the revenue requirement of a utility is functionalized. Functionalization is the division of the revenue requirement based on the functional areas of operations of the utility where a cost is incurred. For example, the revenue requirement can be functionalized into generation, transmission, distribution, and metering and services costs [62]. The functionalized revenue requirement may be further classified based on energy consumption, number of customers, and peak demand. There are several methods and approaches [62] for allocating the functionalized and classified revenue requirement between customer classes. Cost causation is usually kept in mind. Some costs are easy to allocate as only a certain class of consumers are responsible for them. For example, the cost of low voltage distribution lines and transformers that serve residential customers may not be allocated to large industrial users that are serviced at higher voltages. The challenging part of allocating a revenue requirement is the costs that multiple classes benefit from. Representatives of each rate class request for the method that favors their class. In general, residential and small commercial users greatly outnumber industrial users and both classes are responsible for a high percentage of peak demand. Hence, representatives of industrial users advocate for allocating more cost based on number of customers and peak demand [60]. On the other hand, cost allocation based on energy consumption fall equally of all users. Consequently, representatives of residential customers advocate for allocating more of the revenue requirement based on energy consumption.

The revenue allocated to each customer class is divided amongst the customers in the class. For the residential classes, the rates are usually divided into energy and customer charges with the demand related revenue requirement included in the energy or the customer related charges. This is a two-part rate [61]. Demand related revenue requirements are included in either customer charges or in energy charges because residential customers may not have meters capa-

ble of measuring peak demand. For other classes, the rates could be broken into demand charges, energy charges, and customer related charges. This is a three-part rate [61].

Deficiencies of the Cost-of-Service Regulation Construct

The COS regulation construct provides protection for consumers and utilities alike. In theory, it offers price protection (regulation) for consumers and prevents utilities from making excessive profits that will unduly increase costs to consumers. It offers utilities the opportunity to make a fair rate on their investments and it focuses heavily on revenue recovery. Unlike in a competitive environment, however, the COS regulation construct offers only a weak incentive for efficiency. The construct offers little incentive to reduce cost. A utility, whose return is dependent of its rate base and whose cost of capital is less than the rate-of-return, has the incentive for a high rate base, i.e., to overinvest. This is termed the Averch-Johnson effect (see [65]). A regulator may not be in a position to always identify overinvestment. Similarly, there is little incentive for utilities to reduce operating expenses under COS regulation: expenses are passed on to the customers. For a utility that also has non-regulated businesses, expenses, such as cost of corporate liability insurance and headquarters facilities, could be shifted from the competitive side to the non-competitive side of the business [59], [60]. The COS regulation process is also very contentious. A commission has to balance competing interests and its decision may not always be purely technical. For example, there could be political considerations, such as keeping rates low for residential customers who vote.

Even if it were possible to do away with the deficiencies that arise with the implementation of the COS regulation, as discussed in the preceding paragraph, COS regulation cannot match the ability of competitive markets to keep prices at marginal cost and to minimize cost. In theory, COS regulation can be effective in keeping prices at marginal cost or at minimizing cost: it cannot do both well at the same time [2]. In order to keep prices at marginal cost, regulators have to ensure that the revenue recovered, including the cost of capital, is exactly the cost incurred. With such an objective, however, a utility has no incentive to reduce cost since such efficiency gains are given to the consumer. On the other hand, price caps can be imposed. The price cap incentivizes a utility to keep costs low. A utility keeps whatever efficiency saving it makes by keeping costs below the price cap. Price caps, however, have to be set higher than the marginal cost; otherwise, the regulator risks bankrupting the utility. What is obtained in practice is a mix of both. COS regulation is conducted with focus on keeping prices down [2]. Since the rate case process takes a very long time, prices are set for multiple years and must take into consideration the length of time the prices are in place. This result is a bit of price cap even when the regulator is attempting to keep prices close to marginal costs [2].

2.4 Distribution System Rate Structures

Several rate structures arise from the COS regulation construct. The most prevalent include the flat rate (FR), the block rate, and the time-of-use rate (TOU). The FR charges a uniform price per kWh regardless of the consumption level and the time of consumption. The block rate charge a different price as the consumption level of a customer passes a particular threshold. There are two major types of block rates: declining and inverted block rate. Rates reduce as consumption increases in a declining block rate structure, i.e., the rate for each block of consumption level decreases as consumption increases. Declining block rates were used in the early history of the electric utility industry to incentivize electricity applications, such as refrigeration [61]. They

are still used today for a similar purpose. For example, a utility with summer-peaking load and excess capacity in the winter may use the declining block rate to incentivize electric heating [61]. The inverted block rate is the opposite of the declining block rate: rates increase as consumption increase. The inverted block rate is an attempt to incentivize efficient consumption.

The FR and block rates are simple rates that are easy to understand and are easy and cheap to implement. They are, however, determined with a heavy focus on revenue recovery. A rate can do more than recover costs, i.e., a rate can be used to incentivize other objectives. Prices in general are used to incentivize economic efficiency and prices in the distribution system should also be used for the same purpose, in addition to revenue recovery. A distribution system price should be able to incentivize consumption from the most willing consumer (efficient allocation of scare resources in an economy), reduce operation cost in the short-term (generation or fuel cost) and incentivize efficient investment in the long term (efficient mix of generators and optimal transmission and distribution investment).

In general, rates determined based on the COS construct are incapable of effectively achieving economic efficiency. Apart from the attendant problems discussed in the previous section, rates under the COS construct are average rates and are applied to all the customers in the same rate class. While a rate class is supposed to group customers with similarities together, customers in the same rate class could still have different consumption patterns, impact system operation differently, and have different individual preferences for electricity consumption [64]. Average prices that do not take into consideration the individual impact or cost of a load to the system result in cross-subsidies between customers [1], [64]. Some customers pay more than their cost to the system while others pay less. Cross-subsidies occur within the same rate class and it can also occur between rate classes. It distort prices and sends improper signals to consumers. Average rates applied to all customers in the same class also do not provide customers the choice to determine the appropriate level of risk, in terms of price volatility and reliability, they would like to be exposed to [1], [64].

Rates under the COS construct are also in place for a long period of time and are mostly determined based on embedded costs. They do not reflect the true cost of consumption. Hence, they cannot be used to achieve allocative efficiency for short-term operation. The contemporary distribution system is a good illustration of this point. Customers under a flat or block rate pay the same price regardless of time of consumption. The cost to the system during a peak period is highly unlikely to be the same cost during the off-peak period. The flat and block rates imply otherwise. Hence, customers, who may value consumption differently during both periods, have no incentive to consume differently during the periods. The inability of rates, such as the flat and block rates, to achieve allocative efficiency results in improper investments in the long run. For example, a utility may have to carry peak generation capacity, which may be needed for only a few periods in a year.

Incentivizing economic efficiency is more important with the advent of competitive bulk energy markets along with retail access or retail competition. The nature of the price of energy in the competitive markets is such that it could change significantly over time and between locations as a result of system state (network conditions, demand and supply conditions). Consumers in the distribution system may not see the changes under the COS regulation construct, i.e., consumers are insulated from wholesale prices regardless of what happens in bulk energy market. This could negatively impact reliability and lead to inefficiencies, such as the exercise of market

power and unnecessarily high levels of price volatility in the wholesale market. It also limits demand from being used for ancillary services and increases the reserve capacity that must be carried. In general, rates under the COS construct lead to higher operational costs. Other rate types have been proposed or implemented to shore up the perceived weaknesses of the traditional distribution system rates [64], [66], [67]. The prices include the TOU, critical peak price (CPP), and RTP.

The TOU rate is a time differentiated rate with two or three different rates for different time periods. The time periods are peak and off-peak for the two-period TOU rate and peak, partial or shoulder peak, and off-peak for the three-period TOU rate. Rates are fixed in each period. The TOU rate is a compromise between simplicity, cost of implementation, and price predictability and capture of the true nature of electricity prices. While it is time differentiated, the time periods in the TOU rate structure do not effectively capture the time dependence of electricity prices. TOU rates are also fixed for a season or longer and cannot properly reflect system conditions. The TOU rate is essentially an average rate and it is applied equally to all customers in the same rate class. While the TOU rate can be based on long-run marginal cost, a lot of utilities use embedded costs [64]. The CPP is similar to the TOU rate. For a limited number of hours in a year, a utility is allowed to charge a significantly higher rate during critical periods, such as during a contingency, to incentivize reduced consumption. Customers are notified in advance. While such a high rate can incentivize reduced consumption during a critical period, the incentivized consumption level may still be inaccurate since the high rate of a CPP could be independent of the true cost to consume at such periods. In addition, since the CPP is in place for a limited period of time in a year, a COS rate, such as the FR, will be in place for the periods the CPP is not used.

RTPs are generally hourly prices and are the most accurate prices for incentivizing economic efficiency in the contemporary distribution system. Several types of RTPs exist and they expose customers to different levels of price risk. They include the basic RTP, the block and index RTP, the two-part RTP, and the unbundled RTP with self-selected baseline [64]. The basic RTP is simply the wholesale price at the distribution proxy. Customers are charged on an hourly basis at the rate of the proxy LMP. The basic RTP and the block and index RTP are operated in environments with retail competition or retail access. The two-part RTP and the unbundled RTP are operated under the traditional regulated environment. The basic RTP presents the highest level of risk to customers. The block and index RTP provides a hedge for customer. It allows a customer to enter into a forward contract, based on contract for differences, to hedge price risks. A premium is charged for the financial hedge. Consumption in excess of the contracted demand level is charged at real-time rates. Customers are credited at real-time rates for consumption under the fixed level. Under the two-part RTP structure, a utility establishes a customer's baseline consumption (CBL). The CBL consumption is charged at rates that could be based on the COS regulation. This is the first part of the rate structure. A customer's baseline is based on the historical consumption of the customer (usually the consumption level in the year before the RTP is in place) [64]. Consumption above the CBL is charged at real-time rates and consumption below the CBL are credited at real-time rates. This is the second part of the rate. The unbundled RTP separates the cost to generate or procure energy from the cost of other services. The energy cost is charged at real-time rates or based on the estimated system lambda (marginal cost of energy) of a utility [64]. A customer can enter into a contract for difference to hedge risks. Under the contract, customers are allowed to select their own CBL. Consumption below the selected CBL

are credited at real-time rates and consumption above the selected CBL are charged at real-time rates. RTPs have been implemented by different utilities, such as Georgia Power, Progress Energy, and Duke Power [63], [64]. RTP rates are mostly applied to large customers.

2.5 Nodal Pricing in the Distribution System

RTPs capture the nature of the cost in the wholesale market, i.e., the time variation and the reflection of generation availability and transmission system conditions. They do not capture or reflect conditions in the distribution system. While the traditional distribution system has limited price sensitive resources and has no need for active power management or for considering network conditions, the contemporary distribution system and the future distribution system will have such resources and such needs. Hence, improvement in operations and investment may be achieved with a distribution system nodal price that reflects not only the transmission system state but also the distribution system state.

The concept of nodal distribution prices has generated some interest as of late with [42]-[47] discussing or proposing the use of some sort of nodal price in the distribution system. While the applications and the approaches discussed in the papers vary, the motivation behind the proposals or the impetus behind nodal distribution prices is the same – the smart grid initiative. The smart grid initiative is an endeavor to modernize the U.S. electric grid for the 21st Century. It was formally accepted as a policy of the U.S. government by the passage of the Energy Independence and Security Act of 2007 [48]. Title XIII of the bill calls for modernizing the U.S. transmission and distribution grid to provide a reliable and secure grid to meet future demand and to meet certain characteristics. The characteristics, listed in Table 2.1, are the envisioned functions of a modern grid.

Table 2.1. Characteristics of a Smart Grid [49]-[52]

Characteristic	Definition
Intelligent	Capable of autonomous control and operation
Efficient	Better utilization and optimization of system resources and grid operation
Accommodating	Integration of all fuel sources including wind and solar DGs and integration of new technologies, such as energy storage systems
Motivating	Enabling interaction between consumers and utilities such as real-time communication of prices for demand response
Opportunistic	Creating new markets and opportunities through its plug and play capability
Quality-focused	Delivering power-quality befitting of the digital economy
Resilient	Self-healing and resistant to attack and natural disaster

The smart grid is a confluence of information and communication technologies with power systems engineering [53]-[55]. It is the application of a layer of information and communication technologies such as, wide-area network and sensors, to the power systems infrastruc-

ture. The layer of information and communication technologies will enable fundamental communications and control applications, such as two way communication between utilities and customers, advanced metering infrastructure (AMI), distribution management system (DMS), and substation and other distribution system automation. The smart grid is expected to have a marked effect on the distribution system [47], [53]. The smart grid initiative is expected to result in a substantial presence of DGs, energy storage, and demand response at the distribution level. Under such a scenario, the distribution system could become an active meshed network [42], [43], potentially congested, with an operational paradigm that includes economic efficiency, active management and control of power flow, volt/var optimization, and operation of distributed energy resources (DERs) [45]-[47], [54]. A properly determined nodal price that adequately reflects system conditions and optimally couples the distribution and the transmission system can be effectively utilized as a control signal to incentivize efficient behavior of DERs under the smart grid environment.

Distribution nodal prices are proposed in [42] to incentivize increased DG penetration and proper location of DGs in the distribution grid. Reference [42] develops a nodal price similar to the transmission system LMP. The nodal price, which has no congestion component, is calculated based on the energy price at the transmission proxy and the impact of a DG's generation on marginal losses. Reference [42] develops an equation for the nodal price by applying the KKT conditions to an economic dispatch problem that minimizes both real and reactive power costs subject to a node balance constraint. The equation essentially calculates the price at a node by adding to the proxy LMP, the marginal cost of losses that is determined by multiplying the proxy LMP by the sensitivity of losses to the injection at the corresponding node. The authors argue that paying DGs based on their location, rather than a uniform price (proxy price) will provide additional revenue for the DGs and incentivize increased penetration and proper DG location.

A distribution nodal price is proposed in [43] to increase DG benefits, reduce losses in the distribution system, and provide distribution companies a control signal to align private DG operation with the goals of distribution system operation. The nodal price developed in [43] is not the same as the transmission system LMP. Rather, it is based on a loss reduction allocation mechanism. Under the mechanism, a base case is established and the deviation of losses from the base case as a result of a DG's production is used to calculate the nodal price at the DG's bus. Nodal prices are calculated for DG buses only. Load buses pay a uniform price. An iterative approach is employed to consider the possibility of DG output deviating from the output used to calculate a nodal price, i.e., an iterative approach is used to handle the fact that nodal prices are based on DG outputs, which are dependent on nodal prices. In the first iteration, a uniform price that is equal to the transmission proxy LMP is applied to all the buses in a distribution system. The resulting DG outputs are used to calculate distribution nodal prices. The distribution nodal prices are then used to calculate a new set of DG outputs. The iteration continues until convergence is achieved. Note that the iteration is not between the transmission and the distribution system; rather, it is within the distribution system for nodal prices in the distribution system. An artificial neural network (ANN) based mechanism to predict day-ahead distribution nodal prices to help distribution companies forecast DG generation for the next operating period is also developed in [43].

Distribution nodal pricing is proposed as a control signal for distribution system resources in [44] and [45]. The price in [44] is similar to the transmission LMP and it is calculated

based off of a DCOPF formulated as a quadratic programming problem to include losses in the lossless DCOPF. The distribution nodal price scheme in [45] is proposed as a control signal around which multiple distribution operation objectives can be optimized. The work is motivated by the changing control possibilities in the distribution system. The nodal price is calculated based off of transmission proxy LMPs and a marginal loss and congestion cost calculated by a Jacobian based AC distribution factor. The work allows for multiple transmission connection to the distribution system by multiplying the proxy LMPs by a participation factor that represents the contribution of each transmission supply point to the consumption at a node. The distribution nodal price is applied, via a multi-objective programming formulation, for energy management control. The objectives include peak power, peak energy consumed, cost of energy, and the total energy loss in the power electronics of energy storage systems.

2.6 Conclusion

With discussions on the LMP concept, the OPF problem, COS regulation, distribution system rate structures and nodal pricing in the distribution system, this chapter provides the background and context necessary to understand the work in this report. The chapter defined the LMP as the cost to supply an increment of energy at a specific node in the grid and discussed the properties that provide the LMP the capability to incentivize economic efficiency. The chapter discussed the OPF problem, which is used to calculate LMPs. The chapter also discussed the COS regulation as a set-up to exploring the inability of rates, such as the flat rate, the TOU rate, and the CPP, to effectively incentivize economic efficiency. While the RTP represents the most accurate prices that can be obtained in the contemporary distribution system, they may not suffice under an enhanced distribution system environment. Hence, nodal distribution prices have been proposed by several papers to incentivize appropriate behavior of price sensitive distribution system resources.

Chapter 3. The Distribution-Class Locational Marginal Price Index

This chapter discusses the DLMP. It begins with the definition, properties, and benefits of the DLMP in Section 3.1. A two-stage optimization process for calculating the DLMP and for optimally coupling the transmission and the distribution system are discussed in Section 3.2. The chapter discusses the issues of fairness of nodal prices in the distribution system and the issue of customer exposure to price volatility in Section 3.3 and Section 3.4. It concludes with a discussion on the factors that may limit the ultimate usage of the DLMP in the distribution system in Section 3.5.

3.1 The Distribution-class Locational Marginal Price (DLMP) Index

The DLMP proposed in this report is a type of nodal distribution system price. It is the extension of the LMP concept to the distribution system. Apart from the system both are used in, the DLMP has the same definition as the LMP and it has similar properties to the LMP. It is the cost to optimally deliver an increment of energy to a specific node in a distribution system without violating any system security or operational constraints. It reflects the marginal cost of energy and it captures the effect, on congestion and system losses, of delivering incremental energy to a specific location in a distribution grid. Both the transmission system and the distribution system states are considered in calculating the DLMP. Hence, a DLMP reflects the network conditions and generation availability of both the transmission and the distribution systems. The DLMP is proposed for use as a control signal to incentivize DSRs to behave optimally in way that benefits economic efficiency and system reliability, to optimally couple the transmission and the distribution system, and to incentivize DSRs to locate optimally.

The benefit of the DLMP to economic efficiency is similar to that of the LMP to economic efficiency. The DLMP, by being calculated by the interaction of the market supply and demand curves, is economically efficient. This is illustrated by the supply and demand curve in Figure 3.1. At the market clearing price (MCP), the price at which the supply and the demand curve intersects P^*, market surplus (MS) is maximized. MS or social surplus (SS) is a measure of economic efficiency. It is the benefit that accrues to both suppliers and consumers for trading in a market. The benefit that accrues to suppliers is the producer surplus (PS) and the benefit that accrues to consumers is the consumer surplus (CS). PS can be viewed as short-term producer profit and CS as consumer cost savings. MS or SS is the sum of PS and CS. In Figure 3.1, the PS is $D + E + F$, the CS is $A + B + C$, and the MS is $A + B + C + D + E + F$ if the price is P^*. At any price other than the MCP, there is a loss of efficiency, termed dead weight loss (DWL). In Figure 3.1, a DWL equal to G occurs if the price P_1 is imposed on the market. That is, the MS is equal to $A + B + C + D + E + F - G$. Wealth, equal to $D + E + H + I$, is transferred from producers to consumers. The PS is F. If the price P_2 is imposed, a DWL equal to $C + E$ occurs. The MS is equal to $A + B + D + F$. Wealth, $B + D$, is transferred from consumers to producers. The CS is A. Only the MCP supports equilibrium between the desire to consume versus the desire to produce. Imposing a lower price will result in a shortage as the quantity available for consumption will be less than the quantity desired for consumption. Imposing a higher price will result in over-production as the quantity available for consumption will be greater than the quantity desired for consumption. In a power system, a price lower than the MCP will result in over-consumption and a price higher than the MCP will result in under-consumption.

The DLMP is determined based on the interaction of the supply bids of generators and the demand bids of loads. Hence, the DLMP is a MCP and the consumption it will incentivize will, theoretically, maximize bid surplus for a convex market. For a power system, this translates to optimal energy production and consumption. Energy production will be optimal if the cost to generate energy to reliably serve distribution loads is the cheapest possible. That is, subject to reliability, the cheapest DGs and ESSs are dispatched and an optimal mix of production from distribution resources and the transmission system is achieved. Consumption will be optimal, if consumption is from the PR loads that value consumption the most and consumption is matched to generator marginal costs.

In addition to its determination by the interaction of supply offers and demand bids, the DLMP is nodal. The nodal property allows the DLMP to reflect the individual contribution of consumption at a node to system condition and costs. Consequently, the DLMP can capture the individual cost of loads at a node to system conditions and, as such, it is not distorted by and reduces cross-subsidy between customers. Cross-subsidies occur when a consumer does not pay the "true cost to the system" of its consumption. Some customers pay more than their true costs while others pay less. Cross-subsidies distort prices and incentivize suboptimal behavior. Hence, cross-subsidies degrade economic efficiency.

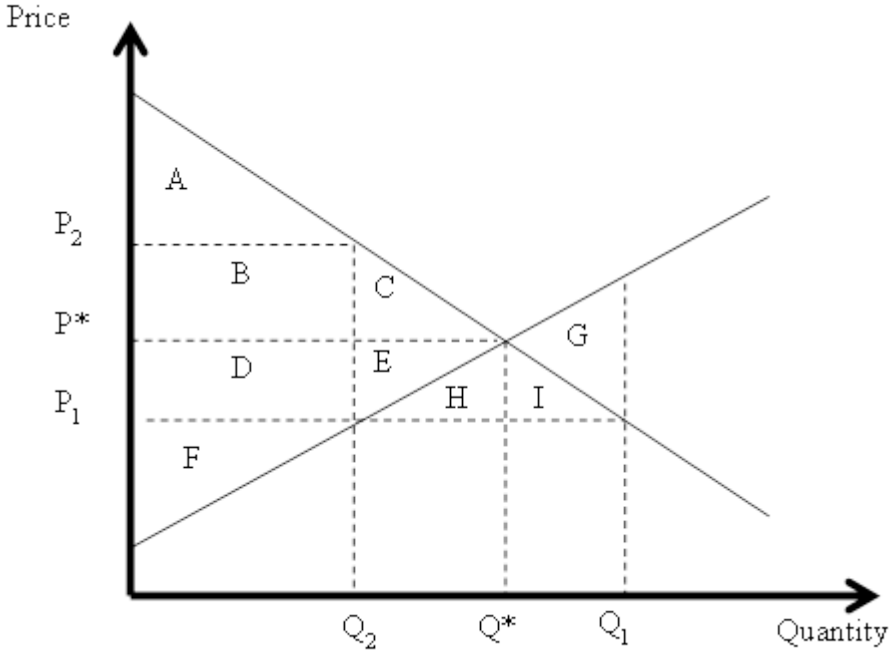

Figure 3.1. Supply and Demand Curve

The benefit of the DLMP to system reliability is also similar to the benefit of the LMP to system reliability. The DLMP, by its nodal property and by reflecting the impact of marginal consumption on network conditions (rather than reflecting embedded costs), can align a DSR's behavior with the system operational objective. If a network is stressed or generation is scarce, the DLMP appropriately incentivizes DSRs to act in a way to help maintain reliability; this is accomplished by matching consumption to generation based on the value loads place on consumption and the marginal cost of generation and reliability.

Incentivizing optimal DSR behavior or improving economic efficiency could lead to reduced operational cost, not only in the distribution system but for the power system as a whole. The benefit of the DLMP to reliability could also be to the power system as a whole. For example, DSRs controlled by the DLMP could potentially be used for demand response (DR) and for ancillary services. In order to realize the benefit of the DLMP at the transmission system level, the transmission and the distribution systems must be optimally coupled. Optimal coupling of both systems can be achieved by the DLMP correctly reflecting both the transmission and the distribution system states.

In the long term, the DLMP is efficient because it can signal where upgrades are most needed and it can be used to guide investment decisions. Information about where upgrades are needed and where resources should be located in a system could be gleaned from the nodal separation of DLMPs. Information about the optimal technology to investment in could be gleaned from the DLMP. The DLMP could also incentivize reduced peak consumption, which could help defer expensive upgrades and help utilize existing resources more efficiently.

3.2 Calculation Approach of the DLMP

Similar to the LMP, the DLMP will be calculated as the dual variable of a node balance constraint in an OPF problem. Ideally, the OPF problem should be solved for a single transmission and distribution system model. Such an approach provides the opportunity to consider the resources and the network condition of the entire power system. The approach may, however, be computationally intractable as a result of size. Consequently, a two-stage optimization approach, illustrated in Figure 3.2, is proposed for calculating DLMPs. The first stage of the optimization process is the transmission system OPF. The details of the distribution network are not modeled in the transmission system OPF. Rather, the distribution system is represented by its aggregate demand. The second stage is the distribution system OPF. The details of the transmission system are not modeled in the distribution system OPF. Rather, the transmission system is modeled as an infinite generator with its marginal cost equal to the distribution proxy LMP in the transmission system OPF. The two-stage decomposition approach is similar to current practices where the transmission and the distribution model are separated to improve computational efficiency. It is also the approach in the other papers [42]-[45] proposing nodal distribution system prices.

The separation of both systems poses a problem regarding accurate modeling of one system in the other. Usually, the distribution system aggregate demand is forecasted and used in the transmission system model. For a distribution system lacking in price sensitive resources and lacking in important network characteristics, such as congestion, it is sufficient to simply use the distribution proxy LMP to calculate DLMPs, which can be described as a single-shot approach. For an enhanced distribution system with price sensitive resources and important network characteristics, it may be more difficult to accurately forecast the distribution system's aggregate demand. Without properly representing the distribution system's network and price sensitive resources in developing forecasts for the distribution system, it is possible that distribution system resources will deviate from the model used in the transmission system OPF. The deviation could result in a sub-optimal solution for both the transmission and the distribution systems OPF and resources may be improperly incentivized.

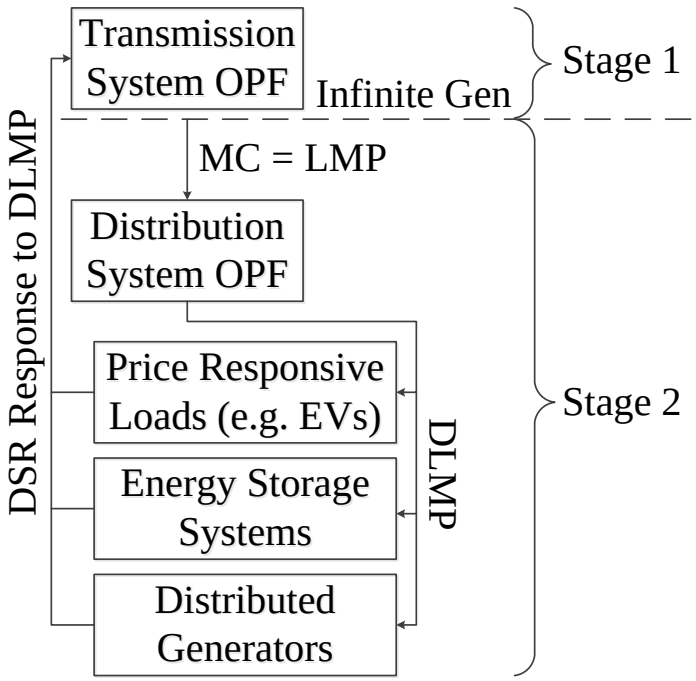

Figure 3.2. DLMP Calculation and Application Framework

In order to ensure an accurate representation of the distribution system for the transmission system OPF and vice versa, the DLMP calculation framework can iterate between the first and the second stages of the optimization process until the problems converge to a solution where further iterations neither leads to changes in LMPs or changes in the distribution system aggregate load. At each iteration, the latest results from the other process will be an input to the optimization problem that is been solved. For example, in the first iteration, the forecasted aggregate load of a distribution system will be used to model the distribution system for the transmission system OPF. The resulting LMPs at the distribution proxies in the transmission system OPF will be the marginal cost of the infinite generators in the distribution system OPF. In the second iteration, the new aggregate load that results from the first distribution OPF is used to model the distribution system in the new transmission system problem and the new LMPs that results from the second transmission system OPF will be used to calculate new DLMPs.

The iterative framework essentially couples the transmission and the distribution system in an optimal manner. The iterative approach allows the price sensitivity of distribution system resources and the distribution system network condition to be accurately modeled for the transmission system OPF and the impact of network conditions and generation availability in the transmission system to be optimally translated into a control signal for distribution system resources. The transmission system state, which will affect transmission LMPs, will be reflected in DLMPs and the benefits of having distribution system resources will be reflected in the distribution system's aggregate demand from iteration to iteration. Optimally coupling the transmission and the distribution systems provides ample opportunities for demand response and for utilizing distribution resources for ancillary services. Demand response can have a marked impact on market efficiency. It is the most effective cure for exercise of market power, which results in price volatility. It is also an effective tool for reliability especially with variable generation. Demand response can be faster than generator ramp rates and demand response could be cheaper

than carrying more reserves or building new facilities to provide reserves. Demand response can also help with peak shaving and deferring expensive system upgrades. While [42]-[45] separate the transmission and the distribution system OPF problems, the calculation approaches in the papers do not iterate between both problems.

Both OPFs in the two-stage optimization process can be based on either the DCOPF or the ACOPF. In this report, the DCOPF formulation is used for both the transmission system OPF and the distribution system OPF. The assumptions used to obtain the DCOPF (discussed in Section 2.2) are, however, based on the characteristics of the transmission system and may not hold for the distribution system. Particularly, the percentage of energy losses in the distribution system is higher than in the transmission system as a result of higher *r/x* ratios and as a result of lower voltage level of operation [32], [46]. To correct for this assumption, a lossy DCOPF model is used for the distribution system OPF. The lossy DCOPF model is also used for the transmission system OPF as it improves on the current practice of marginal loss modeling. The marginal loss modeling technique, which uses a slack or distributed slack bus method to approximate losses, can result in inaccurate dispatch solutions and LMPs. Furthermore, the slack or distributed slack bus method can produce varying LMP results for the same dispatch solution based on the approximation method used to distribute losses [68]. The lossy DCOPF formulation is discussed extensively in Chapter 4. The DCOPF also assumes that voltages are kept within a tight range around 1 p.u. for transmission system operation. Hence, voltages are assumed to be approximately 1 p.u. in the DCOPF. Voltages in the distribution system can deviate significantly from 1 p.u. ANSI C84.1 recommends maintaining service voltage between $\pm 5\%$ of nominal voltage [71]. For the studies in this report, DLMPs are calculated only on the primary distribution system feeders or at the secondary terminals of a distribution transformer. The DCOPF and the ACOPF assume balanced 3-phase operation. The distribution system is unbalanced. This DCOPF assumption is not corrected for the distribution system. Taking into consideration distribution system unbalance requires a 3-phase unbalanced power flow with prices potentially differing between the different phases. The assumption will not impact the studies conducted in this report, which are focused on economic efficiency. Future research can consider expanding the iterative framework to incorporate an unbalanced OPF formulation for the distribution system.

The calculation of the DLMP is assumed, in this work, to be done by the system operator. The system operator will individually optimize the distribution system and centrally optimize the transmission system. The iterative process is conducted for the system as a whole: the transmission system and the distribution systems. The communications and the control infrastructure to support the functions of the DLMP will be available as a result of the smart grid initiative. The DLMP will be suitable for both day-ahead and real-time purposes.

3.3 Fairness of Nodal Prices in the Distribution System

Fairness is a major objective in rate making and in utility regulation [69]. It is a topic that has been discussed in regards to ratemaking for many decades. The question of fairness, for the DLMP, goes to the appropriateness of rate discrimination based on customer location. That is, is it fair to have consumers in the same distribution system pay different prices because they are located at different nodes on the grid? Fairness is difficult to judge as it is dependent on the observer. For example, a load at the end of a feeder may feel unfairly treated if it has to pay more than the load at the beginning of the feeder. At the same time, the load at the beginning of a

feeder may feel unfairly treated if it has to subsidize the losses for the consumer at the end of the feeder. Regardless of the price signal or the rate structure, there are always winners and losers. It is not the goal of this report or the responsibility of an Independent System Operator (ISO) to decide who the winners and the losers are. Rather, the primary objective of the ISO is to maximize social welfare and this is partially achieved by ensuring that the prices are proper economic signals in order to optimally incentivize economically efficient behavior. For a convex market, the DLMP is the optimal pricing mechanism to incentivize efficient and reliable behavior from the market participants.

3.4 Price Volatility with the use of the DLMP

Concerns about customer exposure to price volatility may arise with the implementation of the DLMP. Unlike a flat rate or a TOU rate, which are established and fixed over long time periods, the DLMP can change as frequently as it is calculated and it can theoretically be as high as infinity. Factors that may affect the volatility of the DLMP include the transmission LMP, congestion, and scarcity in the distribution system and bid practices of distribution system resources. The volatility of the LMP represents a major source of volatility for the DLMP. The LMP could be volatile as a result of bid practices in the transmission system and as a result of congestion and scarcity in the transmission system. As an input into the DLMP calculation, the volatility of the LMP at the transmission proxy of a distribution system may translate into volatility for the DLMP. DLMP volatility could also result from system conditions, such as congestion and scarcity. At times when the distribution system is stressed, the system conditions will be reflected through the DLMP. DLMP volatility could also occur, theoretically, as a result of strategic bidding from distribution system resources.

While price volatility may be regarded as undesirable, DLMP volatility as a result of system conditions provides information about the state of the system. For example, a high DLMP as a result of congestion shows there may be need for an upgrade at a location and it incentivizes system resources to behave in a manner to achieve economic efficiency and reliability subject to the congestion. Hedging mechanisms can be developed and offered alongside the DLMP. The mechanism can offer different degree of protection against price volatility for risk-averse consumers. The mechanism can be based on a contract for differences similar to that described in Section 2.4 for contemporary RTPs. Prices for the contracts will be determined by market forces. Unlike contemporary rates, such as the flat, block, or TOU rates, which protects against volatility but are determined based on COS regulation, a market-based hedging mechanism allows for price discovery.

Price volatility as a result of bid practices negatively impacts market efficiency. Strategic behavior can be expected to be insignificant in the distribution system as the option to purchase from the transmission system is always available. A resource can only exercise market power or behave strategically up to the point that the option of purchasing from the transmission system becomes a viable option. The use of the DLMP can help reduce price volatility in bulk energy markets by optimally representing price responsive demands in the bulk energy market. One of the major reasons generators have the opportunity to bid strategically or exercise market power in the transmission system is because loads are assumed to be largely inelastic. Price elasticity of demand can curb strategic behavior because there is always the threat that a generator bidding strategically or exercising market power can miss out on an opportunity to produce. If a genera-

tor does not bid its true marginal cost, the generator's bid in the market may not be cleared if loads view the cost as too high. Hence, the environment surrounding the use of the DLMP can reduce price volatility in the LMP, which can in turn reduce the DLMP volatility. The extent to which demand flexibility can curb strategic behavior will be dependent of the flexibility of demand resources and the amount of flexible resources available.

3.5 Factors that will Affect Ultimate Usage

There are differences between the contemporary distribution system design and the transmission system that can limit the ultimate usage and benefit of the LMP concept in the distribution system. The transmission system is a highly meshed network with multiple generators. There could be multiple congested interfaces in the transmission system and as such, there is a need for the LMP to help manage congestion. The contemporary distribution system often has the transmission system as the major, and sometimes the only, source of energy into the distribution system. The contemporary distribution system is operated predominantly in a radial configuration with power flowing from the distribution substation to loads. As a result of radial power flow, distribution circuits and equipment are overbuilt to avoid congestion. Consequently, the DLMP in a radial distribution system may have no congestion component. Only losses will cause separation between DLMPs at different nodes. As a result, the improvement that may be obtained for such a system, over the FR, the TOU, or a contemporary RTP, may not justify the complexities of administering a DLMP, especially if loads are treated as inelastic and there are limited generation resources. Also, while the transmission system has multiple generators that are price sensitive and, to a lesser extent, price responsive loads and agents, such as virtual bidders and market makers, the distribution system has limited price responsive resources: load is viewed as perfectly or highly inelastic.

The benefits of the DLMP to the contemporary distribution system may be limited but the DLMP is developed for the enhanced distribution grid expected as a result of the smart grid initiative. The enhanced distribution system is expected to have a substantial amount of price responsive resources such as PRLs, ESSs, and DGs. These resources are already materializing in the distribution system. For example, DR is implemented in various forms in electricity markets and rates such as the TOU, CPP, and RTP are an admission that loads do respond to prices. Also, with DGs, there can be multidirectional flows in the future distribution system. For such a grid, the benefit of the DLMP to the distribution system will be impacted by network topology, distribution system losses, and congestion. There will also be a major benefit to the whole power system as the coupling between the transmission and the distribution system will affect economic efficiency and reliability for the whole system.

3.6 Conclusion

The DLMP is defined and its properties and benefits are discussed in this chapter. The objective of introducing the DLMP in enhanced distribution systems is also discussed. The DLMP in envisioned as an efficient control signal for incentivizing optimal DSR behavior such that DSR behavior is aligned with system operation objectives and economic efficiency is improved. The DLMP is also envisioned to optimally couple the transmission and the distribution system. The coupling is proposed to be effected through an iterative approach to calculating DLMPs. The coupling will allow the gains realized from the use of the DLMP to be translated to

economic and reliability gains for the transmission system. Issues, such as fairness and price volatility, surrounding the DLMP usage are also discussed. The DLMP is proposed for use in an enhanced distribution system.

Chapter 4. Lossy DCOPF for DLMP Calculation

As discussed in Section 2.2, the traditional DCOPF is a lossless formulation. Nodal prices and dispatch solutions obtained from a lossless DCOPF do not reflect the effects of real power losses. Real power losses are of particular importance in distribution system applications: distribution system circuits have high resistances and the voltage level is low. Real power losses will also be the only factor that results in nodal price separation in a distribution system that is not congested. As a result, a lossy DCOPF formulation is developed in this chapter for calculating DLMPs. The same formulation can be applied in the transmission system to calculate LMPs. The lossy DCOPF formulation is particularly attractive because loss approximation does not require an iterative process [16] and loss approximation, rather than been conducted ex-post [16], is endogenous to the formulation. The formulation is also attractive because it does not require the definition or existence of a slack bus. Hence, the formulation is not arbitrary as solutions do not change with a changing slack bus definition [7], [17]-[19], which is what occurs with an iterative technique that places losses at the slack or distributed slack bus.

The lossy DCOPF formulation is developed and some issues surrounding its use are presented in this chapter. In Section 4.1, a discussion on the loss approximation technique, the derivation of the linear expressions that approximates the AC loss equation and the lossy DCOPF, formulated as a linear programming problem, is presented. Under the scenario that non-positive DLMPs or LMPs occur in a problem with the lossy DCOPF formulation, artificial losses could be incorrectly created and resulting solutions could be wrong. The scenario and an adjacency and an exclusivity condition, which when satisfied guarantee correct loss approximation and solutions, are discussed in Section 4.2. The occurrence of artificial or non-physical losses is theoretical proven in Section 4.3 using duality theory and the Karush Kunh Tucker (K.K.T.) conditions. The presented theoretical proof is one of the major contributions of this work to the existing body of knowledge in this field. Several publications, e.g., [20]-[22], have used the loss approximation technique without discussing its breakdown. The presented proof goes beyond the scope of the work in [23]-[27]. If the lossy DCOPF formulation breaks down, integer constraints can be applied to enforce the adjacency and the exclusivity conditions. The constraints and a mixed-integer linear programming (MILP)-based lossy DCOPF formulation is presented in Section 4.4. The MILP-based formulation is only used in place of the linear programming-based formulation when the lossy formulation breaks down.

4.1 Lossy DCOPF Formulation

The lossy DCOPF formulation is developed by simply adding linearized real-power loss equations to the standard DCOPF problem. By including the linearized loss equations, the DCOPF formulation endogenously approximates real power losses and endogenously captures the effect of losses on dispatch solutions and prices. By linearizing losses, the linear properties of the DCOPF, discussed in Section 2.1, are retained for the lossy formulation. For example, the lossy DCOPF does not suffer from the convergence issues of the ACOPF and it converges to a solution relatively quickly. The approach employed to develop the linearized equations is the piecewise linear technique discussed in [21] and [22].

The first step in developing the lossy DCOPF formulation is to linearly approximate real power losses. Equation (4.1) is the AC expression for real power losses that is to be linearized. Equation (4.1) is obtained for any line *k* by subtracting the AC power flow expression for the power delivered to the receiving end bus of *k* from the AC power flow expression for the power injected at the sending end of *k* and applying the approximation that bus voltages are approximately 1 p.u. This can be illustrated with the two bus system in Figure 4.1. Equation (4.2), the full AC equation of real power losses on *k* as a result of *k's* resistance and the current it carries, is obtained by subtracting the AC power flow expression of P_k^{nm} from the AC power flow expression of $-P_k^{mn}$. Note that P_k^{mn} is the power injected from bus *n* onto line *k* and its negative is the power delivered to bus *n*. Also note that the AC power flow expression for P_k^{nm} and $-P_k^{mn}$ follow the power flow expression in (2.3). The approximation that bus voltages V_m and V_n are 1 p.u is applied to (4.2) to derive (4.1). The approximation, which is one of the approximations used to develop the DC approximation of the line flow equation, allows for (4.1) to be linearized over $(\theta_n - \theta_m)$, the bus angle difference across *k*.

The non-linear part of (4.1), i.e., $1 - \cos(\theta_n - \theta_m)$, along with a piecewise linear curve approximation is shown in Figure 4.2. The product of the expression that describes the piecewise linear approximation curve and $2G_k$, the conductance term in (4.1), is the linearized loss expression. An expression for the piecewise curve is developed by using the length of the segments of the curve to approximate $(\theta_n - \theta_m)$ as in (4.3) - (4.5). The length and the slope of the segments used in the angle difference approximation are then used to represent the piecewise linear curve as in (4.6). Equation (4.6) is multiplied by $2G_k$ to linearly approximate real power losses as in (4.7),

$$P_n^L = 2G_k\left(1-\cos\left(\theta_n - \theta_m\right)\right) \tag{4.1}$$

$$Loss = \left|V_m^2\right|G_k + \left|V_n^2\right|G_k - 2\left|V_m\right|\left|V_n\right|\left(G_k\cos\left(\theta_n - \theta_m\right)\right) \tag{4.2}$$

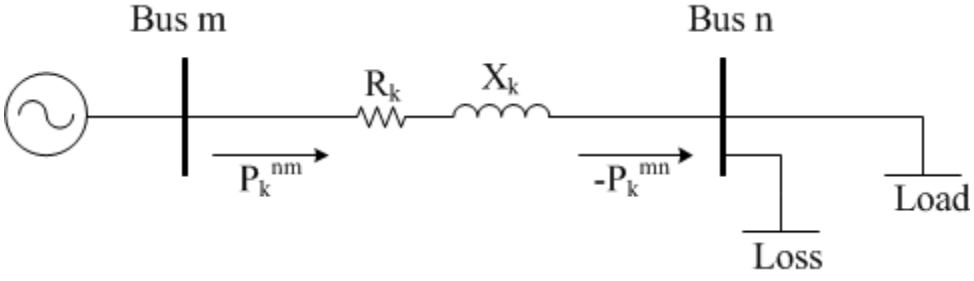

Figure 4.1. Two-Bus System for Real Power Loss Expression Derivation

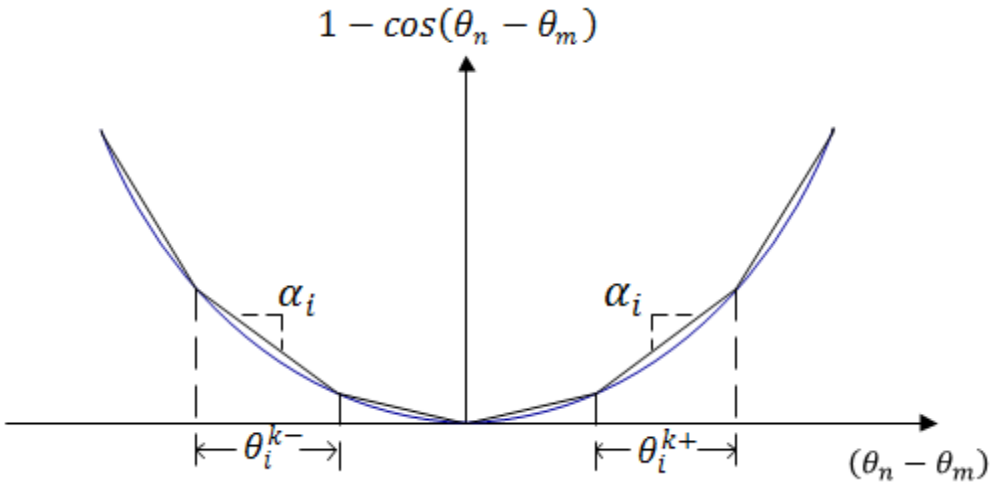

Figure 4.2. Plot of $1-\cos(\theta_n-\theta_m)$ and its Piecewise Linear Approximation Curve

$$(\theta_n-\theta_m)=\left(\sum_{\forall i}\theta_i^{k+}-\sum_{\forall i}\theta_i^{k-}\right) \tag{4.3}$$

$$0\le\theta_i^{k+}\le\theta_i^{\max}\quad\forall i \tag{4.4}$$

$$0\le\theta_i^{k-}\le\theta_i^{\max}\quad\forall i \tag{4.5}$$

$$1-\cos(\theta_n-\theta_m)=\left(\sum_{\forall i}\alpha_i\theta_i^{k-}\right)+\left(\sum_{\forall i}\alpha_i\theta_i^{k+}\right) \tag{4.6}$$

$$P_n^L=\left[\sum_{\forall k(n,;)}2G_k\left(\sum_{\forall i}\alpha_i\theta_i^{k-}\right)\right]+\left[\sum_{\forall k(;,n)}2G_k\left(\sum_{\forall i}\alpha_i\theta_i^{k+}\right)\right]. \tag{4.7}$$

The first term on the RHS of (4.7) is the expression for the loss contribution of lines that have a bus *n* as their receiving end bus and the second term is the expression for the loss contribution for lines that have the bus as their sending end bus. Distinction is made between the two because the real power losses associated with a line is placed as a fictitious demand (FD) at the bus that is receiving a positive injection of real power from the line. Determination of loss placement is done endogenously by the lossy DCOPF formulation based on the sign of the bus angle difference across a line. For the DC approximation of the line flow equation in this report, a negative angle difference indicates that power flow is in the pre-defined direction. Consequently, losses are placed at the designated receiving end of a line if a negative angle difference occurs across the line. A positive angle difference indicates that power flow is in the opposite of the pre-defined direction. Consequently, losses are placed at the designated sending end bus of a line if a positive angle difference occurs across the line. In Figure 4.1, the losses on *k* will be placed at bus *n* because the angle difference across *k* will be negative, i.e., power flow will be to bus *n*. As will be discussed in Section 4.2, the loss approximation technique uses the two terms on the RHS of (4.3), to determine loss or FD placement. The terms correspond to the sum of the lengths of positive and negative orthant segments used to approximate the angle difference across a line respectively.

The lossy DCOPF is formulated as a linear programming problem in (4.8) - (4.20). The formulation is developed by adding (4.3) - (4.5) and (4.7) to the standard DCOPF formulation. Equation (4.8), the objective function of the lossy formulation, represents market surplus (MS) or bid surplus. Constraint (4.9) is the DC approximation of the line flow equation. Constraint (4.10) is the node balance equation. The loss term in the constraint is a variable load and its value is determined using constraint (4.11), the linearized loss equation. The other terms in (4.10) are the sum of the generator injections at a bus, the sum of the power flowing into the bus and the sum of the power flowing out of the bus. Constraint (4.12) is the angle difference approximation from (4.3). Constraints (4.13) - (4.16) are the restrictions in (4.4) and (4.5) that define the minimum and maximum length of the segments in the piecewise linear approximation. Constraint (4.17) and (4.18) are the constraints for line capacity limits and (4.19) and (4.20) are the constraints for generator output limits. A DCOPF can include an angle difference constraint as a proxy for transient stability limit. Rather than include an explicit angle difference constraint, the limit is enforced by the maximum possible sum of the length of the piecewise linear curve used for loss approximation. For example, if the angle difference limit is to be set at 30 degrees, then the maximum possible sum of the length of segments in the same orthant will be 30 degrees,

$$Maximize: \sum_t \sum_d b_{d,t} D_{n,d,t} - \sum_t \sum_g c_{g,t} P_{g,t} \tag{4.8}$$

subject to:

$$B_k \left(\theta_{n,t} - \theta_{m,t}\right) - P_{k,t} = 0 \qquad \forall k,t \tag{4.9}$$

$$\sum_{g \in G_n} P_{g,t} + \sum_{\forall k(n,;)} P_{k,t} - \sum_{\forall k(;,n)} P_{k,t} - P^L_{n,t} - \sum_d D_{n,d,t} = 0 \qquad \forall n,t \tag{4.10}$$

$$P^L_{n,t} - \left[\sum_{\forall k(n,;)} 2G_k \left(\sum_{\forall i} \alpha_i \theta^{k-}_{i,t}\right)\right] - \left[\sum_{\forall k(;,n)} 2G_k \left(\sum_{\forall i} \alpha_i \theta^{k+}_{i,t}\right)\right] = 0 \qquad \forall n,t \tag{4.11}$$

$$\left(\theta_{n,t} - \theta_{m,t}\right) - \left(\sum_{\forall i} \theta^{k+}_{i,t} - \sum_{\forall i} \theta^{k-}_{i,t}\right) = 0 \qquad \forall k,t \tag{4.12}$$

$$\theta^{k+}_{i,t} \geq 0 \qquad \forall i,k,t \tag{4.13}$$

$$\theta^{k-}_{i,t} \geq 0 \qquad \forall i,k,t \tag{4.14}$$

$$-\theta^{k+}_{i,t} \geq -\theta^{\max}_i \qquad \forall i,k,t \tag{4.15}$$

$$-\theta^{k-}_{i,t} \geq -\theta^{\max}_i \qquad \forall i,k,t \tag{4.16}$$

$$P_{k,t} \geq -P^{\max}_k \qquad \forall k,t \tag{4.17}$$

$$-P_{k,t} \geq -P^{\max}_k \qquad \forall k,t \tag{4.18}$$

$$P_{g,t} \geq P^{\min}_g \qquad \forall g,t \tag{4.19}$$

$$-P_{g,t} \geq -P^{\max}_g \qquad \forall g,t \tag{4.20}$$

$$P_{g,t}, P_{k,t}, \theta_{n,t}, P^L_{n,t} \; free.$$

4.2 Conditions for Correct Solutions

Equation (4.12) in the lossy DCOPF formulation is the link between the piecewise linear approximation of losses and the DC approximation of the line flow equation. By coupling (4.9) and (4.11), (4.12) enforces a proportional relationship between the magnitude of the real power losses and the magnitude of the real power flow on a line. Equation (4.12) also pegs the placement of approximated losses to the direction of actual power flow. If the order in which segments are selected in (4.12), to approximate $(\theta_n - \theta_m)$, satisfies an adjacency and an exclusivity condition, the lossy DCOPF formulation will correctly approximate and place losses.

The adjacency condition requires the length of all lower positioned segments to be fully utilized if there is a higher positioned segment in the same orthant that is used to approximate a bus angle difference. Mathematically, this can be written for segments in the positive orthant as:

$$\theta_j^{k+} = 0 \; if \; for \; any \; i < j \; \exists \; \theta_i^{k+} < \theta_i^{max}$$

Since there is no explicit constraint in the linear programming-based lossy DCOPF formulation that defines segments selection order, each $\theta_i^{k-}$and each θ_i^{k+} is treated independently of every other $\theta_i^{k-}$and θ_i^{k+} in the selection process. As a result, segments, regardless of position, can be selected to approximate $(\theta_n - \theta_m)$ in any order. An indirect selection order exists in the form of the slope of the piecewise segments. For segments in the same orthant, segment slopes increase with distance from the origin and each segment has a slope that is different from the slope of every other segment in the same orthant. If the linear programming-based lossy formulation works correctly, artificial losses are not created and the losses associated with a problem are correctly approximated. The increasing slopes of segments in the same orthant forces the formulation to respect the adjacency condition in order to properly reflect power losses. Respecting the adjacency condition ensures correct approximation of losses because (4.11) is a sum of the product of the lengths and the slopes of the segments selected to approximate $(\theta_n - \theta_m)$ in (4.12). Using a higher segment with a higher slope in place of a lower segment with a lower slope to approximate the same angle difference will result in over-estimation of losses, i.e., artificial losses created. If the linear programming-based lossy DCOPF formulation breaks down in such a way that artificial losses are created, the adjacency condition will be violated and losses will be incorrectly approximated by selecting segments with higher slopes in place of segments with lower slopes.

The exclusivity condition requires that all the segments used to approximate an angle difference lie in the same orthant. Segments in the positive orthant must be exclusively used to approximate positive angle differences and segments in the negative orthant must be exclusively used to approximate negative angle differences. Mathematically this can be written as:

$$\theta_i^{k+} = 0 \; when \; (\theta_n - \theta_m) < 0 \; \forall i \; and \; \theta_i^{k-} = 0 \; when \; (\theta_n - \theta_m) > 0$$

As discussed in Section 4.1, loss placement is determined endogenously based on the sign of $(\theta_n - \theta_m)$. Loss placement is effected by the selection of θ_i^{k+} and θ_i^{k-}. The exclusivity condition is necessary because θ_i^{k+} and θ_i^{k-} for a line *k* appear in different FD equations. That is, θ_i^{k+} and θ_i^{k-} appear in (4.11) for different buses. θ_i^{k+} for a line *k* appear in the FD equation for the designated sending end bus and θ_i^{k-} appear in the FD equation for the designated receiving end

bus. If the angle difference across a line is positive and θ_i^{k+}s are selected to approximate the angle difference while the θ_i^{k-}s are zero, losses will be correctly placed at the sending end bus of the line. If the angle difference across a line is negative and θ_i^{k-}s are selected to approximate the angle difference while the θ_i^{k+}s are zero, losses will be correctly placed at the receiving end bus of the line. If in either case, both terms in (4.12) are non-zeros, that is the exclusivity condition does not hold, losses will be placed at both ends of a line in a proportion determined by the split of the angle difference and the slope of the segments selected in each orthant. The split is possible because (4.12) only requires the magnitude of the angle difference across a line to be equal to the sum of the lengths of the segment approximating it. Since each $\theta_i^{k-}$and each θ_i^{k+} is treated independently of every other $\theta_i^{k-}$and θ_i^{k+} and since there is no explicit constraint on selection order, the lossy formulation can select segments in both orthants to approximate an angle difference.

In addition to the incorrect placement of losses, violation of the exclusivity condition also results in the magnitude of the approximated loss being artificially increased. This results from the two terms in (4.12) having opposite signs. If the exclusivity condition is violated, the absolute value of the magnitude of the sum of the lengths of the segments in one orthant must be greater than the absolute value of the angle difference approximated and the sum of the lengths of the segments in the other orthant must be non-zero in order for (4.12) to hold. Since (4.11) is a sum of products of the lengths and slopes of all selected segments in (4.12), losses will be overestimated. The lossy formulation behaves in such a manner when it breaks down in order to artificially increase the losses at a bus without violating a constraint manifested as a binding angle difference limit.

For a problem with strictly positive DLMPs/LMPs, the lossy formulation appropriately estimates losses. A positive DLMP/LMP indicates that additional consumption at a bus will increase total cost. If a load is a parameter, the optimization problem has to secure generation to meet the load regardless of the effect of the consumption on the objective function. In the case of a variable load, such as the approximated loss term in the node balance constraint of the lossy formulation, the optimization problem will prevent additional consumption if such consumption degrades the objective function. Hence, in a problem with strictly positive DLMPs/LMPs, extra losses (artificial losses) beyond the correct approximation of losses will not be created to prevent degrading the objective function (in a bid maximization problem, artificial losses degrade the objective function since there is no bid value assigned to them). On the contrary, if non-positive DLMPs/LMPs occur, additional consumption at a bus may benefit an objective function. If a DLMP/LMP is zero, the optimization problem in indifferent between creating and not creating artificial losses: more consumption neither benefits nor degrades the objective function. If a negative DLMP/LMP occurs at a bus, any additional consumption at the bus will improve the objective function. If additional consumption improves an objective function, the lossy formulation has the opportunity, through the loss approximation technique, to create artificial losses to improve the objective function. The lossy formulation will violate the adjacency condition to create artificial losses at the bus until additional consumption either does not improve the objective function any longer or until a constraint in the problem prevents additional consumption solely at the bus. That is, if there is no reason why additional losses cannot be created, fictitious losses will be created until the negative DLMP/LMP is zero. If a constraint limits the fictitious losses that can be created solely at a bus with a negative DLMP/LMP, then if beneficial, the formula-

tion will violate the exclusivity condition to create losses at an adjacent bus so as to create more losses at the bus with the negative DLMP/LMP.

The breakdown of the lossy DCOPF formulation is illustrated with the 3-bus network in Figure 4.3. The network has an inelastic load; hence, the DCOPF formulations used to study the network have generation cost minimization as their objective. Results of a lossless DCOPF study, Table 4.1, establish the occurrence of a negative LMP at bus 2 of the network. The negative LMP occurs as a result of congestion on the line between bus 2 and bus 3. To supply an additional MW at bus 2, the output of generator 2 (an expensive generator) has to be decreased by 2 MW and the output of generator 1 (a cheaper generator) increased by 3 MW. The re-dispatch will cause a reduction of $50 in total generation cost. In the lossless DCOPF formulation, fixed loads prevent the formulation from taking advantage of the opportunity to further improve the objective function. The lossy DCOPF formulation, however, could take advantage of the opportunity because the FDs that represent the losses on a line are variable loads. The total generation cost in Table 4.1 shows that the objective of the lossy formulation is indeed better than the objective of the lossless formulation. Artificial losses in the lossy formulation caused the system to re-dispatch away from the expensive generator as shown in Table 4.2.

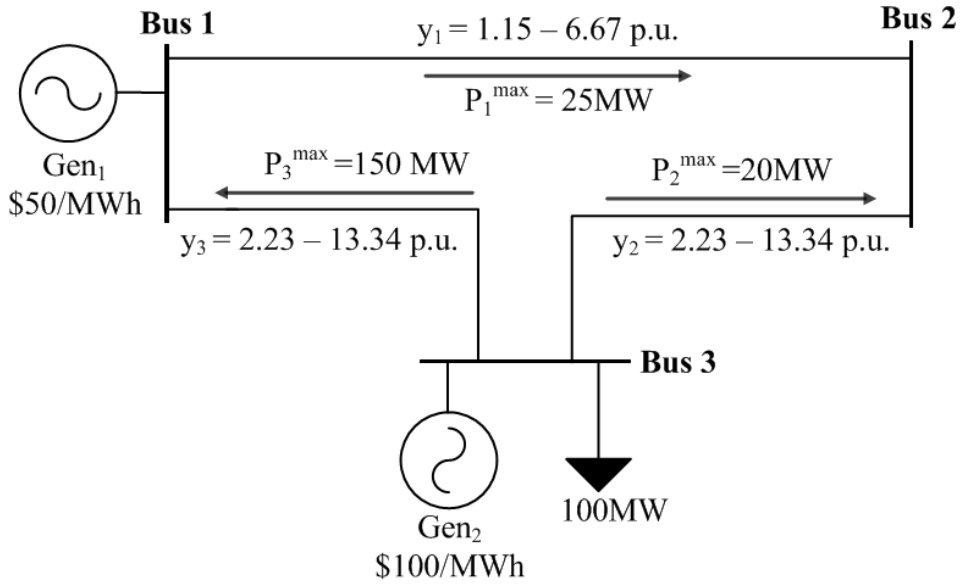

Figure 4.3. Three-Bus Network Example for Illustrating Lossy Formulation Breakdown

Table 4.1. Lossless and Lossy DCOPF LMPs, Losses, and Total Cost Results

Bus No.	Lossless DCOPF	Lossy DCOPF	
	LMP ($/MWh)	LMP ($/MWh)	Losses (MW)
1	50.00	50.00	0.11
2	– 50.00	–5.71	5.00
3	100.00	100.00	0.75
Total Losses (MW)	0	5.86	
Total Cost ($)	6000.00	5830.32	

Table 4.2. Lossless and Lossy DCOPF Generation Dispatch Results

Gen No.	Lossless DCOPF	Lossy DCOPF
	Output (MW)	Output (MW)
1	80.00	95.11
2	20.00	10.75

Examining the piecewise approximation results of the lossy DCOPF study, Table 4.3, indicates that artificial losses were created by violating the adjacency and the exclusivity conditions. Both conditions were violated in approximating the angle difference across the lines connected to bus 2: lines 1 and 2. In the case of line 1, negative orthant segments 10 and 11 were selected to approximate $(\theta_2 - \theta_1)$ while lower segments, 1 through 9, were not selected. Segments 1 through 4 in the positive orthant were also selected to approximate $(\theta_2 - \theta_1)$. Since the power flow on line 1 is to bus 2 and since the flow on line 1 is correctly designated, $(\theta_2 - \theta_1)$ is a negative angle. Consequently, only negative orthant segments should have been selected to approximate the angle difference. In the case of line 2, a negative orthant segment, 11, was one of the segments selected to approximate $(\theta_2 - \theta_3)$, a positive angle difference.

Table 4.3. Piecewise Approximation Result for the Lossy DCOPF Study

Line No. (k)	$\sum_{\forall i} \theta_i^{k+}$	$\sum_{\forall i} \theta_i^{k-}$	i for θ_i^{k+} Used	i for θ_i^{k-} Used
1	0.03076	0.06824	1, 2, 3, 4	10, 11
2	0.01745	0.00246	1, 2	11
3	0.05300	0.00000	1 thru 6	–

The artificial losses created by incorrectly approximating $(\theta_2 - \theta_1)$ are placed at bus 2 and bus 1. For bus 1, this is easily verified by the fact that the FD at bus 1 is not equal to zero, Table 4.1. As shown in Table 4.4, the power flow on line 1 is to bus 2, the power-flow on line 2 is to bus 3 and the power-flow on line 3 is to bus 3. There is no flow into bus 1. As a result, losses should not have been placed at the bus. The artificial losses created by incorrectly approximating $(\theta_2 - \theta_3)$ are placed at bus 2 and bus 3. The artificial losses at bus 2 are responsible for the significant deviation of bus 2's LMP in the lossy formulation from bus 2's LMP in the lossless formulation, Table 4.1.

Table 4.4. Lossless and Lossy DCOPF Line Flow and Line Angle Difference Results

Line No. (k)	Lossless DCOPF		Lossy DCOPF	
	Line Flow (MW)	$\theta_n - \theta_m$ (rad)	Line Flow (MW)	$\theta_n - \theta_m$ (rad)
1	20	–0.0300	25	–0.037
2	–20	0.0150	–20	0.015
3	–60	0.4498	–70	0.053

4.3 Theoretical Proof of Lossy DCOPF Breakdown

It can be shown that the linear programming-based lossy formulation breaks down with the occurrence of negative DLMPs/LMPs by proving theoretically that negative DLMPs/LMPs

cannot result from the lossy formulation if consumption at a bus that is supposed to have a negative DLMP/LMP is not limited by any constraints. That is, if a constraint, e.g., active line, stability or generator output limit, does not limit the amount of energy that could be consumed at all buses that are supposed to have negative DLMPs/LMPs, the lossy formulation will artificially increase the amount of losses at such buses until all the negative DLMPs/LMPs are equal to zero, i.e., until creating artificial losses no longer benefits the objective. Since it is known that a DLMP/LMP can indeed be negative (due to negative bidding and also due to Kirchhoff's laws, i.e., negative DLMPs/LMPs can exist even when all generators submit positive bids), having a formulation that cannot result in negative DLMPs/LMPs shows the lossy formulation improperly create artificial losses to improve the objective function. In the case where additional consumption at a negative DLMP/LMP bus is limited by a constraint, losses are artificially created by violating the adjacency condition, i.e., artificial losses are created through the slope of the segments approximating an angle difference. The mathematical proof for the claims is developed by examining the dual and the K.K.T. conditions of the lossy formulation.

The dual of the lossy formulation, for a single period, is shown in (4.21) - (4.28). For the ease of the reader, the primal formulation for the lossy DCOPF formulation, for a single period, is also shown in (4.29) - (4.41). Perfectly inelastic loads are assumed in the primal formulation for ease of the dual derivation. The variables in braces in the dual formulation are the primal variables for the dual constraint they appear next to and the variables in braces in the primal formulation are the dual variables for the primal constraint they appear next to. The proof holds for the case of elastic loads.

Dual Formulation

$$\begin{aligned} &\textit{Maximize}: \sum_n \lambda_n D_n - \sum_{\forall k} \left(F_k^- + F_k^+\right) P_k^{\max} - \sum_{\forall i,k} \left(\rho_i^{k-} + \rho_i^{k+}\right) \theta_i^{\max} \\ &+ \sum_g \delta_g^- P_g^{\min} - \sum_g \delta_g^+ P_g^{\max} \end{aligned} \tag{4.21}$$

subject to:

$$\lambda_n + \delta_g^- - \delta_g^+ = c_g \qquad \forall g \quad \{P_g\} \tag{4.22}$$

$$\lambda_n - \lambda_m - \xi_k + F_k^- - F_k^+ = 0 \qquad \forall k \quad \{P_k\} \tag{4.23}$$

$$\gamma_n - \lambda_n = 0 \qquad \forall n \quad \{P_n^L\} \tag{4.24}$$

$$\sum_{\forall k(n,;)} B_k \xi_k - \sum_{\forall k(;,n)} B_k \xi_k + \sum_{\forall k(n,;)} \mu_k - \sum_{\forall k(;,n)} \mu_k = 0 \qquad \forall n \quad \{\theta_n\} \tag{4.25}$$

$$-2G_k \alpha_i \gamma_m - \mu_k - \rho_i^{k+} \le 0 \qquad \forall i,k \quad \{\theta_i^{k+}\} \tag{4.26}$$

$$-2G_k \alpha_i \gamma_n + \mu_k - \rho_i^{k-} \le 0 \qquad \forall i,k \quad \{\theta_i^{k-}\} \tag{4.27}$$

$$F_k^-, F_k^+, \delta_g^-, \delta_g^+, \rho_i^{k-}, \rho_i^{k+} \ge 0 \tag{4.28}$$

$$\lambda_n, \mu_k, \xi_k, \gamma_n \textit{ free}$$

Primal Formulation

$$Minimize: \sum_g c_g P_g \tag{4.29}$$

subject to:

$$B_k(\theta_n - \theta_m) - P_k = 0 \qquad \forall k \qquad \{\xi_k\} \tag{4.30}$$

$$\sum_{g \in G_n} P_g + \sum_{\forall k(n,;)} P_k - \sum_{\forall k(;,n)} P_k - P_n^L = D_n \qquad \forall n \qquad \{\lambda_n\} \tag{4.31}$$

$$P_n^L - \left[\sum_{\forall k(n,;)} 2G_k \left(\sum_{\forall i} \alpha_i \theta_i^{k-}\right)\right] - \left[\sum_{\forall k(;,n)} 2G_k \left(\sum_{\forall i} \alpha_i \theta_i^{k+}\right)\right] = 0 \qquad \forall n \qquad \{\gamma_n\} \tag{4.32}$$

$$(\theta_n - \theta_m) - \left(\sum_{\forall i} \theta_i^{k+} - \sum_{\forall i} \theta_i^{k-}\right) = 0 \qquad \forall k \qquad \{\mu_k\} \tag{4.33}$$

$$\theta_i^{k+} \geq 0 \qquad \forall i,k \tag{4.34}$$

$$\theta_i^{k-} \geq 0 \qquad \forall i,k \tag{4.35}$$

$$-\theta_i^{k+} \geq -\theta_i^{\max} \qquad \forall i,k \qquad \{\rho_i^{k+}\} \tag{4.36}$$

$$-\theta_i^{k-} \geq -\theta_i^{\max} \qquad \forall i,k \qquad \{\rho_i^{k-}\} \tag{4.37}$$

$$P_k \geq -P_k^{\max} \qquad \forall k \qquad \{F_k^-\} \tag{4.38}$$

$$-P_k \geq -P_k^{\max} \qquad \forall k \qquad \{F_k^+\} \tag{4.39}$$

$$P_g \geq P_g^{\min} \qquad \forall g \qquad \{\delta_g^-\} \tag{4.40}$$

$$-P_g \geq -P_g^{\max} \qquad \forall g \qquad \{\delta_g^+\} \tag{4.41}$$

$$P_{g,t}, P_{k,t}, \theta_{n,t}, P_{n,t}^L \; free$$

If the lossy formulation artificially increase the amount of losses at a bus with a negative DLMP/LMP by violating the adjacency condition, for such a scenario, there exists at minimum a prior segment *i* and a later segment *j* such that (4.42) and (4.43) hold. Note that while the discussions here are restricted to the negative orthant, the same arguments are true for the positive orthant. From complementary slackness, (4.27) for segment *i* and *j* are equal to zero since the lengths of *i* and *j* are greater than zero. Also from complementary slackness, the dual variable of (4.37) for *i* is equal to zero since the maximum length of *i* is not used in the angle approximation, i.e., (4.37) is not active. Consequently, constraint (4.27) for *i* and *j* can be written as in (4.44) and (4.45). When (4.37) for *j* is also inactive, its dual variable is also equal to zero and (4.45) for *j* is further re-written as in (4.46). It is reasonable to assume constraint (4.37) for *j* is inactive since one of the arguments for this proof is that no constraint limits the creation of artificial losses at the bus with the negative DLMP/LMP. With (4.44) and (4.46) equaling zero, (4.47) must be true

since, as shown in (4.48), the slopes of segments *i* and *j* are not equal. If (4.47) is true, then from (4.24), the DLMP/LMP at bus *n*, which is supposed to be negative, is equal to zero. The proof shows that a lossy DCOPF problem that is supposed to have negative DLMPs/LMPs will have none if additional consumption at all the negative DLMP/LMP busses is not prevented by a constraint,

$$0 < \theta_i^{k-} < \theta_i^{\max} \tag{4.42}$$

$$0 < \theta_j^{k-} \tag{4.43}$$

$$-2G_k \alpha_i \gamma_n + \mu_k = 0 \tag{4.44}$$

$$-2G_k \alpha_j \gamma_n + \mu_k - \rho_j^{k-} = 0 \tag{4.45}$$

$$-2G_k \alpha_j \gamma_n + \mu_k = 0 \tag{4.46}$$

$$\gamma_n = 0 \tag{4.47}$$

$$\alpha_i \neq \alpha_j . \tag{4.48}$$

If a constraint limits the angle difference across a line connected to a bus with a negative DLMP/LMP, such that more power cannot flow across the line to artificially increase the amount of losses at the bus, the lossy formulation may create artificial losses at an adjacent bus. Creating artificial losses at the adjacent bus will allow more artificial losses to be created at the bus with the negative DLMP/LMP and it will further improve the objective function and drive the negative DLMP/LMP closer to zero. This occurs in the 3-bus example in Section 4.2. The artificial losses at bus 2 of the network cause congestion on line 1, seen by comparing the power flow on line 1 for the lossless and the lossy DCOPF studies in Table 4.4, which limits the amount of artificial losses that can be further created solely at bus 2. The congestion on line 1, which is also manifested in the maximum value $(\theta_2 - \theta_1)$ can be, is respected and at the same time while more losses are created at bus 2 to improve the solution, by violating the exclusivity condition. The same occurs for line 2 where artificial losses are created at bus 3 as a result of the congestion on line 2 to create more losses at bus 2. The limit placed on artificial loss creation by congestion on both lines 1 and 2 prevent the LMP at bus 2 from being zero.

As described in Section 4.2, violating the exclusivity condition allows artificial losses to be created without changing the angle difference across a line. If a limiting constraint manifested as a restriction on angle difference limits the flow across a line, the lossy formulation can respect the limit and create artificial losses by selecting segments in both orthants to approximate the angle difference. That is artificial losses are created through the lengths of the segments used to approximate the angle difference. If this occurs, there exists, at minimum, a positive orthant segment *i* and a negative orthant segment *j* such that (4.49) and (4.50) hold. From complementary slackness, (4.26) for segment *i* and (4.27) for *j* are equal to zero and can be written as in (4.51) and (4.52). Equation (4.53) can then be obtained by summing (4.51) and (4.52) together. From (4.28) it is known that the dual variables corresponding to the constraint that defines the maximum length of each segment, (4.36) and (4.37), are both non-negative. Consequently (4.54) can be deduced. When (4.55) and (4.56) holds, that is the angle limitation is not as a result of all the piecewise segments being completely used up, then the dual variables of (4.36) and (4.37) are

equal to zero and (4.54) can be written as in (4.57). From (4.24), (4.57) can be re-written as in (4.58),

$$\theta_i^{k+} > 0 \tag{4.49}$$

$$\theta_j^{k-} > 0 \tag{4.50}$$

$$-2G_k\alpha_i\gamma_m - \mu_k - \rho_i^{k+} = 0 \tag{4.51}$$

$$-2G_k\alpha_j\gamma_n + \mu_k - \rho_j^{k-} = 0 \tag{4.52}$$

$$\alpha_i\gamma_m + \alpha_j\gamma_n = \frac{\rho_i^{k+} + \rho_j^{k-}}{-2G_k} \tag{4.53}$$

$$\alpha_i\gamma_m + \alpha_j\gamma_n \le 0 \tag{4.54}$$

$$\theta_i^{k+} < \theta_i^{\max} \tag{4.55}$$

$$\theta_j^{k-} < \theta_j^{\max} \tag{4.56}$$

$$\alpha_i\gamma_m + \alpha_j\gamma_n = 0 \tag{4.57}$$

$$\alpha_i\lambda_m + \alpha_j\lambda_n = 0\,. \tag{4.58}$$

The proof in (4.49) to (4.58) show that if enough artificial losses cannot be created at a bus because a constraint prevents power flow into the bus or the losses may force the formulation to select a different solution that may be worse off and, if all the lengths of the segments in the piecewise approximation has not been used up, the formulation will create additional artificial losses at an adjacent bus until the weighted sum of the DLMPs/LMPs at both buses is equal to zero, (4.58). This can be explained easily using the simple case where *i* is equal to *j*. For such a case, artificial losses will be created until the sum of the DLMPs/LMPs at both buses is equal to zero. That is, the formulation will create more consumption until the net change in the cost to consume, i.e., the objective function, is zero. This means the formulation will create artificial losses until it cost more to create artificial invalid losses at the adjacent bus than the cost saved by creating artificial invalid losses at the bus with the negative DLMP/LMP. Equation (4.54) can only hold for a combination of a non-positive LMP and a positive LMP and for a combination of non-positive LMPs. Artificial losses can be created at an adjacent bus with either negative, positive or zero DLMP/LMP. A combination of non-positive DLMPs/LMPs can theoretically result in an unbounded situation where the resulting DLMPs/LMPs are as negative as possible. Note that when artificial losses are created at an adjacent bus, the DLMP/LMP at the negative DLMP/LMP bus will not be completely reduced to zero. This can also be seen in the 3-bus example in Section 4.2.

The dual of a standard DCOPF formulation does not have (4.26) or (4.27). These additional constraints are responsible for the lossy formulation approximating bus angle differences in such a way that fictitious losses are created to improve the solution of a problem when negative DLMPs/LMPs occur. It is important to recognize this inadequacy of the lossy DCOPF formulation because the resulting solutions (DLMPs/LMPs, losses, dispatches and line flows), when a negative DLMP/LMP occurs, may be wrong. It is also important to understand how the inade-

quacy is manifested in the DLMPs/LMPs so that the breakdown of the formulation can be readily identified.

4.4 Mixed-Integer Linear Programming (MILP) Formulation

The possibility of loss approximation errors require that the lossy DCOPF solutions be inspected for compliance with the adjacency and the exclusivity conditions. If loss approximation errors occur with the linear programming-based formulation, the lossy DCOPF problem must be converted to a MILP formulation as it is not possible to generate a set of linear constraints to enforce the adjacency and the exclusivity conditions (except by defining the convex hull). In the MILP formulation, (4.59) - (4.66) are added to the original linear programming-based lossy formulation for lines whose angle difference approximation violates the adjacency or the exclusivity conditions. Similar to [27], constraints (4.59), (4.60), (4.65), and (4.66) restrict the formulation to selecting the maximum length of lower segments if higher segments are also used to approximate a bus angle difference. By combining (4.61) with (4.59), (4.60), (4.65), and (4.66), the formulation is restricted from using segments in both orthants to approximate the same angle difference. Note that the mixed-integer linear constraints are applied only to lines whose angle difference approximations have violated the adjacency and exclusivity conditions. This reduces the computational complexity by not requiring these constraints for all lines but simply those corresponding to fictitious loss approximations. The resulting solution from such a decomposition approach must, however, also be checked for loss approximation errors. An algorithm for implementing the MILP formulation is shown in Figure 4.4. While non-positive LMPs are the trigger in the figure, non-positive DLMPs will be the trigger in a distribution system OPF,

$$\theta_{i,t}^{k+} \geq u_{i+1,t}^{k+}\theta_i^{\max} \qquad \forall i,k,t \mid k \in \Lambda^- \tag{4.59}$$

$$\theta_{i,t}^{k-} \geq u_{i+1,t}^{k-}\theta_i^{\max} \qquad \forall i,k,t \mid k \in \Lambda^- \tag{4.60}$$

$$u_{1,t}^{k+} + u_{1,t}^{k-} \leq 1 \qquad \forall k,t \mid k \in \Lambda^- \tag{4.61}$$

$$u_{i,t}^{k+}, u_{i,t}^{k-} \in \{0,1\} \qquad \forall i,k,t \mid k \in \Lambda^- \tag{4.62}$$

$$-\theta_{i,t}^{k+} \geq -\theta_i^{\max} \qquad \forall i,k,t \mid k \in \Lambda^+ \tag{4.63}$$

$$-\theta_{i,t}^{k-} \geq -\theta_i^{\max} \qquad \forall i,k,t \mid k \in \Lambda^+ \tag{4.64}$$

$$-\theta_{i,t}^{k+} \geq -u_{i,t}^{k+}\theta_i^{\max} \qquad \forall i,k,t \mid k \in \Lambda^- \tag{4.65}$$

$$-\theta_{i,t}^{k-} \geq -u_{i,t}^{k-}\theta_i^{\max}. \qquad \forall i,k,t \mid k \in \Lambda^- \tag{4.66}$$

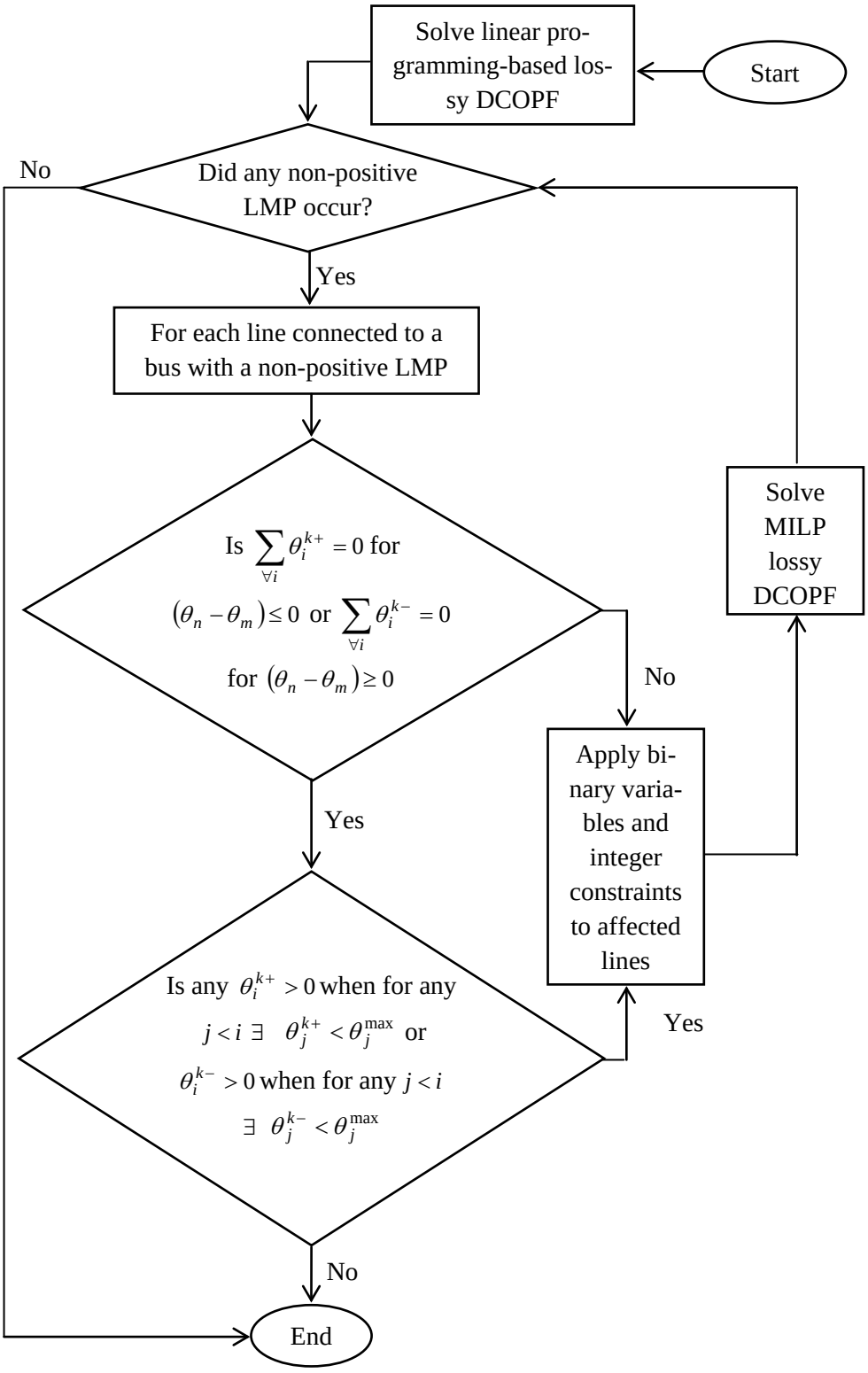

Figure 4.4. MILP Lossy DCOPF Implementation Triggered by Non-positive LMPs

The MILP formulation is used to conduct a study on the 3-bus network in Section 4.2. Its results and the results of the lossless and the linear programming-based lossy formulations are compared in Table 4.5 to Table 4.7. Comparison of the loss results of the linear programming-based lossy DCOPF study to the loss results of the MILP lossy study in Table 4.5 confirms that fictitious losses are created at the 3 buses in the network in the linear programming-based lossy study. Fictitious losses are created at bus 1 and bus 3 in addition to the fictitious losses at bus 2 because of the congestion on lines 1 and 2 respectively, Table 4.7. It is cheaper and more effective to create fictitious losses at the bus with the negative LMP than it is to also create fictitious losses at an adjacent bus with a positive LMP. Consequently, the fictitious losses at bus 2 are approximately 45 times the fictitious losses at bus 1 and approximately 21 times the fictitious losses at bus 3. The total losses in the linear programming-based study are approximately 9.5 times the total losses in the MILP lossy study. Bus 2's LMP in the linear programming-based lossy study is not completely reduced to zero because the congestion on lines 1 and 2 limit the creation of artificial losses. Table 4.7 shows that the congestion on line 1 is purely as a result of the flow of fictitious losses to bus 2. Table 4.6 shows that the dispatch solutions of the linear programming-based lossy study and the MILP study are significantly different. Table 4.5 shows that bus 2's LMP in the linear programming-based lossy study and the MILP study are also significantly different and the total cost in the linear programming study is about $216 less than the total cost in the MILP study.

Table 4.5. LMP, Losses, and Generation Cost Results

Bus No.	Lossless DCOPF	Linear Prog. Lossy DCOPF		MILP Lossy DCOPF	
	LMP ($/MWh)	LMP ($/MWh)	Losses (MW)	LMP ($/MWh)	Losses (MW)
1	50.00	50.00	0.11	50.00	0
2	–50.00	–5.71	5.00	–46.10	0.10
3	100.00	100.00	0.75	100.00	0.52
Total Losses	0 MW	5.86 MW		0.62 MW	
Total Cost	$6000.00	$5830.32		$6046.95	

Table 4.6. Generation Dispatch Results

Gen No.	Lossless DCOPF	Linear Prog. Lossy DCOPF	MILP Lossy DCOPF
	Output (MW)	Output (MW)	Output (MW)
1	80.00	95.11	80.31
2	20.00	10.75	20.31

Table 4.7. Lossless and Lossy DCOPF Line Flow and Line Angle Difference Results

Line No. (k)	Lossless DCOPF		Linear Prog. Lossy DCOPF		MILP Lossy DCOPF	
	Line Flow (MW)	$\theta_n - \theta_m$ (rad)	Line Flow (MW)	$\theta_n - \theta_m$ (rad)	Line Flow (MW)	$\theta_n - \theta_m$ (rad)
1	20	–0.0300	25	–0.037	20.1	–0.0301
2	–20	0.0150	–20	0.015	–20.0	0.0150
3	–60	0.4498	–70	0.053	–60.2	0.0451

4.5 Conclusion

The lossy OPF for calculating DLMPs is developed in this chapter. The OPF formulation uses a piecewise linear approximation technique to approximate real power losses. The lossy DCOPF formulation can be used both for LMPs in the transmission system and the DLMPs in the distribution system. The loss approximation technique places additional constraints on the lossy formulation that may cause the formulation to create fictitious losses. Fictitious losses are created as long as the objective decreases due to fictitious losses, which generally drives negative DLMPs/LMPs to zero or as close to zero as possible depending on binding constraints in the problem. When loss approximation errors occur, the lossy formulation has to be solved as a MILP formulation with binary variables and constraints applied to lines whose angle difference approximations violates an adjacency or an exclusivity condition. It is important to be aware of the loss approximation error and to correct for it because the artificial losses created could be substantial and could lead to a wrong dispatch and wrong DLMPs/LMPs.

Chapter 5. Illustrative Examples of the DLMP

The lossy DCOPF formulation in Chapter 4 is used to calculate DLMPs for different test distribution systems in this chapter. The calculations are conducted for: (1) a traditional distribution system with inelastic loads, radial topology and no congestion, (2) an enhanced distribution system with price responsive loads, radial topology and no congestion, and (3) an enhanced distribution system with price responsive loads, meshed topology and congestion. The iterative framework described in Section 3.2 is also illustrated numerically with an enhanced distribution system with price responsive loads.

5.1 Roy Billinton Test System (RBTS)

The RBTS system is used in all of the studies in this chapter. It consists of a transmission system and five load busses that represent the distribution systems connected to the transmission system. The system was developed in [28] - [31]. Figure 5.1 shows the one-line diagram of the transmission system, which is operated at 230 kV and has a peak load of 185 MW. The transmission system also has 11 generators. Six of the generators are located at bus 1 and the remaining five are located at bus 2. For the purpose of the studies in this chapter, the maximum generation capacity of the transmission system is modified from 240 MW to 222.5 MW. Details of the generators and the marginal costs used in the simulations are shown in Table 5.1. The marginal costs in the table have also been modified from the original RBTS data. Details of the transmission system's branch data are listed in Table A.1 in Appendix A.

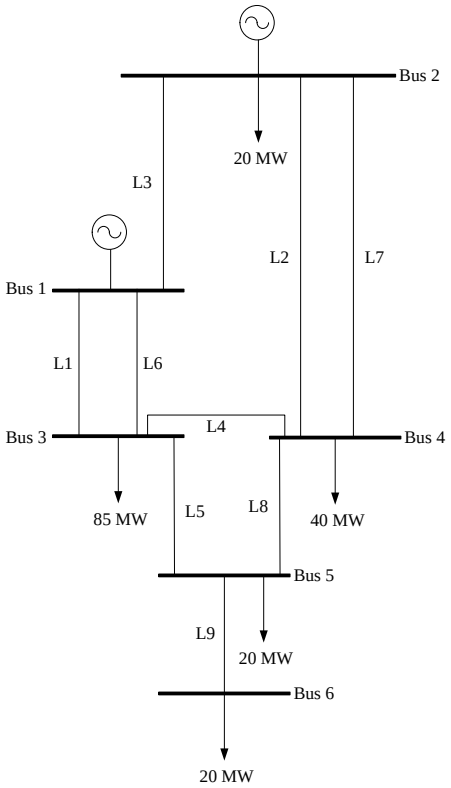

Figure 5.1. RBTS Transmission System

Table 5.1. RBTS System Generator Details

Unit No.	Bus	Marginal Cost ($/MWh)	Min. Output (MW)	Max. Output (MW)
1	1	53	0	22.5
2	1	50	0	40
3	1	80	0	10
4	1	55	0	20
5-6	2	20	0	5
7	2	20	0	40
8-11	2	20	0	20
Maximum Capacity				222.5

The distribution systems at bus 3 and at bus 4 of the transmission system are the test distribution systems. The bus 3 system has a peak load of 85 MW distributed along 8 primary feeders between 44 load points (LP). As shown in Table 5.2, the LPs are aggregates of multiple customers with similar service requirements: residential users, large industrial users, small industrial users, commercial users, and office buildings. The one-line diagram of the system is shown in Figure 5.2. The main substation is energized at 138 kV and the main substation is the only source of energy to the system. The main substation is connected to two other substations by 33 kV lines. Feeders 1 (F1) to F6 are operated at 11 kV and F7 and F8 at 138 kV. The 8 primary feeders in the distribution system have section types listed in Table 5.4. The impedance and the peak loading data for each feeder are listed in Table 5.3. For the simulations in this chapter, two 230/138 kV sub-transmission transformers that connect the transmission system to the substation of the bus 3 distribution system are added between bus 3 and a new bus (bus 7) in the transmission system and the load at bus 3 is moved to the new bus. This was done so that the sub-transmission system transformers could be included in the transmission system network model.

Table 5.2. Bus 3 Distribution System Load Details

Customer type	Peak Load (MW)	Load Points
Residential	0.8367	1, 4-7, 20, 24, 32, 36
	0.85	11, 12, 13, 18, 25
	0.775	2, 15, 26, 30
Large users	6.9167	39, 40, 44
	11.5833	41-43
Small Industrial	1.0167	8, 9, 10
Commercial	0.5222	3, 16, 17, 19, 28, 29, 31, 37, 38
Office Buildings	0.925	14, 27

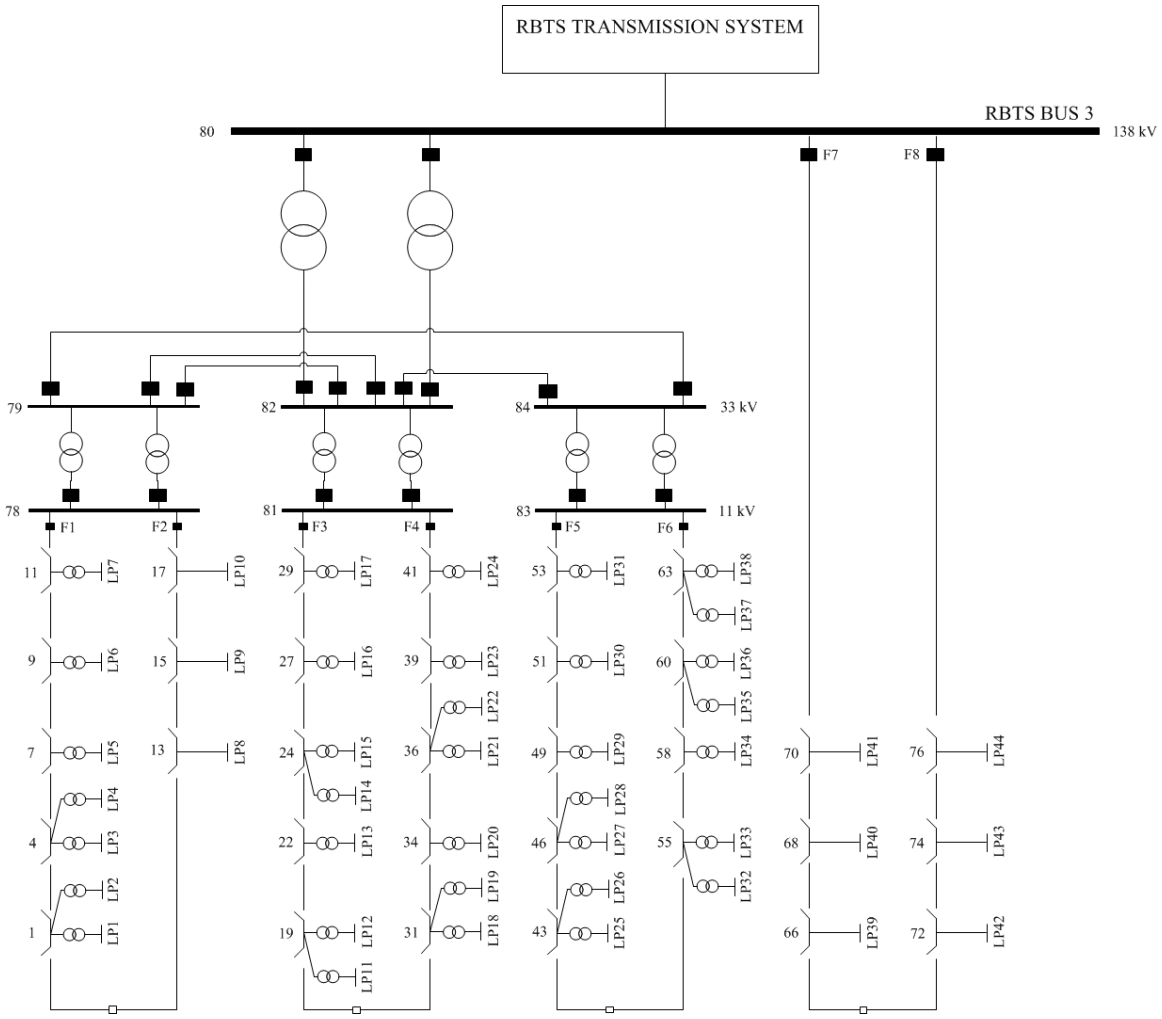

Figure 5.2. Distribution System at Bus 3

Table 5.3. Bus 3 Distribution System Feeder Summary

Feeder	kV Level	Total MW Load	Total Length (mi)	R (Ω/mi)	X (Ω/mi)
1	11	5.4807	5.4057	0.307088	0.62958
2		3.0501	3.0446		
3		5.2944	5.7164	0.187726	0.60014
4		5.5557			
5		4.8916			
6		5.2279	5.1572		
7	138	25.4167	2.8582	0.592606	0.76279
8		30.0833			
Total		85.0004	30.0833		

Table 5.4. Bus 3 Distribution System Feeder Section Length

Section Type	Length (mi)	Section Number
1	0.3728	1, 2, 3, 7, 11, 12, 15, 21, 22, 29, 30, 31, 36, 40, 42, 43, 48, 49, 50, 56, 58, 61, 64, 67, 70, 72, 76
2	0.4971	4, 8, 9, 13, 16, 19, 20, 25, 26, 32, 35, 37, 41, 46, 47, 51, 53, 57, 60, 62, 65, 68, 71, 75, 77
3	0.5592	5, 6, 10, 14, 17, 18, 23, 24, 27, 28, 33, 34, 38, 39, 44, 45, 52, 54, 55, 59, 63, 66, 69, 73, 74

As shown in Table 5.5, the distribution system at bus 4 of the RBTS transmission system has a peak load of 40 MW distributed along 7 primary feeders between 38 LPs. Similar to bus 3, the LPs are aggregates of multiple customers with similar service requirements. The loads are classified into five categories. Type 1 and type 2 are residential loads with peak consumption of 0.8869 MW and 0.8137 MW respectively, type 3 and type 4 are small industrial loads with peak consumption of 1.63 MW and 2.445 MW respectively, and type 5 are commercial loads with a peak consumption of 0.6714 MW. Table 5.6 lists the LPs and their classification. The system is supplied by 3 distribution substations. As shown in the one-line diagram in Figure 5.3, the substations are connected by 33 kV lines and one of the substations is directly connected to the transmission system. The system's branch and detailed load data are provided in Table A.3-Table A.6 in Appendix A. The system has an open-loop topology. For the purpose of this report, the normally open switch between F1 and F7, the normally open switch between F3 and F4 and the normally open switches between F2, F5, and F6 are closed to form a meshed distribution system. A summary of the studies in this chapter and the systems used for each study in presented in Table 5.7

Table 5.5. Summary of Distribution System at Bus 4 of RBTS System

Number of Nodes	75
Number of Branches	84
Number of Distributed Generators	2
Number of Load Points	38
Total Peak Load	40 MW
Capacity of Distributed Generator	2.75 MW

.

Table 5.6. Bus 4 Distribution System Load Type Details

Load Type	Load Points
1	1-4, 11-13, 18-21, 32-35
2	5, 14, 15, 22, 23, 36, 37
3	8, 10, 26-30
4	9, 31
5	6, 7, 16. 17, 24, 25, 38

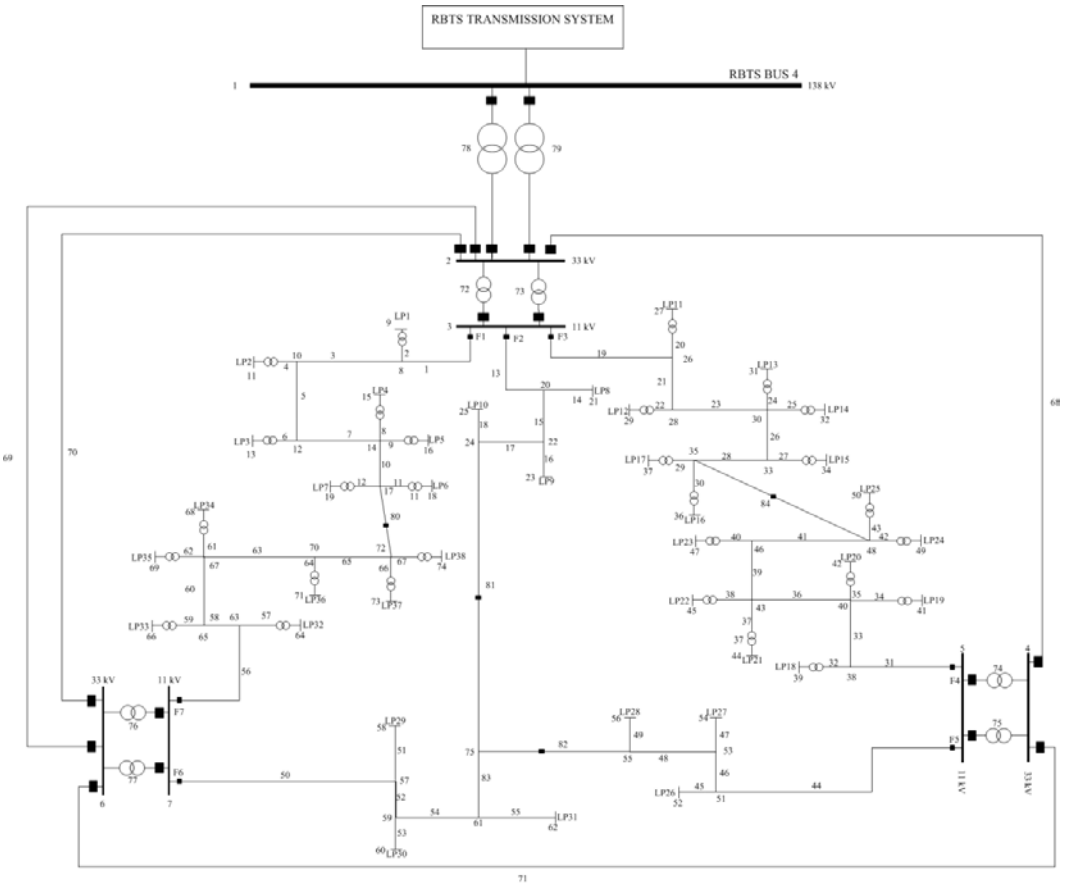

Figure 5.3. Distribution System at Bus 4 with a Meshed Topology

Table 5.7. Summary of Studies and Test Systems Used

Test Distribution System	Section	Characteristics	Study Objectives
Bus 3	5.2	- Radial topology - No congestion - No price sensitive resources	- DLMP trends in a traditional distribution system - Cross-subsidy with average prices
	5.3	- Radial topology - No congestion - PRLs	- Benefit of the DLMP to economic efficiency
	5.5	- Radial topology - No congestion - PRLs	- Importance of iterative approach to calculating DLMPs
Bus 4	5.4	- Meshed topology - Congested - PRLs - DGs	- DLMP in a congested distribution system

5.2 DLMP in a Traditional Distribution System

The test traditional distribution system is the distribution system at bus 3 of the RBTS system. The system is operated radially, the system lacks internal generation resources and all loads in the system are assumed to be perfectly inelastic. Hence, feeders and equipment in the system, as it is in traditional distribution systems, are oversized to avoid congestion. DLMPs in the system have no congestion component as a result. Price separation between nodes results from real power losses. This is reflected in Figure 5.4, the plots of the calculated DLMPs for the peak period of the test distribution system.

Figure 5.4 shows the computed DLMP at the LP nodes on each feeder. The LPs are numbered from the beginning to the end of each feeder (for example LP7 on F1 in Figure 5.2 is LP1 on F1 in the plot). The trend of the plots reflects the locational effect of real power losses. The farther a LP is from the beginning of a feeder, the higher the losses incurred in delivering energy to the LP; thus, the higher the DLMP at its node. This is true for any radial feeder with one injection point; losses incurred to deliver energy to a node will increase as the node gets farther from the source of injection. The notion of DLMPs increasing along a radial feeder is valid even for F1 where there is a decrease in the DLMP between consecutive LPs: the fourth and the fifth LPs. The decrease occurs because both LPs are connected to the same node on the primary feeder via laterals of different lengths. The lateral connecting the LP with the higher DLMP to the primary feeder node is longer than the length of the lateral connecting the LP with the lower DLMP to the primary feeder node. Both the fourth and fifth LPs are connected to node 4 (figure numbering) on F1. The lateral connecting the fifth LP to node 4 is of section type 1 and is 0.3728 miles long while the lateral connecting the fourth LP to node 4 is of section type 2 and is 0.4971 miles long.

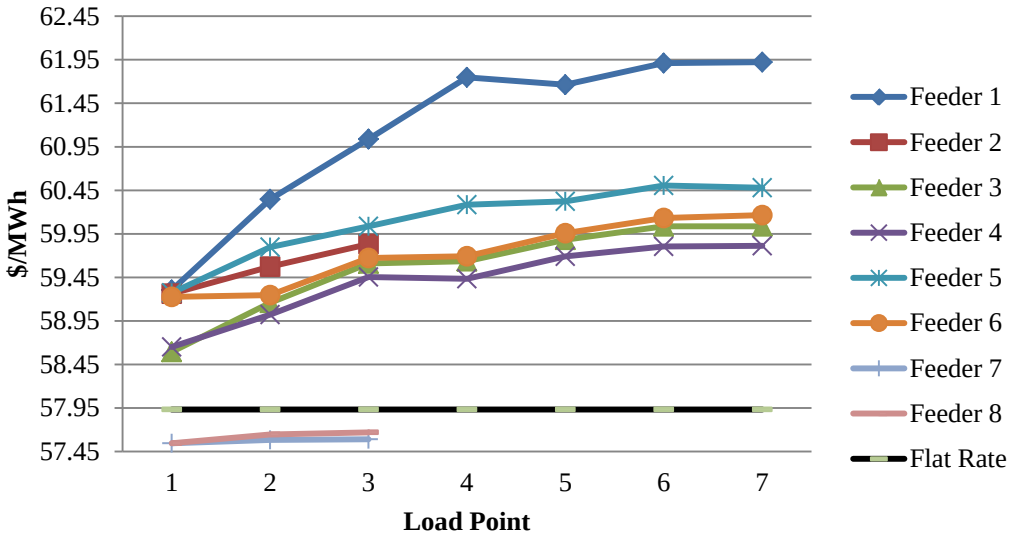

Figure 5.4. DLMP Across Feeders in the Test Distribution System (The LMP at the transmission proxy is indicated by the first point on the vertical axis)

The effect of losses is also apparent between feeders. From Figure 5.4, it can be deduced that the least amount of losses per MWh delivered are incurred on F7 and F8. Despite F7 and F8 having about 65 percent of the total system loading, this resulted because both feeders are direct-

ly connected to the sub-transmission bus. Hence, they are the closet feeders to the source of the system and are operated at 138 kV. F7 and F8 also have the shortest lengths in the system.

Effect of losses between feeders is also reflected in the trend of the DLMP at the first LP of F3 through F6. F3 and F4 are connected to the substation directly energized by the sub-transmission system while F1, F2, F5 and F6 are connected through 33 kV lines to the substation F3 and F4 are connected to. This resulted in the DLMP at the first LP on F3 and F4 being lower than the DLMP at the first LP on F1, F2, F5, and F6. The DLMP at the first LP on F1, F2, F5, and F6 are close because the 33 kV lines connecting each substation to the main substation are of equal lengths and the 33kV/11kV transformers have the same impedance. The divergence of DLMPs further down F1 through F6 is a result of different feeder section lengths, loading, and impedance. The higher impedance of F1 dominates.

The total payment to the transmission system is used to calculate a flat rate (FR) that can be used to represent average rates from COS regulation. The rate, $57.93/MWh, is the cost per MWh to recover the payment (energy and losses) to the transmission system. Cross-subsidization under the FR pricing scheme is apparent. Some LPs pay more than their DLMP while others pay less (DLMP is the accurate marginal cost that captures the individual contribution of each load to losses). Figure 5.4 shows that the loads on F7 and F8 will pay more than their true cost to consume under the FR scheme, i.e., the loads on F7 and F8 will subsidize the other loads in the system. The economic benefit of contributing less to losses will not be realized by the loads on F7 and F8 as a result. In the traditional distribution system where loads are assumed to be perfectly inelastic and there is limited price sensitive resources, operating with average rates may be acceptable. In the enhanced distribution system, however, cross-subsidies will distort prices and send incorrect economic signals to price sensitive resources and negatively affect economic efficiency. The locational information provided by the DLMP, which may not be readily predictable in congested systems, will also be lost with average prices. Note that contemporary RTPs also cause cross-subsidies. While contemporary RTPs capture and reflect conditions in the transmission system, they do not reflect conditions in the individual distribution system they are used in.

5.3 DLMP in an Enhanced Distribution System with Price Responsive Loads

One of the major advantages of the DLMP is its capability to improve economic efficiency by properly incentivizing price sensitive resources to behave optimally in a manner that benefits system operations. The actions incentivized by the DLMP are compared to the action incentivized by a FR to illustrate the capability of the DLMP to improve economic efficiency in this section. The price sensitive resources are flexible loads. The test distribution system is the distribution system at bus 3 of the RBTS system. Twenty percent of the peak load in the test system is considered elastic for the enhanced distribution system. The LPs selected as price responsive loads are listed in Table 5.8. Each price responsive load has a two-step bid. It is assumed that only part of the demand of each price responsive load is sensitive to the price range expected for the DLMPs. The first step of the demand bid represents the portion of the demand of each price responsive LP that is inflexible and the second step represents the flexible portion. The bid value of the inflexible portion is $64.45/MWh for all the price responsive loads. The flexible portion of a load has one of the 4 values in Table 5.8. The values represent different levels of flexibility with the lowest representing the highest flexibility and the highest representing the lowest flexibility. The remaining details of the price responsive loads are listed in Table A.2 in Appendix A.

Table 5.8. Bid Value of Flexible Portion of Demand

Bid Value ($)	Load Point
55	3, 11, 27, 32
57.65	19, 21, 39, 40, 42, 43
58.95	2, 8, 9, 12, 14, 25, 26, 33, 35
61.45	1, 4, 13, 18, 20, 28, 34

The resulting DLMP at the nodes of the flexible LPs, the FR established in Section 5.2, and the bid value of the flexible part of the LPs are plotted in Figure 5.5. The action incentivized by the DLMP and the FR is shown in Table 5.9. Table 5.9 is obtained based on the intersection of a price with the bid value plot. Whenever a price is less than or equal to the value of the flexible portion of a load, the flexible portion of the load is consumed. Whenever a price is higher than the value of the flexible portion of a load, the flexible portion is not consumed. The behavior incentivized by the DLMP is the optimal behavior because the DLMP is an accurate economic signal. The behavior incentivized by the FR deviates from that of the DLMP; hence, it is suboptimal. For example, the behavior of LPs 2, 19, 21, 39, 40, 42, and 43 deviates from the optimal behavior. LP2 is incentivized to consume the flexible portion of its demand even though the value it places on the flexible portion is less that the true cost to consume. LPs 19, 21, 39, 40, 42 and 43 are incentivized not to consume even though the value they place on consumption is higher than the true cost to consume. As discussed in Section 3.1, deviation from optimal behavior leads to a reduction in economic efficiency: deadweight loss. Hence, the FR pricing mechanism is inferior to the DLMP pricing mechanism. In an enhanced distribution system, the benefits of having distribution resources will be reduced as a result of wrong price signals. For example, a load whose consumption further exacerbates the cost of congestion may be incentivized to consume by a FR pricing mechanism during a period when the DLMP would otherwise discourage consumption by sending a higher pricing signal.

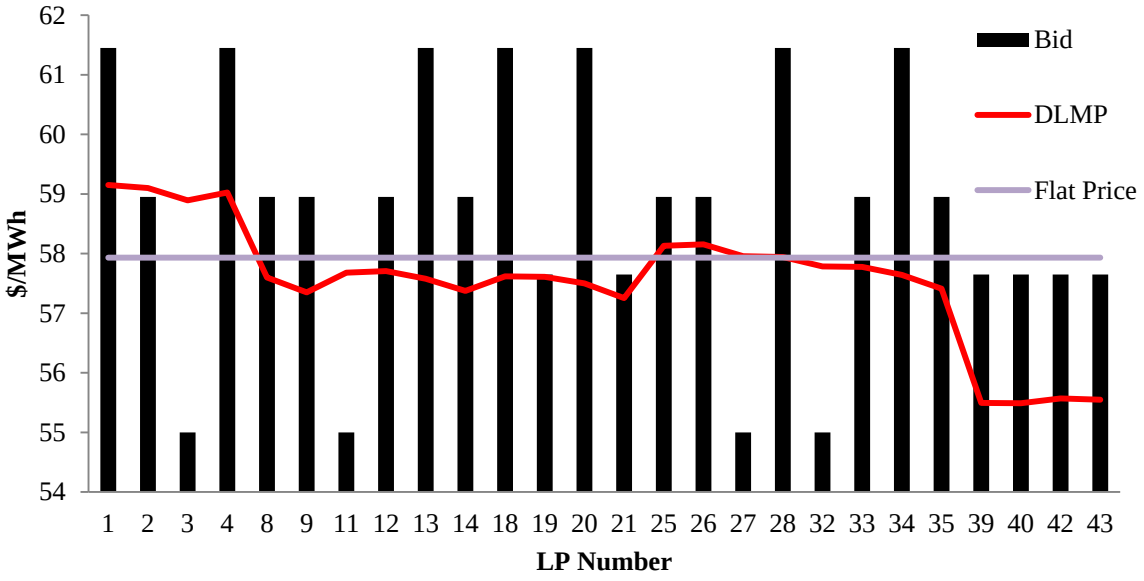

Figure 5.5. Flexible Portion of Demand, DLMP, and Flat Price

Table 5.9. Action Incentivized by DLMP and Flat Price (Black – Consumption both prices, White – No consumption both prices, Red – Consumption one price, No Consumption one price)

LP #	1	2	3	4	8	9	11	12	13	14	18	19	20	21	25
DLMP															
FP															

LP #	26	27	28	32	33	34	35	39	40	42	43
DLMP											
FP											

5.4 DLMP in a Meshed Distribution System with Congestion

Today, there are distribution systems that are meshed; however, they are primarily found in large metropolitan cities. If the existence of meshed distribution systems increases in the future, congestion can cause higher nodal price separation than losses could. Price separation as a result of congestion reflects the ability of the DLMP to internalize congestion management. The distribution system at bus 4 of the RBTS system is used to illustrate DLMPs in a meshed and congested distribution system. To create congestion, the capacity limit for line section 17, between nodes 22 and 24 on F2, is set to 1.9 MW. A 750 kW DG with a marginal cost of $18/MWh is placed at node 22. A 2 MW DG, with a marginal cost of $40/MWh, is placed at bus 4. The DGs are in addition to the transmission system, which is an infinite generator with a marginal cost of $54.63/MWh. Type 1 loads are modeled as perfectly inelastic loads while type 2 through type 5 are elastic loads with the demand bids in Figure 5.6. The development of the demand bids is discussed in details in Chapter 6.

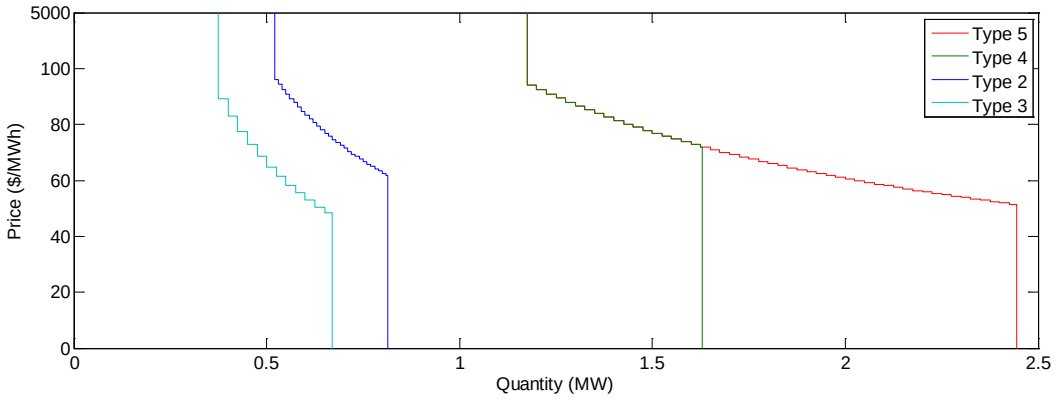

Figure 5.6. Elastic Load Bids

Several DLMP trends that results for the congested system, as shown by Figure 5.7, are different from the trends in the uncongested system, which can be seen by Figure 5.8. The highest DLMP in the congested system ($92.54) is much higher than the highest DLMP in the uncongested system ($60.26) and occurs at different locations: LP3 on F1 and LP8 of F4 in the

congested and uncongested system respectively. The lowest DLMP in the congested system is also lower than the lowest DLMP in the uncongested system and occur at different locations. Of note are the DLMPs on F2, which has the congested segment, and the DLMPs on F5 and F6. While the DLMP on F2 increased between its first and second LPs and decreased between its second and third LPs for the uncongested system, it does the opposite in the congested system. The values of the DLMPs at the first and the second LPs on F2 are also lower in the congested system than in the uncongested system and higher for the third LP in the congested system than in the uncongested system. The lower DLMPs incentivized a 15 percent increase in the consumption at the second LP on F2 and the higher DLMP incentivized a 26 percent decrease in the consumption at the third LP. The DLMPs on F5 and F6 are noticeably affected because both feeders are directly connected to F2. The DLMPs on the feeders are higher in the congested system. The higher DLMPs resulted in a consumption decrease of 9.5 percent at the third LP on F6.

DLMP separation as a result of congestion is a tool for system operation and provides valuable information for system upgrades and resource location. The change in consumption between the congested and the uncongested system aided with respecting the line flow limit of segment 17. For example, the change in the consumption of the second and the third LPs on F2 have the effect of reducing power flow on the segment. Increasing the consumption at the second LP reduces the power flow to segment 17 because the LP is before the congested segment and reducing the consumption at the third LP reduces the power flow because the LP is after the congested segment: the net power flow on the feeder is from the beginning of the feeder to the end. The trend of the DLMPs on F2 also signifies that the nodes on the feeder have the greatest impact on congestion and it will be more effective to locate the DG at node 22, at node 24, or at node 25 to relieve congestion on segment 17. The inversion of the DLMP trend on F2 in the congested test system, as compared with the uncongested system, signifies that the DLMP trend in a congested system may be different from the DLMP trend in a radial system; this also communicates that the trend of the DLMP in a congested system may not be readily predictable.

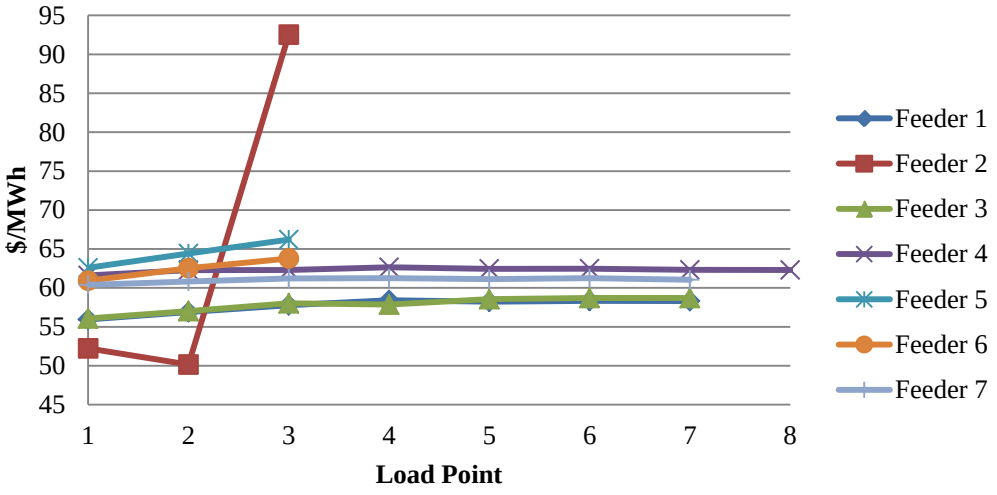

Figure 5.7. DLMPs in Enhanced Distribution System with Congestion

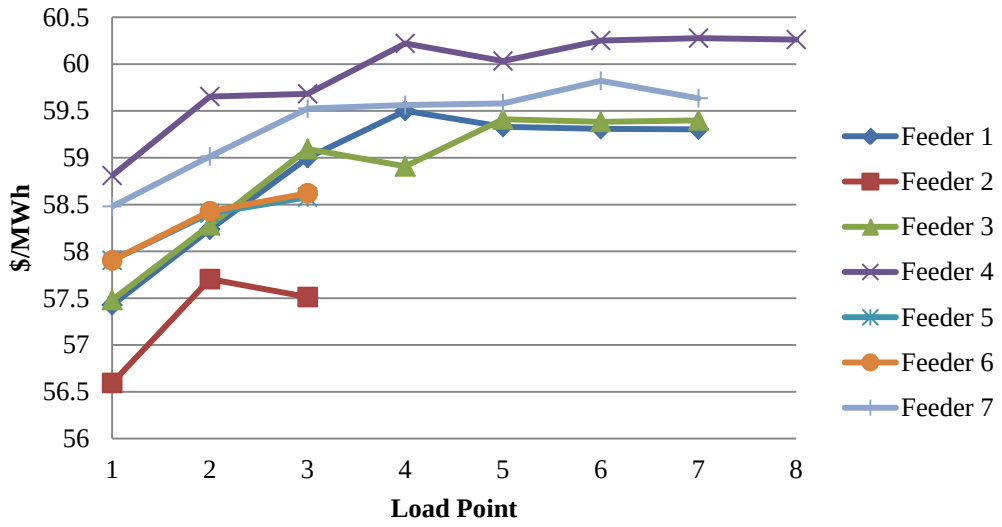

Figure 5.8. DLMPs in Enhanced Distribution System without Congestion

5.5 Optimal Coupling of the Transmission and the Distribution System

If the benefits of the expected DSRs are to be effectively propagated throughout the whole power system, the transmission and the distribution systems must be optimally coupled. This is the reason behind the iterative framework discussed in Section 3.2. Optimal coupling of the transmission and distribution system is illustrated using the test distribution system in Section 5.3 and the RBTS transmission system. The iterative process for the study converged in 3 iterations. The resulting LMPs in the transmission system from the first and the second iterations are shown in Figure 5.9. There is a difference between the LMPs in both iterations because the solutions of the first iteration (single-shot approach) are sub-optimal while the solutions for the second iteration (iterative approach) are optimal. The sub-optimal solutions of the single-shot approach resulted because of an inaccurate representation of the distribution system. The peak load, 85 MW, was the initial load forecast. It resulted in generator 4, with a marginal cost of $55/MWh, being the marginal generator. The resulting LMP at the distribution proxy bus caused the price sensitive distribution loads to deviate from their forecasted peak, resulting in an aggregate distribution consumption of 79.10 MW. The new model of the distribution system resulted in generator 1, with a marginal cost of $53/MWh, becoming the new marginal generator in the second iteration. Generator 1 remained the marginal generator in the third iteration and LMPs remained the same between the second and the third iterations. Since it is not possible to perfectly approximate the flexible resources in the distribution system at the distribution proxy when solving the transmission system, such an iterative framework is preferred in order to achieve an integrated framework between the two systems. Note that in a congested transmission system, LMPs can change between iterations even if the marginal generator remains the same.

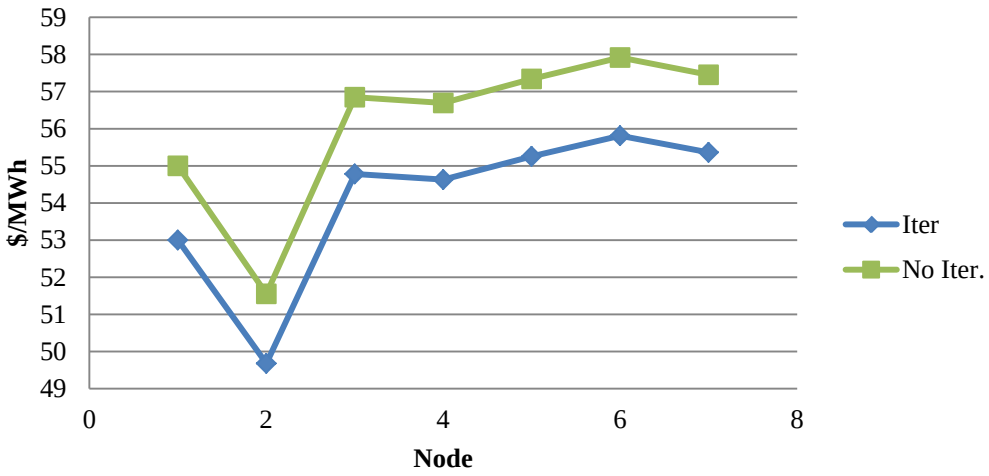

Figure 5.9. Transmission LMP for 1st and 2nd Iterations

The solutions from the single-shot approach are confirmed to be sub-optimal and the results from the iterative approach are confirmed to be optimal by comparing the resulting LMPs and DLMPs from both approaches to that obtained by using a single model of the transmission and the distribution systems. The single model is the true problem and its solution is the global optimal solution. Figure 5.10 shows that the results from the iterative framework converges to the same solution as the single model while the results of the single-shot approach deviates from the results of the combined system.

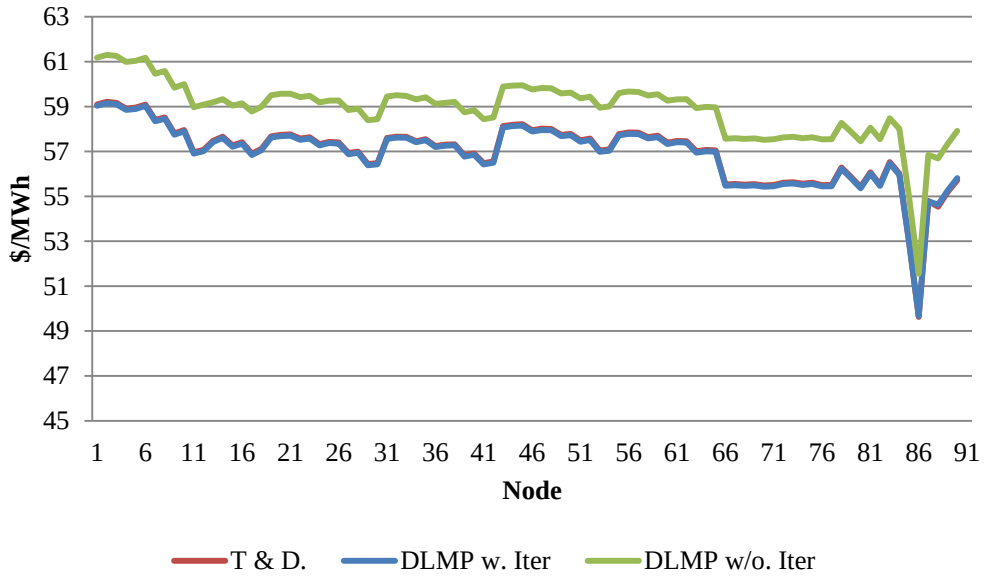

Figure 5.10. Comparison of the Iterative and Single-shot Solutions to the Solutions from a Single Model of the Transmission and the Distribution System

The effect of sub-optimal solutions includes loss of economic efficiency. The sub-optimal prices of the single-shot approach incentivized sub-optimal behavior of the PRL in the distribution system and it would also incentivize sub-optimal behavior of DGs and ESSs. This is illustrated in Figure 5.11 and Table 5.10. Figure 5.11 shows the value of the flexible portion of price

responsive loads in the test distribution system and the DLMP at the price responsive LP nodes for the iterative and the single-shot approach. Table 5.10 shows the action incentivized by both approaches. The consumption incentivized by the single-shot approach deviates from the consumption incentivized by the DLMP for several LPs. The deviation results in efficiency loss as shown in Table 5.11

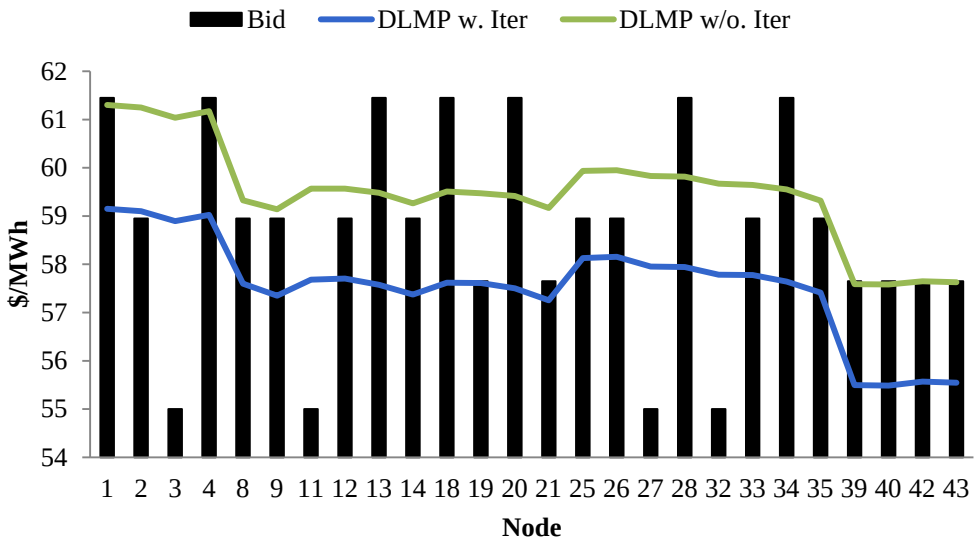

Figure 5.11. Flexible Portion of Demand and DLMP for Iterations 1 and 2

Table 5.10. Action Incentivized by DLMP for Iterations 1 and 2 (Black – Consumption both prices, White – No consumption both prices, Red – Consumption one price, No Consumption one price, Gray – Partial Consumption)

LP #	1	2	3	4	8	9	11	12	13	14	18	19	20	21
DLMP w. Iter.														
DLMP Single-shot														

LP #	25	26	27	28	32	33	34	35	39	40	42	43
DLMP w. Iter.												
DLMP Single-shot												

Table 5.11. Comparison of Resulting Market Surplus for Iterative and Single-shot Approach

Approach	Total Demand Value ($)	Elastic Demand Value ($)	Gen. Cost ($)	Market Surplus ($)
Iterative	5296.68	912.89	4668.04	628.64
Single-shot	5030.01	646.22	4575.00	455.00

While the DLMPs for the single-shot approach are higher than the DLMPs of the iterative process for this study, this trend cannot be guaranteed to always occur. If the study had been started with a low aggregate distribution demand for the first iteration, the DLMPs in the first iteration may have been lower than the DLMPs in the second iteration. What can be guaranteed is the demonstrated improvement in economic efficiency. Optimally coupling the transmission and distribution systems will reduce operational costs and improve reliability. For example, if

DSRs are used for ancillary services, it will be important that the control signal, such DSRs act upon, be accurate for both transmission and distribution system operations.

5.6 Conclusion

Several studies have been used to numerically illustrate the DLMP in this chapter. The studies showed that in the traditional distribution system, where there is no congestion and the network is operated radially, DLMPs increase from the point of generation injection to feeder ends as only losses cause DLMP separation. The study on an enhanced system with price responsive load showed that contemporary prices in the distribution system will reduce economic efficiency in the enhanced distribution system partly because of the cross subsidies that distort prices and wrongly incentivize distribution resources. A study in the chapter shows that in a congested system, the DLMP trend is not as predictable as in an uncongested system as a result of the DLMP internalizing congestion management. The trend of DLMPs in a congested system can provide valuable information for locating resources in an enhanced system. The chapter also illustrated the need to optimally couple the transmission system and the enhanced distribution system. The coupling, which can be achieved through a mechanism, such as the iterative DLMP calculation approach, allows for the proper modeling of the price sensitive resources in both systems in the decomposed OPF problem.

Chapter 6. Comparison of the DLMP to Contemporary Pricing Mechanisms in the Distribution System

Simulation results that compare the impact of the DLMP to the impact of a RTP, a TOU rate, and a FR are reported in this chapter. Multi-period studies are conducted on enhanced distribution systems with price responsive loads and a meshed topology with and without congestion. The test system is described in Section 6.1 and the modeling of the price sensitive loads is described in Section 6.2. The iterative framework discussed in Section 3.2 may fail to converge. The convergence issue is discussed in Section 6.3. An alternative framework, used to calculate DLMPs for the studies in this chapter, and the framework for calculating other tested pricing indices is described in Section 6.4. The results in Section 6.5 through Section 6.8 cover various studies involving different demand elasticity as well as networks with and without congestion. A concluding paragraph is presented in Section 6.9.

6.1 Test System

The test systems reported in this chapter are the IEEE 30 bus system and the distribution system at bus 4 of the RBTS system. The IEEE 30 bus system represents the transmission system; a summary of its characteristics are presented in Table 6.1 and its one line diagram is shown in Figure 6.1. The branch and the load details of the system are listed in Table A.7 and Table A.8 in Appendix A. The data for the IEEE 30 bus system was obtained from test case case30pwl in MATPOWER [34]. The system in case30pwl was modified from the original IEEE test system using data from [35]. Data obtained from [35] include branch limits. For this report, the test distribution system is placed at bus 5. The generator data in case30pwl were replaced with the generator data in Table 6.2. The generator data were obtained from the reliability test system (RTS) [36], [37]. For the studies in this chapter, all transmission loads, except for the load at bus 5, are perfectly inelastic. The perfectly inelastic loads have a 24 hour load profile as shown by Figure 6.2. The load profile is a spring weekday load profile from the RTS system. The hourly load details for the test transmission system are in Table A.8 in Appendix A.

Table 6.1. Summary of IEEE 30-Bus System

Number of Buses	30
Number of Branches	41
Number of Generators	6
Number of Load Points	21
Total Peak Load (incl. distribution system peak load)	229.20 MW
Total Generation Capacity	360.00 MW

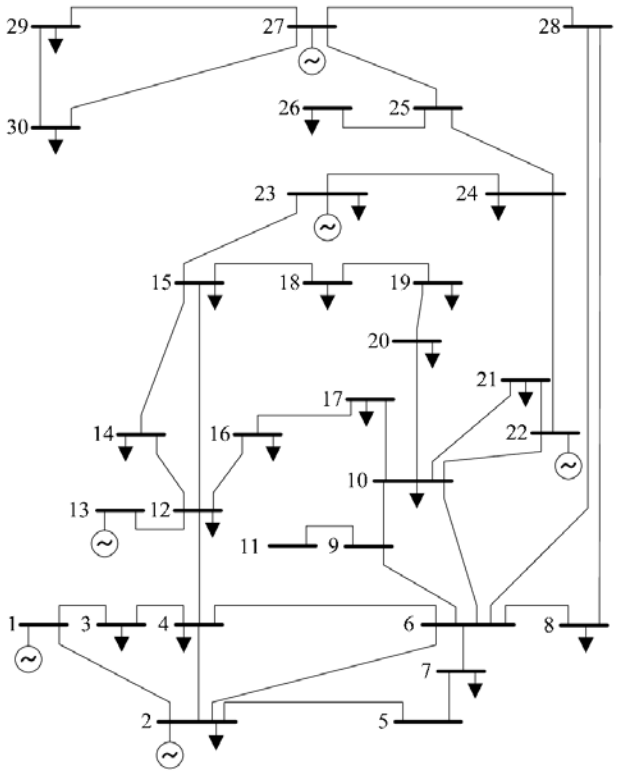

Figure 6.1. One-line Diagram of IEEE 30-Bus System [38] (Test Distribution system at bus 5 not shown)

Table 6.2. Generator Data for the Test Transmission System

Gen No.	Bus No.	Min. Output (MW)	Max Output (MW)	Marginal Cost ($/MWh)	Gen. Type
1	1	0.00	76.00	19.64	Fossil Steam Coal
2	2	0.00	20.00	163.02	Comb Turbine Oil
3	22	0.00	12.00	94.74	Fossil Steam Oil
4	27	0.00	76.00	19.64	Fossil Steam Coal
5	23	0.00	76.00	19.64	Fossil Steam Coal
6	13	0.00	100.00	75.64	Fossil Steam Oil

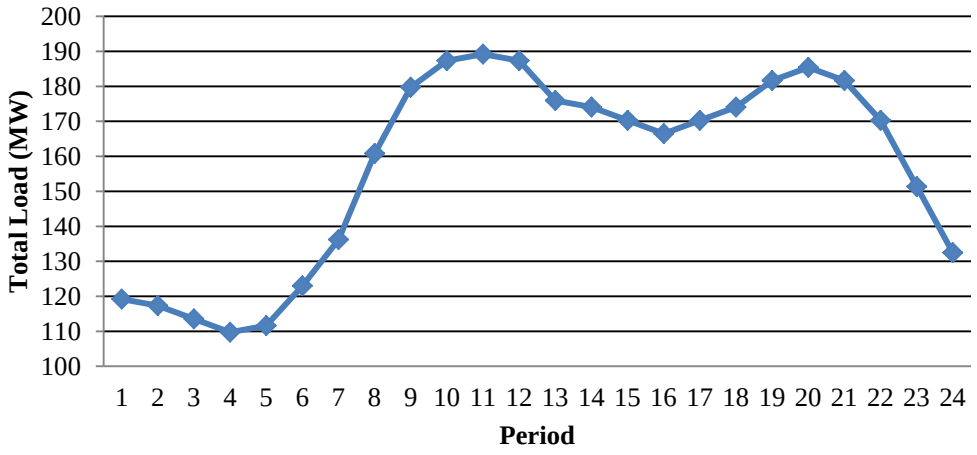

Figure 6.2. Hourly Profile of the Total Inelastic Load in the Test Transmission System

The test distribution system is the distribution system at bus 4 of the RBTS system. It is the same system used for the study in Section 5.4. For Case Study 1 – 3 in this chapter, the test distribution system feeders are sized so that the distribution system is not congested and there are no DGs in the system. Similar to Section 5.4, congestion is created for Case Study 4 and DGs are added to the system. The load data for the simulation is created from the peak load information of the test system, which is provided in Table A.9 in Appendix A. A subset of the loads has demands that do not respond to prices, i.e., perfectly inelastic demand, and a subset has price responsive demands. Load type 1 is classified as perfectly inelastic and load types 2, 3, 4, and 5 are classified as price responsive loads. Table 5.6 presents the details of the LPs. The perfectly inelastic loads have the load profile shown by Figure 6.3. The load profile is obtained from the AEP Ohio Columbus Southern Power Company [39]. It is the load profile for the residential customer class for spring 2012. The peak of 13.30 MW occurs at 8 PM and it is just 33.25 percent of the total possible peak of 40 MW in the test system. The details of the type 1 loads are listed in Table A.10 in Appendix A.

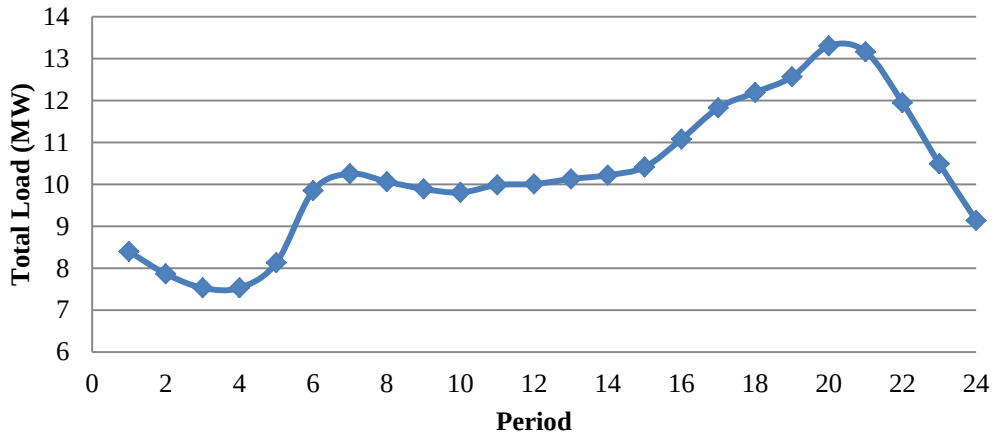

Figure 6.3. Hourly Profile of the Total Perfectly Inelastic Load in the Test Dist. System

6.2 Economic Modeling of Distribution Loads

The assumption of demand response necessitates the modeling of the sensitivity of demand to prices. In the current electricity market environment, some ISOs and Regional Transmission Operators (RTOs) allow loads to submit monotonically non-increasing step bids to purchase electricity. The bids represent the quantity that a load is willing to purchase or consume at a specified price. Price sensitive loads are modeled in the lossy DCOPF using the same approach. The problem of determining the bid curve of a load is complex and several papers have attempted and proposed different solutions to the problem [72]-[74]. The crux of developing a bid function is to determine the consumption level that maximizes the benefit a load receives from consuming at different prices. This is achieved, in this report, with a demand curve. The demand curve is the plot of the price of a good and the quantity of the good that a consumer is willing to consume at each price. Load demand curves are approximated by step functions to form bid curves. Approximating a demand curve by a step function is a simple approach to the problem of determining a bid curve. While a demand curve is developed based on consumer preferences [77], other factors, such as the fact that electricity markets are two-settlement markets, the bids of other loads, and the offer of generators, could affect the consumption level that maximizes the economic benefit a load obtains from consuming at a certain price.

There are several functional forms to the demand curve. These functional forms include linear, exponential, log, and quadratic forms [1]. Each functional form has its own properties. The power form is selected for this report because of its constant elasticity property [1], [75]. Equation (6.1) is a generic form of the power model of a demand curve. P_o and Q_o in the equation represent a reference price and quantity that can be used to scale the demand curve. ε in the equation is the coefficient of price elasticity of demand. In economics, the price elasticity of a good represents the sensitivity of the good to prices. It is quantified by the coefficient of price elasticity ε, which is described by (6.2). The coefficient of elasticity is defined as the percent change in quantity demanded of a good for a percent change in the price of the good. As represented by the negative slope of a demand curve, there is usually an inverse relationship between the price and the quantity of a good demanded. Hence, the coefficient of price elasticity of demand is usually a negative value. The more negative the coefficient of elasticity of a good, the more price sensitive the good is. A coefficient of price elasticity of zero indicates a perfectly inelastic demand, i.e., demand that does not respond to prices. A coefficient of price elasticity greater than -1 (absolute value less than 1 but greater than 0) represents inelastic demand, i.e., a change in price results is a smaller percentage change in demand. A coefficient of price elasticity of -1 represents unit elasticity, i.e., a percent change in price results in a percent change in quantity demanded. A coefficient of price elasticity less that -1 (absolute value greater than 1) represents elastic demand, i.e., a small change in price leads to a greater percentage change in quantity demanded,

$$Q = Q_o \left(\frac{P}{P_o}\right)^{\varepsilon} \tag{6.1}$$

$$\frac{P\,dQ}{Q\,dP}. \tag{6.2}$$

Determining the coefficient of price elasticity of a good is complex. It is estimated by fitting observations from empirical econometric experiments by a demand curve. Over the years

researchers have produced several works estimating the coefficient of elasticity of electricity consumption. The numbers from the studies show a wide degree of variation. According to a summary in [76], the short-run coefficient of price elasticity from different studies range from -0.01 to -0.9. The study in [78] estimates the short-run coefficient to be as high as -2.57 (2.57% change in consumption for a 1% change in price). Several factors are responsible for the variation in estimated coefficient of electricity. The factors include the prices observed data are obtained for, the approach for fitting the observed data, and the environment under which the loads are observed. For example, loads exposed to a RTP may have a different elasticity than loads exposed to a FR. Similarly, smart loads making autonomous decision may have different elasticity from loads controlled by human beings, as a result of the ease that technology provides [70]. It is likely that loads exposed to the DLMP and the smart grid environment will be more elastic than loads in the contemporary distribution system. As a result, studies are conducted in this chapter for elasticity ranging from -0.2 to -4.2. The demand curves, for the elastic load types at the elasticity used in the simulations, are shown in Figure 6.4 – Figure 6.7.

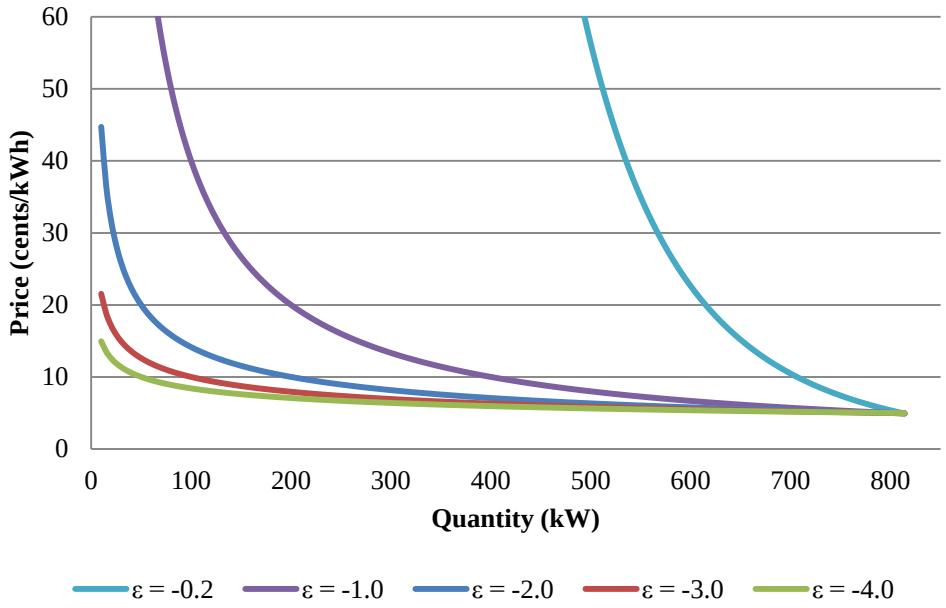

Figure 6.4. Type 2 Demand Curves with Different Coefficient of Elasticity

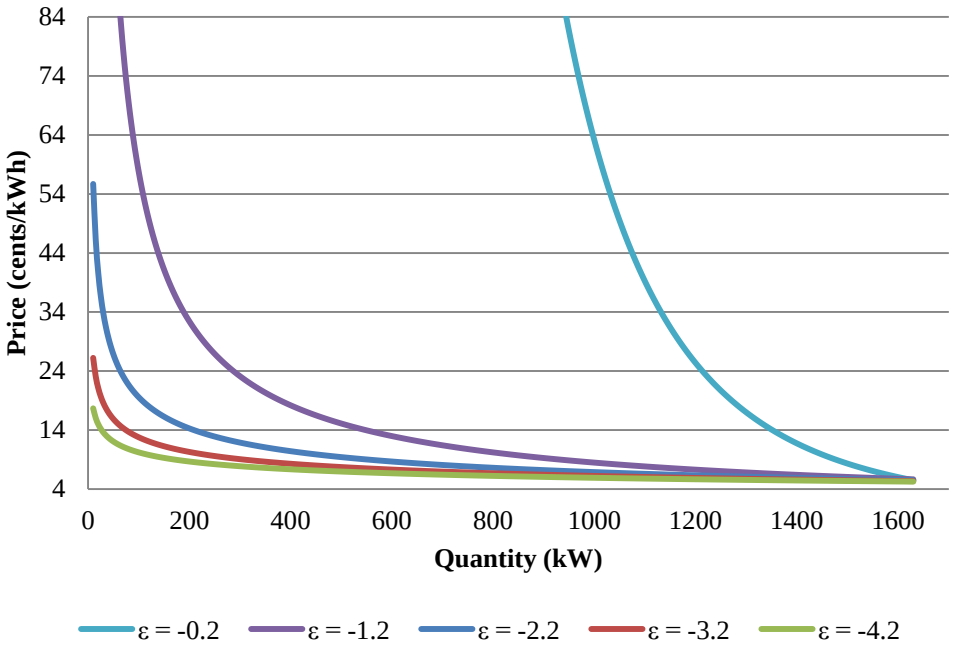

Figure 6.5. Type 3 Demand Curves with Different Coefficient of Elasticity

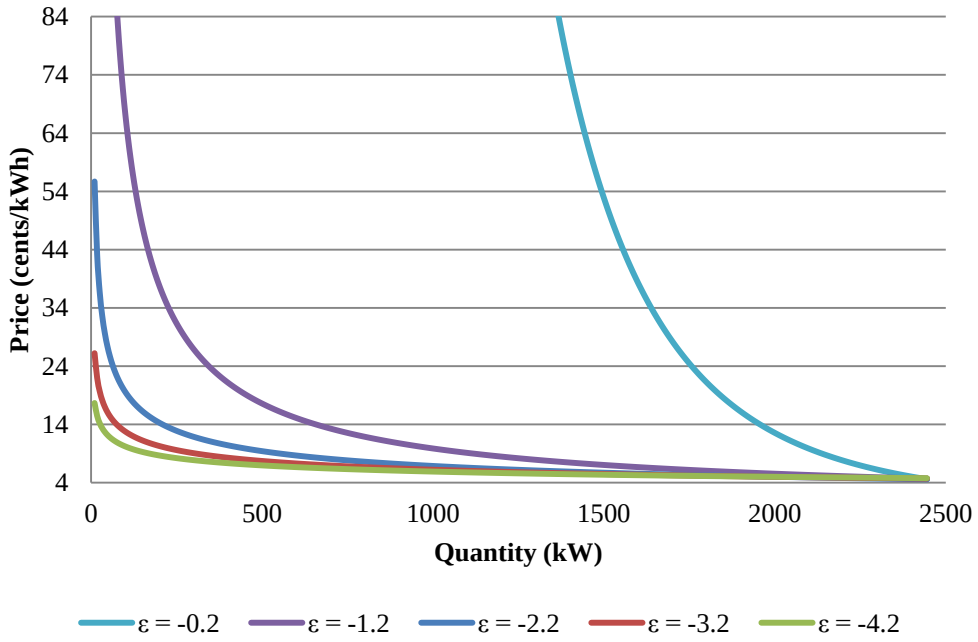

Figure 6.6. Type 4 Demand Curves with Different Coefficient of Elasticity

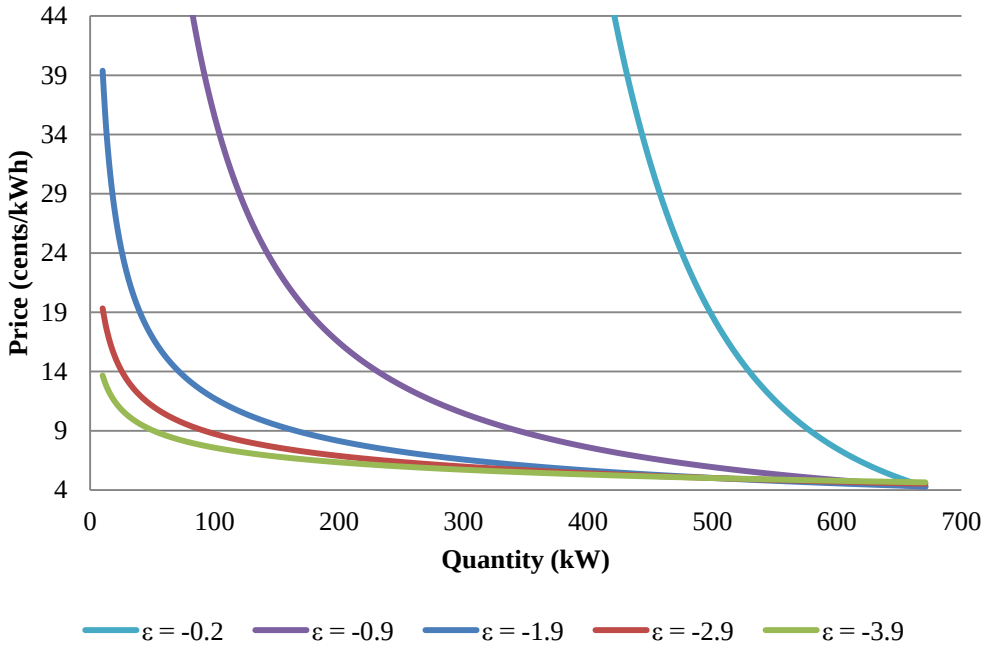

Figure 6.7. Type 5 Demand Curves with Different Coefficient of Elasticity

Note that the price elasticity of demand can be affected by time. Consequently, there is short and long-run elasticity. In economics, short-run signifies a period in which certain parameters are held constant. For example, it can be assumed that the number of generators in a system is fixed in the short-run. Long-run signifies that the parameters held constant in the short-run are variable. Time provides the opportunity to seek out substitutes or alternative; hence, the price elasticity of demand in the long-run is usually higher than in the long-run. The short-run elasticity of demand is used to develop the demand curves in this report.

6.3 Convergence Problems with Iterative Framework

While the iterative framework for calculating the DLMP provides a way to accurately model the price sensitivity of distribution resources for the transmission system OPF and vice versa, there is no guarantee of convergence to a solution or convergence to the correct or optimal solution. One of the major factors that can lead to non-convergence of the iterative framework includes the non-continuity of generator offer curves and load bids. A load or a generator could set the clearing price as a result of the step curves of generator offers and load bids. A generator setting the clearing price is illustrated in Figure 6.8 and a load setting the clearing price is illustrated in Figure 6.9. If a load sets the clearing price in the distribution system OPF, the approximation of the distribution system by a perfectly inelastic curve for the transmission system OPF may be inadequate. A perfectly inelastic demand model of the distribution system sends the signal that distribution loads will consume regardless of proxy LMP. This is inaccurate for a distribution system with price sensitive resources and the inaccuracy matters in the situation where a distribution load sets the clearing price. As shown in Figure 6.10, the inelastic representation results in a non-unique clearing price in the transmission OPF. While the clearing price in the distribution system is a specific price between P_A and P_B, any price between P_A and P_B could be the clearing price in the transmission system OPF: the inelastic representation sends the signal that a

load is willing to consume the fixed demand at any price between P_A and P_B. If the solution algorithm selects any price other than the distribution system clearing price, the distribution system consumption incentivized by the selected price will deviate from the optimal consumption.

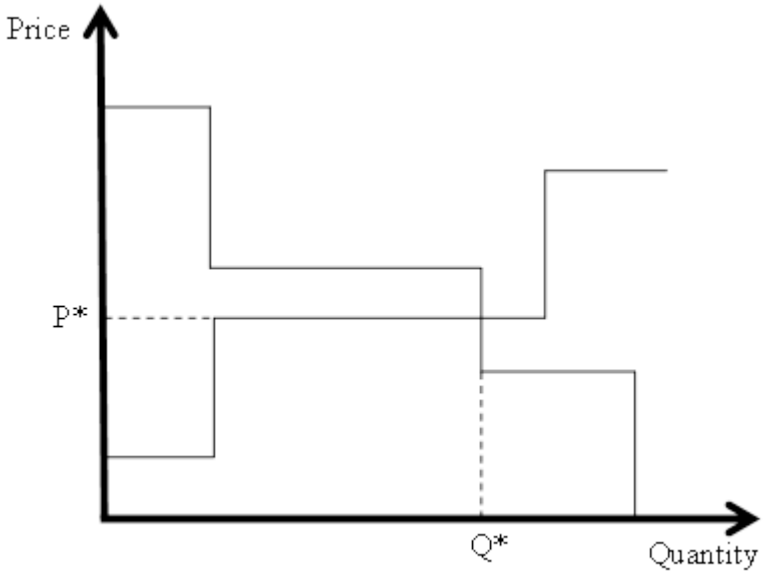

Figure 6.8. Generator Sets Clearing Price

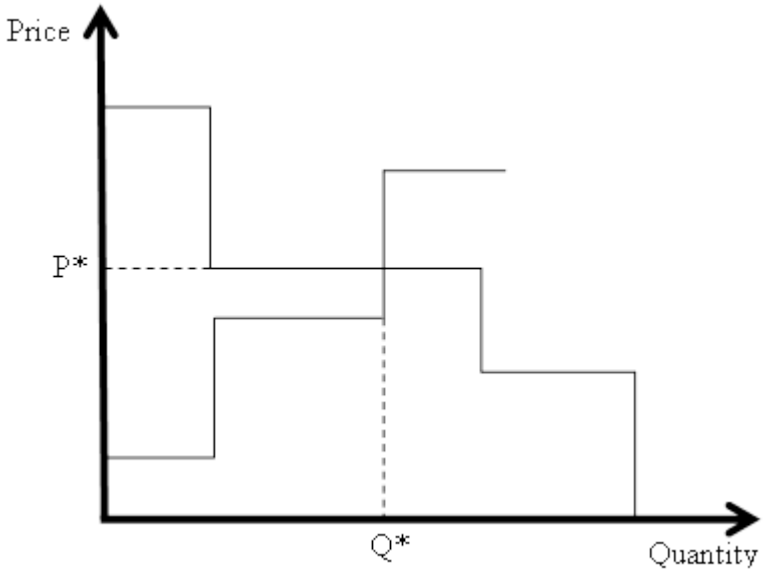

Figure 6.9. Load Sets Clearing Price

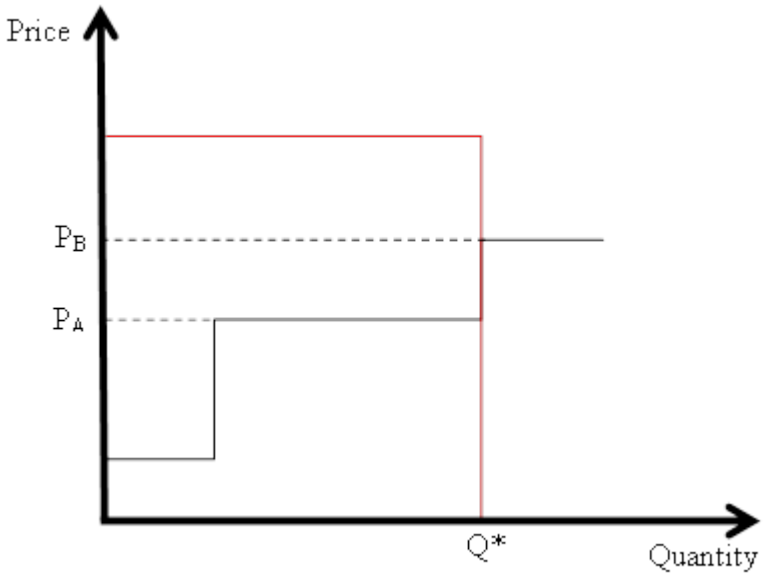

Figure 6.10. Inelastic Distribution Load Sets Clearing Price in Transmission OPF

The situation described in the preceding paragraph occurred in the simulations conducted for this report, Figure 6.11 and Figure 6.12. In Figure 6.11, the proxy LMPs for five iterations and the optimal proxy LMPs are shown. The figure show the proxy LMP jumping between the prices in iterations 1, 3, and 5 and the prices in iterations 2 and 4 for some of the periods, e.g., 3, 5, 13, 17, and 22. The proxy LMPs in the periods could not converge to the optimal price. The prices in Figure 6.11 incentivized the consumption in Figure 6.12, which does not settle to the optimal solution. A representation, more accurate than the inelastic demand curve, is required to solve this convergence problem of the iterative framework. Simply using a step bid rather than an inelastic demand curve may not resolve the problem as the vertical portion of the step demand bid curve can overlap with the vertical portion of the supply curve and cause the same problem.

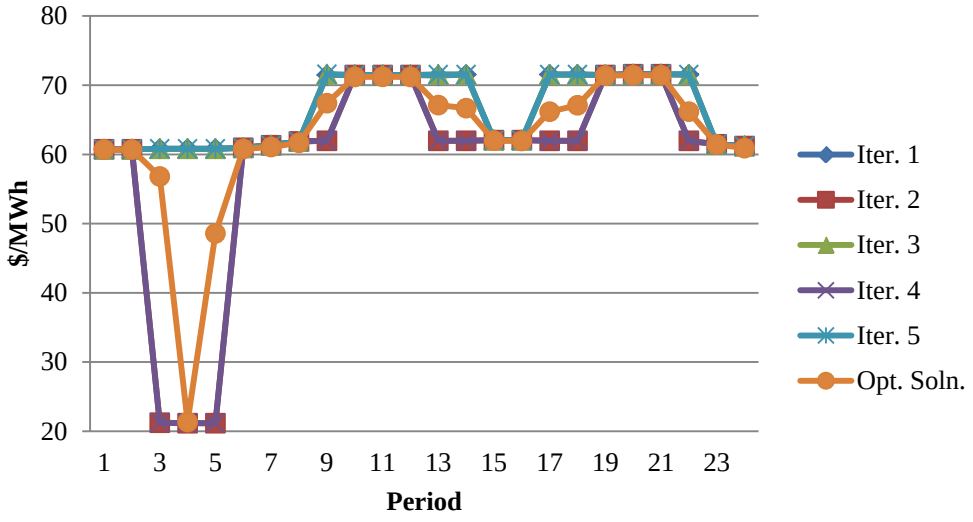

Figure 6.11. Proxy LMP Changing from one Iteration to the other and the Optimal Proxy LMP

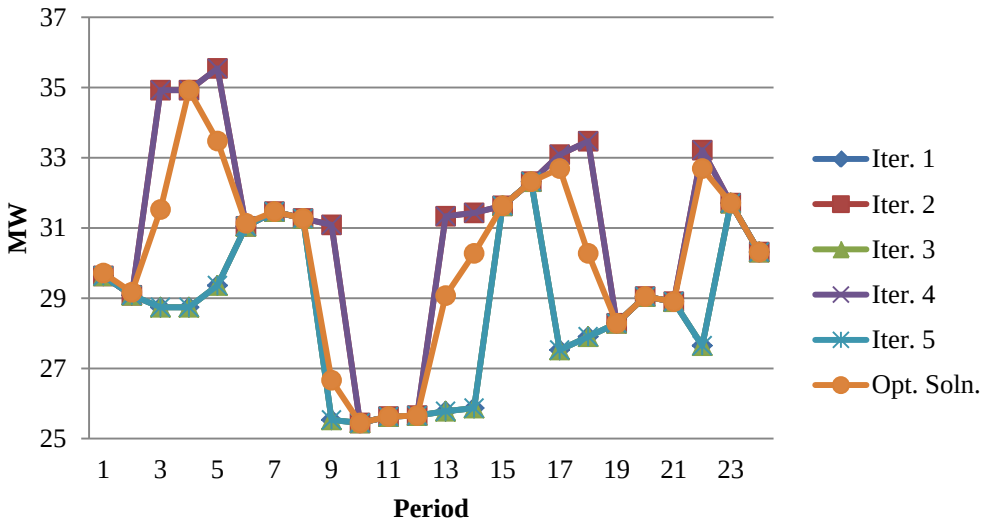

Figure 6.12. Infinite Generator Output Changing from one Iteration to the other and the Optimal Infinite Generator Output

A similar problem could result even when a generator sets the price in the transmission system OPF. The infinite generator model of the transmission system sends the signal that the cost to consume is the fixed marginal cost, distribution proxy LMP, regardless of the consumption level in the distribution system. Hence, the optimization algorithm could select any consumption between Q_A and Q_B as the clearing consumption as shown in Figure 6.13. A consumption level other than the optimal consumption that cleared in the transmission system OPF can cause a change to the proxy LMP. Non-convergence as a result of the infinite generator model can be handled by adding additional constraints to the OPF and a small cost to the objective that penalizes deviation from the optimal consumption.

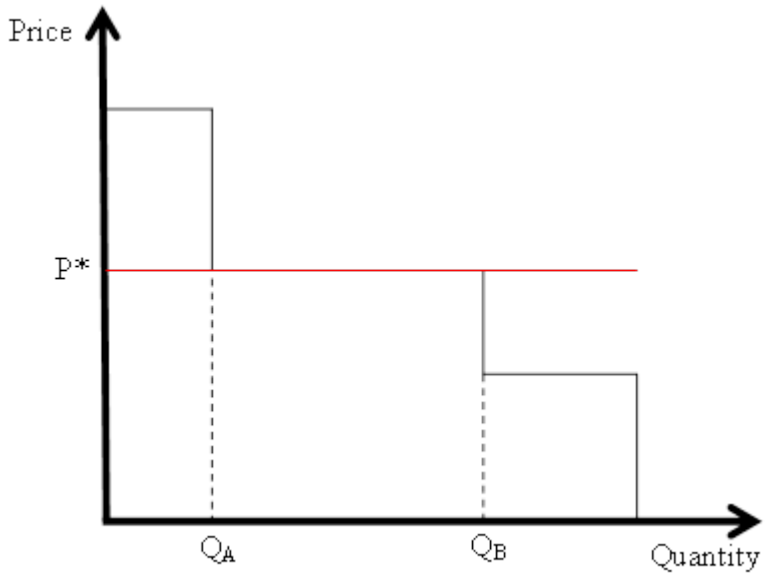

Figure 6.13. Infinite Generator Sets Clearing Price in Distribution OPF

Convergence may also be dependent on the amount of flexibility in the decomposed problem, occurrence of congestion and the initial solution. The iterative framework may have convergence problems if a distribution system has multiple connections to the transmission system, i.e., multiple infinite generators. The dispatch of the infinite generators may change from iteration to iteration as a result of the MC of the generators changing such that it may be cheaper to purchase losses from different generators at different iterations. A similar situation may arise if the transmission system has multiple distribution systems connected. Congestion and changes in the consumption of other distribution systems may cause the proxy LMP at a distribution system to change from iteration to iteration. Congestion may also cause non-monotonicity of LMPs. For example, congestion can cause an LMP to decrease even with increased consumption. Non-monotonicity of LMPs can also cause non-convergence. As will be discussed in the future work section in Chapter 7, the convergence problem of the iterative framework needs to be further investigated.

6.4 Sampling Approach for Calculating Prices

In order to overcome the convergence problem of the iterative framework, for the purpose of conducting the studies in this chapter, a sampling approach [79] was employed for calculating DLMPs. The approach is illustrated in Figure 6.14. An aggregate demand curve is developed by determining the resulting aggregate demand in the distribution system at different sample marginal costs for the infinite generator. The aggregate demand at each sample marginal cost is the infinite generator output obtained by solving the lossy DCOPF for the distribution system. The aggregate demand curve fully represents the price elasticity of distribution system loads, the local generation resources in the distribution system, and the network condition, e.g., congestion, of the distribution system. The process mimics a scenario where information is available to accurately model the prices sensitive resources and the network conditions of a distribution system.

A similar technique is employed for the RTP, TOU, and FR simulations. The process for the RTP simulations is depicted in Figure 6.15. In the RTP process, the aggregate demand at each sample price does not properly capture losses and network conditions in the distribution system. A sample RTP is simply propagated throughout the distribution system without a marginal loss or congestion component. The same is done in the process that determines the final consumption in the distribution system. The prices in the final process are, however, the LMP at the distribution proxy bus. The difference between the DLMP and the RTP processes for the sampling approach represents the difference in the application of the DLMP and the contemporary RTP. While the DLMP is calculated from a distribution system OPF, the RTP is calculated without proper consideration of the distribution network. The RTP could simply be the proxy LMP. Hence, the DLMP reflects both the transmission system and the distribution system network and generation conditions and the price sensitivity of loads and other resources, the RTP reflects the transmission system network and generation conditions. The RTP inaccurately represents the price sensitive resources in the distribution system as it does not reflect the response of the resources to losses and other distribution network conditions.

The TOUs and FRs in these studies are determined based on the total distribution system load payment to the transmission system resulting from the DLMP simulations. The FR is the load weighted average of the load payment to the transmission system. This includes the cost of losses, which is socialized based on MW consumption. Two periods types are used for the TOU.

The peak period runs from 7 a.m. to 9 p.m. and the off-peak period is every period not included in the peak period.

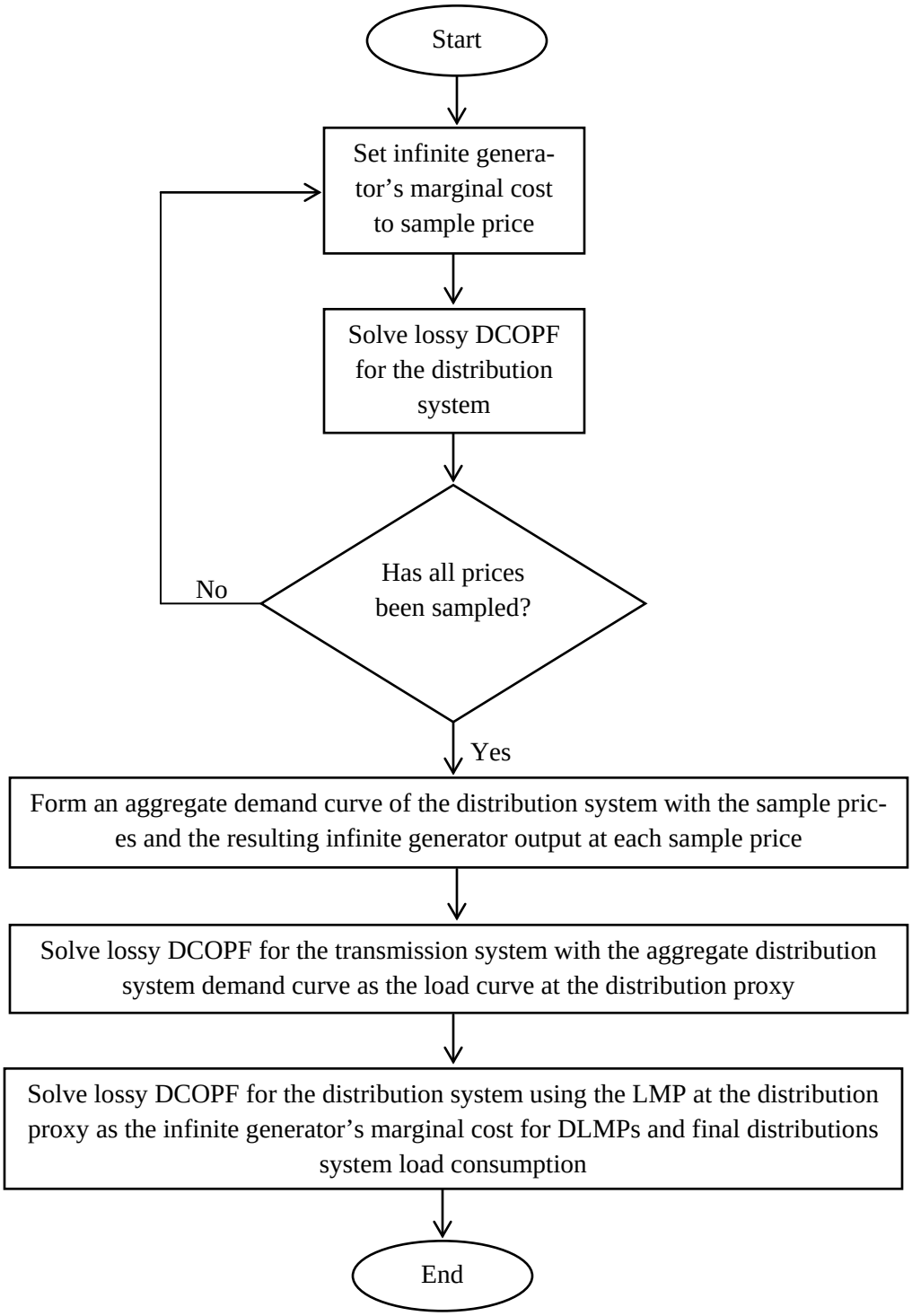

Figure 6.14. Sampling Approach for Calculating DLMP

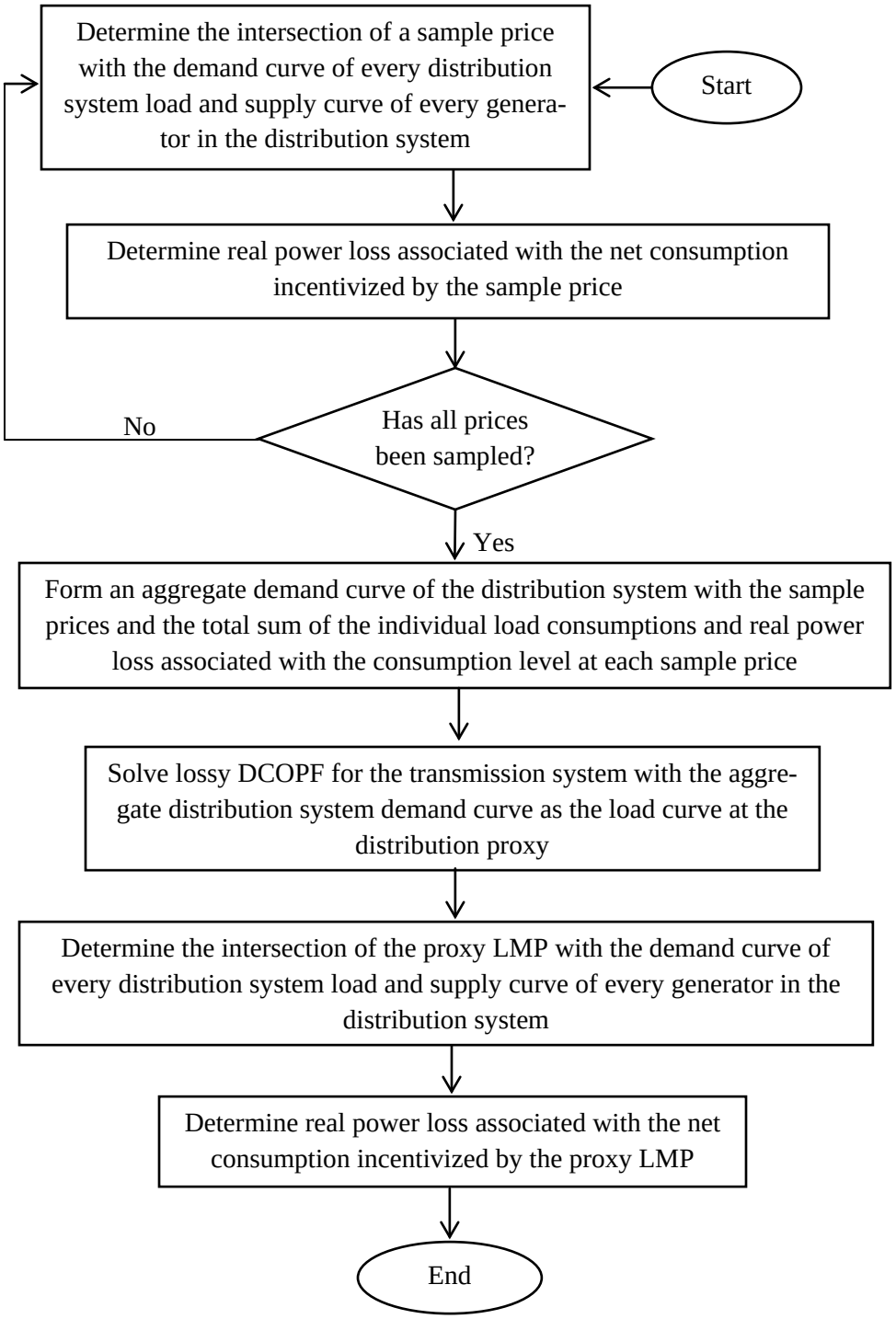

Figure 6.15. Sampling Approach for Calculating RTP

6.5 Case Study 1: ε of -0.2 and No Congestion

As discussed in Section 6.2, a load with a coefficient of elasticity of -0.2 is inelastic. Hence, small changes in consumption are expected for large changes in prices. This is reflected in the results of simulations with ε of -0.2. The prices in the simulations are shown in Figure 6.16 and the aggregate consumption incentivized by the prices in Figure 6.17. Note that the DLMP in Figure 6.16 is for a node, 49, that demonstrates a consistently high deviation from the RTP. The deviation of each price from the DLMP in each hour represents the inaccuracy of the price. Despite the significant inaccuracy shown by Figure 6.17, Figure 6.18 shows that the aggregate consumption incentivized for each period, by all the prices, is largely the same. As shown in Figure 6.18, the absolute percentage deviation from the optimal DLMP aggregate consumption is less than 1.7 percent for the FR for all time periods except for H4, less than 1.5 percent for the TOU rate for all time periods except for H4 and H22, and approximately 1 percent or less for all time periods for the RTP. It takes a very high price differential in H4 to obtain a 4.89 percent deviation in H4 for the FR and 3.32 and 3.01 percent in H4 and H22 for the TOU rate. The inaccuracy of the FR, TOU, and RTP has limited impact on consumption as a result of highly inelastic loads.

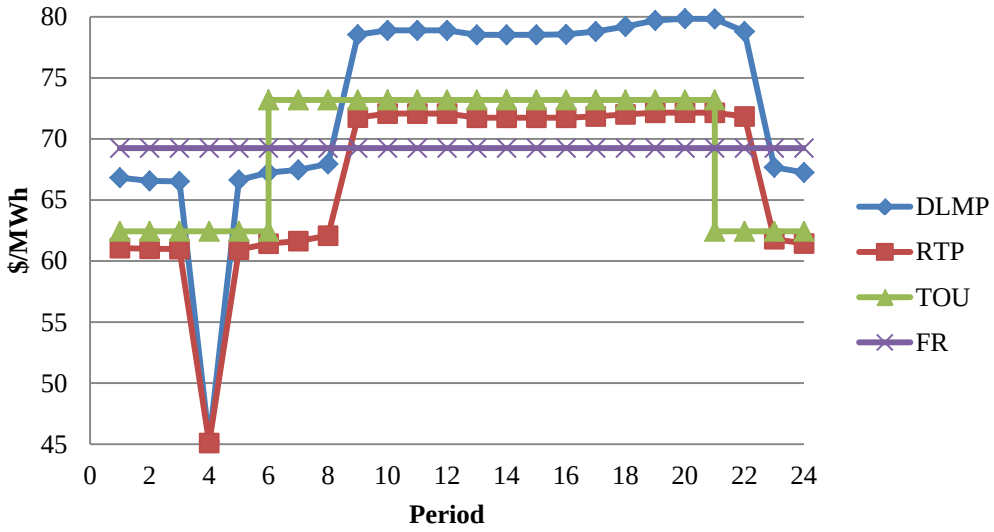

Figure 6.16. Prices at ε of -0.2

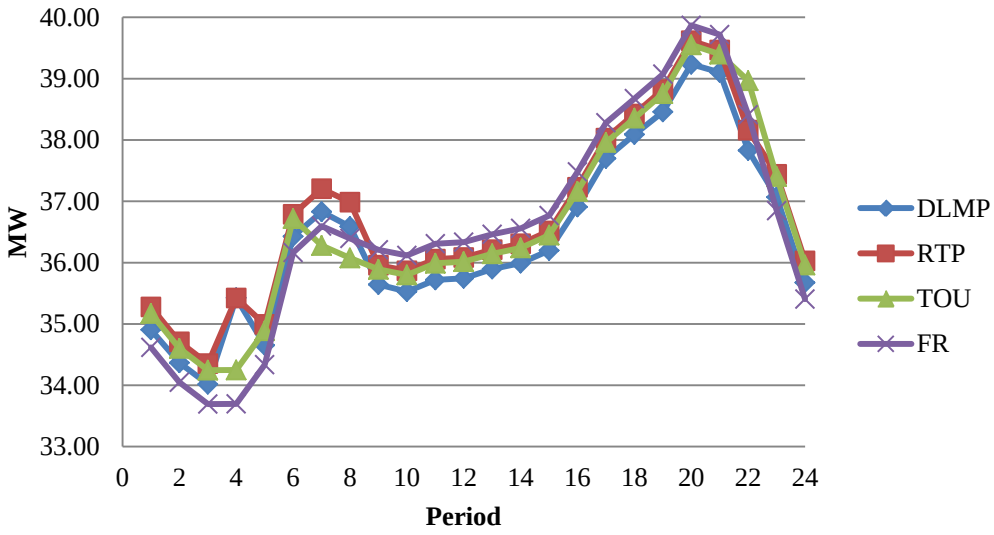

Figure 6.17. 24 Hour Aggregate Load Consumption at ε of -0.2

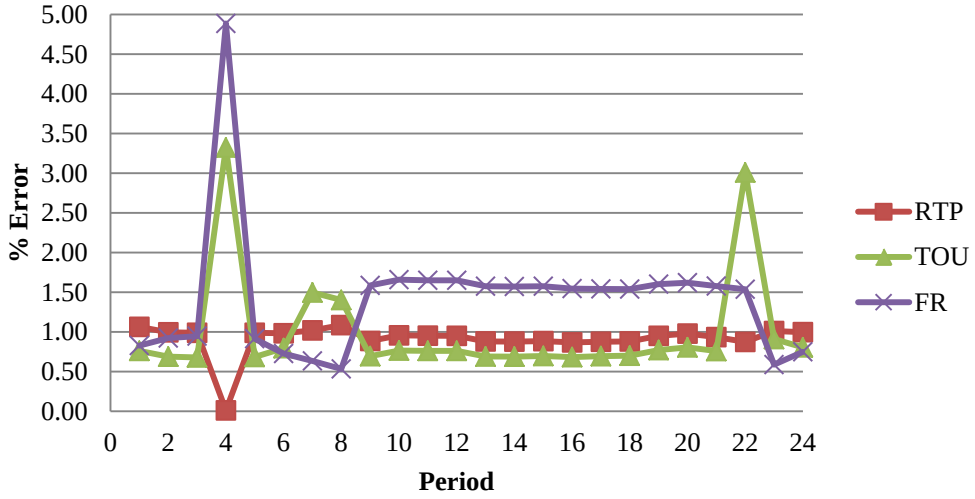

Figure 6.18. Absolute Percentage Deviation from Optimal Aggregate Consumption at ε of -0.2

6.6 Case Study 2: ε around -1.0 and No Congestion

The impact of the inaccuracy of the FR, TOU, and the RTP on consumption are masked in case study 1 because the distribution system loads are highly inelastic. At higher elasticity, the deviation is more pronounced. For price differentials similar to or less than those obtained for ε of -0.2, Figure 6.19, the incentivized aggregate consumption for ε around -1.0, Figure 6.20, show higher deviation from each other. The consumption incentivized by the FR and the TOU show different trends from the optimal consumption incentivized by the DLMP. For example, the consumption incentivized by the DLMP increases from H2 to H4 and decreases from H4 to H6 while the consumption incentivized by the FR and the TOU decrease from H2 to H4 and increase from H4 to H6. In H7 to H22, the FR and the TOU rate are unable to capture the details of the trend of the optimal consumption. While the optimal DLMP consumption increased and de-

creased several times, the FR and the TOU rate consumption simply increased. Figure 6.21 shows that the aggregate consumption incentivized by the FR deviates by higher than 8 percent for half the periods and by 18.98 percent in H4. For the TOU, the deviation is approximately 6 percent or higher for over half of the periods and 11.19 percent and 10.58 percent in H4 and H22.

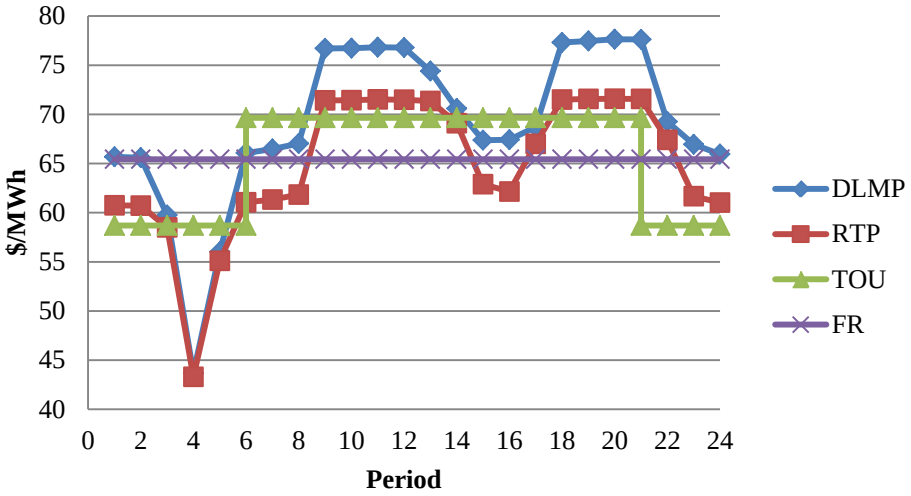

Figure 6.19. Prices at ε around -1.0

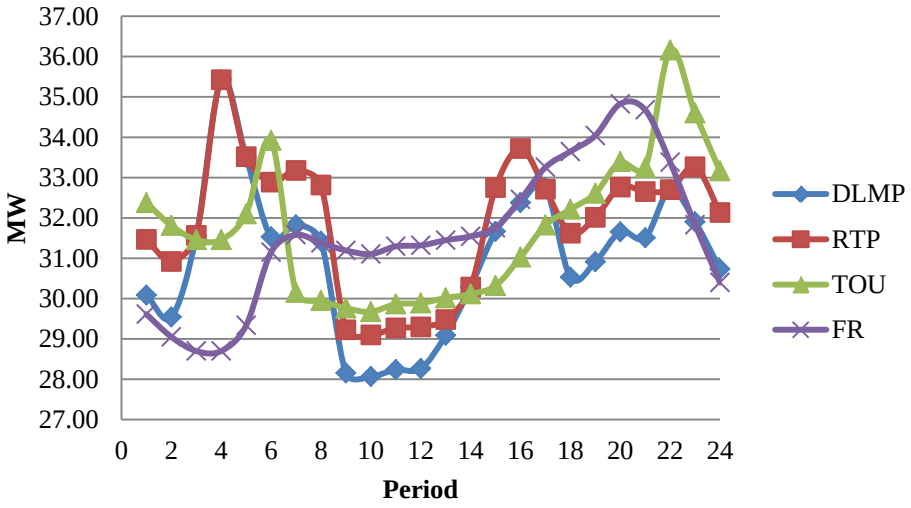

Figure 6.20. 24 Hour Aggregate Load Consumption at ε around -1.0

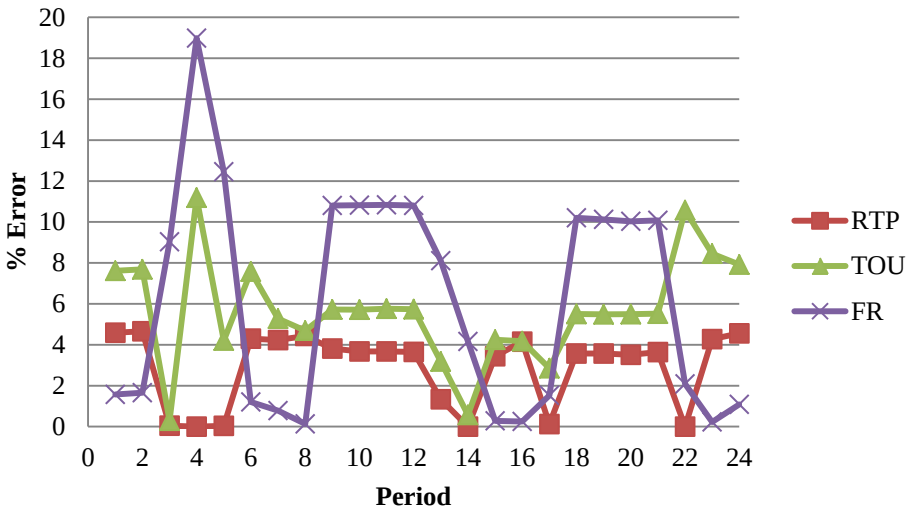

Figure 6.21. Absolute Percentage Deviation from Optimal Aggregate Consumption at ε around -1.0

While the RTP incentivizes consumption with the same trend as the DLMP, the level of consumption for two-thirds of the periods is different from the level of consumption incentivized by the DLMP. The deviation is about 4 percent in most of the periods. Inspecting the real power consumption deviation at the aggregate level somewhat obfuscates the impact of the inaccuracy of the RTP on incentivized consumption. There are inelastic loads in the test system whose deviation from the optimal consumption, including the losses associated with the inelastic consumption, is zero. At the individual load level, the inaccuracy of the RTP is more pronounced. This is reflected in Figure 6.22 – Figure 6.25, the plot of the absolute percentage deviation of the individual load consumption incentivized by the RTP from the individual optimal DLMP consumption. While the maximum deviation at the aggregate level is about 4 percent, the individual deviations are as high as about 8. All of the elastic loads demonstrate individual deviations of about 4 percent or higher in about two-thirds of the periods.

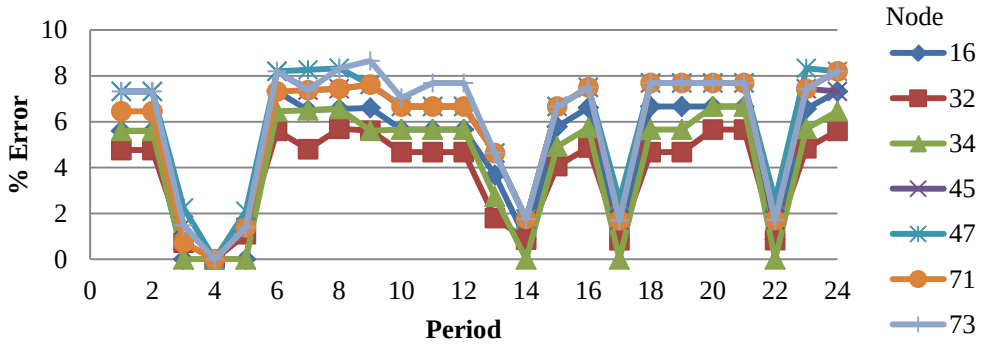

Figure 6.22. Type 2 Loads Absolute Percentage Deviation from Optimal Consumption at ε around -1.0

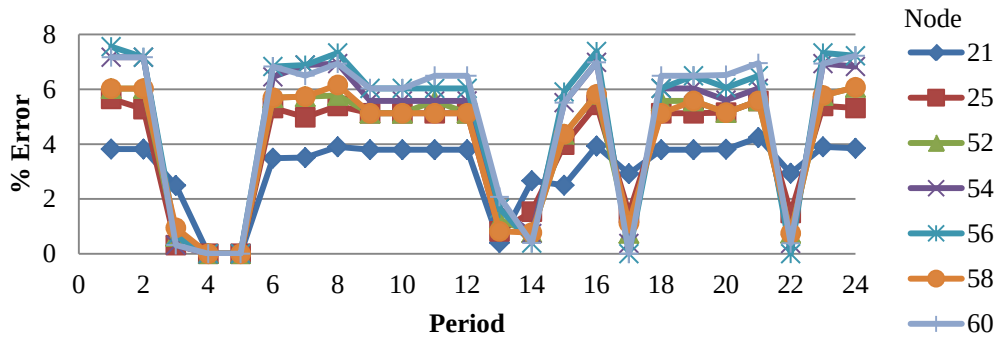

Figure 6.23. Type 3 Loads Absolute Percentage Deviation from Optimal Consumption at ε around -1.0

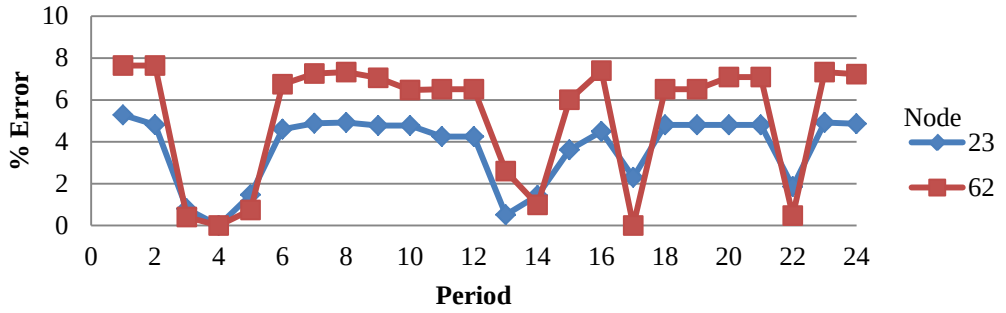

Figure 6.24. Type 4 Loads Absolute Percentage Deviation from Optimal Consumption at ε around -1.0

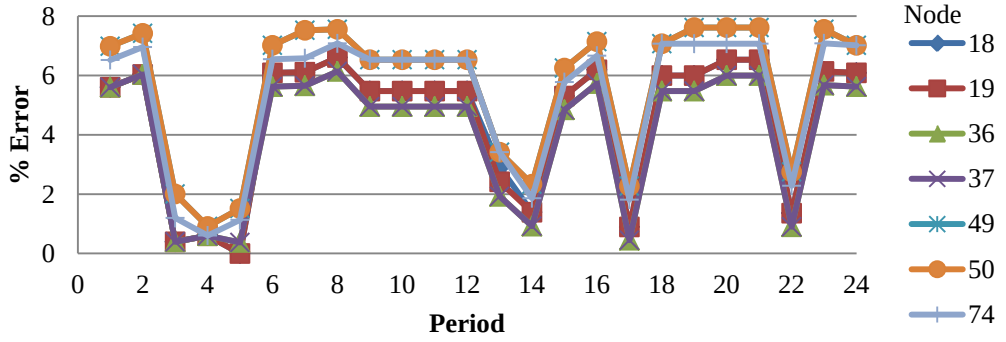

Figure 6.25. Type 5 Loads Absolute Percentage Deviation from Optimal Consumption at ε around -1.0

6.7 Case Study 3: ε from around -2.0 to around -4.0 and No Congestion

The DLMP is best for a distribution system with substantial amount of flexible resources. With increased load flexibility, results of Case Study 3 show that the disadvantage of contemporary prices, in terms of deviation from optimal consumption, also increases. As shown in Figure

6.26, the minimum deviation of the consumption incentivized by the FR for ε around -4.0 is 10.92 percent. Periods in between H7 and H24 for ε around -4.0 have deviations approximately between 15 and 20 percent. In the off-peak period, the deviation is as high as 38.54 percent. For ε around -3.0, the deviation is as high as 34.02 percent and more than two-thirds of the periods have deviations greater than 10 percent. H11 and H20 (for ε around -3.0) and H10 to H12 and H19 to H21 (for ε around -2.0) show higher deviations than for ε around -4.0 as a result of congestion in the transmission system. The increased elasticity, for ε around -4.0, helps relive the congestion. Hence, only a small spike in H20 when ε is around -4.0.

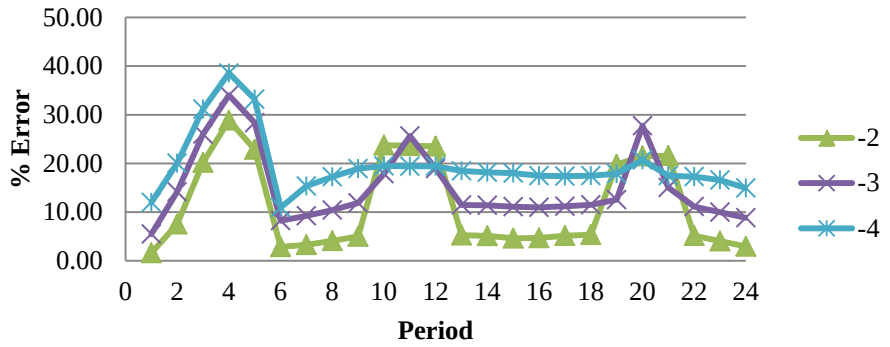

Figure 6.26. FR Absolute Percentage Deviation from Optimal Consumption at Higher ε

In the off-peak period, Figure 6.27 shows that a significant deviation from the optimal consumption is incentivized by the TOU rate. The deviations are as high as about 46 percent, 32 percent, and 20 percent for an ε around -4.0, -3.0, and -2.0 respectively. During the peak period, the results show an interesting trend. Except for H10 – H12 and H19 – H21 (for ε around -2.0), H11 and H20 (for ε around -3.0), and H20 (for ε around -4.0), the deviation in the peak period is less that or approximately 5 percent. This results because of the increased elasticity of the distribution loads, which helps relieve the congestion in the transmission system. The profile of the resulting DLMPs, during the peak periods, became flatter as elasticity increased. Since the TOU rate is determined based on the DLMP and the consumption resulting from the DLMP, the peak TOU rate becomes more accurate than what may be obtained in actual practice. In practice, TOU rates are determined based on consumption and costs over a very large time horizon.

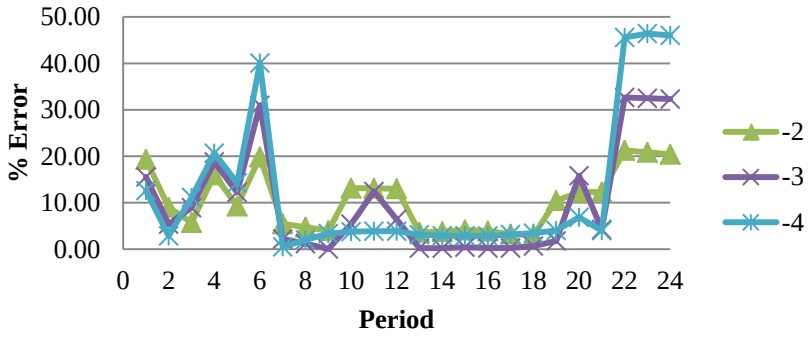

Figure 6.27. TOU Absolute Percentage Deviation from Optimal Consumption at Higher ε

As elasticity increases, the difference between DLMPs and the RTP reduces. In spite of the reduction, the deviation of the consumption incentivized by the RTP from the optimal DLMP

consumption increases as a result of increased load flexibility. This is seen both at the aggregate consumption level, Figure 6.28, and at the individual consumption level Figure 6.29 – Figure 6.40. At the aggregate level, the deviation is approximately between 5 and 7 percent for sixteen periods (for ε around -2.0), approximately between 6.5 and 7.5 percent for thirteen periods (for ε around -3.0), and between 7 and 9 percent for sixteen periods (for ε around -4.0). At the individual consumption level, all type 2 loads exhibit deviations of approximately between 8 and 15 percent for about two-third of the periods (for ε around -2.0), approximately between 10 and 20 percent (for ε around -3.0) for over half of the periods, and approximately between 15 and 29 percent for about two-thirds of the periods (for ε around -4.0). All but one type 3 loads exhibit deviations of approximately between 8 and 12 percent for about two-third of the periods (for ε around -2.0), approximately between 10 and 15 percent (for ε around -3.0) for over half of the periods, and approximately between 15 and 20 percent for about two-thirds of the periods (for ε around -4.0). Similar significant deviations are reflected for the type 4 loads with deviations of approximately between 15 and 19 percent for about 16 periods for one of the loads and deviation between 10 and 15 percent for the other load at ε around -4.0. All type 5 loads exhibit deviations approximately between 8 and 16 percent for about two-third of the periods (for ε around -2.0), approximately between 13 and 20 percent (for ε around -3.0) for over half of the periods, and approximately between 15 and 27 percent for about two-thirds of the periods (for ε around -4.0).

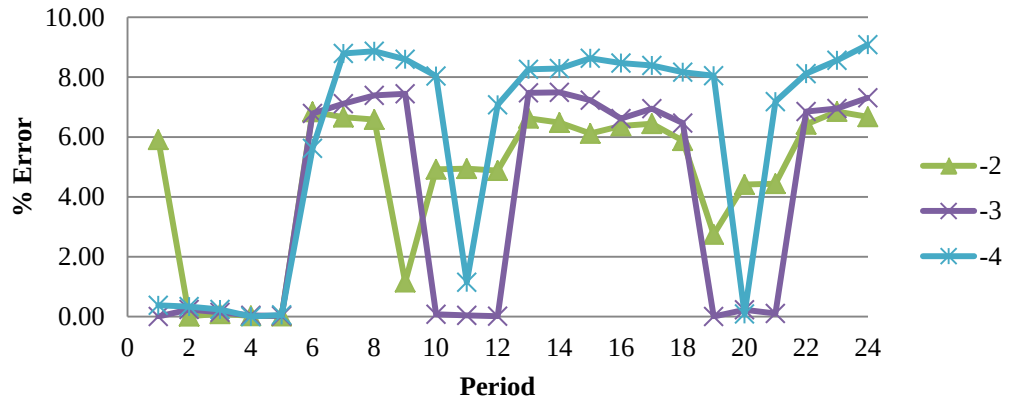

Figure 6.28. RTP Absolute Percentage Deviation from Optimal Consumption at Higher ε

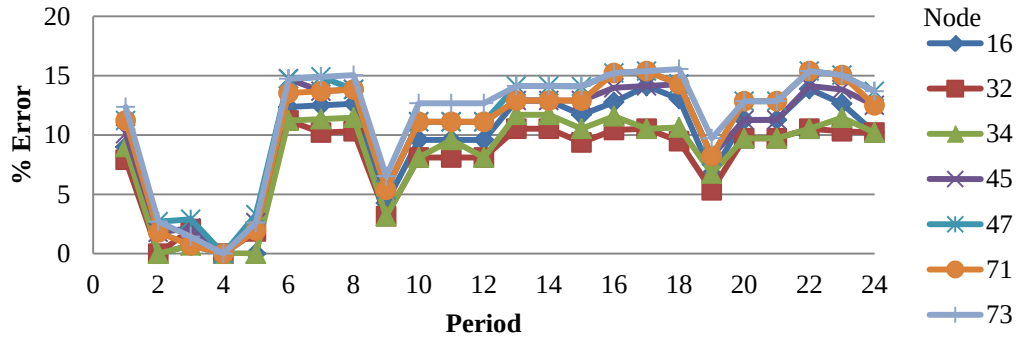

Figure 6.29. Type 2 Loads Absolute Percentage Deviation from Optimal Consumption at ε around -2.0

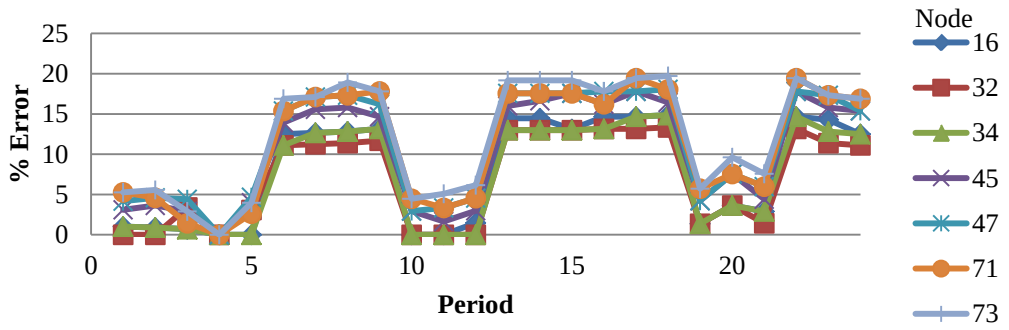

Figure 6.30. Type 2 Loads Absolute Percentage Deviation from Optimal Consumption at ε around -3.0

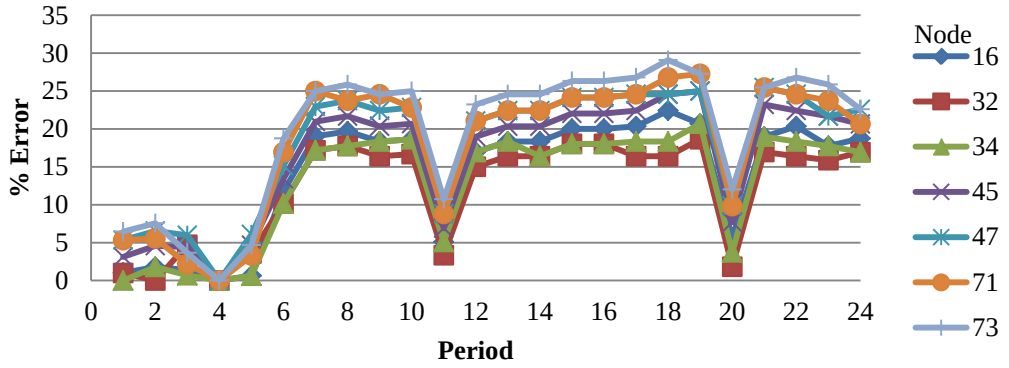

Figure 6.31. Type 2 Loads Absolute Percentage Deviation from Optimal Consumption at ε around -4.0

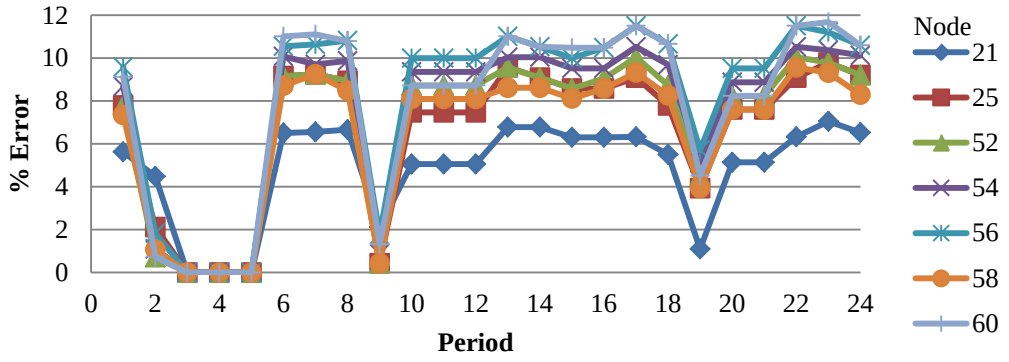

Figure 6.32. Type 3 Loads Absolute Percentage Deviation from Optimal Consumption at ε around -2.0

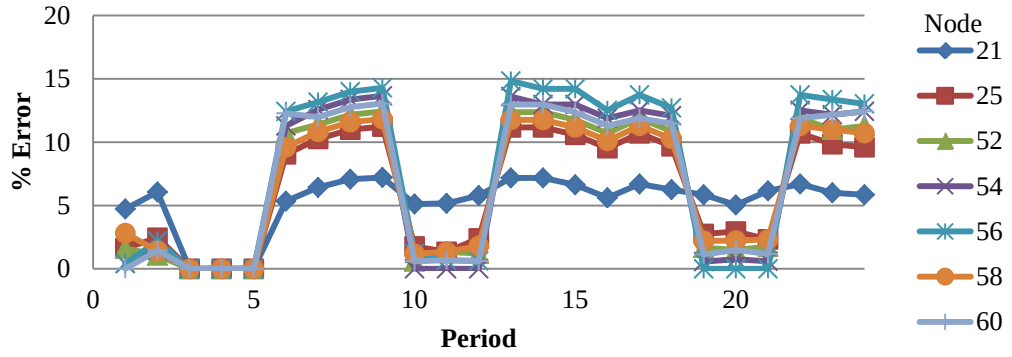

Figure 6.33. Type 3 Loads Absolute Percentage Deviation from Optimal Consumption at ε around -3.0

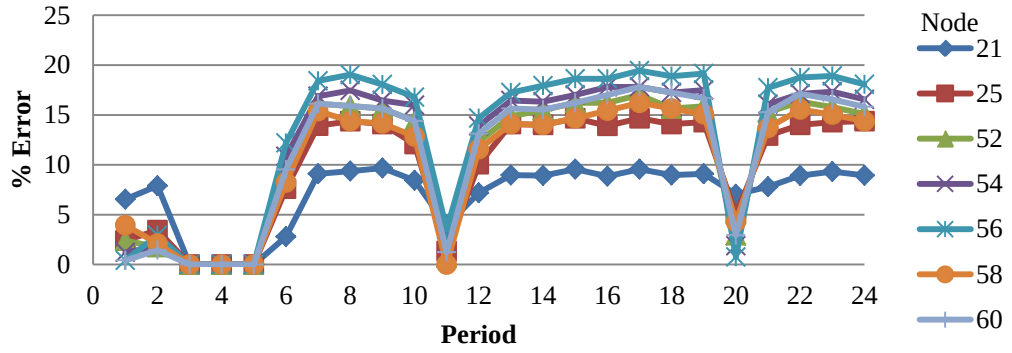

Figure 6.34. Type 3 Loads Absolute Percentage Deviation from Optimal Consumption at ε around -4.0

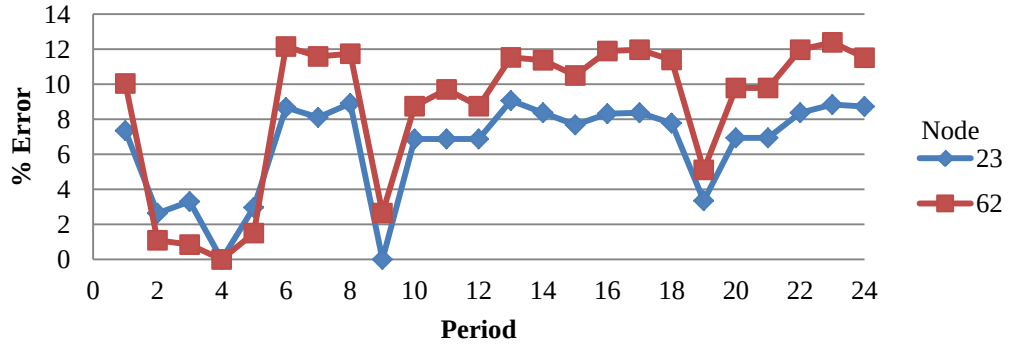

Figure 6.35. Type 4 Loads Absolute Percentage Deviation from Optimal Consumption at ε around -2.0

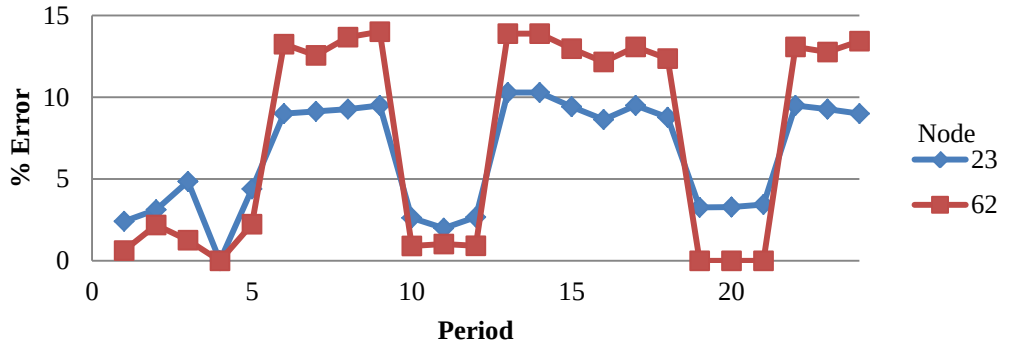

Figure 6.36. Type 4 Loads Absolute Percentage Deviation from Optimal Consumption at ε around -3.0

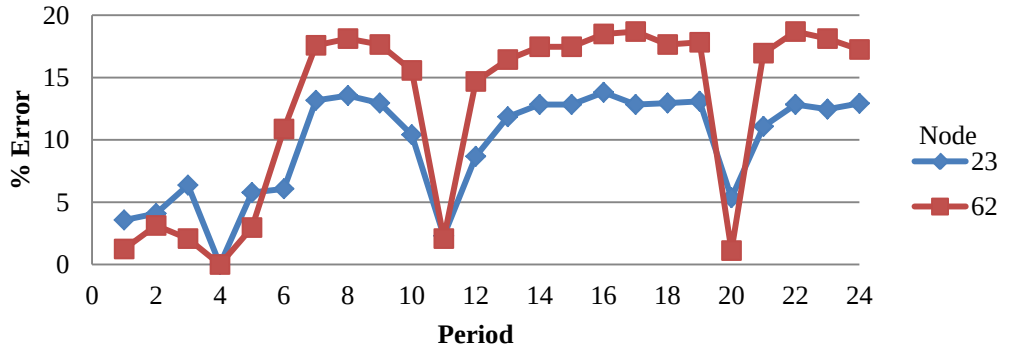

Figure 6.37. Type 4 Loads Absolute Percentage Deviation from Optimal Consumption at ε around -4.0

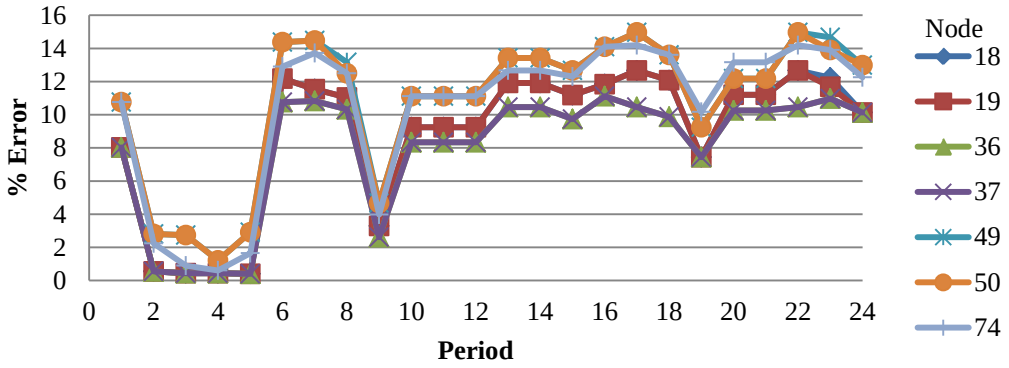

Figure 6.38. Type 5 Loads Absolute Percentage Deviation from Optimal Consumption at ε around -2.0

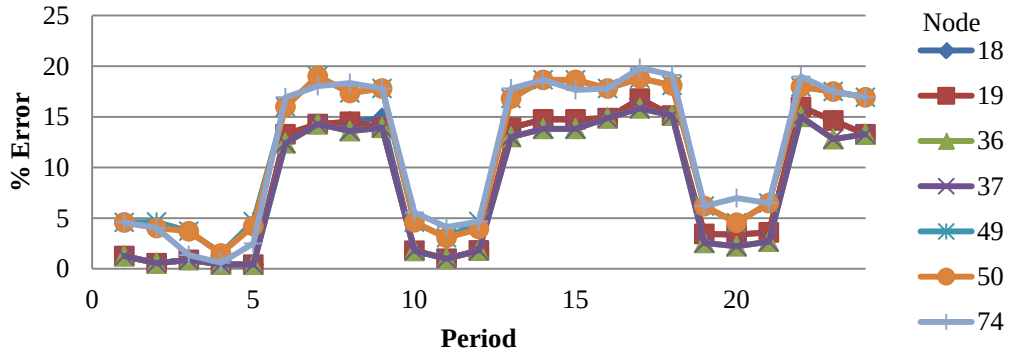

Figure 6.39. Type 5 Loads Absolute Percentage Deviation from Optimal Consumption at ε around -3.0

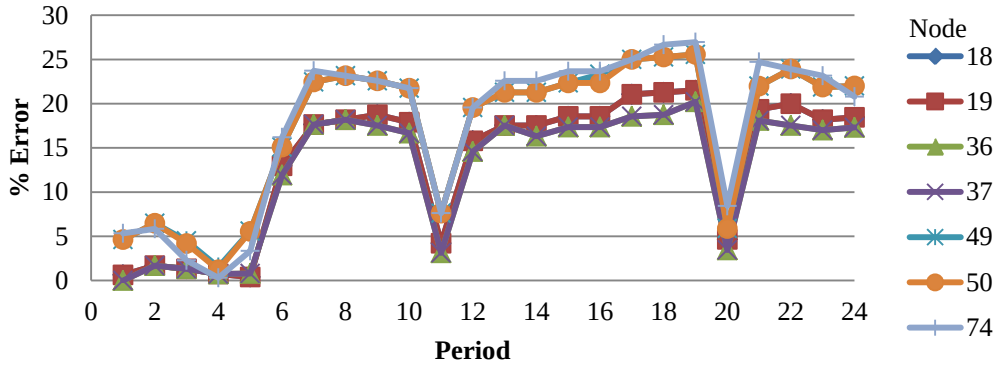

Figure 6.40. Type 5 Loads Absolute Percentage Deviation from Optimal Consumption at ε around -4.0

6.8 Case Study 4: Congested Distribution Network

While inaccurate, the RTPs in case studies 1 – 3 have the same trend as the DLMP and incentivized aggregate consumptions with similar trend as the DLMP's aggregate consumptions. The RTP is able to reflect a similar trend as the DLMP because there is no congestion in the distribution system. The DLMPs take the shape of the LMP at the proxy bus, the RTP, as a result. The inaccuracy of the RTP in case studies 1 – 3 results because the RTP does not properly reflect distribution losses. Congestion in the distribution network could cause the DLMP to take a different trend than the proxy LMP. Hence, the inaccuracy of the RTP could be much more significant in a congested system and the inaccuracy could have significant reliability impacts. In a distribution system with congestion, only the DLMP internalizes congestion. The RTP will result in a need for load curtailment, which may be sub-optimal, to maintain reliability. This is illustrated by conducting studies on the same test system in case studies 1 – 3 but with the rating of segment 17 reduced to 1.6 MW to cause congestion. The test system also has DGs as described in Section 5.4 and the loads have ε around -2.0.

Figure 6.41 shows the plot of the resulting RTP and the DLMPs at one of the nodes significantly impacted by the congestion. The figure shows that the price differential between the DLMP and the RTP in H1 to H5 is significantly high: as high as $52.20 in H3. The consumption

incentivized by both the DLMP and the RTP at node 25 is shown in Figure 6.42 and the difference between the DLMP and the RTP consumption, as a percentage of the optimal consumption, is shown in Figure 6.43. The figures show that the RTP consumption deviates by more than 15 percent from the DLMP consumption for two-thirds of the periods. The deviation in H1 – H5 is especially high. This results from the severity of the congestion in those periods and the significant load curtailment that may be required to rectify the overload on branch 17 as a result of the consumption incentivized by the RTP. This is illustrated in Figure 6.44, which shows the flow on branch 17 in the DLMP study and in the RTP study. The internalization of congestion by the DLMP results in a situation where branch 17 flow is never more than 1.6 MW while the RTP results in a situation where the line flow is more than the line limit in several periods. The periods where the line flow, as a result of the consumption incentivized by the RTP, is much higher than the limit correspond to the periods with the highest deviations, as shown by Figure 6.43. The RTP solution will require an operator to take steps to curtail load to mitigate the overload on branch 17. The operator intervention would be sub-optimal and would not be required for this example when using the DLMP. The deviation of the consumption incentivized by the RTP in the congested system is compared to the deviation incentivized in case study 3, an uncongested system, in Figure 6.45.

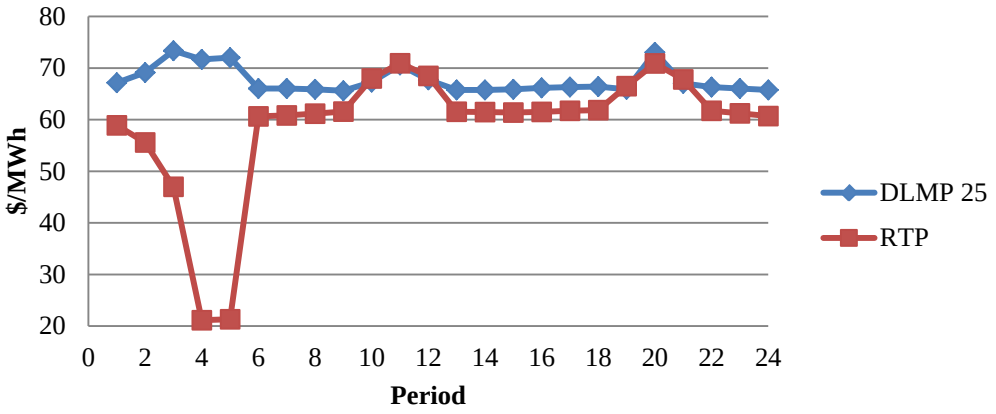

Figure 6.41. DLMP at Node 25 and RTP in Congested Network

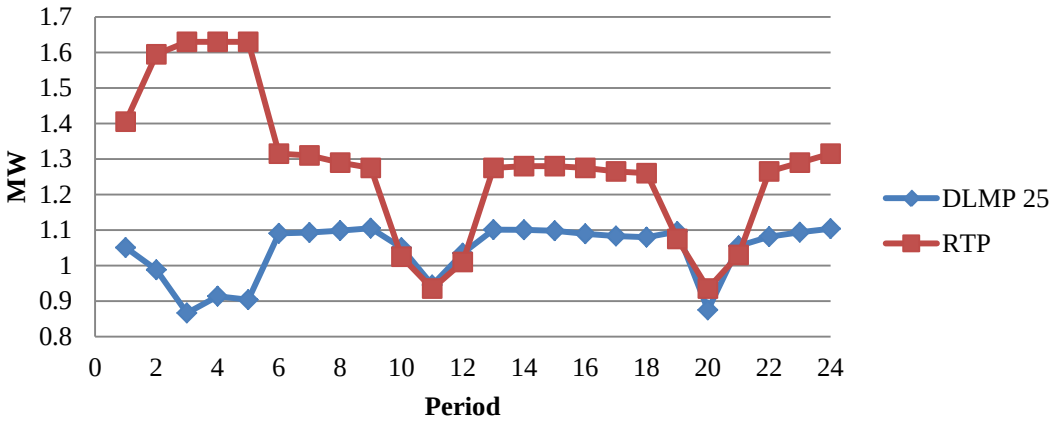

Figure 6.42. Real Power Consumption Incentivized by the DLMP and the RTP at Node 25 in the Congested Network

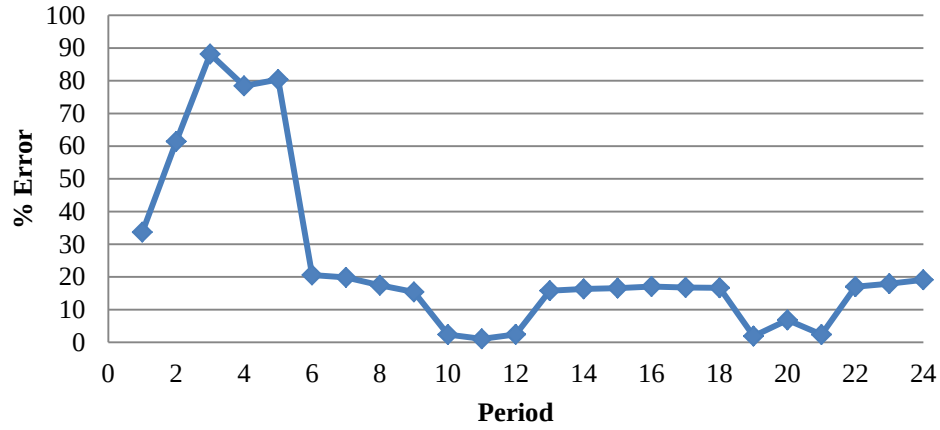

Figure 6.43. Absolute Percentage Deviation of the Consumption the RTP Incentivized at Node 25 from the Consumption Incentivized by the DLMP in the Congested Network

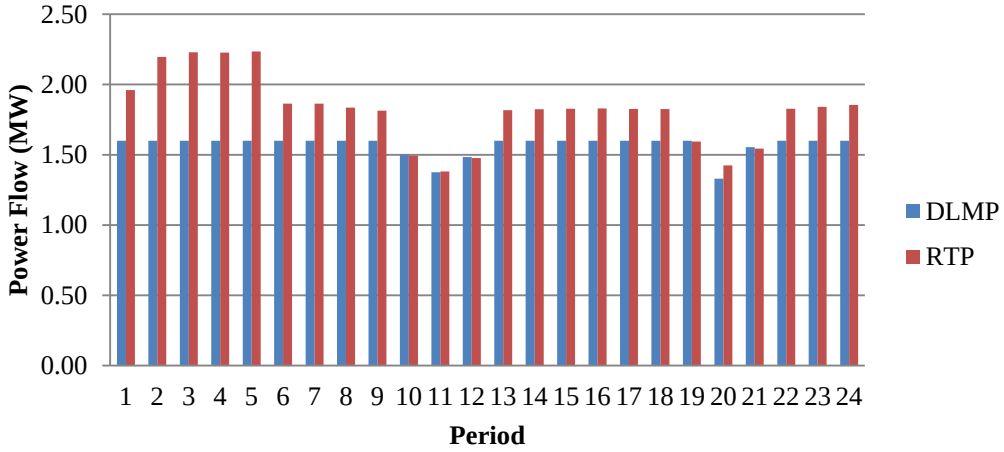

Figure 6.44. Power Flow on Branch 17 as a result of the Consumption Incentivized by the DLMP and RTP in the Congested Network

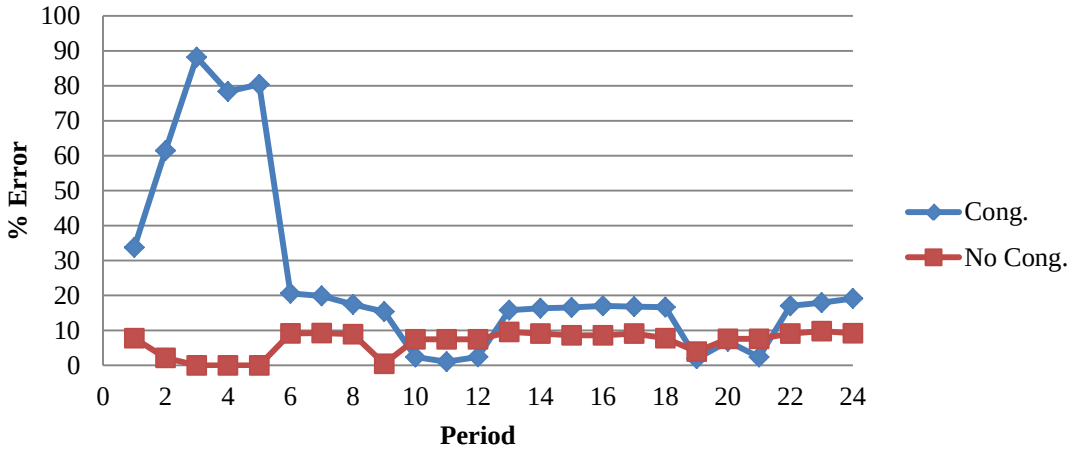

Figure 6.45. Comparison of the Absolute Percentage Deviation of the Consumption Incentivized by the RTP at Node 25 for Congested and Uncongested Network

6.9 Conclusion

The advantage of the DLMP over contemporary prices is tested numerically in this chapter. The DLMP pricing mechanism is tested on enhanced distribution systems with price responsive loads. The simulations are conducted with and without congestion in the enhanced distribution systems. Results of the simulations show that despite the inaccuracy of the FR, TOU, and the RTP, the contemporary prices perform well when the price sensitive loads are highly inelastic. As elasticity increases, the inaccuracy of the prices leads to deviation between the consumption incentivized by the contemporary prices and the optimal consumption incentivized by the DLMP. The deviation becomes significant as elasticity increases and it is more pronounced at individual load levels than at the aggregate level since the inelastic loads averaged out some of the effects. In the case where there are important network characteristics, such as congestion, in the distribution system, the RTP could incentivize significantly inaccurate consumption. The RTP in the congested system also resulted in line overloads, i.e., the inaccuracy of the RTP not only affected economic efficiency negatively, it also affected reliability negatively.

Chapter 7. Conclusions and Future Work

7.1 Conclusions

The use of the DLMP in enhanced distribution systems is proposed in this report. The proposed DLMP is an extension of the LMP concept to the distribution system and the DLMP has similar properties to the LMP. This report defined the DLMP and discussed its properties. The properties provide the DLMP the capability to incentive DSRs to behave optimally in a manner that benefits economic efficiency and reliability.

As part of the calculation approach for the DLMP, this report also discussed a lossy DCOPF formulation that endogenously captures real power losses. The lossy DCOPF formulation uses piecewise linear functions to approximate losses. The approximation technique could break down and lead to incorrect solutions under the scenario that negative DLMPs/LMPs occur. The breakdown was theoretically proven in this work. A MILP formulation for correcting the breakdown is also discussed.

Computational limitations necessitates that the OPF problem for calculating DLMPs be decomposed into a transmission and distribution system OPF. The decomposition requires iteration between both problems to ensure adequate modeling of the distribution system, including its DSRs, for the transmission system OPF and an adequate representation of the transmission system for the distribution system OPF. The iterative process optimally couples the transmission and the distribution systems. Previous work calculated nodal distribution prices using decomposed OPF problems but such approaches did not provide a mechanism that optimally couples the transmission and the distribution systems together. Due to non-convexities resulting from the staircase bid and offer curves as well as non-monotonicity of LMPs, there is no guarantee that the iterative process will converge or converge to a correct or globally optimal solution.

The iterative framework and a sampling approach, which does not suffer from the convergence problems of the iterative framework, are used to demonstrate the superiority of the DLMP over contemporary pricing schemes in the distribution system. The DLMP and contemporary pricing schemes are compared through the incentivized behavior of PRLs. Simulations show that, as the flexibility of loads increase, the contemporary prices incentivized significant sub-optimal behavior of PRLs. The superiority of the DLMP results from its calculation by the interaction of the demand and supply curves, its property as a nodal price, and the capability of the DLMP to adequately reflect the time dependence of energy prices. As such, the DLMP can reflect the network conditions of both the transmission and the distribution system and it can reflect the generation condition in both systems. The contemporary RTP, while reflecting the transmission system state, does not reflect the distribution system state (network and demand and supply conditions). The FR and the TOU do not reflect any system state, do not reflect time dependence of energy prices in the case of FR, and inadequately reflect time dependence of energy prices in the TOU case. Cross-subsidies, which distort prices, also result with the use of the contemporary prices. As a result, contemporary prices are inadequate for operating under the enhanced distribution system environment. The demonstrated superiority of the DLMP is expected to carry through in an enhanced distribution system with other price sensitive resources such as DGs and ESSs.

7.2 Future Work

While this report demonstrated and discussed the potential benefits and the need for the DLMP, additional work is required to fully develop the calculation and the application framework of the DLMP. In the area of the DLMP's calculation framework, the iterative approach of calculating the DLMP must be further investigated to develop solutions to its convergence issues. The solution may include a better representation of the distribution system in the transmission system OPF and the transmission system in distribution OPF model. Further work is also necessary to determine the suitability of the DCOPF for calculating DLMPs and for improving the OPF formulation. As discussed in this work, the assumptions in the DCOPF, while accurate for the transmission system, may be inaccurate for the distribution system. Hence, there may be a need to explore a better OPF model for the distribution system. In the area of the application framework of the DLMP, there is a need to explore the communication architecture between DSR and the market.

While PRLs are studied in this work, there is a need to also study ESSs and DGs with the iterative approach. Part of the benefit of the DLMP is also the benefits to the transmission system; these benefits should also be studied and benefits to congestion management and ancillary services demonstrated.

REFERENCES

[1] F.C. Schweppe *et al.*, *Spot Pricing of Electricity*, Boston, MA: Kluwer Academic Publishers, 1988.

[2] S. Stoft, *Power System Economics*, Piscataway, NJ: IEEE Press, 2002.

[3] T. Orfanogianni, G. Gross, "A general formulation for LMP evaluation," *IEEE Trans. Power Syst*., vol. 22, no. 3, pp. 1163-1173, Aug. 2007.

[4] D. Kirschen, G. Strbac, *Fundamentals of Power System Economics*, New York: John Wiley & Sons, 2010.

[5] H. Liu, L. Tesfatsion, A.A. Chowdhury, "Locational marginal pricing basics for restructured wholesale power markets," in *Proc. 2009 IEEE Power & Energy Society General Meeting*, pp. 1-8, July 2009.

[6] P.R. Gribik, W.W. Hogan, S.L. Pope, Market-Clearing Electricity Prices and Energy Uplift, Tech. Rep. 2007. [Online]. Available: http://www.whogan.com/

[7] E. Litvinov *et al.*, "Marginal loss modeling in LMP calculation," *IEEE Trans. Power Syst*., vol. 19, pp. 880-888, May 2004.

[8] E. Litvinov, "Design and operation of the locational marginal prices-based electricity markets," *Generation, Transmission & Distribution, IET*, vol. 4, no. 2, pp. 315-323, Feb. 2010.

[9] W.W. Hogan, Financial Transmission Right Formulations, Tech. Rep., 2002. [Online]. Available: http://www.whogan.com/

[10] W.W. Hogan, Contract Networks for Electric Power Transmission: Technical Reference, Tech. Rep., 1992. [Online]. Available: http://www.whogan.com/

[11] California ISO. (2012, Nov.). California Independent System Operator Corporation Fifth Replacement FERC Electric Tariff Section 27: CAISO Markets and Processes. [Online]. Available: http://www.caiso.com/Documents/TableOfContents_Nov5_2012.pdf

[12] ISO New England. (2013, Jan.). Manual M-11: ISO New England Manual for Market Operations. [Online]. Available: http://www.iso-ne.com/rules_proceds/isone_mnls/index.html

[13] Electric Reliability Council of Texas. (2013, Feb.). ERCOT Nodal Protocols Section 4: Day-Ahead Operations. [Online]. Available: http://www.ercot.com/mktrules/nprotocols/current

[14] Midwest ISO. (2012, Jan.). Business Practices Manual: Energy and Operating Reserve Markets. [Online]. Available: https://www.midwestiso.org/Library/Tariff/Pages/Tariff.aspx

[15] PJM Interconnection. (2010, Sept.). PJM Open Access Transmission Tariff Section 2: Calculation of Locational Marginal Prices: [Online]. Available: http://www.pjm.com/~/media/documents/agreements/tariff.ashx

[16] F. Li, R. Bo, "DCOPF-based LMP simulation: algorithm, comparison with ACOPF, and sensitivity," *IEEE Trans. Power Syst.*, vol. 22, no. 4, pp. 1475-1485, Nov. 2007.

[17] T. Wu, Z. Alaywan, A. D. Papalexopoulos, "Locational marginal price calculations using the distributed-slack power-flow formulation," *IEEE Trans. Power Syst.*, vol. 20, no. 2, pp. 1188- 1190, May 2005.

[18] J. Meisel, "System incremental cost calculations using the participation factor load-flow formulation," *IEEE Trans. Power Syst.*, vol. 8, no. 1, pp. 357-363, Feb 1993.

[19] Z. Hu *et al.*, "An iterative LMP calculation method considering loss distributions," *IEEE Trans. Power Syst.*, vol. 25, no. 3, pp. 1469-1477, Aug. 2010.

[20] A. L. Motto *et al.*, "Network-constrained multiperiod auction for a pool-based electricity market," *IEEE Trans. Power Syst.*, vol. 17, no. 3, pp. 646- 653, Aug 2002.

[21] N. Alguacil, A. L. Motto, A. J. Conejo, "Transmission expansion planning: a mixed-integer LP approach," *IEEE Trans. Power Syst.*, vol. 18, no. 3, pp. 1070- 1077, Aug. 2003.

[22] H. Zhang *et al.*, "A mixed-integer linear programming approach for multi-stage security-constrained transmission expansion planning," *IEEE Trans. Power Syst.*, vol. 27, no. 2, pp. 1125-1133, May 2012.

[23] B. F. Hobbs *et al.*, "Improved transmission representations in oligopolistic market models: quadratic losses, phase shifters, and DC Lines," *IEEE Trans. Power Syst.*, vol. 23, no. 3, pp. 1018-1029, Aug. 2008.

[24] B. B. Chakrabarti *et al.*, "Alternative loss model for the New Zealand electricity market using SFT," in *Proc. 2011 IEEE Power and Energy Society General Meeting*, pp. 1-8, 24-29 July 2011.

[25] P.S. Martin, “Mejoras en la eficacia computacional de medelos probabilistas de explotación generación/red a medio plazo,” Ph.D. dissertation (in Spanish), Univ. Pontificial de Comillas, Madrid Spain, 1998.

[26] R. Palma-Benhke *et al.*, “Modeling network constrained economic dispatch problems,” Elect. Power Optimization Center, Auckland, Tech Rep., 2009.

[27] P. S. Martin and A. Ramos, “Modeling Transmission Ohmic Losses in a Stochastic Bulk Production Cost Model,” [Online]. Available: http://www.iit.upcomillas.es/~aramos/papers/losses.pdf

[28] R. Billinton and S. Jonnavithula, "A test system for teaching overall power system reliability assessment," *IEEE Trans. Power Syst.*, vol. 11, no. 4, pp. 1670-1676, Nov 1996.

[29] R. N. Allan *et al.*, "A reliability test system for educational purposes-basic distribution system data and results," *IEEE Trans. Power Syst.*, vol. 6, no. 2, pp. 813-820, May 1991.

[30] R. Billinton *et al.*,"A reliability test system for educational purposes-basic results," *IEEE Trans. Power Syst.*, vol. 5, no. 1, pp. 319-325, Feb 1990.

[31] R. Billinton *et al.*, "A reliability test system for educational purposes-basic data," *IEEE Trans. Power Syst.*, vol. 4, no. 3, pp. 1238-1244, Aug 1989.

[32] D. A. Haughton, “State estimation for enhanced monitoring, reliability, restoration and control of smart distribution systems,” Ph.D. dissertation, Arizona State Univ., Tempe U.S.A, 2012.

[33] B. R. Sathyanarayana, “Sensitivity-based pricing and multiobjective control for energy management in power distribution system,” Ph.D. dissertation, Arizona State Univ., Tempe U.S.A, 2012.

[34] R. D. Zimmerman, C. E. Murillo-Sanchez, R. J. Thomas, “Matpower: steady-state operations, planning and analysis tools for power systems research and education," *IEEE Trans. Power Syst.*, vol. 26, no. 1, pp. 12-19, Feb. 2011.

[35] O. Alsac, B. Stott, "Optimal load flow with steady state security," *IEEE Trans. on Power App. and Syst.*, vol. PAS 93, no. 3, pp. 745-751, 1974.

[36] C. Grigg *et al.*, "The IEEE reliability test system-1996. A report prepared by the Reliability Test System Task Force of the Application of Probability Methods Subcommittee," *IEEE Trans. Power Syst.*, vol. 14, no. 3, pp. 1010-1020, Aug 1999.

[37] K. W. Hedman *et al.*, “Co-optimization of generation unit commitment and transmission switching with N-1 reliability, “*IEEE Trans. Power Syst.*, vol. 25, no. 2, pp. 1052-1063, May 2010.

[38] F. Gonzalez-Longatt. *IEEE 30 bus test* [Online]. Available: http://www.fglongatt.org/Test_Case_IEEE_30.html

[39] AEP Ohio. *Columbus Southern Power Company Class Load Profiles Jan-Dec 2012* [Online]. Available: https://www.aepohio.com/service/choice/cres/LoadProfiles.aspx

[40] J. J. Burke, “Utility distribution design fundamentals and characteristics,” in *Power Distribution Engineering Fundamentals and Applications*, New York: Dekker, 1994.

[41] W. H. Kersting, “Introduction to distribution systems,” in *Distribution System Modeling and Analysis*, 2nd ed. Boca Raton: CRC, 2007.

[42] P. M. Sotkiewicz, J. M. Vignolo, "Nodal pricing for distribution networks: efficient pricing for efficiency enhancing DG," *IEEE Trans. Power Syst.*, vol. 21, no. 2, pp. 1013-1014, May 2006.

[43] K. Shaloudegi *et al.*, "A novel policy for locational marginal price calculation in distribution systems based on loss reduction allocation using game theory," *IEEE Trans. Power Syst.*, vol. 27, no. 2, pp. 811-820, May 2012.

[44] N. Steffan, G. T. Heydt, "Quadratic programming and related techniques for the calculation of locational marginal prices in distribution systems," in *Proc. North American Power Symposium (NAPS)*, 2012, pp.1-6, 9-11 Sept. 2012.

[45] B. R. Sathyanarayana, G. T. Heydt, "Sensitivity-based pricing and optimal storage utilization in distribution systems," *IEEE Trans. Power Del.*, vol. 28, no. 2, pp. 1073-1082, April 2013.

[46] G. T. Heydt, "The next generation of power distribution systems," *IEEE Trans. Smart Grid*, vol. 1, no. 3, pp. 225-235, Dec. 2010.

[47] G. T. Heydt *et al.*, "Pricing and control in the next generation power distribution system," *IEEE Trans. Smart Grid*, vol. 3, no. 2, pp.907-914, June 2012.

[48] 110th Congress of United States, "Smart Grid," Title XIII, Energy Independence and Security Act of 2007, Washington DC, December 2007.

[49] Office of Electricity Delivery and Energy Reliability, United States Department of Energy. (2008). *The Smart Grid – An Introduction* [Online]. Available: http://energy.gov/sites/prod/files/oeprod/DocumentsandMedia/DOE_SG_Book_SinSin_Pages%281%29.pdf

[50] Office of Electricity Delivery and Energy Reliability, United States Department of Energy. (2009). *What the Smart Grid Means to You (Utilities) and the People You Serve* [Online]. Available: http://energy.gov/sites/prod/files/oeprod/DocumentsandMedia/Utilities.pdf

[51] Office of Electricity Delivery and Energy Reliability, United States Department of Energy. (2009). *What the Smart Grid Means to Americans (Consumer Advocates)* [Online]. Available: http://energy.gov/sites/prod/files/oeprod/DocumentsandMedia/ConsumerAdvocates.pdf

[52] Office of Electricity Delivery and Energy Reliability, United States Department of Energy. (2009). *What the Smart Grid Means to American's Future (Technology Providers)* [Online]. Available: http://energy.gov/sites/prod/files/oeprod/DocumentsandMedia/TechnologyProviders.pdf

[53] H. Farhangi, "The path of the smart grid," *IEEE Power and Energy Magazine*, vol. 8, no. 1, pp. 18-28, January-February 2010.

[54] F. Xi *et al.*, "Smart Grid — The new and improved power grid: a survey," *IEEE Communications Surveys & Tutorials*, vol. 14, no. 4, pp. 944-980, Fourth Quarter 2012.

[55] V. C. Gungor *et al.*, "Smart grid technologies: communication technologies and standards," *IEEE Trans. Ind. Informat.*, vol. 7, no. 4, pp. 529,539, Nov. 2011.

[56] J. C. Bonbright, *Principle of Public Utility Rates*, New York, NY: Columbia Univ. Press, 1961.

[57] M. H. Dworkin. (2003, Jan.). *The PSB process: the scope, the players, and the rules of practice before the public service board* [Online]. Available: http://gmcboard.vermont.gov/sites/gmcboard/files/PBS041212.pdf

[58] H. S. Parmesano, C. S. Martin, "The evolution in U.S. electric utility rate design," *Annu. Rev. Energy*, vol. 8, pp. 45-94, Nov. 1983.

[59] M. A. Jamison, "Rate of return: regulation," Public Utility Research Center, University of Florida, Tech. Rep. [Online]. Available: http://warrington.ufl.edu/centers/purc/purcdocs/papers/0528_jamison_rate_of_returr.pdf

[60] The Regulatory Assistance Project. (2011, Mar.). *Electricity regulation in the US: a guide* [Online]. Available: www.raponline.org/document/download/id/645

[61] L. J. Vogt, *Electricity Pricing Engineering Principles and Methodologies*, Boca Raton, FL: CRC Press, 2009.

[62] P. Q. Hanser, "Issues in cost allocation – Wisconsin Public Utility Institute," The Brattle Group, Tech. Presentation. [Online]. Available: http://wpui.wisc.edu/wp-content/uploads/2012/07/Cost-Allocation-2012.pdf

[63] G. Barbose *et al.*, "A survey of utility experience with real time pricing" Ernest Orlando Lawrence Berkeley National Laboratory, Berkeley, CA, Tech Rep. DE-AC03-76SF00098, Dec. 2004. [Online]. Available: http://eetd.lbl.gov/ea/ems/reports/54238.pdf

[64] S. Braithwait *et al.*, "Retail electricity pricing and rate design in evolving markets" Edison Electric Institute, Washington, D.C, Tech Rep. [Online]. Available: http://www.eei.org/ourissues/electricitydistribution/Documents/Retail_Electricity_PPricin.pdf

[65] H. Averch, L. Johnson, "The behavior of the firm under regulatory constraint," *Amer. Econ. Rev.*, vol. 52, no. 5, pp. 1052-1069, Dec. 1962.

[66] S. Borenstein "Time-varying retail electricity prices: theory and practice," in Griffin and Puller, eds., *Electricity Deregulation: Choices and Challenges*, Chicago, IL: Univ. of Chicago Press, 2005.

[67] A. Faruqui *et al.*, "Time-varying and dynamic rate design" The Brattle Group, Tech Rep. [Online]. Available: http://www.brattle.com/Experts/ExpertDetail.asp?ExpertID=164

[68] O. W. Akinbode, K. W. Hedman, "Fictitious losses in the DCOPF with a piecewise linear approximation of losses," to be published in *Proc. 2013 IEEE Power and Energy Society General Meeting.*

[69] D. N. Jones, P. C. Mann, "The fairness criterion in public utility regulation: does fairness still matter?" *J. of Econ. Issues*, vol. 35, no. 1, pp. 153-172, Mar. 2001.

[70] M. D. Ilic, J. Donadee, "Distribution pricing and tariff structure: the ongoing US reforms," in *Proc. 2011 IEEE Power and Energy Society General Meeting*, pp. 1-2.

[71] Pacific Gas and Electric Company, "Voltage tolerance boundary," Pacific Gas and Electric Company, [Online]. Available: http://www.pge.com/includes/docs/pdfs/mybusiness/customerservice/energystatus/powerquality/voltage_tolerance.pdf

[72] H. Oh, R. J. Thomas, "Demand-side bidding agents: modeling and simulation," *IEEE Trans. on Power Syst.*, vol. 23, no. 3, pp. 1050-1056, Aug. 2008.

[73] Y. Liu, X. Guan, "Purchase allocation and demand bidding in electric power markets," *IEEE Trans. on Power Syst.*, vol. 18, no. 1, pp. 106-112, Feb. 2003.

[74] G. B. Sheble, "DSM economic marginal demand bidding," in *Proc. 2010 IEEE Power and Energy Society General Meeting*, pp. 1-7.

[75] P. R. Thimmapuram *et al.*, "Modeling and simulation of price elasticity of demand using an agent-based model," in *Proc. 2010 Innovative Smart Grid Technologies (ISGT)*, pp. 1-8.

[76] M. A. Bernstein, J. Griffin, "Regional differences in the price-elasticity of demand for energy," the RAND Corporation, Tech. Rep. [Online]. Available: http://www.rand.org/content/dam/rand/pubs/technical_reports/2005/RAND_TR292.pdf

[77] H. R. Varian, *Intermediate Microeconomics a modern approach*, 8th ed. New York: W. W. Norton, 2010.

[78] M. Filippini, "Electricity demand by time of use: An application of the household AIDS model," *Energy Economics*, vol. 17, no. 3, pp. 197-204, Jul. 1995.

[79] N. Singhal, K. W. Hedman, "An integrated transmission and distribution systems model with distribution-based LMP (DLMP) pricing," submitted to *North American Power Symposium (NAPS)*, 2013.

APPENDIX A

SIMULATION DATA AND RESULTS DETAILS

Appendix A. Simulation Data and Results Details

Table A.1. RBTS Transmission System Branch Data

No.	From Bus	To Bus	Length (mi)	R p.u	X p.u.	B/2 p.u	Current Rating p.u.	MVA Rating (p.u.)
1	1	3	46.6028	0.0342	0.1800	0.0106	0.85	0.85
2	2	4	155.3428	0.1140	0.6000	0.0352	0.71	0.71
3	1	2	124.2742	0.0912	0.4800	0.0282	0.71	0.71
4	3	4	31.0686	0.0228	0.1200	0.0071	0.71	0.71
5	3	5	31.0686	0.0228	0.1200	0.0071	0.71	0.71
6	1	3	46.6028	0.0342	0.1800	0.0106	0.85	0.85
7	2	4	155.3428	0.1140	0.6000	0.0352	0.71	0.71
8	4	5	31.0686	0.0228	0.1200	0.0071	0.71	0.71
9	5	6	31.0686	0.0228	0.1200	0.0071	0.71	0.71
10	3	7	0.0000	0.0128	0.0640	0.0000	1.55	1.55
11	3	7	0.0000	0.0128	0.0640	0.0000	1.55	1.55
100 MVA Base								

Table A.2. Flexible Load Data for RBTS Bus 3 Distribution System

Feeder	Load Point	Peak Load (MW)	Flexible Part of Load (MW)	Inflexible Part of Base Load (MW)	% of Peak Load that is Flexible
F1	LP1	0.8367	0.2740	0.5627	32.75
	LP2	0.7750	0.2740	0.5010	35.36
	LP3	0.5222	0.2740	0.2482	52.48
	LP4	0.8367	0.2740	0.5627	32.75
F2	LP8	1.0167	0.3050	0.7117	30.00
	LP9	1.0167	0.3050	0.7117	30.00
F3	LP11	0.8500	0.2650	0.5850	31.14
	LP12	0.8500	0.2650	0.5850	31.14
	LP13	0.8500	0.2650	0.5850	31.14
	LP14	0.9250	0.2650	0.6600	28.62
F4	LP18	0.8500	0.2780	0.5720	32.68
	LP19	0.5222	0.2780	0.2442	53.20
	LP20	0.8367	0.2780	0.5587	33.20
	LP21	0.8367	0.2780	0.5587	33.20
F5	LP25	0.8500	0.2450	0.6050	28.77
	LP26	0.7750	0.2450	0.5300	31.56
	LP27	0.9250	0.2450	0.6800	26.44
	LP28	0.5222	0.2450	0.2772	46.84
F6	LP32	0.8367	0.2610	0.5757	31.24
	LP33	0.8367	0.2610	0.5757	31.24
	LP34	0.8367	0.2610	0.5757	31.24
	LP35	0.8367	0.2610	0.5757	31.24
F7	LP39	6.9167	2.5400	4.3767	36.75
	LP40	6.9167	2.5400	4.3767	36.75
F8	LP42	11.5833	3.0000	8.5833	25.97
	LP43	11.5833	3.0000	8.5833	25.97

Table A.3. RBTS Bus 4 Distribution System 11 kV Feeder Loading and Impedance Summary

Feeder	Peak Loading (MW)	Conductor Rating (A)	Feeder Length (mi)	R (Ω/mi)	X (Ω/mi)
1	5.70	530.00	5.4370	0.307088	0.629576
2	5.71	530.00	2.7030		
3	5.63	530.00	5.3127		
4	6.52	530.00	5.8098		
5	4.89	530.00	2.6719		
6	5.71	530.00	2.6719		
7	5.85	530.00	5.3438		

Table A.4. RBTS Bus 4 Distribution System Feeder Section Summary

Section Type	Length (mi)	Section Number
1	0.3728	2, 6, 10, 14, 17, 21, 25, 28, 30, 34, 38, 41, 43, 46, 49, 51, 55, 58, 61, 64, 67
2	0.4660	1, 4, 7, 9, 12, 16, 19, 22, 24, 27, 29, 32, 35, 37, 40, 42, 45, 48, 50, 53, 56, 60, 63, 65
3	0.4971	3, 5, 8, 11, 13, 15, 18, 20, 23, 26, 31, 33, 36, 39, 44, 47, 52, 54, 57, 59, 62, 66

Table A.5. RBTS Bus 4 Distribution System 11 kV Network Feeders Impedance Summary

Section #	Length (mi)	R (Ω/mi)	X (Ω/mi)
80	9.32057	0.30709	0.629576
81	3.10686	0.30709	0.629576
82	3.10686	0.30709	0.629576
83	6.21371	0.30709	0.629576
84	6.21371	0.30709	0.629576

Table A.6. RBTS Bus 4 Distribution System 33 kV Feeders Impedance Summary

Branch No.	Peak Loading (MW)	Conductor Rating (A)	Feeder Length (mi)	R (Ω/mi)	X (Ω/mi)
68	5.70	730.00	6.2137	0.187726	0.600135
69	5.71	730.00	9.3206		
70	5.63	730.00	9.3206		
71	6.52	730.00	6.2137		

Table A.7. IEEE 30-Bus System Branch Data

No.	From bus	To bus	kV Base	MVA Base	R (p.u.)	X (p.u.)	G (p.u.)	B (p.u.)	Branch Limit (p.u.)
1	1	2	135	100	0.0200	0.0600	5.0000	-15.0000	1.3
2	1	3	135	100	0.0500	0.1900	1.2953	-4.9223	1.3
3	2	4	135	100	0.0600	0.1700	1.8462	-5.2308	0.65
4	3	4	135	100	0.0100	0.0400	5.8824	-23.5294	1.3
5	2	5	135	100	0.0500	0.2000	1.1765	-4.7059	1.3
6	2	6	135	100	0.0600	0.1800	1.6667	-5.0000	0.65
7	4	6	135	100	0.0100	0.0400	5.8824	-23.5294	0.9
8	5	7	135	100	0.0500	0.1200	2.9586	-7.1006	0.7
9	6	7	135	100	0.0300	0.0800	4.1096	-10.9589	1.3
10	6	8	135	100	0.0100	0.0400	5.8824	-23.5294	0.32
11	6	9	135	100	0.0000	0.2100	0.0000	-4.7619	0.65
12	6	10	135	100	0.0000	0.5600	0.0000	-1.7857	0.32
13	9	11	135	100	0.0000	0.2100	0.0000	-4.7619	0.65
14	9	10	135	100	0.0000	0.1100	0.0000	-9.0909	0.65
15	4	12	135	100	0.0000	0.2600	0.0000	-3.8462	0.65
16	12	13	135	100	0.0000	0.1400	0.0000	-7.1429	0.65
17	12	14	135	100	0.1200	0.2600	1.4634	-3.1707	0.32
18	12	15	135	100	0.0700	0.1300	3.2110	-5.9633	0.32
19	12	16	135	100	0.0900	0.2000	1.8711	-4.1580	0.32
20	14	15	135	100	0.2200	0.2000	2.4887	-2.2624	0.16
21	16	17	135	100	0.0800	0.1900	1.8824	-4.4706	0.16
22	15	18	135	100	0.1100	0.2200	1.8182	-3.6364	0.16
23	18	19	135	100	0.0600	0.1300	2.9268	-6.3415	0.16
24	19	20	135	100	0.0300	0.0700	5.1724	-12.0690	0.32
25	10	20	135	100	0.0900	0.2100	1.7241	-4.0230	0.32
26	10	17	135	100	0.0300	0.0800	4.1096	-10.9589	0.32
27	10	21	135	100	0.0300	0.0700	5.1724	-12.0690	0.32
28	10	22	135	100	0.0700	0.1500	2.5547	-5.4745	0.32
29	21	22	135	100	0.0100	0.0200	20.0000	-40.0000	0.32
30	15	23	135	100	0.1000	0.2000	2.0000	-4.0000	0.16

No.	From bus	To bus	kV Base	MVA Base	R (p.u.)	X (p.u.)	G (p.u.)	B (p.u.)	Branch Limit (p.u.)
31	22	24	135	100	0.1200	0.1800	2.5641	-3.8462	0.16
32	23	24	135	100	0.1300	0.2700	1.4477	-3.0067	0.16
33	24	25	135	100	0.1900	0.3300	1.3103	-2.2759	0.16
34	25	26	135	100	0.2500	0.3800	1.2083	-1.8366	0.16
35	25	27	135	100	0.1100	0.2100	1.9573	-3.7367	0.16
36	28	27	135	100	0.0000	0.4000	0.0000	-2.5000	0.65
37	27	29	135	100	0.2200	0.4200	0.9786	-1.8683	0.16
38	27	30	135	100	0.3200	0.6000	0.6920	-1.2976	0.16
39	29	30	135	100	0.2400	0.4500	0.9227	-1.7301	0.16
40	8	28	135	100	0.0600	0.2000	1.3761	-4.5872	0.32
41	6	28	135	100	0.0200	0.0600	5.0000	-15.0000	0.32

Table A.8. 24 Hour Load Data for the Inelastic Loads in the Test Transmission System

Bus No.	H1	H2	H3	H4	H5	H6	H7	H8
1	0.00	0.00	0.00	0.00	0.00	0.00	0.00	0.00
2	13.67	13.45	13.02	12.59	12.80	14.11	15.62	18.45
3	1.51	1.49	1.44	1.39	1.42	1.56	1.73	2.04
4	4.79	4.71	4.56	4.41	4.48	4.94	5.47	6.46
5	0.00	0.00	0.00	0.00	0.00	0.00	0.00	0.00
6	0.00	0.00	0.00	0.00	0.00	0.00	0.00	0.00
7	14.36	14.14	13.68	13.22	13.45	14.82	16.42	19.38
8	18.90	18.60	18.00	17.40	17.70	19.50	21.60	25.50
9	0.00	0.00	0.00	0.00	0.00	0.00	0.00	0.00
10	3.65	3.60	3.48	3.36	3.42	3.77	4.18	4.93
11	0.00	0.00	0.00	0.00	0.00	0.00	0.00	0.00
12	7.06	6.94	6.72	6.50	6.61	7.28	8.06	9.52
13	0.00	0.00	0.00	0.00	0.00	0.00	0.00	0.00
14	3.91	3.84	3.72	3.60	3.66	4.03	4.46	5.27
15	5.17	5.08	4.92	4.76	4.84	5.33	5.90	6.97
16	2.21	2.17	2.10	2.03	2.07	2.28	2.52	2.98
17	5.67	5.58	5.40	5.22	5.31	5.85	6.48	7.65
18	2.02	1.98	1.92	1.86	1.89	2.08	2.30	2.72
19	5.99	5.89	5.70	5.51	5.61	6.18	6.84	8.08
20	1.39	1.36	1.32	1.28	1.30	1.43	1.58	1.87
21	11.03	10.85	10.50	10.15	10.33	11.38	12.60	14.88
22	0.00	0.00	0.00	0.00	0.00	0.00	0.00	0.00
23	2.02	1.98	1.92	1.86	1.89	2.08	2.30	2.72
24	5.48	5.39	5.22	5.05	5.13	5.66	6.26	7.40
25	0.00	0.00	0.00	0.00	0.00	0.00	0.00	0.00
26	2.21	2.17	2.10	2.03	2.07	2.28	2.52	2.98
27	0.00	0.00	0.00	0.00	0.00	0.00	0.00	0.00
28	0.00	0.00	0.00	0.00	0.00	0.00	0.00	0.00
29	1.51	1.49	1.44	1.39	1.42	1.56	1.73	2.04
30	6.68	6.57	6.36	6.15	6.25	6.89	7.63	9.01
Total	119.20	117.30	113.52	109.74	111.63	122.98	136.22	160.82

Bus No.	H9	H10	H11	H12	H13	H14	H15	H16
1	0.00	0.00	0.00	0.00	0.00	0.00	0.00	0.00
2	20.62	21.48	21.70	21.48	20.18	19.96	19.53	19.10
3	2.28	2.38	2.40	2.38	2.23	2.21	2.16	2.11
4	7.22	7.52	7.60	7.52	7.07	6.99	6.84	6.69
5	0.00	0.00	0.00	0.00	0.00	0.00	0.00	0.00
6	0.00	0.00	0.00	0.00	0.00	0.00	0.00	0.00
7	21.66	22.57	22.80	22.57	21.20	20.98	20.52	20.06
8	28.50	29.70	30.00	29.70	27.90	27.60	27.00	26.40
9	0.00	0.00	0.00	0.00	0.00	0.00	0.00	0.00
10	5.51	5.74	5.80	5.74	5.39	5.34	5.22	5.10
11	0.00	0.00	0.00	0.00	0.00	0.00	0.00	0.00
12	10.64	11.09	11.20	11.09	10.42	10.30	10.08	9.86
13	0.00	0.00	0.00	0.00	0.00	0.00	0.00	0.00
14	5.89	6.14	6.20	6.14	5.77	5.70	5.58	5.46
15	7.79	8.12	8.20	8.12	7.63	7.54	7.38	7.22
16	3.33	3.47	3.50	3.47	3.26	3.22	3.15	3.08
17	8.55	8.91	9.00	8.91	8.37	8.28	8.10	7.92
18	3.04	3.17	3.20	3.17	2.98	2.94	2.88	2.82
19	9.03	9.41	9.50	9.41	8.84	8.74	8.55	8.36
20	2.09	2.18	2.20	2.18	2.05	2.02	1.98	1.94
21	16.63	17.33	17.50	17.33	16.28	16.10	15.75	15.40
22	0.00	0.00	0.00	0.00	0.00	0.00	0.00	0.00
23	3.04	3.17	3.20	3.17	2.98	2.94	2.88	2.82
24	8.27	8.61	8.70	8.61	8.09	8.00	7.83	7.66
25	0.00	0.00	0.00	0.00	0.00	0.00	0.00	0.00
26	3.33	3.47	3.50	3.47	3.26	3.22	3.15	3.08
27	0.00	0.00	0.00	0.00	0.00	0.00	0.00	0.00
28	0.00	0.00	0.00	0.00	0.00	0.00	0.00	0.00
29	2.28	2.38	2.40	2.38	2.23	2.21	2.16	2.11
30	10.07	10.49	10.60	10.49	9.86	9.75	9.54	9.33
Total	179.74	187.31	189.20	187.31	175.96	174.06	170.28	166.50

Bus No.	H17	H18	H19	H20	H21	H22	H23	H24
1	0.00	0.00	0.00	0.00	0.00	0.00	0.00	0.00
2	19.53	19.96	20.83	21.27	20.83	19.53	17.36	15.19
3	2.16	2.21	2.30	2.35	2.30	2.16	1.92	1.68
4	6.84	6.99	7.30	7.45	7.30	6.84	6.08	5.32
5	0.00	0.00	0.00	0.00	0.00	0.00	0.00	0.00
6	0.00	0.00	0.00	0.00	0.00	0.00	0.00	0.00
7	20.52	20.98	21.89	22.34	21.89	20.52	18.24	15.96
8	27.00	27.60	28.80	29.40	28.80	27.00	24.00	21.00
9	0.00	0.00	0.00	0.00	0.00	0.00	0.00	0.00
10	5.22	5.34	5.57	5.68	5.57	5.22	4.64	4.06
11	0.00	0.00	0.00	0.00	0.00	0.00	0.00	0.00
12	10.08	10.30	10.75	10.98	10.75	10.08	8.96	7.84
13	0.00	0.00	0.00	0.00	0.00	0.00	0.00	0.00
14	5.58	5.70	5.95	6.08	5.95	5.58	4.96	4.34
15	7.38	7.54	7.87	8.04	7.87	7.38	6.56	5.74
16	3.15	3.22	3.36	3.43	3.36	3.15	2.80	2.45
17	8.10	8.28	8.64	8.82	8.64	8.10	7.20	6.30
18	2.88	2.94	3.07	3.14	3.07	2.88	2.56	2.24
19	8.55	8.74	9.12	9.31	9.12	8.55	7.60	6.65
20	1.98	2.02	2.11	2.16	2.11	1.98	1.76	1.54
21	15.75	16.10	16.80	17.15	16.80	15.75	14.00	12.25
22	0.00	0.00	0.00	0.00	0.00	0.00	0.00	0.00
23	2.88	2.94	3.07	3.14	3.07	2.88	2.56	2.24
24	7.83	8.00	8.35	8.53	8.35	7.83	6.96	6.09
25	0.00	0.00	0.00	0.00	0.00	0.00	0.00	0.00
26	3.15	3.22	3.36	3.43	3.36	3.15	2.80	2.45
27	0.00	0.00	0.00	0.00	0.00	0.00	0.00	0.00
28	0.00	0.00	0.00	0.00	0.00	0.00	0.00	0.00
29	2.16	2.21	2.30	2.35	2.30	2.16	1.92	1.68
30	9.54	9.75	10.18	10.39	10.18	9.54	8.48	7.42
Total	170.28	174.06	181.63	185.42	181.63	170.28	151.36	132.44

Table A.9. RBTS Bus 4 Distribution System Bus and Load Details

Bus No.	Type	Peak Load kW	Bus No.	Type	Peak Load kW	Bus No.	Type	Peak Load kW
1	1	0	26	1	0	51	1	0
2	1	0	27	1	886.9	52	3	1630
3	1	0	28	1	0	53	1	0
4	1	0	29	1	886.9	54	3	1630
5	1	0	30	1	0	55	1	0
6	1	0	31	1	886.9	56	3	1630
7	1	0	32	2	813.7	57	1	0
8	1	0	33	1	0	58	3	1630
9	1	886.9	34	2	813.7	59	1	0
10	1	0	35	1	0	60	3	1630
11	1	886.9	36	5	671.4	61	1	0
12	1	0	37	5	671.4	62	4	2445
13	1	886.9	38	1	0	63	1	0
14	1	0	39	1	886.9	64	1	886.9
15	1	886.9	40	1	0	65	1	0
16	2	813.7	41	1	886.9	66	1	886.9
17	1	0	42	1	886.9	67	1	0
18	5	671.4	43	1	0	68	1	886.9
19	5	671.4	44	1	886.9	69	1	886.9
20	1	0	45	2	813.7	70	1	0
21	3	1630	46	1	0	71	2	813.7
22	1	0	47	2	813.7	72	1	0
23	4	2445	48	1	0	73	2	813.7
24	1	0	49	5	671.4	74	5	671.4
25	3	1630	50	5	671.4	75	1	0

Table A.10. Hourly Inelastic Loads in the RBTS Bus 4 Distribution System

Period	kW	Per Unit based on Peak kW
1	559.90	0.63
2	524.34	0.59
3	502.09	0.57
4	502.17	0.57
5	542.23	0.61
6	656.69	0.74
7	683.66	0.77
8	671.01	0.76
9	659.45	0.74
10	653.78	0.74
11	665.70	0.75
12	667.30	0.75
13	675.30	0.76
14	681.34	0.77
15	694.35	0.78
16	738.63	0.83
17	788.44	0.89
18	813.02	0.92
19	837.74	0.94
20	886.90	1.00
21	877.59	0.99
22	796.59	0.90
23	699.37	0.79
24	609.35	0.69